Energy, Mines and Resources Canada
Énergie, Mines et Ressources Canada

CANMET

Canada Centre for Mineral and Energy Technology
Centre canadien de la technologie des minéraux et de l'énergie

**Mining Research Laboratories**
**Laboratoires de recherche minière**

# PARADOXICAL SECULAR DISEQUILIBRIUM OF RADIOISOTOPES IN URANIUM MINE TAILINGS

T.P. LIM ELLIOT LAKE LABORATORY

OCT 1987

DIVISIONAL REPORT MRL 89-34 (OP)

Canada

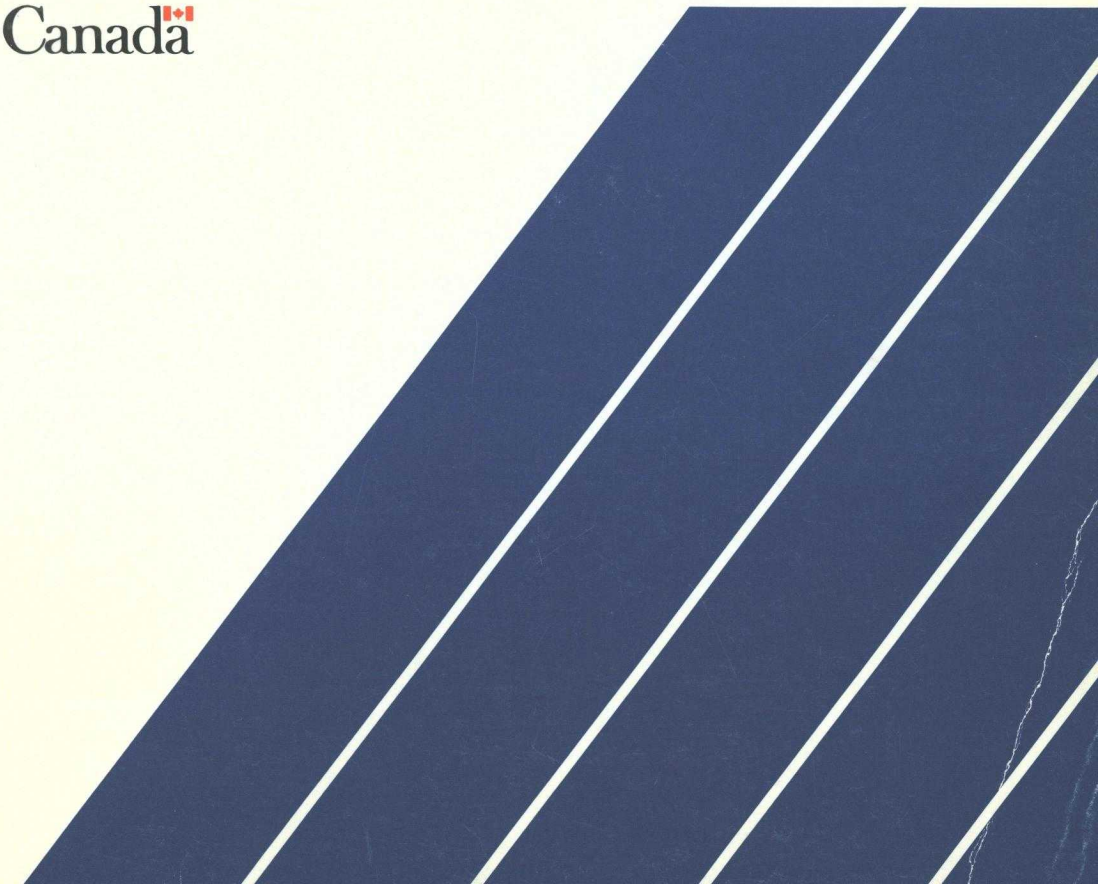

# PARADOXICAL SECULAR DISEQUILIBRIUM OF RADIOISOTOPES IN URANIUM MINE TAILINGS

by

Tjoe-Pa Lim

Submitted in partial fulfilment

of the requirements for the degree of

Master of Science in Physics

School of Graduate Studies

Laurentian University

Sudbury, Ontario

## ABSTRACT

The activity ratios of daughter/parent of radioisotope species in groundwater seldom equal 1.0, indicating that isotopic disequilibrium is a common occurrence. The most common expectation of many researchers for the secular disequilibrium parameters is that this activity ratio will be less than 1.0 for parent isotopes with a very long half-life, and daughter isotopes with a very short half-life, since the activity of the daughter isotopes depends on the existence of the parent isotopes.

A review of non-mining related studies shows that activity ratios of the $^{238}U$, $^{232}Th$ and $^{235}U$ decay series could differ greatly between sites, and may or may not show trends among sites. Some extreme values of activity ratios (from less than 1.0 up to 3000 with most higher than 1.0) have been observed. The review of uranium mining related studies indicates less drastic ratio values ranging from 1.0 to 241 with predominant values between 1.0 and 2.0.

The deviation of the activity ratio from the expected theoretical value of less than 1.0 (for normal secular disequilibrium) is called paradoxical secular disequilibrium.

This thesis presents an in-depth study of interactions between liquid and solid media containing members of radioisotope decay chains, in a uranium tailings deposit. Paradoxical secular disequilibrium is seen in many of the activity ratios obtained with ratios depending on the location of the sample in the tailings pile, the nature of the isotopes involved, and the geochemical processes taking place. Laboratory experiments conducted to demonstrate the existence of paradoxical secular disequilibrium using $^{223}Ra$ and $^{224}Ra$ as natural tracers, are also described.

The importance of taking this disequilibrium into account in designing sampling and analysis procedures for systems such as a tailings area is outlined.

## RÉSUMÉ

Les rapports de l'activité du précurseur à celle des descendants pour les radioisotopes des eaux souterraines sont rarement égaux à 1,0, ce qui indique que les déséquilibres isotopiques sont fréquents. Pour les paramètres du déséquilibre séculaire, beaucoup de chercheurs s'attendent à ce que le rapport des activités soit inférieur à 1,0 pour les précurseurs à très longue période et les descendants à très courte période, puisque l'activité des descendants dépend de l'existence de précurseurs.

Un examen des études ne portant pas sur les activités minières montre que les rapports des activités pour les séries de désintégration de $^{238}U$, $^{232}Th$ et $^{235}U$ peuvent varier beaucoup d'un endroit à un autre et qu'il n'y a pas nécessairement de tendances parmi les différents endroits. On a observé des valeurs très divergentes pour ces rapports des activités (depuis moins de 1,0 jusqu'à 3000, mais la plupart du temps plus de 1,0). L'examen des études relatives à des activités minières montre par contre beaucoup moins de divergences (de 1,0 à 241 seulement) et la plupart des valeurs sont entre 1,0 et 2,0.

L'écart entre le rapport des activités et la valeur théorique prévue inférieure à 1,0 (pour le déséquilibre séculaire normal), s'appelle le déséquilibre séculaire paradoxal.

Cette thèse contient une étude détaillée des interactions entre les milieux solides et liquides d'un dépôt de résidus de mine d'uranium contenant des séries isotopiques en désintégration. Le déséquilibre séculaire paradoxal se retrouve dans nombre des rapports des activités obtenus, ceux-ci dépendant de l'endroit où l'on a prélevé l'échantillon dans les résidus, de la nature des isotopes et des processus géochimiques qui se produisent. On décrit les expériences faites au laboratoire pour démontrer l'existence du déséquilibre sécularie paradoxal en utilisant $^{223}Ra$ et $^{224}Ra$ comme traceurs.

Enfin, on décrit l'importance de prendre en considération ce déséquilibre lorsque l'on concort les méthodes d'échantillonnage et d'analyse pour les systèmes comme les dépôts de résidus miniers.

## ACKNOWLEDGEMENTS

The author wishes to thank N.K. Dave, Ph.D (Supervisor), D. Hallman, Ph.D. (Supervisor), K.A. Morin, Ph.D., and R. Tervo, Ph.D. for their technical guidance and moral support during this study.

Special thanks to Mr. A.J. Vivyurka, Senior Environmental Engineer, Rio Algom Ltd., for allowing me the use of data from the Nordic Main Tailings Project, and for all the technical discussions on this project during the last ten years. Also thanks go to Rio Algom Ltd for allowing me to work on their property.

A special thanks to Dr. J. Bland, University of Calgary, Dept. of Physics, for his help and suggestions in the past when developing radium analysis procedures using the alpha-spectroscopy system, and for his technical guidance as the external examiner of this thesis.

A very special acknowledgement, and many thanks to Mrs. Y. Boucher for her assistance in doing radiochemical analyses in the last eight years, and to Mrs. A. Webster for her assistance in searching references and her patience in typing and proofreading this thesis.

My deep appreciation goes to Dr. J.R. Deans and Dr. N.W. Chiu of Monenco Consultants Ltd. for their time and assistance in discussing radioanalytical methods, and also for their patience during the undertaking of analytical work for the radionuclides presented in this thesis.

A special thanks to the tax payers of Canada, especially to CANMET, Elliot Lake Laboratory, for allowing me to continue my education and the use of instrumentation and laboratories while carrying out my duties as Environmental Scientist.

I am very grateful for the assistance of Mr. H. Jurgens, summer student, in doing graphics, cross-section contour mapping, and other computer

programming related duties.

Also special thanks to Miss. C. Neveau, summer student, Ms. A. Eden B.Sc., and Mr. D. Evans, summer student, who helped compile the data for this project.

Most of all I would like to acknowledge my father, Eng-Tjin Lim and my mother Heng-Nio Kwa for their inspiration and efforts to help me fulfill my dream of becoming a scientist, and my wife, Yong Lim, for her understanding, patience and moral support throughout my studies. This thesis would never have materialized without the help and support of these people.

I hope this work will become an inspiration for my children and others so that they can fulfill a dream by working hard and not waiting for something to happen.

## TABLE OF CONTENTS

## LIST OF FIGURES

## LIST OF TABLES

# CHAPTER 1

## INTRODUCTION

The aqueous migration of radioactive elements of various mobilities is commonly studied. This migration produces geochemical plumes that can be detected by measurements of gamma and beta emissions, and alpha-particle counting, and the differential mobilities leading to decay-series disequilibrium within the plumes.

Many studies have been done in the vicinities of the uranium ore deposits and uranium mill tailings. The migration of the radionuclides within the uranium ore deposit reflects their solubility and aqueous behaviour, and the formation of the plumes, having an analog in the contaminant geohydrochemistry of uranium mill tailings.

Uranium mill tailings can represent an extreme example of radioactive deposits in which the ore is fine grained and unconsolidated. The porewater contains strong leaching chemicals, and since most of the uranium has been removed during milling, the decay equilibrium which initially existed within the ore is disturbed (1). The contaminated porewater, which is commonly replenished by infiltration of precipitation and/or mill effluent, often drains downward into underlying groundwater flow systems ((1) in review). Therefore, radionuclide-laden porewater seepage into the ground water provides opportunities for researchers to examine the radionuclide migration and its deviation from decay series equilibrium.

This thesis presents a study of disequilibrium in the decay series of uranium species in the uranium tailings area within the aqueous and solid tailings media. It shows in-depth studies of interactions between aqueous and solid media, which in turn affect the radionuclide equilibrium. A general review of previous studies of isotope disequilibrium in groundwater,

and some detailed reviews on analytical methods are presented to assist in comprehending the framework of this thesis.

# CHAPTER 2

# RADIOISOTOPE DECAY

## 2.1 A QUICK REVIEW OF THE URANIUM DECAY SERIES

All elements found in natural sources with atomic numbers greater than 83 (bismuth) are radioactive. They belong to chains of sucessive decays, and all the species in one such chain constitute a radioactive family or series (3). Three of these families include all the natural activities in this region of the periodic chart. One of them is $_{92}U^{238}$ with a general formula for the approximate mass of 4n+2, where n is an integer. Therefore, the uranium series is also known as the 4n+2 series. Figure 2.1 shows U (with mass 238) as parent substance, and after fourteen transformations (eight of them by α-particle emission, and six by β-particle emission) it reaches a stable end product $_{82}Pb^{206}$ known as Radium B.

The second series is known as the 4n Thorium series with its parent $_{90}Th^{232}$ and a stable end product $_{82}Pb^{208}$ (Figure 2.2). The third series is known as the 4n+3, or actinium series, with $_{92}U^{235}$ as parent and a stable end product $_{82}Pb^{207}$ (Figure 2.3).

Isotopes are referred to an atomic species of the same atomic number, i.e., belonging to the same element, but having a different mass number. For example, a $_{17}Cl^{35}$ nucleus having a mass number of A=35 and an atomic number of Z=17, contains 17 protons and 18 neutrons. The number of protons in a nucleus equals its atomic number Z, and the total number of neutrons and protons (collectively called nucleons) equal its mass number A. Therefore, the neutron number N = A-Z. The difference N-Z or (A-2Z) between the number of neutrons and protons in a nucleus is referred to as its neutron excess or isotopic number. The symbol used to denote a nuclear species is the chemical

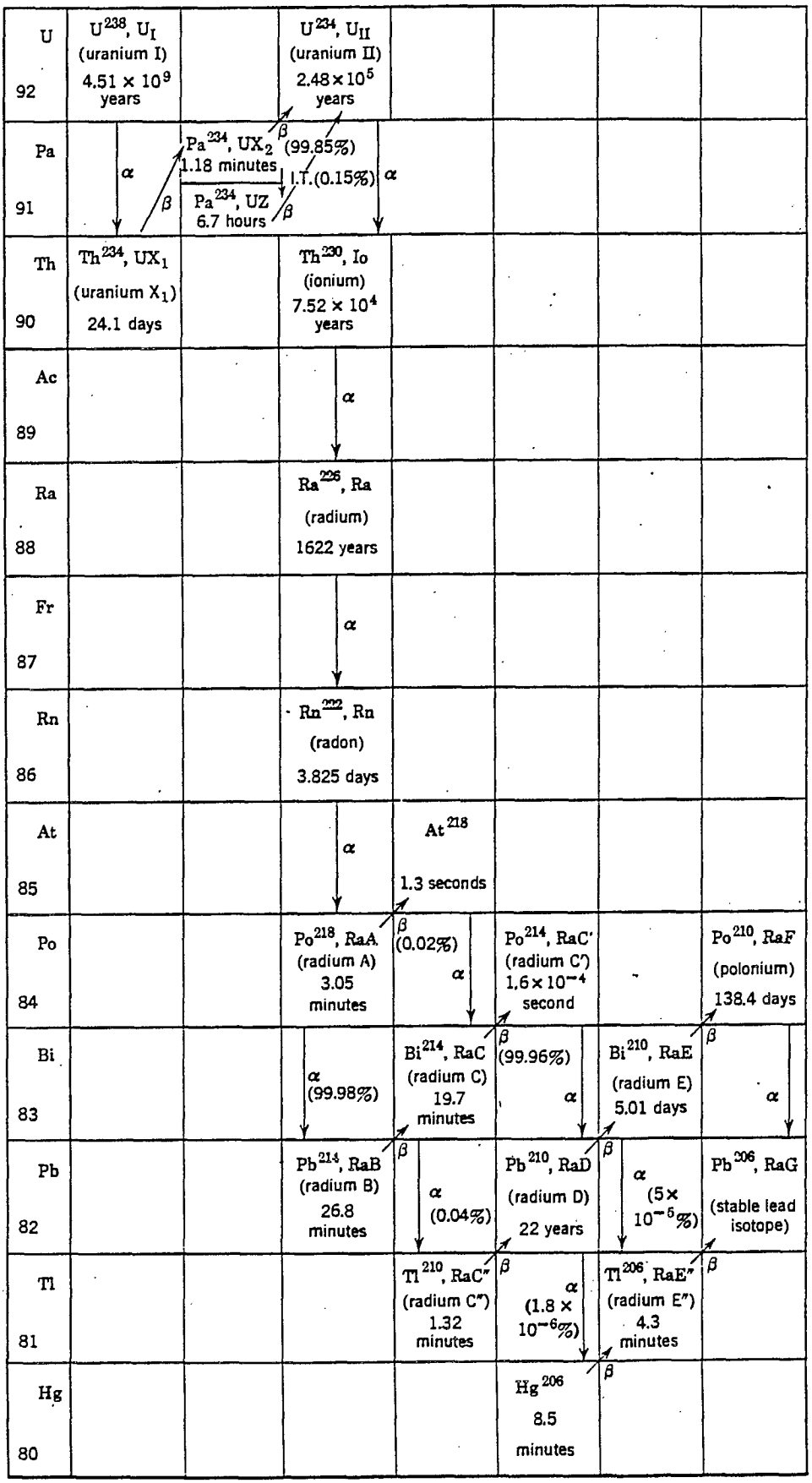


Fig. 2.1 - The uranium (4n+2) series. (From Nuclear and Radiochemistry (3)).

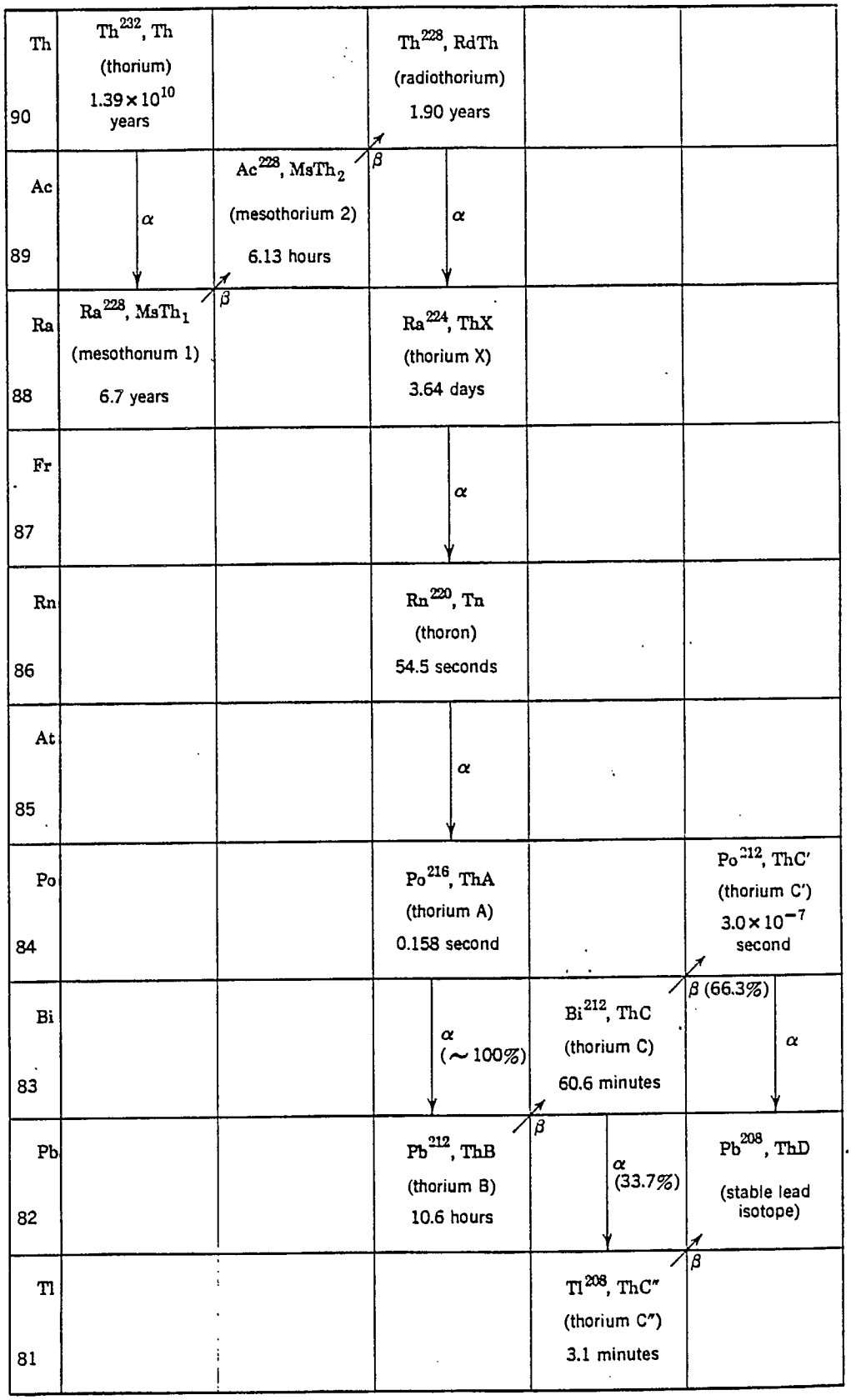


Fig. 2.2 - The thorium (4n) series. (From Nuclear and Radiochemistry (3)).

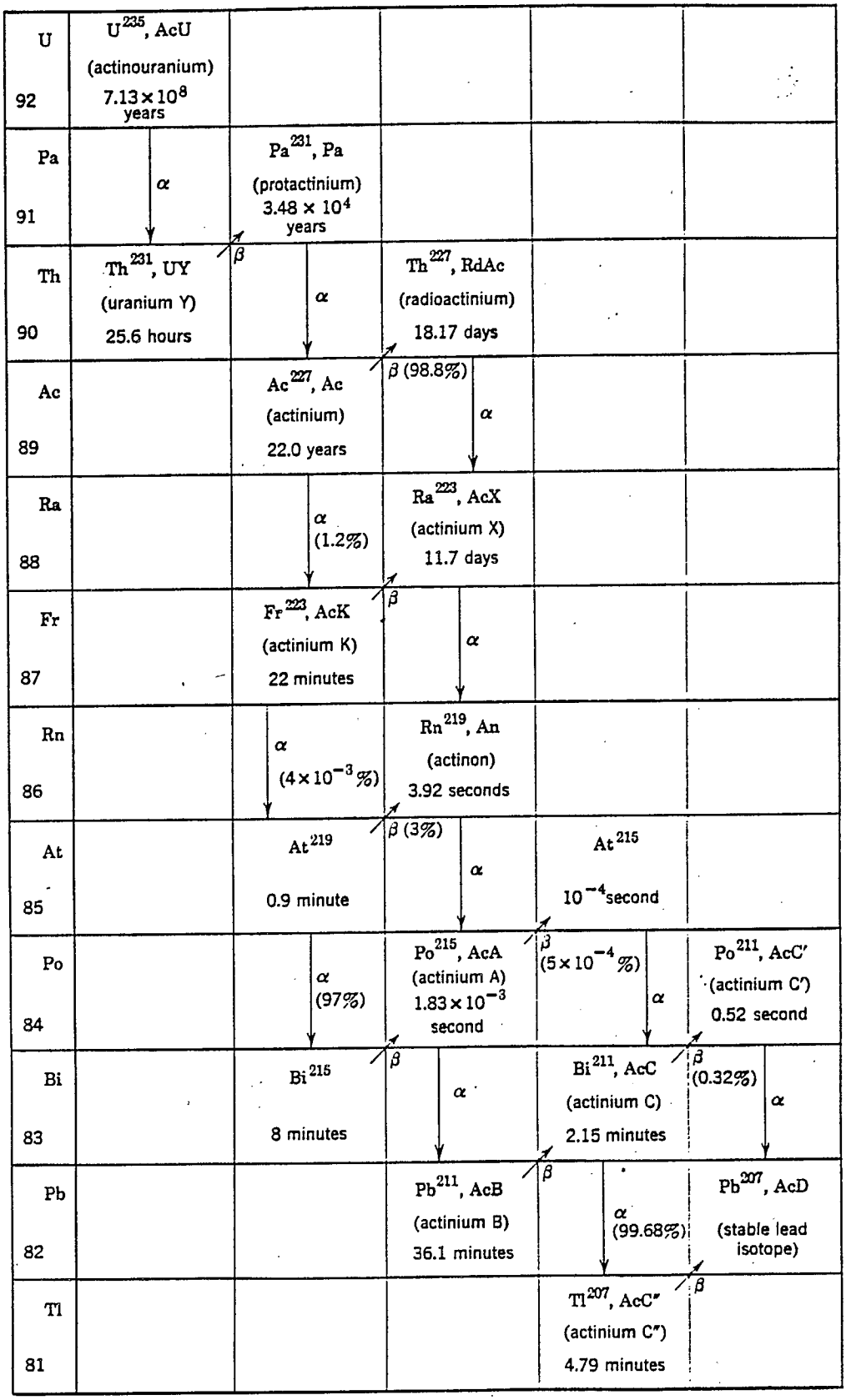


Fig. 2.3 - The actinium (4n+3) series. (From Nuclear and Radiochemistry (3)).

symbol of the element with the atomic number as a left subscript and the mass number as a superscript (in the U.S.A. it is usually written to the right, elsewhere to the left). The atomic number is often omitted because it is uniquely determined by the chemical symbol.

## 2.2 A QUICK REVIEW OF RADIOACTIVE DECAY AND GROWTH

The decay of a radioactive substance follows the exponential law $N=N_0e^{-\lambda t}$, where $N$ is the number of unchanged atoms at time $t$, $N_0$ is the number present when $t=0$, and $\lambda$ is a constant characteristic of the particular radioactive species.

The decay rate, $-dN/dt$, is set proportional to the number of atoms present: $-dN/dt = \lambda N$. On integration the result is $\ell n\ N = -\lambda t+\alpha$, and the constant $\alpha$ is evaluated from the limit $N=N_0$ when $t=0$ : $\alpha=\ell n\ N_0$. Combining these terms we have: $\ell n\ (N/N_0) = -\lambda t$, or $N/N_0 = e^{-\lambda t}$. The characteristic of a radioactive decay may be given in terms of half-life $t_{1/2}$, which is the time required for an initial (large) number of atoms to be reduced to half that number by transformation. Thus, at time $t=t_{1/2}$, $N=N_0/2$ and $\ell n(1/2) = -\lambda t_{1/2}$ or $t_{1/2} = \frac{\ell n\ 2}{\lambda} = \frac{0.69315}{\lambda}$. However, in practical work the number of atoms $N$ is not directly measured. The usual procedure is through indirect methods, such as measurement of its electric, photographic, or other effect, which yield a quantity proportional to its $\lambda N$. The term used for this quantity is 'activity' A, with $A = c\lambda N = c(-dN/dt)$, where $c$ is the coefficient for instrumentation efficiency. Care must be taken to keep the coefficiency factor constant throughout a series of measurements. The decay law can be written as $A=A_0e^{-\lambda t}$ (3), and is commonly used in that form.

### 2.2.1 Secular Equilibrium

In an undisturbed sample containing $N_1$ atoms of a parent isotope, a steady state is established in which the rate of formation of the daughter

isotope $N_2$ is just equal to their rate of decay. This means $-dN_1/dt = \lambda_2 N_2$, in this case because the formation of daughters is the same rate as the decay rate of the parent. Therefore, using the earlier relationship, it can now be expressed as $\lambda_1 N_1 = \lambda_2 N_2$, where $\lambda_1$ and $\lambda_2$ are the respective decay constants. This is sometimes more conveniently expressed as $N_1/(t_{1/2})_1 = N_2/(t_{1/2})_2$. This event is known as **secular equilibrium**. The same relationship, $\lambda_1 N_1 = \lambda_2 N_2 = \lambda_3 N_3$, etc. may be used when several short-lived daughters arise from successive decays beginning from a long-lived parent. However, secular equilibrium only exists under one strict condition, that the material is **undisturbed**, that is, no daughter substances are removed or allowed to escape for a sufficient length of time for secular equilibrium to be established (Figure 2.4).

## 2.2.2 Transient Equilibrium

Let us consider the general equation for the decay of radioactive species $N_1$ and $N_2$, where $N_1$ is the parent isotope and $N_2$ is the daughter. The behaviour of $N_1$ is $-(dN_1/dt) = \lambda_1 N_1$, and $N_1 = N_1^o e^{-\lambda_1 t}$, where $N_1^o$ denotes the value of $N_1$ at time $t=0$. Now the daughter is formed at the rate of $\lambda_1 N_1$, which decays at the rate $\lambda_2 N_2$. Thus:

$$\frac{dN_2}{dt} = \lambda_1 N_1 - \lambda_2 N_2$$

$$\frac{dN_2}{dt} + \lambda_2 N_2 - \lambda_1 N_1^o e^{-\lambda_1 t} = 0 \qquad \text{Eq 1}$$

The solution to this equation may be obtained by standard method and gives:

$$N_2 = \frac{\lambda_1}{\lambda_2 - \lambda_1} N_1^o \left(e^{-\lambda_1 t} - e^{-\lambda_2 t}\right) + N_2^o e^{-\lambda_2 t} \qquad \text{Eq 2}$$

where, $N_2^o$ is the value of $N_2$ at time $t=0$.

In the case where the parent isotope is longer-lived than the daughter ($\lambda_1 < \lambda_2$), after radioactive equilibrium is reached, the ratio of

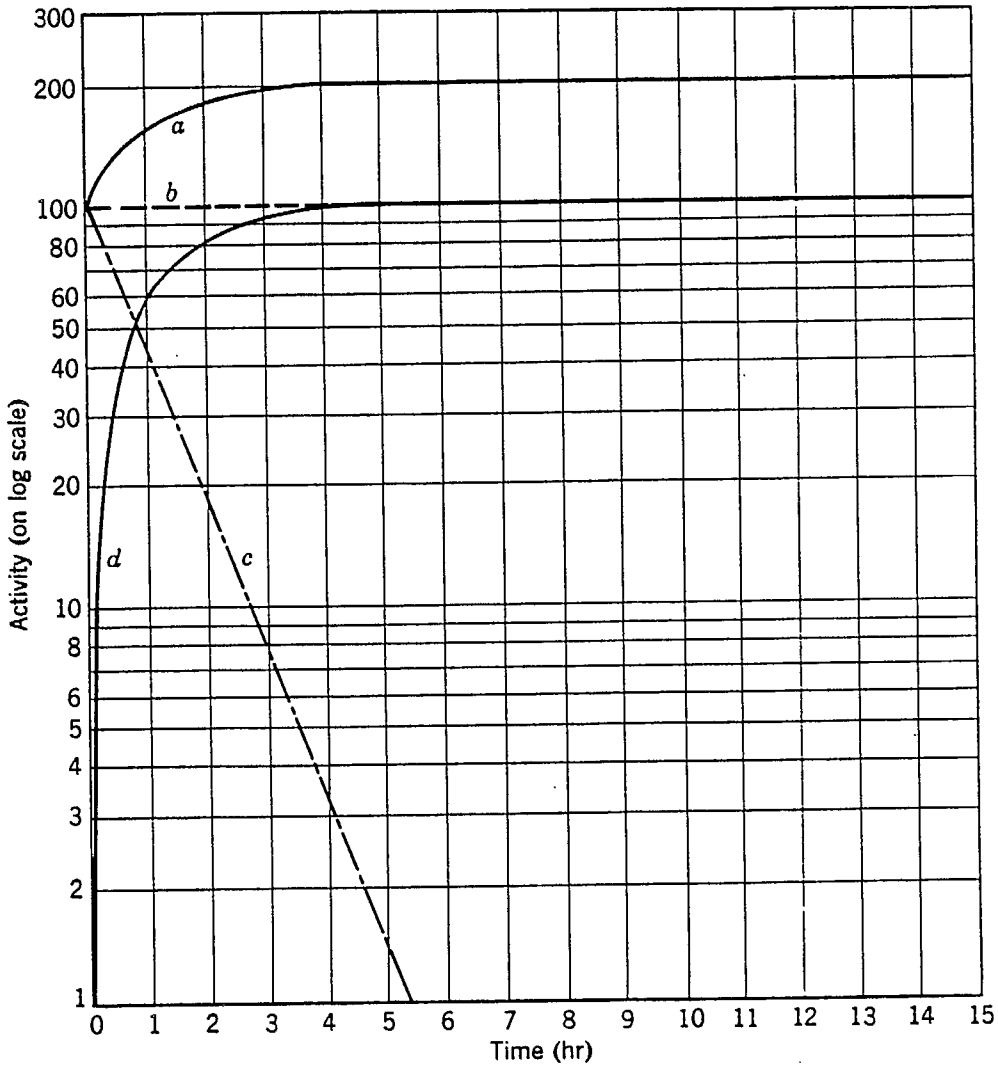


Fig. 2.4 - Secular equilibrium. (From Nuclear and Radiochemistry (3)).

Note: a) total activity of an initially pure parent fraction;
b) activity due to parent ($t_{1/2} = \infty$); this is also the total daughter activity in parent-plus-daughter fractions;
c) decay of freshly isolated daughter fraction ($t_{1/2} = 0.80$ h);
d) daughter activity growing in freshly purified parent fraction.

the number of atoms and the ratio of the integration rates between parent and daughter become constant. From Equation 2 it can be seen that after t becomes sufficiently large, $e^{-\lambda_2 t}$ is negligible in comparison with $e^{-\lambda_1 t}$, and $N_2^o\ e^{-\lambda_2 t}$ also becomes negligible, then:

$$N_2 = \frac{\lambda_1}{\lambda_2-\lambda_1} N_1^o\ e^{\lambda_1 t}$$

and since, $N_1 = N_1^o\ e^{\lambda_1 t}$, then $\frac{N_1}{N_2} = \frac{\lambda_2-\lambda_1}{\lambda_1}$ . Eq 3

The relation between two activities from $A_1 = c_1\lambda_1 N_1$ and $A_2 = c_2\lambda_2 N_2$ is found to be:

$$\frac{A_1}{A_2} = \frac{c_1(\lambda_2-\lambda_1)}{c_2\lambda_2} \qquad \text{Eq 4}$$

In most cases $c_1=c_2$, therefore $A_1/A_2 = 1-(\lambda_1/\lambda_2)$, and may have a value between 0 and 1, depending on the ratio of $\lambda_1$ and $\lambda_2$ (when it is in equilibrium the daughter activity will be greater than the parent activity by a factor of $\lambda_2/(\lambda_2-\lambda_1)$.

In transient equilibrium, the condition is $\lambda_2>\lambda_1$, and the sum of parent and daughter integration rates in an initially pure parent fraction goes through a maximum before transient equilibrium is achieved (Figure 2.5). The general condition for the total measured activity $(A_1+A_2)$ of an initially pure parent fraction to exhibit a maximum is $c_2/c_1>\lambda_1/\lambda_2$. This condition holds regardless of the relative magnitudes of $\lambda_1$ and $\lambda_2$. The condition of:

$$(\lambda_1-\lambda_2)/\lambda_2 \leqslant c_2/c_1 \leqslant \lambda_1/\lambda_2$$

will give a maximum in the total measured activity which occurs at a negative time.

### 2.2.3 The Case of No Equilibrium

If the parent is shorter lived than its daughter $(\lambda_1>\lambda_2)$, it is evident that no equilibrium is achieved at any time. If the parent is made initially free of daughters, then as the parent decays the amount of daughters will rise, pass through a maximum, and eventually decay with the

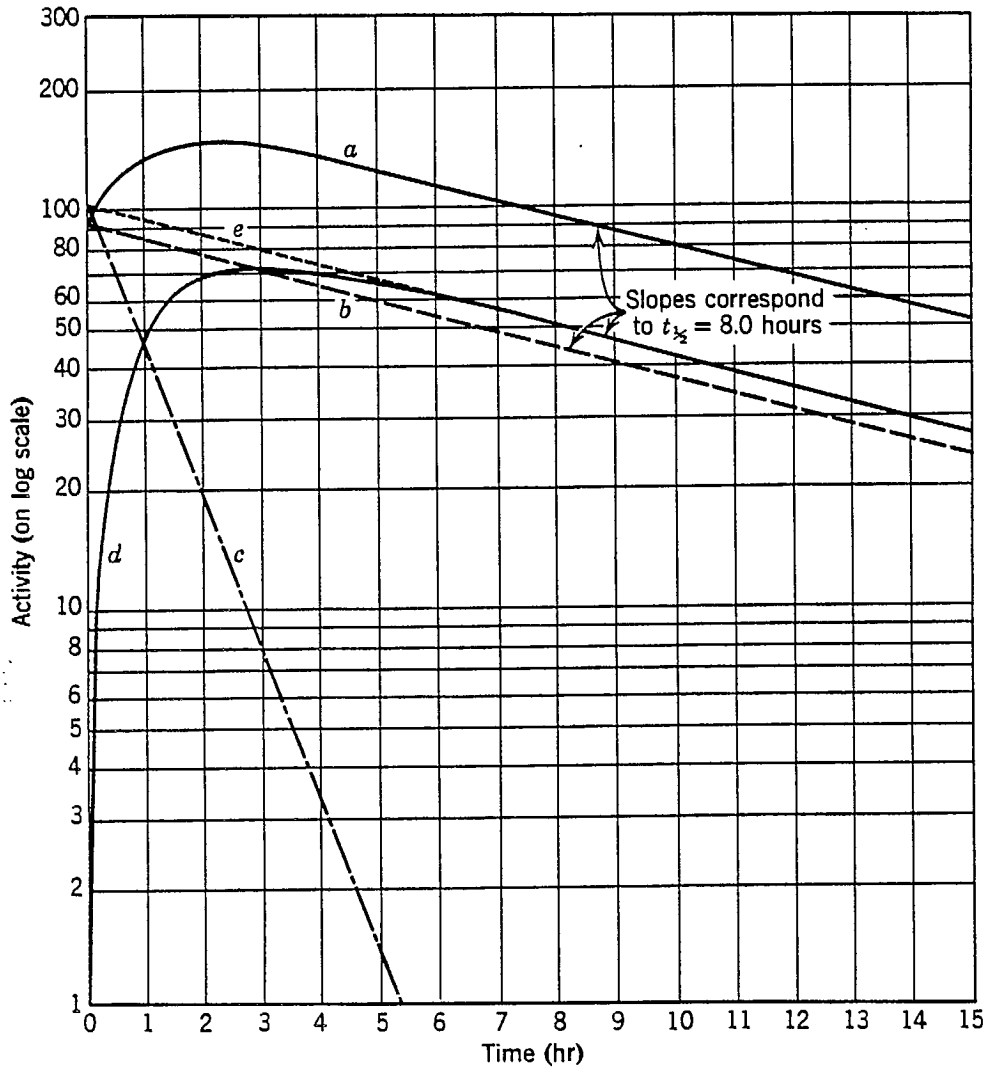


Fig. 2.5 - Transient equilibrium. (From Nuclear and Radiochemistry (3)).

Note: a) total activity of an initially pure parent fraction;
b) activity due to parent ($t_{1/2}$ = 8.0 h);
c) decay of freshly isolated daughter fraction ($t_{1/2}$ = 0.80 h);
d) daughter activity growing in freshly purified parent fraction;
e) total daughter activity in parent-plus-daughter fractions.

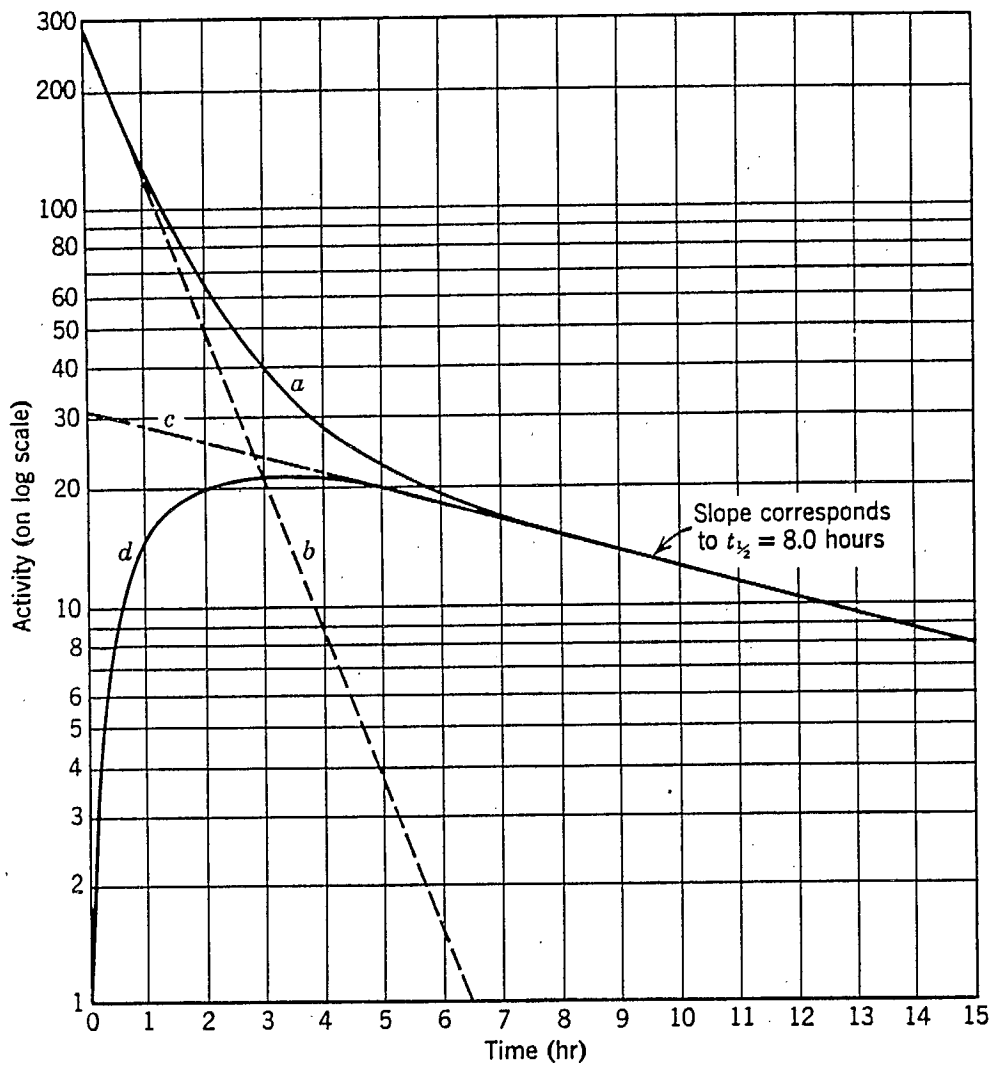


Fig. 2.6 - The case of no equilibrium. (From Nuclear and Radiochemistry (3)).

Note: a) total activity;
b) activity due to parent ($t_{1/2}$ = 0.80 h);
c) extrapolation of final decay curve to time zero;
d) daughter activity in initially pure parent.

characteristic half-life of the daughter (Figure 2.6). The final exponential decay of the daughter is extrapolated back to time $t$=0. This method is useful if $\lambda_1 >> \lambda_2$, when the intercept measures the activity $c_2\lambda_2 N_1^o$. The $N_1^o$ atoms give rise to $N_2$ atoms so early that $N_1^o$ may be set equal to the extrapolated value of $N_2$ at time $t$=0. The ratio of the initial activity, $c_1\lambda_1 N_1^o$, to this extrapolated activity gives the ratio of the half-lives if the relationship between $c_1$ and $c_2$ is known:

$$\frac{c_1\lambda_1 N_1^o}{c_2\lambda_2 N_1^o} = \frac{c_1}{c_2} \times \frac{\lambda_1}{\lambda_2} = \frac{c_1}{c_2} \times \frac{(t_{1/2})_2}{(t_{1/2})_1} \qquad \text{Eq 5}$$

If $\lambda_2$ is not negligible compared to $\lambda_1$, then the ratio $\lambda_1/\lambda_2$ can be replaced by $(\lambda_1-\lambda_2)/\lambda_2$ and the expression involving half-lives changes accordingly.

The transient and no equilibrium cases are often analyzed in terms of time, $t_m$, for the daughter to reach its maximum activity when growing in a freshly separated parent fraction.

By differentiating Equation 2, it was found that:

$$\frac{dN_2}{dt} = -\frac{(\lambda_1)^2}{\lambda_2-\lambda_1} N_1^o e^{-\lambda_1 t} + \frac{\lambda_1\lambda_2}{\lambda_2-\lambda_1} N_1^o e^{-\lambda_2 t}$$

and by setting $dN_2/dt$=0 when $t$=$t_m$, then:

$$\frac{\lambda_2}{\lambda_1} = e^{(\lambda_2-\lambda_1)t_m} \quad \text{or} \quad t_m = \frac{2.303}{\lambda_2-\lambda_1} \log \frac{\lambda_2}{\lambda_1}$$

At this time the daughter decay rate, $\lambda_2 N_2$, is equal to the rate of formation, $\lambda_1 N_1$ (Figures 2.4, 2.5 and 2.6).

It should be noted that time, $t_m$, is infinite for secular equilibrium (3).

### 2.2.4 Many Successive Decays

If we consider a chain of three or more radioactive products, it is clear that the equations already derived for $N_1$ and $N_2$ as functions of time are valid, and $N_3$ may be found by solving the new differential equation:

$$\frac{dN_3}{dt} = \lambda_2 N_2 - \lambda_3 N_3 \qquad \text{Eq 5}$$

This is entirely analogous to the equation for $dN_2/dt$, but the solution calls for more labour, since $N_2$ is a much more complicated function than $N_1$. The next solution for $N_4$ is still more tedious. H. Bateman (3) has given the solution for a chain of $n$ members with the special assumption that at $t$=0 the parent substance alone is present, that is, $N_2^0 = N_3^0 = \cdots N_n^0 = 0$. This solution is:

$$N_n = C_1 e^{-\lambda_1 t} + C_2 e^{-\lambda_2 t} + \cdots C_n e^{-\lambda_n t},$$

$$C_1 = \frac{\lambda_1 \lambda_2 \cdots \lambda_n - 1}{(\lambda_2 - \lambda_1)(\lambda_3 - \lambda_1) \cdots (\lambda_n - \lambda_1)} N_1^0,$$

$$C_2 = \frac{\lambda_1 \lambda_2 \cdots \lambda_n - 1}{(\lambda_1 - \lambda_2)(\lambda_3 - \lambda_2) \cdots (\lambda_n - \lambda_2)} N_1^0. \quad \text{etc.} \qquad \text{Eq 6}$$

If we do require a solution to the more general case with $N_2^0$, $N_3^0 \cdots N_n^0 \neq 0$, we may construct it by adding to the Bateman solution for $N_n$ in an $n$-membered chain, a Bateman solution for $N_n$ in an $(n - 1)$-membered chain with substance 2 as the parent, and, therefore, $N_2 = N_2^0$ at $t$-0, and a Bateman solution for $N_n$ in an $(n - 2)$-membered chain, etc. (3).

2.2.5 Branching Decay

Another variant that is met in general decay schemes is the branching decay, illustrated by:

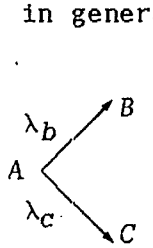


Here the two partial decay constants, $\lambda_b$ and $\lambda_c$, must be considered when the general relations in either branch are studied because, for example, the substance $B$ is formed at the rate $\lambda_b N_A$, but $A$ is consumed at the rate $(\lambda_b + \lambda_c)N_A$. Notice that $A$ can have but one half-life, in this case $t_{1/2} = 0.693/(\lambda_b + \lambda_c)$. By definition the half-life is related to the total rate of disappearance of a substance, regardless of the mechanism by which it disappears.

If the Bateman solution is to be applied to a decay chain containing branching decays, the λ's in the numerators of the equations defining $C_1$, $C_2$, etc., should be replaced by the partial decay constants; that is, $\lambda_i$ in the numerators should be replaced by $\lambda_i^*$, where $\lambda_i^*$ is the decay constant for the transformation of the $i$th chain member to the $(i + 1)$th member. If a decay chain branches, and subsequently the two branches are rejoined as in the natural radioactive series, the two branches are treated by this method as separate chains; the production of a common member beyond the branch point is the sum of the numbers of atoms formed by the two paths (3).

# CHAPTER 3

# PREVIOUS STUDIES OF AQUEOUS DISEQUILIBRIUM

Since there are many papers published on disequilibrium in soil, rock formations and water, only a small selection of typical studies will be reviewed in this thesis.

The natural decay of uranium series are named for the primary parent radionuclides: $^{238}U$, $^{232}Th$ and $^{235}U$. The $^{238}U$-series, which is the usual one examined in the natural environments, begins with $^{238}U$ and ends with the stable isotope $^{206}Pb$. The intermediate radionuclides from $^{238}U$-series usually examined are $^{234}U$, $^{230}Th$, $^{226}Ra$, $^{222}Rn$ and $^{210}Pb$ (Ivanovich et al. (62). The variations in activity ratios between daughter/parent, such as $^{234}U/^{238}U$ and $^{226}Ra/^{230}Th$, along the groundwater flowpath reflect the effects of radioactive decay and its interaction with groundwater and rock formations (over time and distance). An understanding of the decay series (2), and the complex behaviour of radionuclides in groundwater flow systems is necessary to understand the framework of this thesis (Chapter 2).

## 3.1 NON-MINING RELATED STUDIES

In a study of the Floridan Aquifer in northern Florida, Kaufman et al. (12) found that $^{234}U/^{238}U$ activity ratios ranged from 0.5 to 1.2 in uranium concentrations from 0.21 to 3.42 µg/L with an activity ratio less than 1.0 indicating relative depletion of $^{234}U$ in groundwater.

Titayeva et al. (25) studied the disequilibrium of the $^{232}Th$ and the $^{238}U$ series in Polar URAL groundwater. Six $^{234}U/^{238}U$ activity ratios ranging from 0.9 to 1.27, and two $^{230}Th/^{238}U$ values ranging from 0.63 to 1.11 were reported. The mean values for uranium and thorium concentrations were 0.08

and 0.11 µg/L, respectively.

For the $^{232}Th$ series, four values of $^{228}Th/^{232}Th$ ranging from 7.5 to 17.7 were reported. In addition, the activity ratio of $^{232}Th/^{230}Th$ varied from 0.34 to 1.9. Titayeva et al. (25) found that enrichment of the ratio in water (<1) generally corresponded with depleted ratios in rock.

Kronfeld (13) reported sixteen $^{234}U/^{238}U$ activity ratios ranging from 0.92 to 12.25 in a study of groundwater from the Trinity Aquifer in central Texas. Uranium concentrations were between 0.02 and 0.12 µg/L with two extreme concentrations of 1.870 and 15.46 µg/L. Kronfeld attributed the high activity ratios to alpha-recoil ejection from the solid phase uranium into groundwater during the decay of $^{238}U/^{234}Th$, and the subsequent rapid decay of the aqueous $^{234}Th$ ($t_{1/2}$ = 24.1 days) to $^{234}Pa$ ($t_{1/2}$ = 1.2 min) (63).

Surface waters in the recharge area were found to have relatively high uranium concentrations and activity ratios of $^{234}U/^{238}U$ around 1.0 to 2.0.

After tens of kilometers of subsurface flow, uranium concentrations were relatively low, and activity ratios rose from 5 to 12, and there appeared to be a trend of increasing activity ratios with greater distance.

Osmond and Cowart (22) described a scenario in the Carrizo Sandstone of southern Texas similar to Kronfeld's study.

Groundwater near a recharge outcrop had $^{234}U/^{238}U$ activity ratios less than 1.0, and uranium the concentration of approximately 1.0 ppb. The ratio rose to about 9.0, and the concentration decreased to about 0.01 ppb after flowing downdip for approximately 15 km. These trends were attributed to α-recoil (63), and the transition from relatively oxidizing to reducing conditions, respectively. Further downdip, the activity ratio decreased to about 2.0. This decrease was attributed to geochemical effects rather than decay effects. Frohlich et al. (8) simulated the differential behaviour of the two uranium isotopes at this site through sorption processes.

In Texas, Cowart (6) studied variations of $^{234}U/^{238}U$ activity ratios in the Edward Carbonate Aquifer. From the recharge area, and along tens of kilometers of flowpath, the activity ratio remained in the range 1.07 to 1.22 with uranium concentrations of 0.662 to 0.820 µg/L. Parallel to the flowpath, a portion of the aquifer containing slower-moving, higher TDS (Total Dissolved Solids) groundwater, had activity ratios of 1.62 to 2.66, and uranium concentrations of 0.046 to 0.101 µg/L. The mixing zone of the two waters had an anomalous uranium concentration of 0.071 to 4.59 µg/L, and the activity ratio ranged from 0.79 to 1.40 which Cowart attributed to changes in location of the redox boundary rather than simple mixing of the oxidized and reduced groundwater.

Laul et al. (14) studied the Palo Duro Basin groundwater (Texas) and reported radionuclide analyses of $^{238}U$ and $^{232}Th$ series in two brines.

The values for $^{238}U$ activity ratios were:

$$^{234}Th/^{238}U = 25\text{-}50$$
$$^{234}U/^{234}Th = 0.025 \text{ to } 0.050$$
$$^{234}U/^{238}U = 1.1 \text{ to } 1.3$$
$$^{230}Th/^{234}U = 0.19 \text{ to } 1.11$$
$$^{226}Ra/^{230}Th = 2.0 \times 10^4 - 3.0 \times 10^4$$
$$^{222}Rn/^{226}Ra = 0.8 \text{ to } 2.4$$

The activity ratios for $^{232}Th$ series were:

$$^{228}Ra/^{232}Th = 800 \text{ to } 2040$$
$$^{228}Th/^{228}Ra = 0.009 \text{ to } 0.010$$
$$^{228}Th/^{232}Th = 7 \text{ to } 23$$
$$^{224}Ra/^{228}Th = 90 \text{ to } 100$$
$$^{224}Ra/^{228}Ra = 0.9 \text{ to } 1.0$$

Cowart (5) examined the $^{234}U/^{238}U$ activity ratio and $^{226}Ra$ activities in groundwater in the Cambrian/Ordovician aquifers in the Tri-State region (Missouri, Kansas and Oklahoma) of the U.S.A. In the aquifer's calcium carbonate water, the usual ratio is around 7 to 10, and uranium concentrations around 0.3 to 0.5 µg/L. The flow is westward, and eventually

mixes with sodium chloride, $H_2S$-bearing (more reducing) groundwater. Within the mixing zone, $^{226}Ra$ increases from around 0.5 Bq/L up to 0.32 Bq/L, uranium precipitates from 0.02 to 0.04 µg/L, and notably, uranium activity ratios remain essentially constant.

Although the decrease in uranium concentration is consistent with reduction in Eh (redox potential), Cowart could only speculate on explanations for a steady uranium ratio and an increase in $^{226}Ra$. If the uranium concentrations reported as pCi/L in Cowart's Table II (5) essentially represent $^{238}U$, then the calculated values for the $^{226}Ra/^{234}U$ ratio increase from 0.5 to about 1.5, and there is a sharp increase of 6 to 236 in the mixing zone. Under the assumption made for the calculation, this trend indicates that there is a relatively strong aqueous enrichment of $^{226}Ra$ over $^{234}U$ during mixing, probably synonymous with the parallel decrease in uranium concentration.

CBCL Limited (58) carried out a detailed study of a small, post glacial, uraniferous peat deposit at the base of a granitic talus slope near Portland Creek, Newfoundland. Piezometer nests were installed in a line perpendicular to the talus slope. The groundwater in the peat was low TDS, calcium-sodium-bicarbonate water with a pH constant near 6. Uranium decreased with distance from the slope by a factor of 1.7 from 415 µg/L. Many ratio values for the $^{238}U$ series have been calculated and are shown here (Table B-5 (58)).

The values for $^{238}U$ activity ratios were:

$$^{234}U/^{238}U = 1.2 \text{ to } 1.04$$
$$^{230}Th/^{234}U = 2.73 \times 10^{-3} \text{ to } 3.52 \times 10^{-2}$$
$$^{226}Ra/^{230}Th = >1.4 \text{ to } 0.38$$
$$^{210}Pb/^{226}Ra = 10.15 \text{ to } 26.74$$
$$^{210}Po/^{210}Pb = 0.50 \text{ to } 0.64$$

The significant variations in $^{230}Th/^{234}U$ and $^{210}Pb/^{226}Ra$ may be the result of an increase in the activity of $^{230}Th$. The relatively high values

for $^{210}Pb/^{226}Ra$ suggest the accumulation of $^{222}Rn$ gas in the past.

The activity ratio of $^{234}U/^{238}U$ in the uraniferous peat samples varied from 0.92 to 1.26, averaging 1.13. The $^{234}U$ tends to be more soluble than $^{238}U$ because of the ejection of the $^{234}U$ daughter from the uranium bearing mineral by the effect of mass recoil when $^{238}U$ decays. When the uranium derived from the mineralized source is subsequently precipitated it will retain the same elevated $^{234}U/^{238}U$ ratio. Being a recent deposit (i.e., less than 10,000 to 15,000 years old), little time has been available for the ingrowth of radionuclide daughter products of uranium. The deposition of uranium with the peat deposit is considered to be an on-going process.

The activity ratios from the above papers are summarized in Table 3.1. The most obvious observation is that activity ratios spanning a natural decay series are not usually examined along the groundwater flowpath. Nevertheless, the available data indicate that a high degree of variability exists between sites and significant changes in ratio can occur along a flowpath at a site. This variability reflects the numerous processes affecting the migration of radionuclides in groundwater (1).

## 3.2 URANIUM MINING RELATED STUDIES

Because of the potential of near-surface contamination from uranium tailings impoundments, several detailed studies have been undertaken near the impoundments. There are several studies of major ion chemistry and total concentrations in the vicinity of uranium tailings. However, only a few provide a number of ratios along a flowpath, and most only report $^{226}Ra$ activities as it is considered the most toxic component in the tailings seepage.

Cherry et al. (4) reviewed several uranium tailings sites and listed chemical analyses for tailings porewater, or pond water, at three sites in

Wyoming, U.S.A. and one site in Canada. At the four sites, tailings water pH was limited to 1.8 to 2.7; TDS ranged from 12,200 to 18,000 mg/L; and major ion composition could generally be described as predominantly iron, hydrogen and sulphate. If the reported 'U=nat. (mg/L)' is assumed to essentially represent $^{238}U$, then calculated $^{230}Th/^{234}U$ ratios are 12.29 and 23.46 for two Wyoming sites, and 0.01 for the Ontario site (the Nordic Main Impoundment will be discussed later in this thesis). The Wyoming values generally agree with the ratios calculated from 'typical concentrations in tailings solutions' (Table 1a of reference 23): 1.00 for $^{230}Th/^{238}U$, and 27.78 for $^{230}Th/^{234}U$. Based on available activities, two $^{226}Ra/^{230}Th$ ratios for Wyoming sites are 0.011 and 0.058, which are over an order of magnitude higher than Taylor's typical ratio of 0.0027, and the Nordic Main site in Ontario provides a ratio of 7.37. The differences in ratios in the upper portion of the $^{238}U$ series between the Wyoming sites and the Nordic Main site can mostly be attributed to four orders of magnitude higher $^{230}Th$ activities at the Wyoming sites. The three available $^{210}Pb/^{226}Ra$ ratios in Wyoming are 0.17, 0.57, and 14.57. Taylor's typical ratio is 1.00, and the Nordic Main ratio is 12.14.

Because of the variability in ore characteristics passing through a mill, the variability in mill processing, and the physical and chemical variabilities produced during and after discharging a slurry to an impoundment, the activity ratio can be expected to vary with lateral and vertical distance in an impoundment.

Moffett and Tellier (15) who examined the Nordic West Arm tailings adjacent to the Nordic Main Impoundment, classified one 'high acid' and two 'low acid' lateral regions within the tailings pile. The high acid region displays no definite trends along its length, and assuming that the total uranium represents $^{238}U$, then the $^{230}Th/^{238}U$ activity ratio was 4 to 22. The

$^{226}Ra/^{232}Th$ ratio was around 5.8 x $10^{-4}$ to 1.7 x $10^{-3}$, and the $^{210}Pb/^{226}Ra$ ratio varied strongly from 2.05 to 240.88. For the $^{232}Th$ series, the $^{228}Th/^{232}Th$ activity ratio was around 0.36 to 2.00, and the $^{227}Th$ interference was noted for some analyses. For comparison of the magnitude of the two thorium series, the $^{228}Th/^{230}Th$ rate was around 0.031 to 0.27.

Highland et al. (10) examined the chemical composition of 'tailings liquor' from one of the Wyoming ponds mentioned previously and the average groundwater from a point approximately 1 km down gradient from the pond. From their data, pH increases from 1.9 in the pond to 6.2 in the distant groundwater. TDS decreases from 15,000 to 1,820 mg/L, $^{230}Th/^{238}U$ decreases from 1.28 to 0.012, and $^{210}Pb/^{226}Ra$ decreases from 14.27 to 0.79. The change in ratios is caused by the significant decrease in the activities of radionuclides, particularly a nearly three orders of magnitude decrease in $^{230}Th$. Hoffman and Playton (11) examined another Wyoming tailings site. The chemical data suggests an intermediate point in the above 'flowpath' of Highland et al. (10): pH = 3.6 to 3.7; TDS 15,984 to 17,970 mg/L; $^{226}Ra/^{230}Th$ = 0.001 to 0.098; $^{210}Pb/^{226}Ra$ - 8.41 to 8.73; and $^{210}Po/^{210}Pb$ = 0.0 to 0.33.

Taylor and Antommaria (24), Taylor (23) and Haji-Djafari and Antommaria (9), describe a Wyoming tailings area which is sufficiently instrumented to describe a four point flowpath:

| Distance from Piezometer | Tailings (m) | pH | TDS (mg/L) |
|---|---|---|---|
| Tailings pond | 0 | 1.95 | 11810 |
| WM-6S | 0 | 3.00 | 4274 |
| WN-14H | 390 | 5.50 | 4042 |
| WN-1HDA | 1070 | 7.25 | 1395 |

The corresponding activity ratios are listed in Table 3.2, and good trends are apparent for decreasing $^{230}Th/^{238}U$, generally constant $^{226}Ra/^{230}Th$, and decreasing $^{210}Po/^{226}Ra$. The sharpest change in ratios occurs between WN-6S and WN-14H where pH increases from 3.00 to 5.50.

Veska studied groundwater seepage emanating from a uranium-mine waste rock pile near Bancroft, Ontario. A set of piezometers were chosen from Veska's Appendix 5.12 (26) to depict general trends. The chosen piezometers are:

| Piezometer | Source Distance (m) | pH | Elec. Cond. (μS/cm) |
|---|---|---|---|
| L | 0 | 3.7 | 900 |
| GR4 | 9 | 4.6 | 400 |
| GR6 | 12 | 5.0 | 304 |
| M3-4.76 | 20 | 6.0 | 442 |
| M4-8.83 | 30 | 6.2 | 305 |
| M5-11.00 | 39 | 6.5 | 320 |
| M6-14.00 | 47 | 6.8 | 320 |
| M7-15.17 | 56 | 7.5 | 290 |
| M8-14.59 | 76 | 7.6 | 300 |
| M9-15.25 | 94 | 7.6 | 320 |

Variations in activity ratios show trends of increasing $^{234}U/^{238}U$, decreasing $^{226}Ra/^{234}U$, and initially decreasing then increasing $^{210}Pb/^{226}Ra$, Table 3.2. Sharp changes in $^{226}Ra/^{234}U$ can be attributed to the factor of five decreases in $^{226}Ra$. The sharp rise in $^{234}U/^{238}U$ between GR6 and M3, and the continued trend of relative $^{234}U$ enrichment were attributed to a scenario requiring preferential leaching of $^{234}U$ from the waste rock in the 6+ oxidation state ($UO_2^{2+}$), stronger adsorption of $^{238}U$ (as $U^{4+}$) over $^{234}U$ (as $UO_2^{2+}$) in the sand aquifer, and little redox exchange between the 4+ and 6+ states (26).

Table 3.2 summarizes the activity ratios reviewed in this section. Based on the limited data for $^{234}U/^{238}U$, there is near equilibrium (0.86 to 2.07) in tailings water unlike that generally noted in Table 3.1. The $^{234}U/^{238}U$ ratios of Veska (26) show a trend of increasing value along the flow path. Below $^{234}U$ in the $^{238}U$-series, notable disequilibrium occurs, but general trends can be seen. Ratios for $^{230}Th/^{238}U$ are typically greater than 4 in tailings, but decrease to less than 0.1 in the flow path. The $^{226}Ra/^{230}Th$ ratios are variable and usually less than 0.13. The ratio of $^{226}Ra/^{234}U$ spans a wider range and data of Veska (26) indicates the ratio decreases along the flow path. The $^{210}Pb/^{226}Ra$ and $^{210}Po/^{226}Ra$ ratios are variable, but appear to be somewhat less than 1 in most groundwater seepage. There are insufficient data to evaluate the lowest portion of the $^{238}U$ series. Furthermore, no data could be located on variations in ratios along flow paths for the $^{232}Th$ and $^{235}U$ series.

## 3.3 HYDROGEOCHEMISTRY, NORDIC MAIN TAILINGS, ONTARIO. FIELD STUDY OF RADIOISOTOPE DISEQUILIBRIUM IN THE SEEPAGE AREA.

In studies of groundwater seepage from the Nordic Main tailings, near Elliot Lake, Ontario, Morin (16) identified four seepage areas around the impoundment perimeter. The major seepage area, seepage area 'A', was studied from 1979 to 1984. In particular, Morin et al. examined the effect of the various processes of sorption, mineral precipitation-dissolution, coprecipitation, aqueous speciation, and decay of radionuclide migration in area 'A'. The seepage plume is located just beneath the water table at a general depth of 1-2 metres. For simplicity of discussion, one piezometer in each nest was selected to represent the centre of the plume and the flowpath that passes through each of these piezometers is called the 'centreline' of the plume. Morin also recognized that a high degree of analytical error is

expected when dealing with the measurement of relatively low radionuclide activities in high TDS and geochemically reactive water. The study was concentrated mostly along a groundwater flowpath of 20.8 m. Because the groundwater requires approximately 24 days to travel this length of flowpath, the observed variations during one sampling event are predominantly the result of relatively fast geochemical and radioisotope decay processes and are not closely related to temporal variations in the radioactive source (the solid tailings), which can account for variations along flowpaths in slow moving groundwater systems. However, fluctuation in annually measured values at each piezometer can reflect temporal source fluctuations. The $^{234}U/^{238}U$ ratio, for example, increases from 1.23 to 3.92, and $^{227}Th/^{227}Ac$ decreases from 1.88 to 1.26 along the flowpath. Also isotopes of an element display different aqueous behaviour, which is dependent on the relative contribution of the isotope to the total element concentration in the molal bases. For example, $^{230}Th$ steadily decreases along the flowpath from 1370 to <19 mBq/L, whereas $^{228}Th$ initially increases from 130 to 190 mBq/L then decreases to <19 mBq/L. The variations in radionuclide activity ratios along groundwater flowpaths are controlled by the particular set of geochemical and decay mechanisms that regulate each isotope of each element (Morin et al.)(1).

## 3.4 SUMMARY

In general, most of the authors observed similar disequilibrium occurrences, decrease or increase of ratios between daughters and their parent isotopes with distance from the source. However, the explanation of the disequilibrium mechanism itself was not very satisfactory.

Titayeva et al. (25) found that enrichment of ratios in water (values greater than 1) generally corresponded with depleted ratios in rock.

Kronfield (13) found that activity ratios rose to 5-12, and there

appeared to be a trend of increasing activity ratio with further distance. The uranium concentrations were relatively low after tens of kilometres of subsurface flow. Kronfield also attributed the high ratios to alpha-recoil ejection from solid phase uranium into groundwater.

Osmond and Cowart (22) attributed the disequilibrium to geochemical effects rather than decay effects.

Cowart (6) attributed the disequilibrium to changes in the location of the redox boundary rather than simple mixing of oxidized and reduced groundwater.

CBCL Ltd. (58) made an interesting observation on the uraniferous peat sample, in which the activity ratio of $^{234}U/^{238}U$ averaged 1.13. The explanation by CBCL Ltd. was that $^{234}U$ tends to be more soluble than $^{238}U$ due to the ejection of the $^{234}U$ daughter from the uranium bearing mineral by the effect of mass recoil when $^{238}U$ decays. When the uranium derived from the mineralized source is subsequently precipitated it will retain the same elevated $^{234}U/^{238}U$ ratios. The deposition of the uranium with the peat deposit is considered to be an on-going process. Being a recent deposit (i.e., less than 10,000 years old) little time has been available for the ingrowth of radionuclide daughter products of uranium.

Similar relations were found on studying disequilibrium related to uranium mining activities, where the ratios could increase or decrease with distance away from the source (1,19-21). Morin examined the effect of the various processes of sorption, mineral precipitation-dissolution, aqueous speciation and decay on radionuclide migration. This type of pathway analysis study was probably the best approach towards a more reasonable explanation of disequilibrium mechanism.

Taylor (23) listed typical ratios of 1.0 for $^{210}Bi/^{210}Pb$ and $^{210}Po/^{210}Bi$, indicating that rapidly attained equilibrium is often expected

because of short half-lives in this portion of the series. This is an important statement and will be discussed further elsewhere in this thesis, especially in dealing with sampling, sample treatment, timing and analytical procedures.

Veska (26) found that the sharp rise in $^{234}U/^{238}U$, and the continued trend of relative $^{234}U$ enrichment were attributed to a scenario requiring preferential leaching of $^{234}U$ from the waste rock in the 6+ oxidation state ($UO_2^{2+}$), stronger adsorption of $^{238}U$ (as $U^{4+}$), over $^{234}U$ (as $UO_2^{2+}$) in the sand aquifer, and little redox exchange between the 4+ and 6+ states (26). The validity of this explanation was tested with the aid of the cell model, in which a solution spiked with $^{238}U(IV)$, $^{238}U(VI)$, $^{232}Th(IV)$, $^{226}Ra(II)$ and $^{210}Pb(II)$ was added by increments to the groundwater solution.

It is possible that during the decay chain from $^{238}U$ to $^{234}U$, the uranium isotopes lost 2 of their electrons. As an atom progressively decays through a decay series, its chemoelectrical properties, including valence, vary. However, for example, the upper portion of the $^{238}U$ decay series indicates the following transitions for a $^{238}U$ atom: $^{238}U^{4+,5+or6+} \rightarrow {}^{234}Th^{4+} \rightarrow {}^{234}Pa^{5+} \rightarrow {}^{234}U^{4+,5+or6+} \rightarrow {}^{230}Th^{4+} \rightarrow {}^{226}Ra^{2+}$ (Morin) (27). Therefore, as was shown by Morin, $^{238}U$ or $^{234}U$ could exist as (IV), (V) or (VI) valence and the reasoning as described by Veska as preferential leaching could be misleading and misconstrue the real cause of disequilibrium mechanisms in the field.

In addition, it does not appear feasible to practically detect preferential leaching, as described by Veska, in the groundwater sample itself, without the higher concentration of a standard spiked solution. However, Veska's experiment to solve the mystery of disequilibrium was interesting and it demonstrated the level of difficulties involved in solving these complex problems.

TABLE 3.1

Summary of activity ratios at non-mining-related sites (From Morin and Cherry (1)).

$^{238}U$ DECAY SERIES

| Site | Place in flow sys. | $\frac{^{234}Th}{^{238}U}$ | $\frac{^{234}U}{^{238}U}$ | $\frac{^{230}Th}{^{234}U}$ | $\frac{^{226}Ra}{^{234}U}$ | $\frac{^{226}Ra}{^{230}Th}$ | OTHER |
|---|---|---|---|---|---|---|---|
| Floridan Aq | gen* | | 0.5-1.2 | | | | |
| Polar Ural | gen | | 0.9-1.27 | 0.90,0.56 | | | |
| Trinity Aq | recharge | | 1-2 | | | | |
| | 10's of km | | 5-12 | | | | |
| Carrizo Sdst | recharge | | <1.0 | | | | |
| | 15 km | | 9 approx. | | | | |
| | >15 km | | 2 approx | | | | |
| Edwards Aq | gen, oxid | | 1.07-1.22 | | | | |
| | gen, red | | 1.62-2.66 | | | | |
| | gen, mixed | | 0.79-1.40 | | | | $\frac{^{222}Rn}{^{226}Ra}$ |
| Palo Duro Bas | gen | 25-50 | 1.1-1.3 | 0.19-1.11 | | $2-3x10^4$ | 0.8-2.4 |
| Tri-St. Reg | unmixed | | 7-10 | | 0.5-1.5 | | |
| | mixed | | 7-10 | | 6-236 | | $\frac{^{210}Pb}{^{226}Ra}$ $\frac{^{210}Po}{^{210}Pb}$ |
| Newfoundland | begin. | | 1.20 | 0.00273 | | >1.4 | 10.15 0.50 |
| | 135 m | | 1.04 | 0.0352 | | 0.38 | 26.74 0.64 |

(* gen = general, no clear flowpath)

$^{232}Th$ DECAY SERIES

| Site | $\frac{^{228}Ra}{^{232}Th}$ | $\frac{^{228}Th}{^{232}Th}$ | $\frac{^{224}Ra}{^{228}Th}$ |
|---|---|---|---|
| Polar Ural | | 7.5-17.7 | |
| Palo Duro Bas | 800-2040 | 7-23 | 90-100 |

$^{235}U$ DECAY SERIES

| Site | $\frac{^{231}Pa}{^{235}U}$ |
|---|---|
| Newfoundland | <0.04 |

TABLE 3.2

Summary of activity ratios at uranium-mining-related sites (From Morin and Cherry (1)).

| Ref.-Location | $\frac{^{234}U}{^{238}U}$ | $\frac{^{230}Th}{^{238}U}$ | $\frac{^{226}Ra}{^{230}Th}$ | $\frac{^{226}Ra}{^{234}U}$ | $\frac{^{210}Pb}{^{226}Ra}$ | OTHER | |
|---|---|---|---|---|---|---|---|
| Cherry et al. (1982) | | | | | | | |
| Wyo. tailings | | 12.29–23.46* | 0.011–0.058 | | 0.17,0.57; 14.57 | $\frac{^{210}Bi}{^{210}Pb}$ | $\frac{^{210}Po}{^{210}Bi}$ |
| Nordic Main | | 0.01* | 7.37 | | 12.14 | | |
| "Typical" | 1.00 | 27.78 | 0.0027 | | 1.00 | 1.00 | 1.00 |
| Moffett & Tellier (1978) | | | | | | | |
| High-acid | | 4–22* | 0.00058–0.0017 | | 2.05–240.88 | | |
| Low-acid | | | | | 0.25–0.60 | | |
| Highland et al. (1981) | | | | | | $\frac{^{210}Po}{^{210}Pb}$ | |
| Tailings | | 12.29 | 0.012 | | 14.27 | | |
| "Intermed. data" | | 4.09* | 0.001–0.098 | | 8.41–8.73 | 0–0.33 | |
| Average groundwater | | 0.076 | 1.28 | | 0.79 | | |
| Taylor (1980) | | | | | | $\frac{^{210}Po}{^{226}Ra}$ | |
| Tailings | | 11.73* | 0.115 | | | 0.196 | |
| WN-6S | | 3.73* | 0.116 | | | 0.015 | |
| WN-14H | | 0.034* | 0.0031 | | | 0.0 | |
| WN-1HDA | | 0.068* | 0.125 | | | 0.0 | |
| Veska (1983) | | | | | | | |
| L | 0.97 | | | 0.33 | 1.15 | | |
| GR4 | 0.87 | | | 1.63 | 0.05 | | |
| GR6 | 0.86 | | | 1.23 | 0.27 | | |
| M3 | 1.20 | | | 0.35 | 0.66 | | |
| M4 | 1.28 | | | 0.15 | <0.45 | | |
| M5 | 1.27 | | | 0.05 | <1.00 | | |
| M6 | 1.57 | | | 0.08 | <0.38 | | |
| M7 | 1.75 | | | 0.10 | <0.61 | | |
| M8 | 1.88 | | | 0.10 | <0.67 | | |
| M9 | 2.07 | | | <0.65 | – | | |

* = $^{238}U$ calculated from total uranium

# CHAPTER 4

# STUDY OF NORDIC MAIN TAILINGS

In Canada alone there are approximately 120 million tonnes of uranium tailings spread over an area of approximately 635 hectares. It is expected that by the time the present uranium ore reserves are mined there will be about 1 billion tonnes of uranium tailings which will require proper management technology, **without much human involvement, in limiting the release of contaminants to the environment.**

Hydrogeochemical investigations of the Nordic Main Tailings area have been on-going since 1978. Radioisotope and chemical profile studies of solid and liquid phases have been conducted on various sites.

Some studies have also focused on the identification and quantification of the routes of radionuclide escape from the tailings and their entry into the biosphere. However, in this thesis, only a part of the tailings studies related to the disequilibrium of radioisotopes will be discussed.

## 4.1 FIELD STUDY STRATEGY

The first phase of an investigation of the chemical composition (including radioisotopes) of subsurface water and the hydrochemical processes in and near the abandoned Nordic tailings at Elliot Lake, Ontario, was conducted in 1979. The study had three components which included:

1. Monitoring of the groundwater flow and the chemical composition of water in the tailings;
2. Monitoring the flow pattern and chemical composition of groundwater in the sandy aquifer adjacent to the tailings embankment; and

3. Development of a hydrogeological and hydrochemical framework to account for the observed chemical profiles in the tailings and the contaminant distribution in the aquifer (28-30).

Most of the groundwater research was carried out through team work between the University of Waterloo, Rio Algom Ltd., and the Mining Research Laboratory, Elliot Lake, Canada Centre for Mineral and Energy Technology (CANMET), Energy, Mines and Resources Canada.

However, since solid tailings and porewater exist together, the chemical and radioisotope distribution profile of the solid tailings was also determined in a supplementary study to the groundwater research (31-32).

## 4.2 MINING HISTORY AND TAILINGS DEPOSITION

The Nordic Mine is one of ten present and past uranium mining and milling operations in the Elliot Lake area, Figure 4.1. It was in continuous production from 1957 up to its closure in 1968. The mine was operated with a milling capacity ranging from 2,500 tones to 3,300 tonnes per day, and milled a total of 12,300,000 tonnes of ore before closure (Robertson (33)).

The uranium ore is a quartz pebble conglomerate containing 5-15% pyrite. The principal ore minerals are uraninite (pitchblende), brannerite and minor monazite. The ore contains 0.11% $U_3O_8$, 0.020% $ThO_2$ and 0.056% rare earths (yttrium, cerium and neodymium oxides).

The ore milling process at Nordic Mine, and at currently operating mines, involves grinding the ore to 50% minus 200 mesh followed by acid digestion of oxide ore minerals with dilute sulphuric acid. The resulting pregnant liquor is passed through ion-exchange columns to remove the uranium. The uranium is eluted from the ion exchange columns using nitric acid, and then reacted with ammonia to precipitate ammonium diuranate, known as yellow cake. The process effluent water containing $SO_4^{+2}$, $NO_3^{-1}$, $NH_4^{+1}$, $Th^{2+}$ and

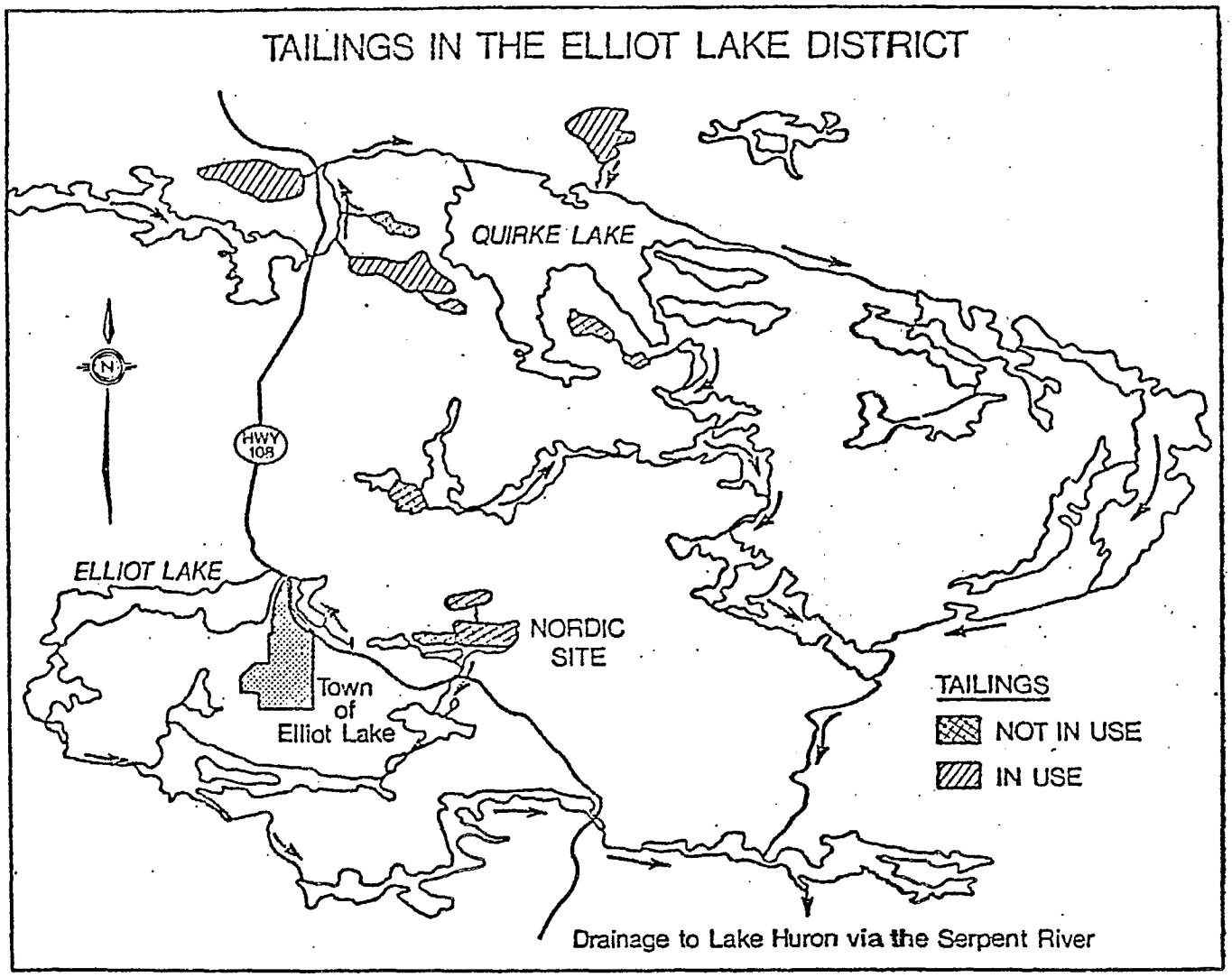


Fig. 4.1 - General location and plan.
(From Blair et al. (28)).

$^{226}Ra$ is collected at the end of the mill circuit along with the leached ore pulp. The effluent water and pulp were neutralized with limestone and lime and discharged to the tailings pond. The average $U_3O_8$ recovery was 95%, and to a certain extent, $ThO_2$ and rare earths were recovered from the leach liquor.

The tailings consists of a mixture of sand and silt, 50% passing the 200 mesh size, and is comprised of quartz, feldspar, approximately 5% pyrite and minor sericite. Gypsum formed from precipitation following lime neutralization of the mill effluent was also present. The tailings were slurried with neutralized mill effluent and discharged to the tailings pond where settling took place in broad low angle alluvial fans. The coarse sand size fraction settled close to the point of discharge, and the fine silt-size or slime fraction settled in the distal area of the impoundment. The coarse sized fraction progressively advanced out over the fine distal fraction in a deltaic fashion (28).

The Nordic Main Tailings Pond occupies an area of approximately 85 hectares, measuring 1460 m east-west, and 550 m north-south, to a depth of 10 m, Figure 4.2. The tailings were deposited in a level valley on an area formerly occupied by a spruce bog. The tailings pond is confined along the north and west perimeter by prominent bedrock ridges. The eastern and southern perimeter of the pond are contained by a 10 to 12 m high rockfill dam.

Deposition of the tailings began in 1957 at the southwest corner of the basin and extended outward to the north and east. The Nordic tailings pond was filled to its capacity and became inactive with closure of the mine in 1968. In 1975, a rehabilitation program by revegetation on the surface of the tailings was started. The surface of the tailings was first treated with lime and crushed limestone and regrowth of grasses was established over the

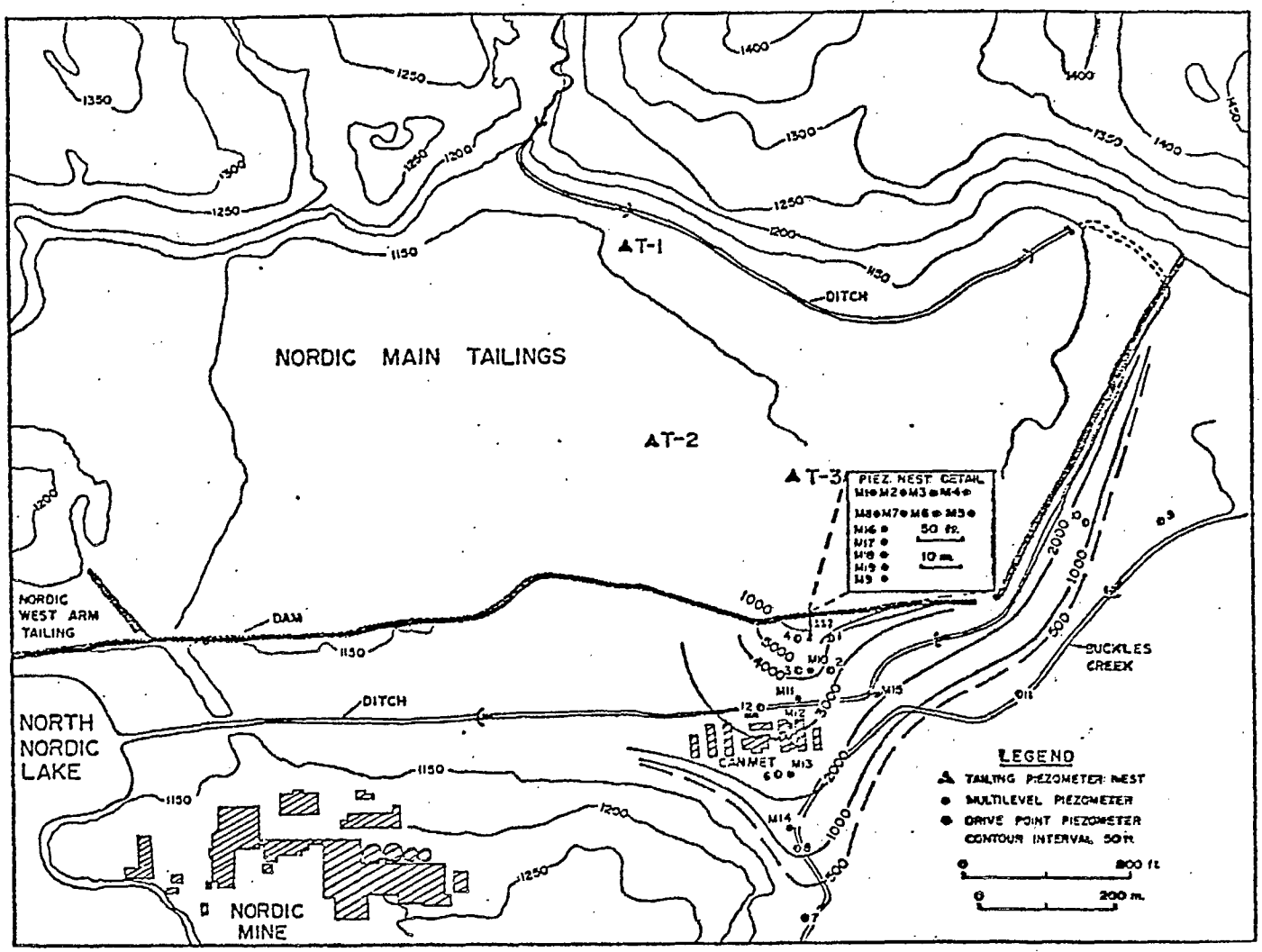


Fig. 4.2 - Nordic mine hydrogeochemistry, piezometer instrumentation and sulphate plume. (From Blair et al. (28)).

period 1975 to 1979 until the vegetation was self-sustaining.

## 4.3 SITE GEOLOGY

The Nordic mine tailings site is located in an east-west trending valley flanked by parallel trending bedrock ridges. The ridges are formed from lower Proterozoic arenaceous meta-sedimentary rocks that strike east-west and dip 10 to 15° north forming a dip and scarp topography. The surface elevations range from 340 to 345 m ASL.

The Nordic Valley is infilled with Pleistocene glacial deposits comprised of basal till overlain by glaciofluvial outwash sands and gravel with a combined thickness varying up to 30 m. The glaciofluvial deposits of the Nordic Mine Valley extend to Buckles Mine Valley in the south.

The glaciofluvial sands form a fairly uniform deposit of fine to coarse-grained micaceous quartz-feldspathic sand with occasional pebble-gravel interbeds. Drilling for peizometer installation indicated that the depth of sand varied from 10 m to greater than 15 m (Blair et al. (28)). The glaciofluvial deposits are overlain throughout much of the valley area by a layer of black peat 0.5 to 1.0 m thick which was formed under a recent spruce bog that existed in the area south of the tailings dam and in the vicinity of the old CANMET Laboratory, Figure 4.3.

The area receives approximately 1 m of precipitation annually. The peak stream flow periods are experienced during the spring snow melt in April and May, and during the fall rains in October and November. The stream flow varies seasonally from $7.5 \times 10^{-3}$ to $2.7 \times 10^{-1}$ $m^3$/sec.

## 4.4 METHODS OF INVESTIGATION: WATER SAMPLING INSTRUMENTATION

### In the Tailings Pile

Piezometer nests were installed in the tailings area approximately 250 m apart. The piezometers at each nest had tips at intervals of 1.5 m and

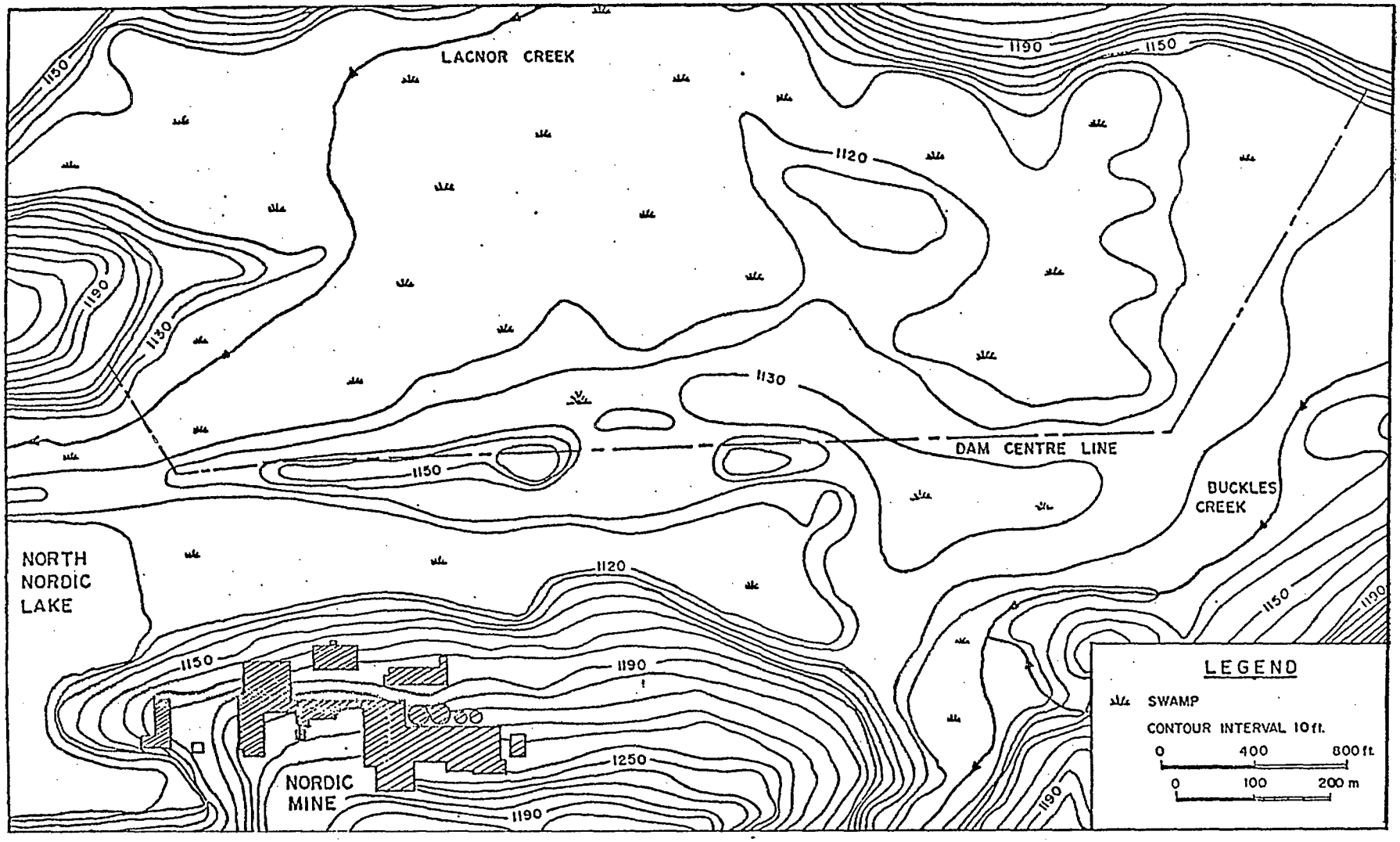


Fig. 4.3 - Nordic mine tailings basin original topography (1956). (From Blair et al. (28)).

were spaced vertically from the water table to about 1 m below the tailings. To obtain a representative porewater sample from a desired depth, the piezometer tip was placed in contact with the tailings causing as little disturbance as possible during the installation.

A modified Casagrande drive-point stand-pipe piezometer constructed entirely of 1.125 in (2.86 cm) schedule 80 PVC pipe (Figure 4.4) was used in an area of fine-grained tailings. A porous polyethylene cartridge (VYON) with a 50 μ pore size was used for the piezometer screen. The porous Vyon cartridge was sandwiched between the drive point tip and a straight female coupling and sealed with caulking compound. This was found to be very useful in preventing silt-sized tailings particles from entering the piezometer.

A vehicle-mounted hollow-stem auger drill was used to install the piezometer in and beneath the tailings where gravel was encountered. The hollow-stem auger was used to drill into the tailings at 1 m above the desired depth. A hand-operated gasoline powered rock drill was used to advance the piezometer point to its desired position. The tailings below the water table liquified around the piezometer pipe allowing the piezometer to advance easily. The tailings then settled back tightly around the piezometer. Bentonite was poured in to fill the void between the piezometer and the hollow-stem auger and the auger was then removed allowing the tailings to collapse around the assembly.

In the Sand Aquifer

Based on the reconnaissance investigation, a detailed groundwater monitoring network was designed along the toe of the dam to intercept chemicals and radioisotopes contaminating the groundwater migrating from the tailings. The monitoring was accomplished with multi-level bundle-type piezometers that provided individual water samples from many different depths over the thickness of the aquifer. The multi-level assemblies were

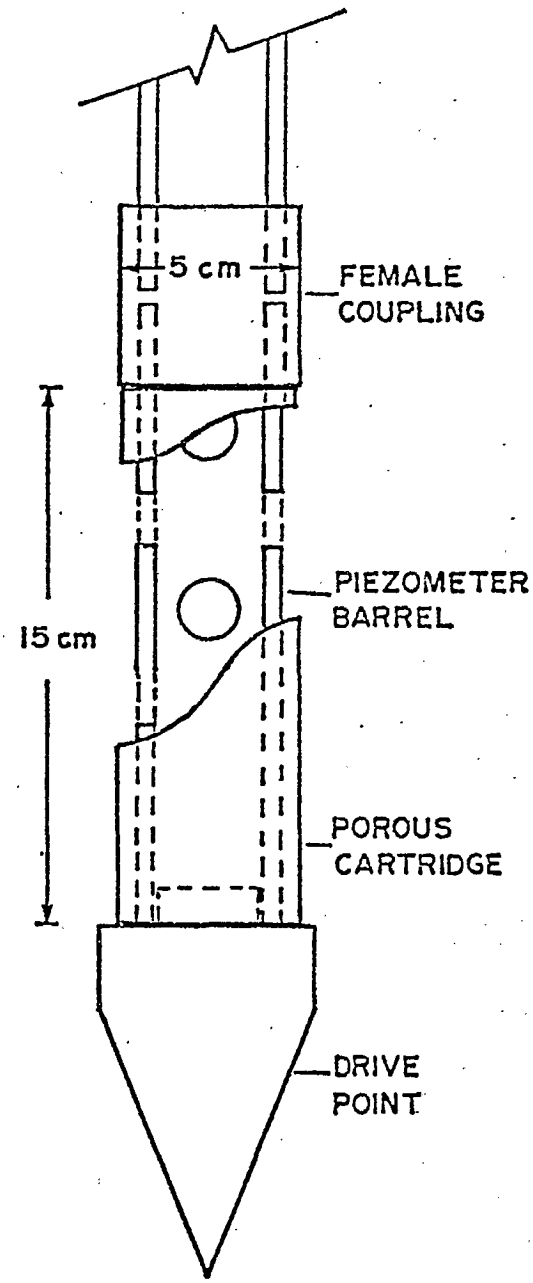


Fig. 4.4 - Design of piezometer drive point tips used in tailings (From Blair et al. (28)).

constructed of a bundle of 12 mm (0.5 in) O.D. polyethylene tubes, each tube with a 10 cm screened interval at the end, fastened at different intervals to a central 12 mm I.D. PVC pipe. The multi-level assemblies were installed using a hollow-stem auger to a maximum depth of 15 m. The cohesionless sand collapsed around the assembly immediately upon withdrawal of the auger (Morin et al. (18-21)).

## 4.5 TAILINGS SOLID SAMPLING METHOD

Solid cores were taken during the hydrogeological investigation. Samples were extracted by drilling or augering a hole down to the required depth and collecting the samples from the undisturbed formation with a split spoon sampler, or short Shelby tube. During the drilling and sampling at the West Arm tailings area, drilling mud (a suspension of bentonite in water) was used for lubricant and washing, and it is suspected that by using this method some sample contamination and ionic imbalance could occur because of the churning action of the drill (31,34,35).

Later, a new method was introduced and used for sampling tailings solids in the Nordic Main tailings area. A vehicle mounted hollow-stem auger was used, and at a shallow depth above the saturated zone, the sampling was done by using a short Shelby tube or split spoon sampler. The hollow-stem auger with centre plug was advanced to a desired depth and the split spoon sampler was lowered through the centre of the hollow stem-auger after the plug has been removed. After the sample was obtained the centre plug was placed back into the hollow stem auger and advanced further into the next desired position. From the water table downward a 30 ft (9.1 m) long tube of thin walled aluminum pipe 3 in (7.62 mm) O.D. was used. The long tube was slowly pushed down and hammered slightly at the same time until it penetrated

the black peat layer and hit the gravel formation beneath. The bottom of the thin aluminum pipe was crimped closed after a few hammer blows against the gravel formation to form a plug.

The pipe was lifted and placed against the drilling tower where it was cut in sections starting at the top in 6 in (15 cm) intervals.

During the drilling and sampling operation all important stratification data, such as starting depth, length of sample, compaction, sample interval, colour, and odour such as $H_2S$ gas, etc. were recorded.

Piezometer nests were installed at the same location where the solid tailings were sampled in such a way that the water samples at certain depths could be directly correlated with tailings solids of the same location and depth.

Locations of piezometer nests T-1, T-2, T-3, T-7, and T-8 are shown in Figure 4.5 and a general cross-section of the Nordic Main Tailings in Figure 4.6.

## 4.6 FIELD PREPARATION

### Water Sampling and Field Preparation

Before the ground water samples were collected, the piezometer well was first pumped nearly dry to clear the stagnant water in the well and allow fresh water from the formation to enter. The water sample was collected following the recovery of the piezometer so that the water retrieval was representative of the tailings formation water in the immediate vicinity of the piezometer screen.

The height of the hydraulic head was monitored before and after pumping to test the response of the piezometer well and to collect hydrology data.

Groundwater samples were collected from the piezometers in the

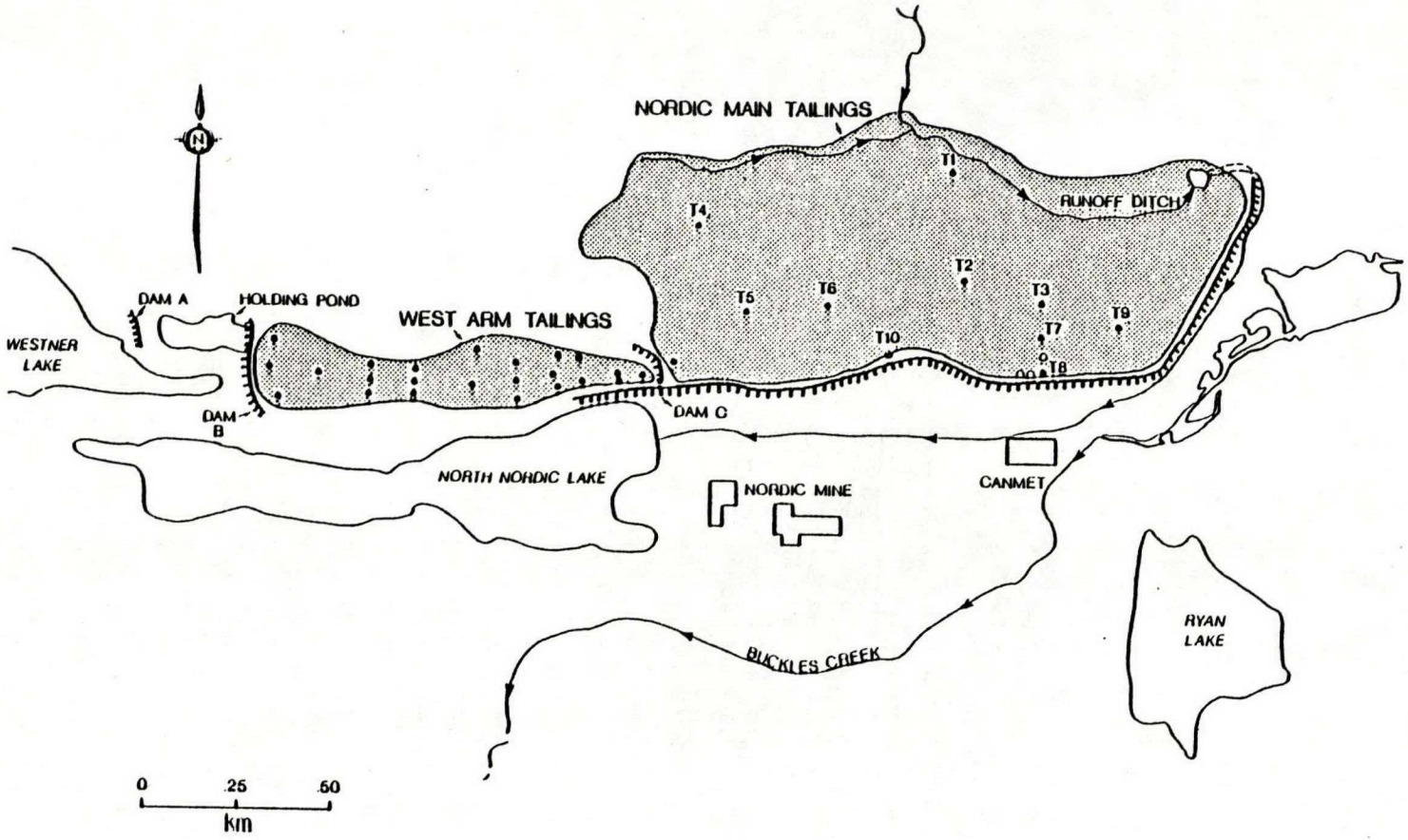


Fig. 4.5 - Location map and monitoring sites at the Nordic main and Nordic west arm tailings. (From Cherry et al. (29)).

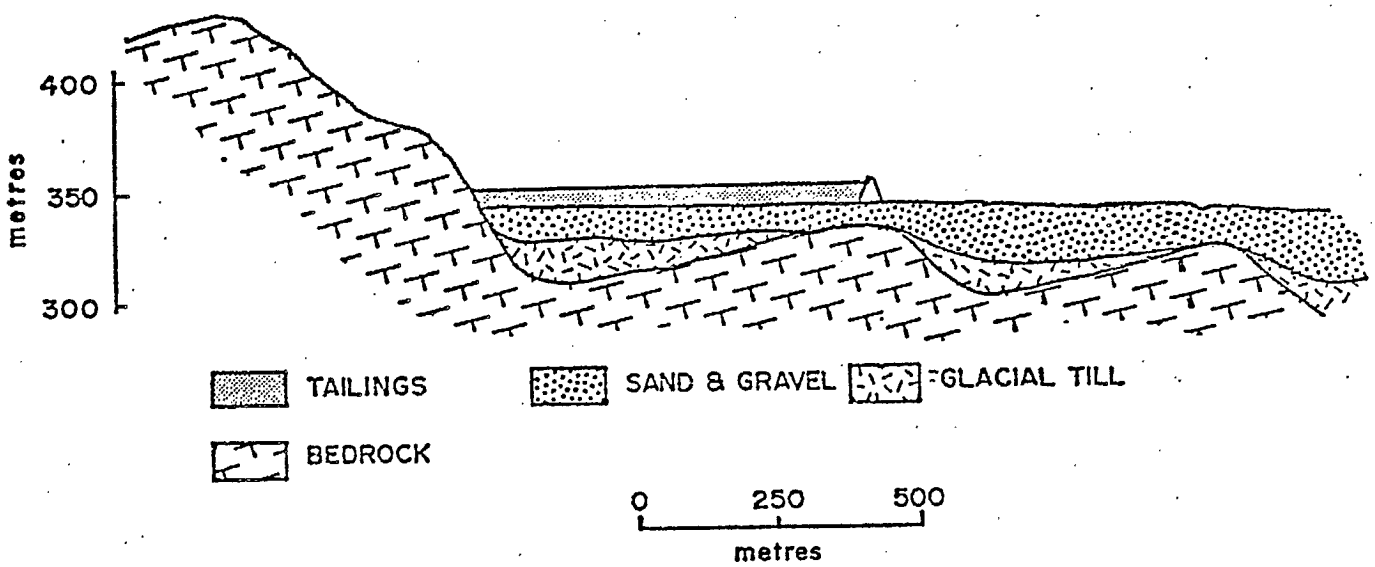


Fig. 4.6 - Geological cross-section of the Nordic main tailings pond and surficial deposits. (From Blair et al. (28)).

tailings and in the sand aquifer using a peristaltic pump and passed through an 0.45 μm, 127 mm diameter, filtration assembly at the end of the pressure side of the peristaltic pump.

The clear pre-filtered water was then analyzed as soon as possible for formation temperature, pH, electrical conductivity, redox potential, iron (II), alkalinity and acidity by titration methods. Other elements such as sulphate, heavy metals, and some radioisotopes such as $^{226}Ra$, $^{232}Th$, $^{228}Th$, $^{230}Th$ and $^{210}Pb$ were analyzed later in the laboratory after the sample had been preserved with hydrochloric acid to pH = 1.

All the sample bottles were labelled with sample identification such as location, depth of sample, date and time of sampling, etc.

## 4.7 HYDROGEOLOGY OF THE TAILINGS

The depth of most of the Nordic Main tailings area, where the piezometer nests were located was approximately 10 m. A layer of compact black peat, approximately 1 m thick, forms an intermittent layer under most of the tailings pond area, separating the tailings from the underlying sand and gravel. A peat layer was not present at T-3 location which corresponded to the elevated areas in the original basin topography, Figure 4.3.

### Water Table

The water table in the tailings has a fairly constant slope from the northside of the tailings area, where the water table is 1 m below surface, to the south side of the tailings adjacent to the dam where the water table is estimated to be 10 m below the surface of the tailings. The average water table fluctuation observed during the period August to December was 0.5 m. The water table elevation declined through the dry summer and early fall, then rose in response to heavy rainfall in November. The response at piezometer nest T-1 location was very rapid, where the water table was within

1.5 m. The rapid response suggested that the tension-saturated zone above the shallow water table was near the surface of the tailings. This rapid response was not observed at piezometer nests T-2, T-3, T-7 or T-8 where the water table was greater than 4 m.

Hydraulic Gradient

The vertical hydraulic gradient in the Nordic Main tailings is strongly downward with an average of 0.2 m/m, and is affected by the presence of the peat layer at locations T-1 and T-2 which causes a sharp increase in gradient. The average gradient across the tailings at T-1 and T-2 is fairly constant at 0.06 m/m, then increases sharply to 1.45 m/m across the peat layer in response to lower hydraulic conductivity in the peat layer compared to that for the overlying tailings. At T-3, where there is no peat layer, the gradient is constant at 0.2 m/m through the tailings into the gravel.

The horizontal hydraulic gradient in the tailings and underlying gravel aquifer is 0.0065 m/m towards the south, approximately 3 orders of magnitude less than the vertical hydraulic gradients. The horizontal gradient increases slightly towards the toe of the dam (Blair et al. (28)).

Hydraulic Conductivity

Each piezometer located below the water table in the tailings was bailed dry and the water levels recorded as recovery occurred. Hydraulic conductivity in the tailings was then calculated by the rising head method of Hvorslev (59), and was found to range from $1 \times 10^{-4}$ cm/s to $3.1 \times 10^{-6}$ cm/s. The individual hydraulic conductivity and the corresponding depth locations within the tailings are represented in Table 2 of Blair (28).

The range of hydraulic conductivity values obtained reflect stratification within the tailings of layers with different grain sizes. In general, the lower hydraulic conductivities are located near the bottom of the tailings and are overlain by tailings of higher hydraulic conductivity.

Groundwater Flux and Velocity

The Darcy equation (28) was used to obtain estimates of the groundwater flux in the tailings. The average groundwater velocity was obtained by dividing the Darcy flux by the porosity, which is approximately 0.30. The observed gradients and bulk average hydraulic conductivity of 1 x $10^{-5}$ cm/s were used in the calculations. The flux values obtained at the piezometer nests are listed in Table 1 of Blair et al. (28).

The average downward groundwater flux at piezometer nests T-1 and T-2 was approximately 0.14 $m^3/m^2$/year with a downward velocity of 0.5 m/year. The corresponding value at T-3 was greater by a factor of 3.5. The downward flux was approximately 0.5 $m^3/m^2$/year with a downward velocity of 1.6 m/year.

The higher ground water flux at T-3 corresponds to the absence of flow restraints caused by the low hydraulic conductivity of the peat layer.

The groundwater seepage fluxes and velocities for the surficial aquifer are determined from the Darcy equation using measured hydraulic gradients and a representative hydraulic conductivity of 1 x $10^{-2}$ cm/s. The average lateral groundwater seepage flux in the surficial aquifer is in the order of 20 $m^3/m^2$/year with an average velocity of 70 m/year.

These values increase towards the toe of the tailings dam where the hydraulic gradient is larger. Between piezometers M-1 to M-8, the specific discharge from beneath the toe of the tailings dam attains an average value of 167 $m^3/m^2$/year with a seepage velocity of 550 m/year. The specific discharge and velocity diminish rapidly southward from the point of discharge as the seepage flowpaths diverge outward away from the bedrock ridge restriction, located in the dam west of the piezometers.

## 4.8 HYDROGEOCHEMICAL PROCESSES

The hydrogeochemical processes that control the chemical composition of the porewater in the tailings and the chemical composition of contaminated groundwater in the sandy aquifer are the subject of on-going research. In this thesis only a brief description of the major hydrogeochemical processes will be discussed.

The most important influence on the chemistry of porewater in the tailings, and subsequently in the groundwater in the surficial aquifer near the tailings, has been the oxidation of pyrite ($FeS_2$) in the tailings. This process can be expressed as:

$$FeS_2 + 3\ O_2 + 2\ H_2O \rightarrow Fe^{+2} + 2\ SO_4^{2-} + 4\ H^+$$

The production of hydrogen ions causes a progressive decline in the pH of the porewater from the initial pH of about 8, which existed when the tailings discharged from the mill, to a pH that is currently about 3 in the groundwater zone just below the water table. At a pH of 3 or lower, ferric ion rather than oxygen becomes the most dominant agent in pyrite oxidation (Nordstrom (37)).

The bacterium Thiobacillus ferrooxidans in the presence of oxygen and water oxidizes ferrous ions previously released from the pyrite to ferric ion, and then the ferric ion oxidizes in a manner that can be represented as:

$$FeS_2 + 14\ Fe^{3+} + 8\ H_2O \xrightleftharpoons{\text{T. ferrooxidans}} 15\ Fe^{2+} + 2\ SO_4^{2-} + 16\ H^+$$

$$7\ H_2O \rightleftharpoons 3\tfrac{1}{2}\ O_2 + 14\ H^+$$

A similar explanation was introduced by Dave et al. (31) as follows:

In the presence of moisture and oxygen, pyrite is being oxidized by Thiobacilli ferrooxidans in the uppermost layer of the tailings producing $H^+$ ions (acidity) and high TDS porewater, represented by:

$$FeS_2 + H_2O + \frac{7}{2} O_2 \xrightarrow{T.ferrooxidans} Fe^{2+} + 2\ H^+ + 2\ SO_4^{2-}$$

$$Fe^{2+} \xrightarrow{T.ferrooxidans} Fe^{3+} + e^-$$

$$Fe^{3+} + FeS_2 + 2\ H_2O + 3\ O_2 + e^- \xrightarrow{T.ferrooxidans} 2\ Fe^{2+} + 4\ H^+ + 2\ SO_4^{2-}$$

The acid produced further leaches out other trace metals and radionuclides. With the downward infiltration of this porewater during recharge events, neutralization and precipitation take place in the neutralized buffer zone in the presence of residual alkalinity in the form of calcite ($CaCO_3$), or lime (CaO), precipitating gypsum and siderite.

$$CaCO_3\ (s) + H^+ \longleftrightarrow Ca^{2+} + HCO_3^-$$

$$CaO\ (s) + 2\ H^+ \longleftrightarrow Ca^{2+}\ H_2O$$

$$Fe^{2+} + SO_4^{2-} + CaCO_3\ (s) + 2\ H_2O \longleftrightarrow FeCO_3\ (s) + CaSO_4.2H_2O\ (s)\ .$$

The solutes are transferred back to the solid phase in a lower zone which continuously progresses downwards with the consumption of the alkaline buffer and replacement of the original porewater by highly acidic, high TDS porewater.

An understanding of the hydrogeochemical aspects of the tailings and aquifer system is an essential prerequisite for the development of predictive models of the long-term evolution of water quality in the drainage basins in which tailings exist (Blair et al. (28)).

Oxidation of pyrite is the major cause of acidification of the uranium tailings porewater, where the original neutralized porewater is gradually replaced by acidic porewater that leaches and mobilizes the radionuclides and heavy metals in the tailings (Cherry et al. (29)).

The hydrogeochemical interactions within the tailings itself produce a dynamic mixture of oxidation, leaching, desorption, solute transportation, neutralization, precipitation, coprecipitation and sorption processes which gradually contribute to the evolution of a solid phase profile (Dave et al. (31)).

# CHAPTER 5

## CHEMICAL ANALYSES

Fractions of the water samples taken in the field were immediately analyzed for temperature, electrical conductance, pH, redox potential, acidity, alkalinity and ferrous ion content before the characteristics of the samples were changed by an oxidation reaction to the atmospheric conditions.

This analysis is a very important aspect of the field investigation, because it ensures the precision and accuracy of the data collected from every sampling point at various depths within the tailings pile.

After the basic field data were analyzed, the samples were stabilized and preserved by adding hydrochloric acid to pH = 1 for further laboratory analyses.

Ferrous ion was determined in the field by potassium dichromate titration as described in the manual "Standard Methods of Chemical Analysis", (36). Acidity and alkalinity were also determined using the titration method.

The pH, redox potential and ferric/ferrous ions ratio are indicators used to determine the extent of oxidation of the tailings with depth. The ferric content was obtained by subtracting the ferrous ions from the amount of total iron determined in the laboratory.

Electrical conductance is a quick indicator used in the field to determine the amount of dissolved electrolytes in the sample, which could also be used to gauge the amount of dissolved sulphate from the porewater of pyritic tailings. Therefore, this was also used as a useful indicator to determine dilution factors or sample cuts for sulphate analyses in the laboratory. The correlation test of electrical conductance versus concentration of sulphate is shown in Figure 5.1.

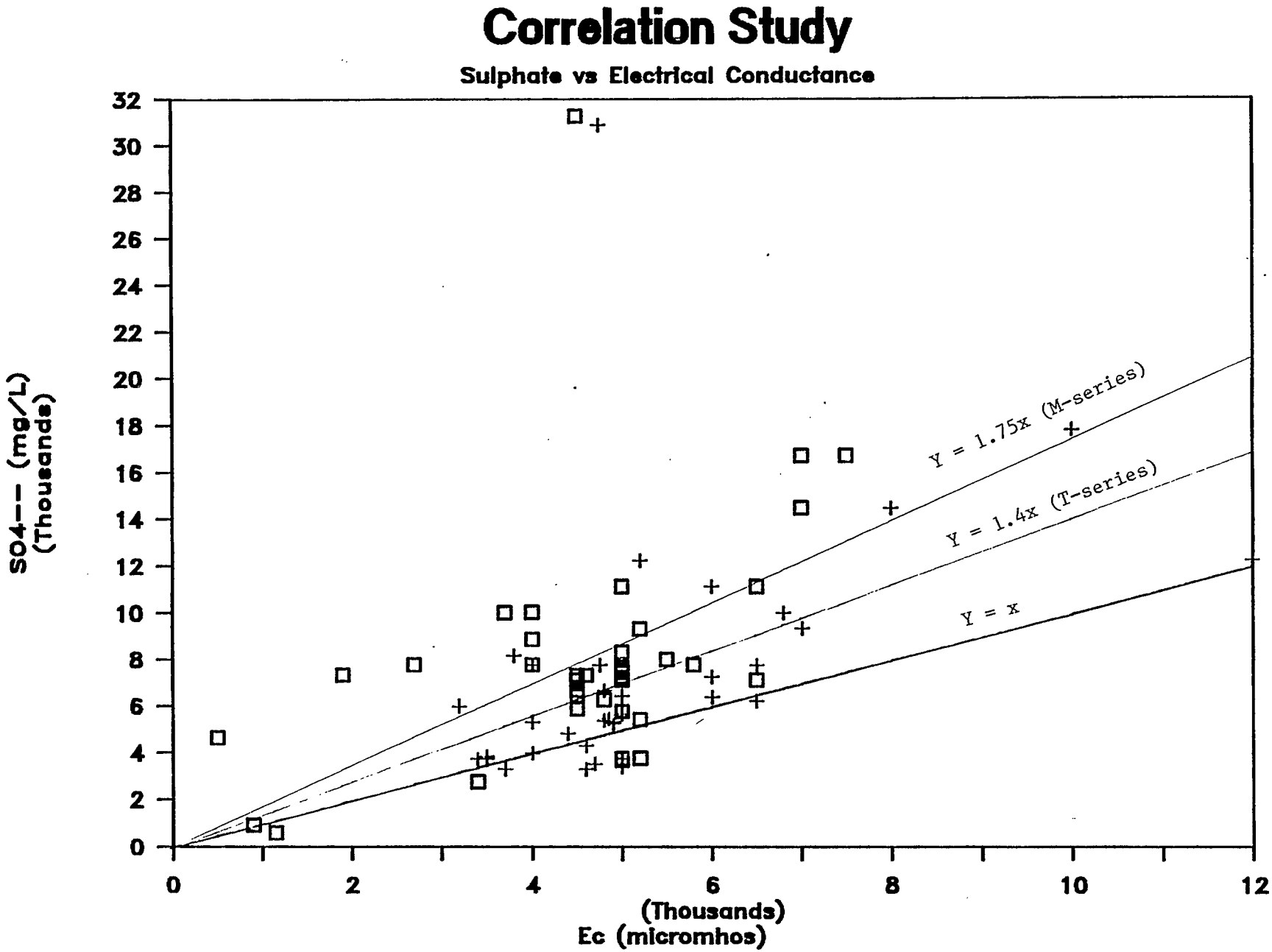


Fig. 5.1 - Correlation study of sulphate versus electrical conductance.
Linear regression for M-series □, and T-series +.

Heavy metals and earth alkali metals, and other inorganic elements from porewater and solid tailings, such as total Fe, B, U, Th, Mn, Ca, Mg, etc., were analyzed at the Canada Centre for Mineral and Energy Technology (CANMET), Elliot Lake, Ontario. Some of these samples were analyzed by contractors such as Guelph Chemical Laboratory Ltd., Guelph, Ontario, and Chemex Laboratories Ltd., Vancouver, B.C.

## 5.1 MEASUREMENT OF SAMPLE pH

The solid samples were prepared using freshly made distilled water in 1:1 ratio by weight, and the pH was measured using a glass electrode with a saturated calomel electrode as a reference electrode. The pH meter used for the measurement was a research grade instrument capable of measuring pH to ± 0.002 units, and was equipped with automatic temperature compensation. The glass electrode system had the capability of measuring the entire pH range from 0 to 14.

The reference electrode was dipped into a potassium chloride solution. The glass electrode consisted of a glass membrane filled with saturated potassium chloride. The potential of the electrode system was tested to ensure that it followed the Nernst equation (55):

$$E_g = E_o + \frac{RT}{F} \ln C_{H^+}$$

where, $R$, $T$ and $F$ represent the gas constant, the absolute temperature, and the Faraday, respectively. $E_o$ is the constant of the electrode system, and $C_{H^+}$ is the concentration of $H^+$ ions.

In the presence of extremely high alkaline solutions, especially when $Na^+$ is also present, negative deviations from the true pH may be caused by the migration of $Na^+$ to the glass membrane. A special glass electrode was used to eliminate error due to the salt effects and to give highly accurate pH values up to pH 13.

To ensure the precision and accuracy of the pH measurement, the instrument was calibrated first using a NBS buffer standard solution such as potassium hydrogen-phthalate (pH = 4.00 at 25°C), and a tetraborate buffer (pH = 9.00 at 25°C).

Precautions were taken to ensure that the electrodes were adequately washed on completion of each determination to avoid cross-contamination.

## 5.2 PRETREATMENT FOR SOLID TAILINGS ANALYSIS

Prior to the chemical analysis, the solid tailings were first weighed accurately, 1 g net weight (solid sample cut on dry basis) and placed in a platinum crucible. Drops of water and reagent grade $HClO_4$ (perchloric acid) were added, and the crucible was agitated slightly to ensure that the sample was thoroughly wetted. Then 10-20 mL of 48% HF (hydrofluoric acid) was added to the crucible and it was put on a hot plate with the temperature set at approximately 200°C to allow the solution to evaporate to dryness (2 to 3 hours). White fumes appeared before the solution evaporated to a complete dryness which indicated that an excess of perchloric acid was present. (Note: precautions should always be taken when working with perchloric acid. A fumehood should be especially designed for this purpose with a washout system in the output stack to prevent explosive powder from building up.)

The crucible was then allowed to cool, and a mixture of 30% borax flux and 70% sodium carbonate were added. The mixture was then heated using a blast burner at a high temperature to bring it to the melting point. While heating it was continuously whirled in a gentle motion for approximately 15 minutes. The melt was allowed to cool off and a solution was then made up by dissolving the melt in 1 N HCl into a litre volume.

This solution was used in the analysis for most of the chemicals and radioisotope components in the solid tailings sample.

## 5.3 SULPHATE

After complete dissolution of solid samples, using the method described in 5.2, or the stabilizing and preserving of prefiltered porewater from the field, soluble sulphate ion concentration was determined by Guelph Chemical Laboratories Ltd. using a spectrophotometric technique.

This sulphate determination involved the reaction between barium chloranilate with sulphate in acid solution to give barium sulphate and acid-chloranilate ion:

$$SO_4^{2-} + BaC_6Cl_2O_4 + H^+ \longleftrightarrow BaSO_4 + HC_6Cl_2O_4$$

The amount of acid-chloranilate liberated is proportional to the sulphate ion concentration. The reaction was carried out in 50% aqueous ethanol, buffered at pH 4.

To eliminate interferences from other cations, the sample containing sulphate ions was first filtered through an ion-exchanger column in hydrogen form. The pH of the effluent was adjusted to 4 with dilute hydrochloric acid or ammonia solution. The eluted sulphate was then made up to a known volume in a volumetric flask for further stoicheiometric calculations.

At pH 4, the acid-chloranilate ion gives a broad peak of 530 nm. This wavelength was used for sulphate determination in the range between 2 to 400 ppm. A much more intense absorption occurs in the ultraviolet: a sharp band at 332 nm will enable the limit of detection of sulphate ions to be extended to 0.06 ppm with accuracy and precision to 5 μg/g ± 3%.

### Calibration

An aliquot containing freshly made standard sulphate ions was prepared. The pH 4 buffer (a 0.04 m solution of analytical reagent grade potassium hydrogenphthalate) and ethanol were added. A weighed quantity of barium chloranilate was added and the flask was shaken for 10 minutes. The excess barium chloranilate and the precipitated barium sulphate were filtered. The absorbance of the filtrate was then measured at 530 nm against

a blank which was prepared in the same manner. A calibration curve using standard potassium sulphate solution was thus prepared from the A.R. grade salt.

For a sample solution containing less than 2 ppm sulphate, the measurement was carried out at a shorter wavelength as described above with an appropriate calibration curve.

Later in this thesis, another new method of sulphate analysis will be discussed. This method involves the radioisotope Ba-133 as a tracer to determine the amount of sulphate present in the solution.

## 5.4 SILICA

### Determination of Silica as $SiO_2$

Insoluble silicate was fused with sodium carbonate, and the melt which contains the silicate in acid-decomposable form was then treated with hydrochloric acid. The acid solution of decomposed silicate was evaporated to dryness in the water bath to separate the gelatinous silicic acid as insoluble silica $SiO_2.yH_2O$; the residue was heated at 110-120°C to partially dehydrate the silica and render it as insoluble as possible. The residue was then extracted with hot dilute hydrochloric acid to remove salts of iron, aluminum and other metals which might be present as interferences. The greater portion of the silica remained undissolved, and was therefore filtered off next. The filtrate was evaporated to dryness, and the residue was heated to dryness at 110-120°C as before which rendered insoluble the small amount of silicic acid that escaped dehydration. The residue was then treated again with dilute hydrochloric acid as before and the second portion of silica was filtered off on a fresh filter.

The two washed precipitates were combined and ignited in a platinum crucible at about 1050°C to produce silicon oxide and then weighed. The

ignited residue is not usually a pure silicon oxide, generally containing a small amount of impurities as determined by treating the weighed residue in the platinum crucible with an excess of hydrofluoric acid and a little concentrated sulphuric acid.

The silica will be expelled as the volatile silicon tetrafluoride; the impurities (e.g., $Al_2O_3$ and $Fe_2O_3$) will first be converted into fluorides which pass into the sulphates in contact with the less volatile sulphuric acid following the subsequent brief ignition (at 1050-1100°C for a few minutes).

The loss of weight therefore represents the amount of pure silicon dioxide present.

The determination of silica in a 'soluble' silicate was carried out by the same procedure (Guelph Chemical Laboratories Ltd.). The accuracy and precision of this method was checked against the NBS standard and found to be excellent with a coefficient variance of less than 2%.

Dalton (38-40), using the X-ray diffraction method, reported the silica content as quartz.

## 5.5 METALS

### Atomic Absorption

Fe, Ca, Al, Pb, Mg and K were analyzed using an atomic absorption spectrophotometer, dual beam Varian CR-90, equipped with automatic background correction and digital readout. The equipment is suitable for both flame and flameless (graphite furnace) spectrophotometry. The detection limit for flame spectrophotometry for various elements required to be analyzed are given in Table 5.1.

### Sequential Atomic Emission Spectrophotometer

Routine analysis of Fe, Ca, Mg, Al, Pb, Mn, U, Th, Si, K, Ni, Co, Cu,

**TABLE 5.1**

Lower limit of detection of metals to be analyzed

| Element | Conc. in Solution ppm (mg/L) | Conc. in Solids 1 gm in 10 mL soln (µg/g) |
|---|---|---|
| Al | 0.5 | 5 |
| Ca | 0.01 | 0.1 |
| Fe | 0.02 | 0.2 |
| Pb | 0.1 | 1.0 |
| Mg | 0.003 | 0.03 |
| K | 0.003 | 0.03 |

Note: In calcium and magnesium determination, trivalent lanthanum chloride was added as a releasing agent to suppress the Na and K enhanced reading.

In potassium determination, CsCl was added to the sample to attain a high degree of accuracy in A.A. measurement.

etc., was carried out with a high energy plasma excitation source (DCP), at the Elliot Lake Laboratory.

The direct current plasma (DCP) emission spectrophotometer employs a three electrode configuration as a plasma excitation source and an echelle grating monochromator. The grating is used in combination with a quartz prism for order separation and provides a two directional spectral pattern covering 190 nm to 800 nm. With the diffraction of collimated incident radiation the peak efficiency of all wavelengths occurs in a succession of different orders, which are vertically stacked, and within these orders the wavelengths are dispersed horizontally. The echelle system has a focal length of only 0.75 m and provides an average reciprocal linear dispersion of 0.12 nm/mm, and an average resolution of 0.003 nm. The detection system on the sequential DCP spectrophotometer uses a single photomultiplier tube and a wavelength is selected by moving the grating and prism within a calibrated scale. The two dimensional spectrum can also be photographed using a Polaroid camera attachment to permit spectrographic qualitative analysis.

During routine operation of the DCP spectrophotometer, it was observed that the overall stability of the instrument was quite short-lived, sometimes as short as 10 to 15 minutes.

The lowest limit of detection, and the ranges of some metals analyzed routinely at the Elliot Lake Laboratory are shown in Table 5.2.

## 5.6 THORIUM AND URANIUM ANALYSES

Chemical thorium and uranium analyses were also done by Neutron Activation Analysis (NAA). This is a very sensitive and accurate method which analyzes thorium and uranium with LLD in the range of microgram and picogram, depending on the form in which the sample is available. The thorium was done by NAA-Gamma Spectroscopy, and the uranium by Delayed

**TABLE 5.2**

Lower limit of detection of metals analyzed by
DCP Sequential Spectrophotometer

| Element | Wavelength (nm) | LLD (mg/L) | LDR (mg/L) | BEC (mg/L) | Precision (RSD) at...xBEC...% |
|---|---|---|---|---|---|
| Al | 236.705 | 1 | 10-1000 | 40 | 2 xBEC 0.6% |
| | 308.215 | 0.08 | 0.8-100 | 2 | 2 xBEC 0.9% |
| | 396.152 | 0.02 | 0.02-100 | 0.04 | 25 xBEC 1.3% |
| Ca | 315.887 | 0.03 | 0.3-100 | 1 | 10 xBEC 0.8% |
| | 445.478 | 0.09 | 0.9-100 | 2 | 5 xBEC 0.7% |
| Co | 236.379 | 0.02 | 0.2-1000 | 0.8 | 1 xBEC 0.7% |
| Cu | 224.7 | 0.03 | 0.3-1000 | 2 | 10 xBEC 1.5% |
| Fe | 259.94 | 0.007 | 0.07-100 | 0.2 | 5 xBEC 0.6% |
| | 371.994 | 0.005 | 0.05-1000 | 0.1 | 10 xBEC 1.0% |
| Pb | 220.353 | 0.2 | 2-1000 | 10 | 1 xBEC 1.3% |
| | 368.348 | 0.01 | 0.1-600 | 0.4 | 20 xBEC 0.8% |
| Mg | 279.553 | 0.0002 | 0.002-60 | 0.006 | 2 xBEC 0.8% |
| Mn | 259.373 | 0.002 | 0.02-100 | 0.06 | 5 xBEC 0.6% |
| Ni | 243.789 | 0.09 | 0.9-1000 | 3 | 10 xBEC 0.8% |
| K | 404.414 | 0.9 | 9-100 | 20 | 1 xBEC 9.0% |
| Th | 401.913 | 0.02 | 1-10 | 2 | ? |
| U | 424.167 | 0.04 | 0.4-1000 | 1 | 10 xBEC 0.4% |

Note: LLD = Lowest limit of detection.
LDR = Linear dynamic range.
BEC = Background equivalent concentration.
RSD = Relative standard deviation.

Neutron Counting.

One of the most important advantages of the NAA method is its unique freedom from the effects of accidental cross-contamination of the sample with the element being determined. The maximum pretreatment necessary for most samples is grinding and homogenization before bombardment with neutrons.

The disadvantage of this technique is that only a few companies have the necessary reactor facilities. In this case, most of the work was contracted out to Atomic Energy of Canada Ltd.

## 5.7 DISCUSSION

Most of the chemical analyses carried out, as described in Chapter 5, were an essential prerequisite to the understanding of the hydrogeochemical processes which may have a connection with the mechanism of radioisotope disequilibrium in the system.

# CHAPTER 6

# RADIOCHEMICAL ANALYSES

A review of recent literature pertaining to the radiochemical measurement of certain, naturally occurring, radioactive elements was prepared in the form of a laboratory manual by Smithson et al. (42), and Chiu et al. (43). It gave detailed analytical methodology for the measurement of gross alpha, gross beta, gross gamma, uranium, $^{226}Ra$, $^{228}Ra$, $^{210}Pb$, $^{232}Th$, $^{230}Th$, $^{228}Th$, total thorium, $^{222}Rn$, $^{220}Rn$ and $^{219}Rn$.

A summary of the $^{238}U$, $^{235}U$ and $^{232}Th$ decay series is shown in Figure 6.1. However, in this thesis only a few radiochemical analyses will be discussed in relation to the subject of disequilibrium of radioisotopes from the vicinity of uranium tailings.

## 6.1 RADIUM-226 ($^{226}Ra$)

$^{226}Ra$ is the most frequently determined radionuclide because of its potential health hazard as a bone seeking element and its long half-life of 1602 years. Therefore, it is used as an indicator of the radioactive contamination level in the environment surrounding the uranium mining and milling operation.

$^{226}Ra$ can be determined by five different methods, namely, the gross alpha measurement, the radon emanation method, the alpha-spectroscopy method, by gamma ray spectroscopy, or by coincidence spectroscopy.

### 6.1.1 Gross Alpha Counting

This is the simplest and most economical method. It involves the separation of radium as sulphate from the sample solution with a lead sulphate carrier. Radium sulphate is then isolated by dissolving the radium-

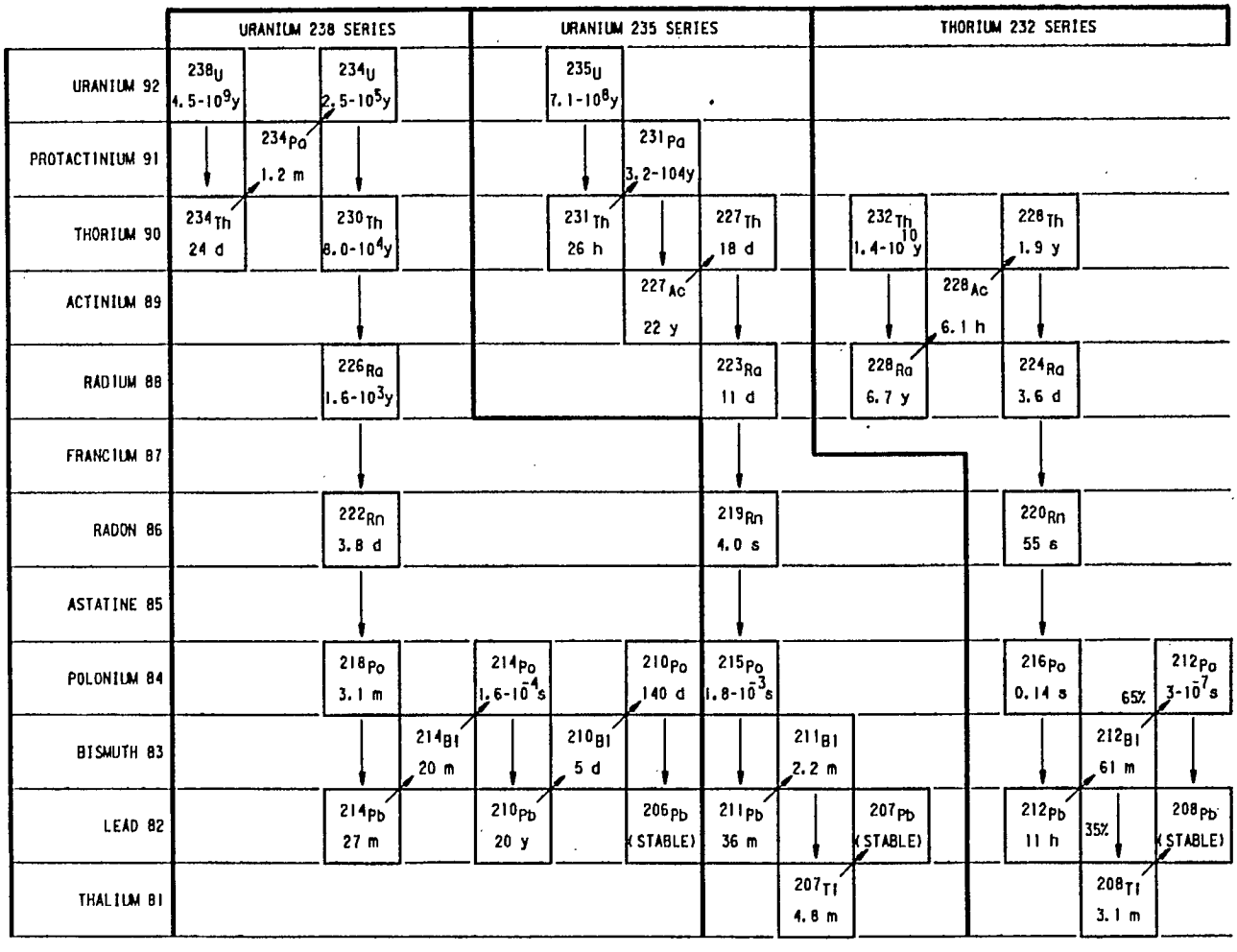


Fig. 6.1 - Some important characteristics of the $^{238}U$, $^{235}U$ and $^{232}Th$ series decay chains (taken from Chiu et al. 1986 (43)).

lead sulphate in alkaline EDTA or DTPA and coprecipitating with a barium sulphate carrier at pH 4.8. The radium-barium sulphate carrier is then counted on a gross alpha counter.

To obtain accurate $^{226}Ra$ activities, correction should be made for the presence of $^{223}Ra$ and $^{224}Ra$ by differential analysis. However, this is not an easy correction to do since gross alpha counting cannot differentiate the partitioning between $^{223}Ra$ and $^{224}Ra$ activities.

The simplest way to eliminate this uncertainty is to wait and count 66 days after the time of separation, that is after the $^{223}Ra$ and $^{224}Ra$ have decayed (Chiu et al. (43)).

### 6.1.2 Radon Emanation Method

The radon emanation method is an indirect method based on the relationship between the activity of the $^{222}Rn$ daughter measured against the $^{226}Ra$ parent present.

Radium, as pure as possible, is separated from the sample solution (as described in the gross alpha counting 6.1.1). and the radium-barium sulphate is redissolved in alkaline EDTA solution.

The redissolved solution is then placed in a bubbler from which the gaseous radon is stripped from the solution to zero concentration of radon in the bubbler.

The bubbler is then sealed off and isolated to allow radon gas to grow in the solution. After a suitable ingrowth period has elapsed, the radon gas is again stripped from the solution and is transferred to a ZnS scintillation (Lucas) cell.

With this method, there may be a considerable delay between sealing the bubbler and stripping the gaseous radon from the solution. For example, if a 50% equilibrium between $^{226}Ra$ and $^{222}Rn$ is desired, a waiting period of one half-life is required, i.e., about four days (Chiu et al. (43)).

Later $^{226}Ra$ can be indirectly determined by counting the activity on a scintillation counter after allowing time (3.5 hours) for $^{222}Rn$ to come to equilibrium with its daughters, namely, $^{218}Po$ and $^{214}Po$.

In the presence of $^{223}Ra$ and $^{224}Ra$, some of their daughters, namely $^{219}Rn$ and $^{220}Rn$, respectively, interfere with $^{226}Ra$ determination. Correction can be made by using a long transfer tube from the bubbler to the Lucas cell to prevent $^{219}Rn$ and $^{220}Rn$ arriving in the Lucas cell, as they will decay along the tube before their arrival in the cell. However, if the concentrations of $^{223}Ra$ and $^{224}Ra$ are very high, this method will become ineffective, as a long tube can cause many changes in the total volume and more errors could be introduced into the system. Furthermore, it is difficult to determine the length of the tubing required, as the system is not designed to differentiate between the isotopes.

### 6.1.3 High-Resolution Gamma Spectroscopy

High-resolution gamma-spectroscopy requires the use of Ge(Li) or high-purity N-type Ge detectors. This technique is based on the simultaneous determination of radionuclides by measurement of emitted gamma photons from 40-2000 KeV. In certain instances it can be complicated and time consuming because of the presence of large numbers of gamma photopeaks, but simplification is possible if the radionuclide(s) of interest is (are) physically separated from the others (Chiu et al. (43)). For example, Michel et al. (44) sucessfully determined the activities of $^{226}Ra$ and $^{228}Ra$ by separating radium with barium carrier from the sample.

For determination of $^{226}Ra$, photopeaks of its daughters $^{214}Pb$ (295 KeV, 352 KeV), and $^{214}Bi$ (609 KeV, 1120 KeV) were used. In the absence of $^{235}U$, the 185 KeV line of $^{226}Ra$ can be used, especially after extraction of the radium as previously mentioned, or if dealing with samples from uranium tailings, where the uranium has been extracted during the milling process.

Similarly, for $^{228}Ra$, the photopeaks of its daughters $^{228}Ac$ at 338 KeV, 911 KeV, and 965 KeV were used.

Other investigators have reported the use of gamma-spectroscopy to determine uranium (45), thorium (45), and $^{210}Pb$ (46).

However, high-resolution gamma-detectors usually have a very low detector efficiency. Therefore, to achieve good counting statistics, a large sample and a long counting time are needed.

### 6.1.4 Coincidence Spectroscopy

Coincidence spectroscopy has recently been reported for the determination of $^{224}Ra$, $^{226}Ra$ and $^{228}Ra$. The coincidence spectrometer consists of a NaI(Tl) gamma-detector, and an alpha- beta-detector which are connected to a coincidence analyzer and associated electronics (Chiu et al. (43)).

This technique is based on separate measurement of the coincident alpha-gamma transitions of $^{226}Ra$ and $^{224}Ra$, and the coincident beta-gamma transitions of $^{228}Ac$, the daughter of $^{228}Ra$. Chemical separation and purification of radium into a source is necessary. $^{224}Ra$ and $^{226}Ra$ are measured directly, and $^{228}Ra$ is measured indirectly via its daughter $^{228}Ac$ (6.13 hours).

### 6.1.5 Alpha-Spectroscopy

Alpha-spectroscopy involves the direct measurement of the alpha-emission from $^{226}Ra$. Source preparation usually involves coprecipitation of radium sulphate with barium sulphate. The spectral resolutions obtained depend on the quantity of barium carrier, the size of the barium sulphate crystals, and the presence of other insoluble impurities. However, when the quantity of the barium carrier is reduced to improve the resolution, the chemical yield decreases.

Lim and Dave, (47), reported alpha-resolutions of 229 KeV to 496 KeV (FWHM) for 100 µg to 1 mg of barium carrier, coupled with a chemical yield of 65% to 85%. The main advantage of this approach is that $^{133}Ba$, a gamma-emitter and a proven tracer for radium, is used for the chemical yield calculation.

Dean and Chiu, (48), reported alpha-resolutions of 120, 156 and 221 KeV (FWHM) for 68, 138 and 276 µg of barium carrier, respectively.

Sill (49) indicated recently that with complete sample dissolution, a modification of barium precipitation procedure, and removal of insoluble impurities from all reagent solutions, a high alpha-resolution (60 KeV) and a high chemical yield can be obtained. Electron microscopy has shown that barium sulphate crystals obtained by normal precipitation from hot DPTA solution are angular and relatively large, at least 1 µm on a side. They tend to form a cluster on the membrane filter so that the fraction of the total available filter area actually covered is small. Consequently, the effective thickness of the deposit is much larger than for a uniform distribution of smaller crystals. On the other hand, barium sulphate crystals obtained by precipitation from DTPA solution at room temperature, using a barium sulphate seeding suspension, are almost amorphous (<1 µm), and cover the entire surface area of the filter.

The high resolution and low background of the solid state surface barrier detectors provide specificity and high sensitivity.

Based on these electronic properties and the simplicity of the chemical separation method for $^{226}Ra$ analysis, a field laboratory was set up in Elliot Lake, specializing in $^{226}Ra$ analysis. This field laboratory was designed especially to handle field investigation and research related to environmental studies surrounding uranium mining and milling activities across Canada.

For a laboratory manual of $^{226}Ra$ analysis used by the Elliot Lake Laboratory, see reference 47. Data pertaining to $^{226}Ra$ from Nordic tailings area were obtained using this manual. Some analyses were contracted out to Monenco Ltd. who used the technique described by Chiu et al. (43).

## 6.2 RADIUM-228 ($^{228}Ra$)

Because of the difficulty in measuring the very low energy beta emission of $^{228}Ra$ (0.055 MeV), all techniques reported to date are based on the indirect measurement of its daughters, $^{228}Ac$ (6.1 h half-life), $^{228}Th$ (1.9 y half-life), or $^{212}Pb$ (10.6 h half-life). The application of gamma spectroscopy and beta-gamma coincidence spectroscopy has been discussed earlier.

The most widely used technique is beta counting of $^{228}Ac$, which requires less than two days for equilibration between $^{228}Ra$ and $^{228}Ac$.

A few procedures use alpha-spectroscopy to measure the long-lived daughter $^{228}Th$ or beta-counting of the short-lived daughter $^{212}Pb$. Both of these procedures require 6-12 months for the ingrowth of daughters which is unacceptable for routine measurement.

$^{228}Ra$ must be separated from other radionuclides before its daughter $^{228}Ac$ is allowed to grow in. A faster and more efficient method is used by Chiu and Dean (50). Radium is separated and purified in the form of barium-radium sulphate. After the ingrowth of $^{228}Ac$, the sulphate is redissolved in alkaline EDTA or DTPA and the $^{228}Ac$ is precipitated as hydroxide with cerous hydroxide as a carrier and collected on a membrane filter for immediate beta-counting. The entire procedure takes less than 30 min, which permits the preparation of one sample to be completed just as the beta-counting of another sample is finished, thereby reducing the risk of decreased

sensitivity while an $^{228}Ac$ source is waiting to be counted (Chiu et al. (43)).

## 6.3 LEAD-210 ($^{210}Pb$)

The radioactivity of $^{210}Pb$ is normally measured indirectly by alpha-counting of its daughter $^{210}Po$ (5.3 MeV, 138 d half-life), or by beta-counting of its daughter $^{210}Bi$ (1.17 MeV, 5 d half-life) because of the low energy beta emission of $^{210}Pb$ (0.018 MeV).

The appropriate methodology depends on the state of equilibrium between $^{210}Pb$, $^{210}Po$ and $^{210}Bi$ (Chiu et al. (43)).

### 6.3.1 Lead-210 ($^{210}Pb$) in Equilibrium With Polonium-210 ($^{210}Po$)

If radioactive equilibrium is known to exist, the measurement of $^{210}Po$ by alpha-spectroscopy is preferred. $^{210}Po$ in aqueous solution can be extracted by spontaneous deposition as the free element on a disc of a less noble metal, such as copper, nickel or silver. Copper or nickel are better than silver for the extraction of $^{210}Po$, although nickel also extracts $^{210}Bi$ and $^{210}Pb$ (up to 20%). However, since $^{210}Po$ is an alpha-emitter, and $^{210}Bi$ and $^{210}Pb$ are beta-emitters, this method is specific for the indirect determination of $^{210}Pb$. It is very sensitive because of the high-resolution alpha source obtained. The chemical procedure is relatively short and the plating can be done in two hours at 60-65°C, and $^{208}Po$ which is also an alpha-emitter is recommended as a tracer.

### 6.3.2. Lead-210 ($^{210}Pb$) in Disequilibrium

In most of the uranium tailings studies, the degree of radioactive equilibrium is unknown, however, in this case three techniques are available.

The first method is to measure $^{210}Po$ in a sample three to six months after the removal of initial $^{210}Po$ by spontaneous deposition on a nickel

disc. The second method is to measure the $^{210}Bi$ ingrowth five or more days after separating $^{210}Pb$ from the sample, and the third method is to allow the sample to age for 30 days after separation of $^{210}Pb$ from the sample, during which time complete equilibrium between $^{210}Pb$ and $^{210}Bi$ will be ensured to be greater than 98%. The $^{210}Bi$ is separated from $^{210}Pb$ and determined by beta-counting.

### 6.3.3 Lead-210 ($^{210}Pb$) Separation

$^{210}Pb$ can be separated by several techniques such as electroplating, solvent extraction, ion exchange chromatography and electrochromatography. All these techniques are labour-intensive and very time-consuming.

The simplest method involves a single extraction of $^{210}Bi$ with an 0.1% solution of DDTC in chloroform from a 2 N hydrochloric acid solution. $^{210}Bi$ is subsequently precipitated as bismuth oxychloride and collected on a membrane filter for beta-counting, and $^{207}Bi$ gamma-emiting tracer is used for chemical recovery measurement (Chiu et al. (43)).

A recent report by Schery (51) indicates that the direct measurement of a 47 KeV photon emitted by $^{210}Pb$ has not been successful in the past because of the self-absorption in the sample and the low sensitivity to low-energy photons.

However, a new generation of high purity N-type germanium detectors now available are characterized by improved sensitivity to low energy photons and increased active surface area. Therefore, direct assay of $^{210}Pb$ in moderately sized environmental samples may be possible by measuring the 47 KeV photon.

## 6.4 THORIUM ISOTOPES

The long-lived thorium isotopes from the uranium and thorium series, such as $^{230}Th$ ($8 \times 10^4$ y half-life), $^{232}Th$ ($1.4 \times 10^{10}$ y half-life) and its

daughter $^{228}Th$ (1.91 y half-life, emit alpha-particles with energies of 4.6 MeV, 4.0 MeV and 5.3 MeV, respectively. They can be determined simultaneously after separation from all other radionuclides and deposited as a uniform and thin source for the best alpha spectrometric resolution.

The purification of thorium by solvent extraction has been found to be effective using bis(2-ethyl-hexyl)phosphoric acid, Aliquot-336, thenoyltrifluoroacetone, trilaurylamine, etc., and is also used in combination with ion exchange. Electrodeposition on a polished stainless steel disc has been found to be the best method of preparing a uniform thin source for the best resolution of alpha-spectroscopy. However, this method is time-consuming and requires elaborate electrodeposition apparatus.

Sill and Williams (52), have developed an alternative method. The purified thorium isotopes are precipitated as hydroxides with 50 µg of cerium carrier from a strongly alkaline solution of EDTA or DPTA and is collected on an 0.1 µm membrane filter for high resolution alpha-spectroscopy. For chemical recovery, $^{234}Th$ tracer is commonly used.

Another method uses a combination of high resolution gamma-spectroscopy and alpha-spectroscopy. $^{228}Th$ is measured on the original sample by gamma-spectroscopy, and the isotopic ratios of $^{228}Th$, $^{230}Th$ and $^{232}Th$ are determined by alpha-spectroscopy on the thorium source after extraction. By means of the $^{228}Th$ activity and the isotopic ratios so obtained, the activity of $^{230}Th$ and $^{232}Th$ are calculated (Durham et al. (53)).

Dean and Chiu (48) measured $^{228}Th$ indirectly via its $^{224}Ra$ daughter using alpha-spectroscopy. After ensuring equilibrium between $^{228}Th$ and $^{224}Ra$ (20 d half-life), $^{224}Ra$ is co-precipitated with barium sulphate for alpha-spectroscopy.

## 6.5 RADON

Radon isotopes occur in all three naturally occurring radioactive decay series. $^{222}Rn$ (3.82 d half-life) from the $^{238}U$ series, $^{219}Rn$ (4.0 s half-life) from the $^{235}U$ series, and $^{220}Rn$ (55.3 s half-life) from the $^{232}Th$ series.

Radon is an inert gas and the distance each isotope can travel from its origin depends on its half-life, and therefore $^{222}Rn$, which has the longest half-life (3.82 d) can be transported further.

The most common and simplest measurement technique is the counting of alpha-disintegrations in a Lucas cell as previously mentioned in $^{226}Ra$ determinations (Chapter 6.1.2).

There are other methods of radon determination, such as a pulse-type ionization counting chamber, track-etch detection, and thermoluminescence. The most appropriate technique largely depends on the application of the measured data.

However, in this thesis the discussion will be limited to the subject of disequilibrium of radioisotopes in groundwater, therefore, only sampling and radon determinations related to this subject will be mentioned. For instance the determination of dissolved $^{222}Rn$ in a water sample originating from an artesian well near Elliot Lake was as follows:

A water sample was collected in a 1 litre bottle. A rubber stopper with three port holes was used to seal the bottle, and a long length of tubing was installed far enough into one of the port holes to reach the bottom of the bottle. This port hole was used to sample the water by flooding the bottle from the bottom upward, thus preventing turbulence and degassing while sampling. Another long length of tubing attached to a bubbler was inserted into the second hole until it rested on the bottom of the bottle. This port hole was used to bubble radon gas out of the water.

The third port hole was connected to a short length of tubing as an outlet to transfer radon gas into a Lucas cell (2.5 mL) (Figure 6.2).

A water sample was taken by completely immersing a long length of tubing into an artesian well. A rubber cork with a hole in it was used to access the other end of the tubing, thus sealing the well and as such restricting the water flow through the tubing and preventing diffusion of radon gas before sampling. The tubing from the well was then connected to the first port hole in the sample bottle and the water sample was allowed to flow into the bottle by flooding it from the bottom upward. The water sample was allowed to overflow through port holes No. 2 and 3 for 5 min, after which it reached a steady state condition and the inlet tubing was disconnected. The excess water was decanted to a litre mark and all three port holes were plugged with clamps.

Radon gas was transferred in the laboratory using the vacuum pump transfer system and the alpha-disintegrations were counted after $^{222}Rn$ reached equilibrium with its daughters.

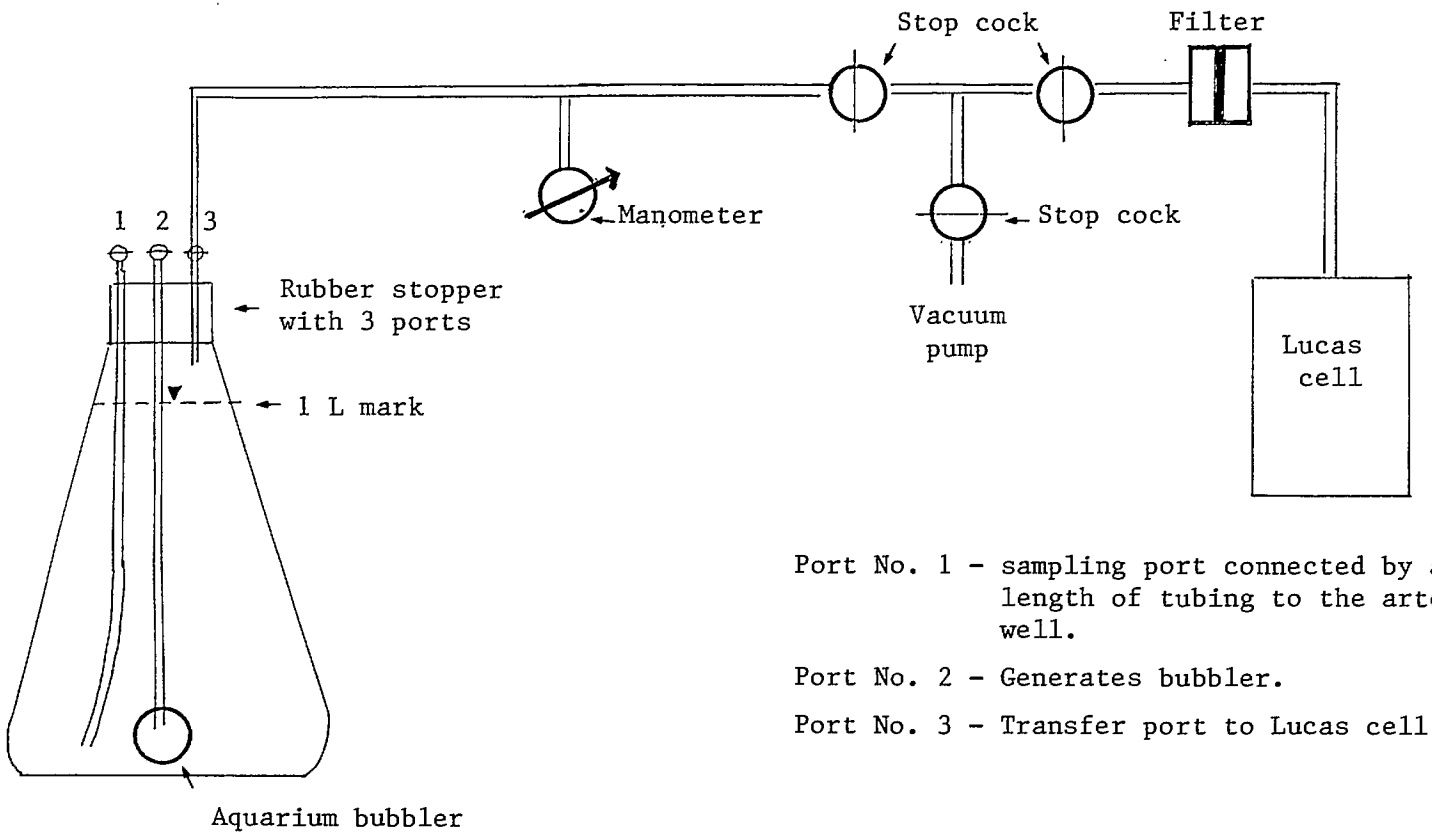


Port No. 1 - sampling port connected by a long length of tubing to the artesian well.

Port No. 2 - Generates bubbler.

Port No. 3 - Transfer port to Lucas cell

Fig. 6.2 - Radon bubbler and transfer system to Lucas cell.

# CHAPTER 7

## NORDIC MAIN TAILINGS - RESULTS AND DISCUSSION

Parts of the data pertaining to the Nordic Main uranium tailings project, which are necessary to form a general cross-section of the tailings pile, are displayed in this Chapter. The data for the solid samples are shown in Tables 7.1 to 7.8, and from 7.9 to 7.12 for the liquid phase porewater samples, respectively. Data for the radioisotope ratios in the solid tailings samples are displayed in Tables 7.13 to 7.16.

Additional data from location T-5 within the Nordic Main tailings are summarized in Tables 7.17 to 7.18. A general cross-sectional view of the Nordic Main tailings is shown in Figure 7.1, and a general flow pattern within the tailings pile is shown in Figure 7.2. The flow net patterns were drawn from interpretation of data from the hydraulic head measurements, and were translated into equipotential line contour mapping using the Kriging technique (53,54).

The Kriging technique is a method used to create a grid pattern using a regional variable theory. The Kriging algorithm assumes an underlying linear variogram, which produces a more accurate contour in comparison to the conventional inverse distance algorithm (Surfer $^{TM}$ version 3.0) (54).

Results for the chemical and radioisotope stratification at various depths for each station are presented in units of µg/g or mBq/g for solid samples, and in mg/L or mBq/L for liquid phase porewater samples, respectively, and are plotted in Figures 7.3 to 7.55. Only the parts of the stratification figures, which are related to the subject of radioisotope disequilibrium are presented here. For example, the stratification figures for thorium and uranium in the solid tailings originating from locations T-1, T-2, T-3, T-7 and T-8 are presented in Figures 7.3 to 7.12, respectively, and

for the liquid phase porewater samples, are presented in Figures 7.13 to 7.17, respectively.

Results for the stratification of lead content in the solid and liquid phases are presented in Figures 7.18 to 7.25, respectively. $^{210}Pb$ content is presented in Figures 7.26 to 7.30. $^{226}Ra$ content is presented in Figures 7.31 to 7.40. The stratification of $^{228}Th$, $^{230}Th$ and $^{232}Th$ of solid tailings samples from locations T-1, T-2, T-3, T-7 and T-8 are presented in Figures 7.41 to 7.55, respectively. No thorium isotope data were obtained from the liquid phase porewater samples.

Contour maps outlining the concentration intervals of the tailings cross-section, from North to South, are presented in Figures 7.56 to 7.90. The stratification figures and the contour maps were derived from data obtained from Tables 7.1 to 7.12.

The distribution coefficient $K_d$ is a widely used parameter in studies of groundwater contamination, which reflect the partitioning of solutes between liquid and solid phases in a porous medium, and can be expressed as:

$$K_d = \frac{\text{mass of solute on the solid phase/unit mass of solid phase}}{\text{concentration of solute in solution}}$$

The measured $K_d$ values are normally reported in mL/g (Freeze and Cherry, Chapter 9 (53)).

The distribution coefficients for sulphate are presented in Figures 7.62 and 7.63 (Table 7.14). The first figure is based on the partitioning of the liquid phase and the bulk mass of sulphate in the solid phase. The second figure reflects the partitioning between the liquid phase and the mass of sulphate adsorbed, or precipitated on the solids per gram of bulk dry tailings.

The major difference between the two sets of sulphate data is the procedure for the pretreatment of samples prior to sulphate analyses. The

bulk mass of sulphate in the solid phase was obtained by fusing the solid tailings sample using borax flux, which resulted in a complete dissolution of the solids. This pretreatment method gave an abnormally high reading of the measured sulphate level in the solid phase which did not reflect the true value of the adsorbed or precipitated sulphate on the solid. This method is simpler and more economical to perform. The second data sets were obtained by leaching the adsorbed and precipitated sulphate out of the solid. This pretreatment method gave a more accurate set of data regarding the partitioning between the liquid phase and the adsorbed or precipitated sulphate on the solid, however, it is time consuming and results vary from sample to sample unrepeatably since the measurement depends on the size distribution, i.e., the sample cannot be homogenized by pulverizing it prior to analysis.

Comparison of the contour shapes between Figures, 7.62 and 7.63, indicate that both show the same trend, i.e., enrichment of sulphate in the liquid phase as the porewater moves downward (Figure 7.2), and the calcium distribution coefficient seems to follow the same trend as sulphate (Figure 7.69). This probably occurred because these constituents exist in the form of calcium sulphate (Dalton) (38-40). The magnesium distribution coefficient, Figure 7.72, also follows the same trend as calcium, i.e., enrichment of magnesium in the liquid phase as the porewater moves downward (Figure 7.2).

The distribution coefficients for Fe, Al, Th and U, show reverse trends to those for the sulphate, i.e., enrichment of Fe, Al, Th and U into the solid phase either by adsorption or reprecipitation as the porewater moves downward. The results are shown in Figure 7.66, 7.75 and 7.78, respectively.

These events are very well known, since these species, especially Fe,

Al, U, Th and Pb are pH dependent. As the porewater moves downward from the low pH zone within the upper layer of the water table, it carries leachable products, such as heavy metals and other trace elements. The porewater gradually reacts with a buffering agent within the tailings pile, such as calcium carbonate and calcium hydroxide (lime), which were added as a neutralizing agents in the mill circuit before discharge into the tailings pond. Therefore, the pH is gradually increased as the porewater moves downward, and at the same time Al, Fe, U, Th and Pb are reprecipitated with the increase of pH. Most of the trace elements, such as radium, and probably protactinium, actinium, polonium, bismuth and thalium are dependent on other scavenger elements, such as aluminium, iron and manganese as hydroxide to coprecipitate with, or barium if present, in the solution (47.57). However, the study of scavenging is beyond the scope of this work.

As these elements move downward from the upper layer of the water table, their concentration in the water phase diminishes, and their concentration in the solid phase shows enrichment as a product of reprecipitation, coprecipitation and adsorption (1,4,16-21,27-32).

The activity ratios of daughter/parent isotopes within the solid tailings are shown in Figures 7.91 to 7.93 (Tables 7.13 to 7.16). The activity ratios for $^{210}Pb/^{226}Ra$ show an expected secular disequilibrium pattern with a ratio of less than 1.0 (Figure 7.91). However, the activity ratios for $^{226}Ra/^{230}Th$ and $^{228}Th/^{232}Th$ show an unusual pattern with a high ratio of approximately 20:1 close to the surface of the tailings which decreases with depth on approaching 1.0 at the peat layer.

Unfortunately, no analyses of $^{210}Pb$, $^{224}Ra$, $^{228}Th$, $^{230}Th$ or $^{232}Th$ on the liquid phase were performed, therefore, there are no activity ratio data available for comparison with liquid samples from T-1, T-2, T-3, T-7 or T-8

cross-sections. However, limited data are available for the T-5 location (Tables 7.17 and 7.18) and the results show that the activity ratio between daughter/parent, especially for $^{210}Pb/^{226}Ra$ ratio in the liquid phase is as high as 164, and is approximately 200 times larger than the ratio in the solid phase. These ratios are very puzzling since, in general, it is expected that secular equilibrium should exist between the short-lived daughters and long-lived parents, and at least, if disequilibrium should exist, the ratio of daughter to parent should be less than 1.0, or within the permissible statistical limit of the analytical method used. This type of secular disequilibrium should be called paradoxical secular disequilibrium since its behaviour is very irregular and beyond the boundary of the expected ratio for secular equilibrium. There were a number of arguments in the past caused by misunderstanding, since most of the time researchers are concentrating their efforts on finding the solution to the problems by investigating only the liquid phase. This paradoxical secular disequilibrium behaviour of radioisotopes has some similarity with most of the data observed by other investigators in Chapter 3 (1-26).

However, if one reviews the other basic rule of secular equilibrium, that the sample should be undisturbed, and no parent or daughter substances removed or allowed to escape for a time long enough for secular equilibrium to be established, then it is expected, that if parts of the daughters or the parents are removed, disequilibrium will exist in the total bulk mass. Also, in the solid phase, if the parent is removed by a leaching process, or a daughter is gained by reprecipitation and adsorption at a rate faster than the time required to gain equilibrium, then a paradoxical secular disequilibrium may exist. A paradoxical secular disequilibrium also exists in the liquid phase, if the daughter activity is gained by preferential leaching, or if the parent isotopes reprecipitate at a faster rate than the

time needed to reach equilibrium.

As an example, let us compare the solubilities of the three main elements in Figure 7.91 to 7.93, i.e., radium, lead, uranium and thorium with the majority of the anion as sulphate. The solubilities of the sulphate salts are obtained from the Handbook of Chemistry and Physics (55) and tabulated in Table 7.19. The solubility table shows that radium sulphate is almost insoluble, followed by lead sulphate, thorium sulphate, and uranium sulphate which is very soluble. Therefore, it can be shown and concluded here, that the behaviour of the activity ratio distribution of $^{210}Pb/^{226}Ra$ (less than 1.0) in the solid tailings cross-section is caused by preferential leaching or removal of $^{210}Pb$ from the solid phase over $^{226}Ra$, and at a faster rate than $^{226}Ra$, decays into $^{210}Pb$ to reach secular equilibrium (Figure 7.91).

The activity ratio in the liquid phase is controlled more by the pH, solubility or chemical equilibrium constant of $^{210}Pb$ $(SO_4)$, and $^{226}Ra$ $(SO_4)$, and the residence time of the porewater (Chapter 7, Freeze and Cherry (53)). This ratio is sometimes extremely high, caused by the higher availability of $^{210}Pb$ with the increase of $^{226}Ra$ activity present in the bulk mass, and a higher solubility with decreases in pH.

It can also be shown that a similar process occurs for the $^{226}Ra/^{230}Th$ activity ratio in the solid phase, where thorium sulphate is more soluble, and therefore is more easily leached than the radium sulphate (Figure 7.92).

The differences in the activity ratios of $^{226}Ra/^{230}Th$ from $^{210}Pb/^{226}Ra$, i.e., $^{226}Ra/^{230}Th$ values, are mostly between 1 to 10, caused by the long half-life of $^{230}Th$ (half-life = $8x10^4$ y), and therefore, long production time to produce $^{226}Ra$. Because of the high solubility of thorium sulphate, the $^{230}Th$ was removed faster by the leaching process than its production rate for $^{226}Ra$.

Whatever the initial $^{226}Ra$ activity was, this isotope was assumed to be in equilibrium with $^{230}Th$ at the time of the initial tailings disposal from the milling process. $^{226}Ra$ is leached at a much slower rate than the $^{230}Th$, and therefore, reflects a higher activity ratio, larger than 1.0 in the solid sample.

$^{210}Pb$ is a product of a much faster rate of decay from $^{226}Ra$ (1.6 x $10^3$ y), and since the lead sulphate solubility is much lower than $^{230}Th$ sulphate, but much higher than radium sulphate, it is therefore, possible for $^{210}Pb$ to build up its activity to near secular equilibrium as the geochemical dynamic leaching process of the tailings continues to leach lead sulphate faster than the radium sulphate. This results in an activity ratio of less than 1.0 in the solid phase.

Another interesting case is the activity ratio of $^{228}Th/^{232}Th$, in which the activity ratio shows a similar trend to that in $^{226}Ra/^{230}Th$, although $^{228}Th$ and $^{232}Th$ belong to the same species and have the same chemical property (solubility). The $^{232}Th$ decay series (Figure 6.1) shows that $^{228}Th$ is a product of a decay series from $^{232}Th \rightarrow {}^{228}Ra \rightarrow {}^{228}Ac \rightarrow {}^{228}Th$, and therefore, $^{228}Th$ is not a direct product of $^{232}Th$. It is assumed that the activity ratio of $^{228}Ra/^{232}Th$ was initially at, or near, secular equilibrium for the tailings deposited, and as the dynamic geochemistry process continued, the $^{232}Th$ was leached at a much faster rate than the $^{228}Ra$.

On taking into account that the half-lives of $^{232}Th$ (1.4 x $10^{10}$ y), and $^{228}Ra$ (6.7 y), to $^{228}Ac$ (6.1 h), and to $^{228}Th$, it can be concluded that $^{228}Ra$ is the controlling factor causing the segregation of $^{232}Th$ and $^{228}Th$.

It has been shown that in the low pH water carrying the leached product of $^{232}Th$, the $^{228}Ra$ movement is retarded by the low solubility of radium sulphate, and $^{228}Th$ is continuously generated by $^{228}Ra$, resulting in a

trend of activity ratio similar to $^{226}Ra/^{230}Th$, which has a high ratio near the surface of the tailings pile and decreases downward towards a ratio of 1.0 near the peat layer.

According to Veska (26), similar cases with a sharp rise of $^{234}U/^{238}U$ in the liquid phase and a continued trend of relative $^{234}U$ enrichment were attributed to a scenario requiring preferential leaching of $^{234}U$ in the $6^+$ oxidation state ($UO_2^+$), a stronger absorption of $^{238}U$ (as $U^{4+}$), over $^{234}U$ (as $UO_2^+$) in the sand aquifer, and little redox exchange between the 4+ and 6+ state. This explanation is not entirely valid, as was mentioned by Morin (27), since $^{238}U$ or $^{234}U$ can exist in a 4+, 5+ or 6+ state.

However, preferential leaching for $^{234}U/^{238}U$ exists, and can also be caused differently, for example, in a scenario where the initial activity ratios of $^{238}U$, $^{234}Th$, $^{234}Pa$ and $^{234}U$ in the solid phase are in secular equilibrium. As the solid phase is leached by low pH water, the $^{238}U$ and $^{234}U$ leach out at an equal ratio, since they both behave as chemical uranium.

Our results show that $^{234}Th$ and $^{234}Pa$ were leached out at a lower rate than the uranium (uranium sulphate is more soluble than thorium sulphate, see Table 7.19). We expect that the movement of $^{234}Th$ could be retarded, resulting in enrichment of $^{234}Th$ in the solid phase, and at the same time $^{234}Th$ decays and generates its daughter $^{234}Pa$, which also decays into $^{234}U$. Since the half-life of $^{234}Th$ and $^{234}Pa$ is very short in comparison to $^{238}U$ and $^{234}U$, the increase of $^{234}U$ activity is also very rapid. Thus, the actual rapid increase of $^{234}U/^{238}U$ activity ratio in the liquid phase can be attributed to the additional activity of $^{234}U$ in the liquid phase through the retardation of $^{234}Th$ movement in the solid phase. Therefore, the $^{234}U/^{238}U$ activity ratio in the liquid phase reflects the enrichment of $^{234}Th$ in the solid phase and it increases with distance from the source as the $^{234}Th$ generates $^{234}U$.

CBCL Ltd. (58), claimed that $^{234}U/^{238}U$ activity ratio in the uraniferous peat samples, averaging 1.13, was attributed to the mass recoil and ejection of $^{234}U$ from $^{238}U$ in the uranium ore bearing mineral when $^{238}U$ decays, resulting in higher solubility of $^{234}U$ than $^{238}U$. Assuming that:

- all uranium originally dissolved in the groundwater was precipitated or adsorbed within the peat (supported by $^{234}U/^{238}U$ ratios);
- $^{230}Th$ has low solubility (i.e., no $^{230}Th$ was transported off site);
- all of the $^{232}Th$ produced remained in the deposit; and
- $^{238}U$ and $^{234}U$ are in equilibrium, then $^{238}U$ activity could be estimated and adjusted from the measured total uranium concentration. Therefore, CBCL Ltd. concluded that the peat layer is a recent deposit (i.e., less than 10,000 to 15,000 years) since little time has been available for the ingrowth of radionuclide daughter products of uranium (Table 21 of CBCL report (58)). The deposition of uranium within the peat deposit is considered to be an on-going process.

The explanation given for $^{234}U/^{238}U$ ratio of 1.13 average as being caused by mass recoil and ejection of $^{234}U$ from $^{238}U$ is probably inaccurate. As mentioned earlier, $^{234}U$ is not a direct daughter of $^{238}U$. Mass recoil and ejection of daughters can also happen to $^{234}Th$ and $^{234}Pa$ during their decay chains.

$^{234}Th$ (24.1 d) and $^{234}Pa$ (1.2 m) could disappear quickly from the solution because of its short half-life and transform through decay chains into $^{234}U$ ($2.5 \times 10^5$ y), therefore resulting in a higher activity ratio of $^{234}U/^{238}U$ in groundwater, consistent with those of soil samples. In Table 21 of the CBCL Ltd. report (58), the age of the uranium mineralization within the deposit was estimated from the ratios of measured $^{230}Th$ activities and calculated $^{238}U$ activities and the decay rate of uranium. As was mentioned by CBCL, the uranium deposition is considered to be an on-going process,

i.e., the hydrogeochemical process is very active. Thus it can be concluded that the age measurement, as reported by CBCL Ltd., could be seriously in error since $^{234}U$ could be added to the peat layer as the dynamic hydrogeochemical process is actively on-going. Thus, the more $^{234}U$ added to the peat layer, the more $^{230}Th$ will be produced, and hence the $^{230}Th/^{238}U$ ratio could be higher than expected. Maybe it would be better if the age dating was determined using a $^{230}Th/^{234}U$ activity ratio instead of $^{238}U$, assuming that $^{230}Th$ is not in the peat layer to begin with.

Therefore, one must be very careful when interpreting data for the dynamic decay chain, especially when dealing with radiochemistry and related subjects, such as radioactive dating, uptake of radioactive materials into biological matter as part of the food chain, etc. within the hydrogeochemical dynamic environmental conditions.

It can be concluded here, that the solid phase system is acting as an indicator of the long term results of hydrogeochemical evolution, which appears to be a very slow-moving process. Solid phase results are extremely valuable in the study of the evolution of radioisotope species from the uranium tailings. In comparison, the liquid phase system is a much faster short term indicator of what happens from day to day, and sometimes the changes are so rapid, such as the oxidation mechanism of iron species, that complex problems arise in the design of mathematical models for the long term tailings events. There are many more parameters to deal with in the liquid phase.

On the basis of our studies, we conclude that when dealing with the solid phase, especially with the radioisotope species, a non-destructive analytical method, such as the use of borehole spectral gamma-logging could be more economical, even though it will probably require a longer time interval for sampling. The mathematical modelling could probably be

simplified by using only an empirical model.

However, both solid and liquid phases exist together, and at the present time interest is concentrated in the effluent discharge, which is directly related to environmental pollution control. The liquid phase is still the major issue in this tailings study. Studies of the solid phase serve to enhance our knowledge of the hydrogeochemical evolution.

Our study has shown that, when dealing with hydrogeochemical processes and field data interpretation for radioisotope migration, one must have an in-depth understanding of the physics of radioisotope decay, the chemical behaviour of the isotopes, and the groundwater hydrology of the system.

A laboratory test to demonstrate the paradoxical secular disequilibrium and hydrogeochemical processes will be discussed in Chapter 8.

Table 7.1 - Nordic main tailings data. Solid phase sample results of chemical and radioisotope analyses from locations T-1, T-2, T-3, T-7 and T-8 at various depths in concentration/gram.

||Solid Sample Study

| SAMPLE DESCRIPTION DEPTH (m) | Northing (m) (x10) | Elevation (m) | Pb-210 (mBq/g) +/-10% | Ra-224 (mBq/g) | Ra-226 (mBq/g) +/-10% | Th-228 (mBq/g) +/-20% | Th-230 (mBq/g) +/-20% | Th-232 (mBq/g) +/-20% | Al (mg/100g) | Ca (mg/g) | Fe (mg/g) |
|---|---|---|---|---|---|---|---|---|---|---|---|
| T - 1 - 1.00 | 544.80 | 350.79 | 13764.0 | | 17760.0 | 3219.0 | 1258.0 | 185.0 | 3840 | 13.65 | 9.30 |
| T - 1 - 1.50 | 544.80 | 350.79 | 7955.0 | | 9768.0 | 703.0 | 5106.0 | 851.0 | | | |
| T - 1 - 2.00 | 544.80 | 350.79 | 15873.0 | | 21201.0 | 1813.0 | 22126.0 | 2738.0 | | | |
| T - 1 - 2.00 | 544.80 | 350.79 | 15947.0 | | 17131.0 | 2220.0 | 23199.0 | 3034.0 | | | |
| T - 1 - 2.00 | 544.80 | 350.79 | 17760.0 | | 21423.0 | 2775.0 | 23680.0 | 3034.0 | 3919 | 35.30 | 24.50 |
| T - 1 - 2.50 | 544.80 | 350.79 | 13653.0 | | 14171.0 | 1073.0 | 8991.0 | 1332.0 | | | |
| T - 1 - 3.00 | 544.80 | 350.79 | 11803.0 | | 14726.0 | 888.0 | 13209.0 | 1332.0 | 3806 | 21.58 | 26.80 |
| T - 1 - 4.00 | 544.80 | 350.79 | 15799.0 | | 14245.0 | 407.0 | 2035.0 | 999.0 | | | |
| T - 1 - 4.00 | 544.80 | 350.79 | 18537.0 | | 18056.0 | 2368.0 | 9805.0 | 2627.0 | | | |
| T - 1 - 4.00 | 544.80 | 350.79 | 15799.0 | | 18167.0 | 1443.0 | 6327.0 | 1147.0 | | | |
| T - 1 - 4.25 | 544.80 | 350.79 | 12950.0 | | 12506.0 | 888.0 | 2775.0 | 962.0 | | | |
| T - 1 - 4.50 | 544.80 | 350.79 | 5846.0 | | 6105.0 | 333.0 | 851.0 | 148.0 | | | |
| T - 1 - 4.60 | 544.80 | 350.79 | 10471.0 | | 11840.0 | 814.0 | 8325.0 | 962.0 | | | |
| T - 1 - 4.75 | 544.80 | 350.79 | 32264.0 | | 21830.0 | 3330.0 | 6660.0 | 2035.0 | | | |
| T - 1 - 5.00 | 544.80 | 350.79 | 14615.0 | | 15540.0 | 2183.0 | 6919.0 | 1517.0 | | | |
| T - 1 - 5.25 | 544.80 | 350.79 | 31968.0 | | 25752.0 | 1036.0 | 3182.0 | 999.0 | | | |
| T - 1 - 5.50 | 544.80 | 350.79 | 12950.0 | | 13653.0 | 1036.0 | 1924.0 | 888.0 | | | |
| T - 1 - 5.75 | 544.80 | 350.79 | 13135.0 | | 16132.0 | 666.0 | 2701.0 | 851.0 | | | |
| T - 1 - 6.00 | 544.80 | 350.79 | 15651.0 | | 15836.0 | 407.0 | 3885.0 | 1221.0 | 3053 | 14.65 | 32.50 |
| T - 1 - 6.00 | 544.80 | 350.79 | 16502.0 | | 18500.0 | 1480.0 | 5106.0 | 1332.0 | 3022 | 15.15 | 32.50 |
| T - 1 - 6.00 | 544.80 | 350.79 | 18796.0 | | 18537.0 | 1517.0 | 6031.0 | 1295.0 | | | |
| T - 1 - 6.00 | 544.80 | 350.79 | 12950.0 | | 14208.0 | 1147.0 | 11729.0 | 1332.0 | | | |
| T - 1 - 6.25 | 544.80 | 350.79 | 10175.0 | | 9398.0 | 1036.0 | 3145.0 | 925.0 | | | |
| T - 1 - 6.50 | 544.80 | 350.79 | 13542.0 | | 14134.0 | 592.0 | 2664.0 | 592.0 | | | |
| T - 1 - 6.75 | 544.80 | 350.79 | 8806.0 | | 8954.0 | 370.0 | 2146.0 | 888.0 | | | |
| T - 1 - 7.00 | 544.80 | 350.79 | 19277.0 | | 14430.0 | 481.0 | 3885.0 | 814.0 | | | |
| T - 1 - 7.00 | 544.80 | 350.79 | 12247.0 | | 13468.0 | 740.0 | 4847.0 | 592.0 | 2890 | 9.55 | 33.50 |
| T - 1 - 7.25 | 544.80 | 350.79 | 5883.0 | | 4810.0 | 74.0 | 259.0 | 74.0 | | | |
| T - 1 - 7.40 | 544.80 | 350.79 | 17057.0 | | 20609.0 | 2331.0 | 9398.0 | 1036.0 | | | |
| T - 1 - 7.50 | 544.80 | 350.79 | 8954.0 | | 10989.0 | 296.0 | 2516.0 | 481.0 | | | |
| T - 1 - 7.60 | 544.80 | 350.79 | 10619.0 | | 12728.0 | 962.0 | 6031.0 | 703.0 | | | |
| T - 1 - 7.60 | 544.80 | 350.79 | 10619.0 | | 12469.0 | 2627.0 | 6697.0 | 777.0 | | | |
| T - 1 - 7.60 | 544.80 | 350.79 | 10360.0 | | 11507.0 | 666.0 | 8695.0 | 1332.0 | 3810 | 17.25 | 34.00 |
| T - 1 - 7.75 | 544.80 | 350.79 | 16539.0 | | 15096.0 | 555.0 | 2590.0 | 703.0 | | | |
| T - 1 - 8.00 | 544.80 | 350.79 | 3885.0 | | 6068.0 | 2109.0 | 14393.0 | 1036.0 | 2326 | 7.90 | 37.00 |
| T - 1 - 8.00 | 544.80 | 350.79 | 23754.0 | | 19610.0 | 1813.0 | 6105.0 | 2035.0 | | | |
| T - 1 - 8.25 | 544.80 | 350.79 | 35853.0 | | 24494.0 | 2627.0 | 6364.0 | 1554.0 | | | |
| T - 1 - 8.50 | 544.80 | 350.79 | 19388.0 | | 22459.0 | 925.0 | 7770.0 | 1036.0 | | | |
| T - 1 - 8.50 | 544.80 | 350.79 | 24901.0 | | 19092.0 | 666.0 | 2960.0 | 1036.0 | | | |
| T - 1 - 8.50 | 544.80 | 350.79 | 26307.0 | | 20239.0 | 3145.0 | 10360.0 | 2775.0 | | | |
| T - 1 - 9.00 | 544.80 | 350.79 | 18759.0 | | 20239.0 | 1924.0 | 14948.0 | 1554.0 | | | |
| T - 1 - 9.00 | 544.80 | 350.79 | 18685.0 | | 21497.0 | 1665.0 | 14652.0 | 1480.0 | | | |
| T - 1 - 9.00 | 544.80 | 350.79 | 15725.0 | | 18241.0 | 2738.0 | 16428.0 | 1887.0 | 5053 | 45.15 | 33.30 |
| T - 1 - 9.60 | 544.80 | 350.79 | 16761.0 | 1295.0 | 13579.0 | 1476.3 | 18107.8 | 1587.3 | 5785 | 41.60 | 39.50 |
| T - 1 - 9.60 | 544.80 | 350.79 | 17908.0 | 1480.0 | 17782.2 | 1968.4 | 22618.1 | 2234.8 | 6475 | 43.70 | 37.00 |
| T - 1 -10.20 | 544.80 | 350.79 | 20646.0 | 2849.0 | 20398.1 | 2886.0 | 26551.2 | 2667.7 | 6000 | 42.60 | 37.00 |
| T - 1 -10.60 | 544.80 | 350.79 | 621.6 | 74.0 | 3307.8 | 59.2 | 292.3 | 25.9 | 946 | 22.00 | 4.07 |
| T - 1 -10.70 | 544.80 | 350.79 | 218.3 | 74.0 | 266.4 | 55.5 | 310.8 | 77.7 | 1676 | 17.45 | 2.32 |

Table 7.2 - Nordic main tailings data. Solid phase sample results of chemical and radioisotope analyses from locations T-1, T-2, T-3, T-7 and T-8 at various depths in concentration/gram.

||Solid Sample Study

| SAMPLE DESCRIPTION DEPTH (m) | Northing (m) (x10) | Elevation (m) | Pb-210 (mBq/g) +/-10% | Ra-224 (mBq/g) | Ra-226 (mBq/g) +/-10% | Th-228 (mBq/g) +/-20% | Th-230 (mBq/g) +/-20% | Th-232 (mBq/g) +/-20% | Al (mg/100g) | Ca (mg/g) | Fe (mg/g) |
|---|---|---|---|---|---|---|---|---|---|---|---|
| T - 1 -10.77 | 544.80 | 350.79 | 12062.0 | 2072.0 | 13908.3 | 1857.4 | 18396.4 | 1713.1 | 4125 | 43.00 | 22.32 |
| T - 1 -10.80 | 544.80 | 350.79 | 225.7 | 70.3 | 336.7 | 85.1 | 188.7 | 51.8 | 2454 | 8.85 | 4.54 |
| T - 1 -11.18 | 544.80 | 350.79 | 484.7 | 122.1 | 588.3 | 129.5 | 762.2 | 136.9 | 5837 | 12.20 | 16.80 |
| T - 1 -12.57 | 544.80 | 350.79 | 18796.0 | | 17168.0 | 2146.0 | 25345.0 | 2442.0 | | | |
| T - 2 - 1.00 | 518.74 | 351.58 | 14689.0 | | 16391.0 | 370.0 | 444.0 | 22.2 | 3779 | 24.25 | 6.30 |
| T - 2 - 1.40 | 518.74 | 351.58 | 10138.0 | | 13764.0 | 666.0 | 1480.0 | 185.0 | | | |
| T - 2 - 2.00 | 518.74 | 351.58 | 12987.0 | | 17575.0 | 2886.0 | 18907.0 | 3293.0 | 3604 | 21.15 | 29.50 |
| T - 2 - 3.00 | 518.74 | 351.58 | 8140.0 | | 9805.0 | 1480.0 | 11211.0 | 1961.0 | | | |
| T - 2 - 4.00 | 518.74 | 351.58 | 14504.0 | | 12506.0 | 925.0 | 11211.0 | 1369.0 | | | |
| T - 2 - 4.00 | 518.74 | 351.58 | 18130.0 | | 16909.0 | 2220.0 | 10582.0 | 1221.0 | | | |
| T - 2 - 4.00 | 518.74 | 351.58 | 17834.0 | | 15762.0 | 1184.0 | 10841.0 | 1258.0 | | | |
| T - 2 - 4.60 | 518.74 | 351.58 | 15096.0 | | 15836.0 | 666.0 | 4921.0 | 629.0 | 3022 | 65.60 | 31.80 |
| T - 2 - 5.00 | 518.74 | 351.58 | 10693.0 | | 13061.0 | 2294.0 | 21090.0 | 2146.0 | | | |
| T - 2 - 5.79 | 518.74 | 351.58 | 22163.0 | | 18796.0 | 1332.0 | 11914.0 | 925.0 | | | |
| T - 2 - 6.02 | 518.74 | 351.58 | 25197.0 | | 23495.0 | 1628.0 | 17834.0 | 1776.0 | | | |
| T - 2 - 6.93 | 518.74 | 351.58 | 21571.0 | | 22829.0 | 1147.0 | 16465.0 | 1739.0 | | | |
| T - 2 - 7.24 | 518.74 | 351.58 | 32745.0 | | 27824.0 | 2479.0 | 22977.0 | 2442.0 | | | |
| T - 2 - 8.00 | 518.74 | 351.58 | 23495.0 | | 21978.0 | 2812.0 | 22718.0 | 2812.0 | 3984 | 44.80 | 39.50 |
| T - 2 - 8.31 | 518.74 | 351.58 | 14319.0 | | 14726.0 | 1184.0 | 10804.0 | 1591.0 | | | |
| T - 2 - 8.76 | 518.74 | 351.58 | 22089.0 | | 22459.0 | 2146.0 | 23569.0 | 2590.0 | | | |
| T - 2 - 8.76 | 518.74 | 351.58 | 21867.0 | | 25937.0 | 1887.0 | 21608.0 | 2849.0 | 5437 | 43.00 | 37.30 |
| T - 2 - 8.76 | 518.74 | 351.58 | 23902.0 | | 22866.0 | 1961.0 | 22903.0 | 2516.0 | | | |
| T - 2 - 9.07 | 518.74 | 351.58 | 33522.0 | | 26566.0 | 3626.0 | 29267.0 | 3256.0 | | | |
| T - 2 - 9.07 | 518.74 | 351.58 | 31968.0 | | 28897.0 | 3108.0 | 29822.0 | 3996.0 | | | |
| T - 2 - 9.07 | 518.74 | 351.58 | 30414.0 | | 26862.0 | 2997.0 | 28934.0 | 3737.0 | 6074 | 55.00 | 47.50 |
| T - 2 - 9.61 | 518.74 | 351.58 | 27491.0 | | 31931.0 | 3552.0 | 27306.0 | 3034.0 | 6026 | 60.40 | 46.00 |
| T - 2 - 9.77 | 518.74 | 351.58 | 37259.0 | | 42180.0 | 3996.0 | 42624.0 | 4810.0 | 5497 | 71.50 | 49.00 |
| T - 2 - 9.79 | 518.74 | 351.58 | 27972.0 | 2664.0 | 35786.4 | 2934.1 | 48421.9 | 2941.5 | 6558 | 73.20 | 51.00 |
| T - 2 - 9.87 | 518.74 | 351.58 | 33633.0 | 5254.0 | 35989.9 | 4632.4 | 51788.9 | 5820.1 | 6050 | 49.50 | 50.00 |
| T - 2 - 9.94 | 518.74 | 351.58 | 27750.0 | 3034.0 | 29326.2 | 2856.4 | 35353.5 | 5220.7 | 5215 | 58.50 | 46.00 |
| T - 2 -10.15 | 518.74 | 351.58 | 321.9 | 7.4 | 492.1 | 14.8 | 236.8 | 37.0 | 898 | 18.20 | 9.93 |
| T - 2 -10.25 | 518.74 | 351.58 | 181.3 | 92.5 | 858.4 | 85.1 | 159.1 | 40.7 | 4032 | 7.80 | 5.00 |
| T - 2 -10.33 | 518.74 | 351.58 | 233.1 | 44.4 | 318.2 | 96.2 | 103.6 | 18.5 | 6144 | 17.05 | 18.00 |
| T - 3 - 1.00 | 509.62 | 350.83 | 15540.0 | | 17538.0 | 888.0 | 925.0 | 114.7 | | | |
| T - 3 - 1.30 | 509.62 | 350.83 | 12876.0 | | 13061.0 | 1221.0 | 6512.0 | 777.0 | | | |
| T - 3 - 2.00 | 509.62 | 350.83 | 9583.0 | | 9842.0 | 666.0 | 2516.0 | 222.0 | | | |
| T - 3 - 2.60 | 509.62 | 350.83 | 24383.0 | | 19055.0 | 1332.0 | 14800.0 | 1332.0 | | | |
| T - 3 - 3.00 | 509.62 | 350.83 | 11803.0 | | 10582.0 | 703.0 | 6549.0 | 703.0 | | | |
| T - 3 - 3.00 | 509.62 | 350.83 | 11655.0 | | 11618.0 | 555.0 | 7400.0 | 814.0 | | | |
| T - 3 - 3.00 | 509.62 | 350.83 | 11433.0 | | 11211.0 | 592.0 | 5846.0 | 666.0 | | | |
| T - 3 - 4.00 | 509.62 | 350.83 | 5476.0 | | 7511.0 | 407.0 | 1628.0 | 444.0 | 4435 | 39.40 | 30.50 |
| T - 3 - 4.30 | 509.62 | 350.83 | 26011.0 | | 27084.0 | 2183.0 | 23051.0 | 2553.0 | | | |
| T - 3 - 4.30 | 509.62 | 350.83 | 27232.0 | | 24457.0 | 1998.0 | 21904.0 | 2368.0 | | | |
| T - 3 - 4.30 | 509.62 | 350.83 | 27528.0 | | 23828.0 | 2072.0 | 21460.0 | 2257.0 | | | |
| T - 3 - 5.00 | 509.62 | 350.83 | 11359.0 | | 14874.0 | 1443.0 | 9250.0 | 1295.0 | 2787 | 14.25 | 28.50 |
| T - 3 - 6.93 | 509.62 | 350.83 | 48285.0 | | 49136.0 | 6549.0 | 41773.0 | 6808.0 | | | |
| T - 3 - 6.93 | 509.62 | 350.83 | 44474.0 | | 53465.0 | 4884.0 | 40959.0 | 6660.0 | 5619 | 61.40 | 38.50 |
| T - 3 - 6.93 | 509.62 | 350.83 | 48248.0 | | 44067.0 | 4514.0 | 39849.0 | 5661.0 | | | |

Solid Sample Data

Table 7.3 - Nordic main tailings data. Solid phase sample results of chemical and radioisotope analyses from locations T-1, T-2, T-3, T-7 and T-8 at various depths in concentration/gram.

||Solid Sample Study

| SAMPLE DESCRIPTION DEPTH (m) | Northing (m) (x10) | Elevation (m) | Pb-210 (mBq/g) +/-10% | Ra-224 (mBq/g) | Ra-226 (mBq/g) +/-10% | Th-228 (mBq/g) +/-20% | Th-230 (mBq/g) +/-20% | Th-232 (mBq/g) +/-20% | Al (mg/100g) | Ca (mg/g) | Fe (mg/g) |
|---|---|---|---|---|---|---|---|---|---|---|---|
| T - 3 - 7.25 | 509.62 | 350.83 | 20868.0 | | 19166.0 | 777.0 | 4551.0 | 1036.0 | | | |
| T - 3 - 7.25 | 509.62 | 350.83 | 22089.0 | | 17131.0 | 1924.0 | 4662.0 | 851.0 | | | |
| T - 3 - 7.25 | 509.62 | 350.83 | 19869.0 | | 22792.0 | 1887.0 | 5550.0 | 1295.0 | | | |
| T - 3 - 7.50 | 509.62 | 350.83 | 22089.0 | | 17427.0 | 1850.0 | 4810.0 | 1332.0 | | | |
| T - 3 - 7.54 | 509.62 | 350.83 | 22422.0 | | 24679.0 | 2294.0 | 24198.0 | 2664.0 | 4771 | 19.60 | 34.30 |
| T - 3 - 7.75 | 509.62 | 350.83 | 12839.0 | | 12617.0 | 851.0 | 2257.0 | 592.0 | | | |
| T - 3 - 7.85 | 509.62 | 350.83 | 28194.0 | | 32116.0 | 2849.0 | 41329.0 | 3848.0 | | | |
| T - 3 - 7.85 | 509.62 | 350.83 | 29489.0 | | 34891.0 | 4810.0 | 42328.0 | 4995.0 | | | |
| T - 3 - 7.85 | 509.62 | 350.83 | 28194.0 | | 37481.0 | 3071.0 | 39257.0 | 3515.0 | 4634 | 66.40 | 40.00 |
| T - 3 - 7.96 | 509.62 | 350.83 | 2479.0 | | 3071.0 | 296.0 | 1110.0 | 185.0 | | | |
| T - 3 - 7.97 | 509.62 | 350.83 | 29970.0 | | 27972.0 | 1184.0 | 3330.0 | 666.0 | | | |
| T - 3 - 8.01 | 509.62 | 350.83 | 1406.0 | | 1813.0 | 148.0 | 74.0 | 18.5 | | | |
| T - 3 - 8.06 | 509.62 | 350.83 | 518.0 | | 518.0 | 74.0 | 222.0 | 74.0 | 7243 | 18.85 | 42.50 |
| T - 3 - 8.29 | 509.62 | 350.83 | 418.1 | 74.0 | 710.4 | 88.8 | 1098.9 | 107.3 | | | |
| T - 3 - 8.53 | 509.62 | 350.83 | 1554.0 | 218.3 | 1872.2 | 203.5 | 1491.1 | 244.2 | 2938 | 14.25 | 34.00 |
| T - 7 - 1.00 | 496.41 | 351.95 | 10027.0 | | 12506.0 | 481.0 | 1184.0 | 148.0 | | | |
| T - 7 - 1.30 | 496.41 | 351.95 | 13949.0 | | 17094.0 | 888.0 | 2183.0 | 296.0 | | | |
| T - 7 - 2.00 | 496.41 | 351.95 | 8103.0 | | 12136.0 | 629.0 | 740.0 | 66.6 | | | |
| T - 7 - 3.00 | 496.41 | 351.95 | 16095.0 | | 19610.0 | 888.0 | 18870.0 | 1628.0 | | | |
| T - 7 - 3.00 | 496.41 | 351.95 | 10841.0 | | 11803.0 | 1147.0 | 17020.0 | 2516.0 | | | |
| T - 7 - 4.00 | 496.41 | 351.95 | 14615.0 | | 14615.0 | 1850.0 | 8436.0 | 1110.0 | | | |
| T - 7 - 5.00 | 496.41 | 351.95 | 12432.0 | | 17242.0 | 1480.0 | 9879.0 | 1332.0 | | | |
| T - 7 - 5.00 | 496.41 | 351.95 | 12506.0 | | 15096.0 | 1406.0 | 8658.0 | 999.0 | | | |
| T - 7 - 5.00 | 496.41 | 351.95 | 12247.0 | | 19425.0 | 2183.0 | 9805.0 | 1517.0 | | | |
| T - 7 - 6.00 | 496.41 | 351.95 | 11914.0 | | 15244.0 | 1406.0 | 8547.0 | 1184.0 | | | |
| T - 7 - 6.40 | 496.41 | 351.95 | 14245.0 | 1480.0 | 18437.1 | 1420.8 | 14448.5 | 1139.6 | 3293 | 15.43 | 32.80 |
| T - 7 - 6.90 | 496.41 | 351.95 | 30081.0 | 2960.0 | 29511.2 | 3204.2 | 28915.5 | 3193.1 | 4734 | 36.00 | 39.50 |
| T - 7 - 6.90 | 496.41 | 351.95 | 27972.0 | 2775.0 | 28342.0 | 2516.0 | 26880.5 | 3178.3 | 4531 | 33.95 | 34.30 |
| T - 7 - 7.00 | 496.41 | 351.95 | 26344.0 | | 31043.0 | 2072.0 | 17760.0 | 2886.0 | | | |
| T - 7 - 7.20 | 496.41 | 351.95 | 28194.0 | 2960.0 | 27539.1 | 3204.2 | 32844.9 | 3470.6 | 4463 | 40.00 | 39.50 |
| T - 7 - 7.70 | 496.41 | 351.95 | 14578.0 | 1517.0 | 14037.8 | 1716.8 | 15273.6 | 2604.8 | 3262 | 21.40 | 32.80 |
| T - 7 - 7.81 | 496.41 | 351.95 | 7770.0 | 444.0 | 5846.0 | 532.8 | 4181.0 | 377.4 | 2760 | 14.30 | 29.00 |
| T - 7 - 7.86 | 496.41 | 351.95 | 15355.0 | 2183.0 | 15318.0 | 1920.3 | 16265.2 | 2379.1 | 4550 | 22.05 | 37.00 |
| T - 7 - 7.91 | 496.41 | 351.95 | 24198.0 | 2886.0 | 25382.0 | 2941.5 | 28893.3 | 4699.0 | 4881 | 58.00 | 42.30 |
| T - 7 - 7.96 | 496.41 | 351.95 | 16021.0 | | 16354.0 | 1332.0 | 10952.0 | 1369.0 | | | |
| T - 7 - 8.38 | 496.41 | 351.95 | 2812.0 | 333.0 | 2797.2 | 355.2 | 1938.8 | 270.1 | 6255 | 12.00 | 37.00 |
| T - 7 - 8.99 | 496.41 | 351.95 | 814.0 | 111.0 | 888.0 | 122.1 | 362.6 | 96.2 | 5856 | 16.55 | 38.00 |
| T - 8 - 1.00 | 490.78 | 353.47 | 7474.0 | | 8954.0 | 703.0 | 407.0 | 44.4 | | | |
| T - 8 - 2.00 | 490.78 | 353.47 | 5920.0 | | 6438.0 | 259.0 | 296.0 | 48.1 | | | |
| T - 8 - 3.00 | 490.78 | 353.47 | 5402.0 | | 7178.0 | | 2220.0 | 2405.0 | | | |
| T - 8 - 3.00 | 490.78 | 353.47 | 6068.0 | | 7918.0 | 333.0 | 1739.0 | 148.0 | | | |
| T - 8 - 4.00 | 490.78 | 353.47 | 7178.0 | | 10989.0 | 296.0 | 481.0 | 77.7 | | | |
| T - 8 - 5.00 | 490.78 | 353.47 | 6697.0 | | 8991.0 | 666.0 | 10656.0 | 851.0 | | | |
| T - 8 - 6.00 | 490.78 | 353.47 | 7733.0 | | 8695.0 | 518.0 | 8325.0 | 703.0 | | | |
| T - 8 - 6.00 | 490.78 | 353.47 | 7622.0 | | 9324.0 | 629.0 | 8066.0 | 703.0 | | | |
| T - 8 - 6.00 | 490.78 | 353.47 | 8399.0 | | 8880.0 | 592.0 | 8140.0 | 888.0 | | | |
| T - 8 - 7.00 | 490.78 | 353.47 | 19499.0 | | 21497.0 | 1665.0 | 14837.0 | 1739.0 | | | |
| T - 8 - 7.60 | 490.78 | 353.47 | 18056.0 | 1591.0 | 14474.4 | 1539.2 | 17131.0 | 1502.2 | 3634 | 20.50 | 36.50 |

Solid Sample Data

Table 7.4 - Nordic main tailings data. Solid phase sample results of chemicals and radioisotope analyses from locations T-1, T-2, T-3, T-7 and T-8 at various depths in concentration/gram.

||Solid Sample Study

| SAMPLE DESCRIPTION DEPTH (m) | Northing (m) (x10) | Elevation (m) | Pb-210 (mBq/g) +/-10% | Ra-224 (mBq/g) | Ra-226 (mBq/g) +/-10% | Th-228 (mBq/g) +/-20% | Th-230 (mBq/g) +/-20% | Th-232 (mBq/g) +/-20% | Al (mg/100g) | Ca (mg/g) | Fe (mg/g) |
|---|---|---|---|---|---|---|---|---|---|---|---|
| T - 8 - 8.40 | 490.78 | 353.47 | 8991.0 | 1961.0 | 7437.0 | 1879.6 | 8376.8 | 703.0 | 2487 | 7.35 | 35.00 |
| T - 8 - 8.40 | 490.78 | 353.47 | 7511.0 | 851.0 | 8658.0 | 1172.9 | 7440.7 | 1354.2 | 2625 | 7.95 | 34.30 |
| T - 8 - 8.76 | 490.78 | 353.47 | 14652.0 | 1628.0 | 14999.8 | 1572.5 | 13149.8 | 1609.5 | 3310 | 10.80 | 36.30 |
| T - 8 - 9.07 | 490.78 | 353.47 | 26640.0 | | 28823.0 | 5254.0 | 19055.0 | 2664.0 | | | |
| T - 8 - 9.37 | 490.78 | 353.47 | 16687.0 | 1406.0 | 15351.3 | 973.1 | 10855.8 | 862.1 | 5540 | 16.95 | 42.50 |
| T - 8 - 9.98 | 490.78 | 353.47 | 41736.0 | | 42809.0 | 5624.0 | 40145.0 | 3811.0 | | | |
| T - 8 -10.29 | 490.78 | 353.47 | 24790.0 | | 26973.0 | | | | | | |
| T - 8 -10.29 | 490.78 | 353.47 | 30081.0 | | 26196.0 | 3293.0 | 31302.0 | 3700.0 | | | |
| T - 8 -10.29 | 490.78 | 353.47 | 29045.0 | | 31524.0 | 1924.0 | 21201.0 | 2109.0 | | | |
| T - 8 -11.05 | 490.78 | 353.47 | 23347.0 | | 24013.0 | 1665.0 | 25530.0 | 2664.0 | | | |
| T - 8 -11.20 | 490.78 | 353.47 | 22385.0 | | 22200.0 | 1776.0 | 21127.0 | 2257.0 | | | |
| T - 8 -11.44 | 490.78 | 353.47 | 33781.0 | | 32893.0 | 2553.0 | 28379.0 | 2627.0 | | | |
| T - 8 -11.49 | 490.78 | 353.47 | 12543.0 | | 12432.0 | 518.0 | 15170.0 | 962.0 | | | |
| T - 8 -11.60 | 490.78 | 353.47 | 5328.0 | | 6956.0 | 1184.0 | 2183.0 | 222.0 | | | |
| T - 8 -11.65 | 490.78 | 353.47 | 9324.0 | 1110.0 | 9224.1 | 865.8 | 10145.4 | 965.7 | | | |
| T - 8 -11.65 | 490.78 | 353.47 | 9805.0 | | 10434.0 | 925.0 | 9287.0 | 888.0 | 2988 | 12.90 | 32.80 |
| T - 8 -12.24 | 490.78 | 353.47 | 6845.0 | | 7422.2 | 740.0 | 7248.3 | 825.1 | 3566 | 12.05 | 30.50 |

Table 7.5 - Nordic main tailings data. Solid phase sample results of chemicals and radioisotope analyses from locations T-1, T-2, T-3, T-7 and T-8 at various depths in concentration/gram

| SAMPLE DESCRIPTION DEPTH (m) | K (mg/g) | Mg (mg/g) | Pb (mg/100g) | Silica Acid extract (mg/g) | Silica Fused w/ NaHCO3 (mg/g) | Soluble Sulphate (mg/g) | Total Sulphate (mg/g) | Th (ppm) | U (ppm) |
|---|---|---|---|---|---|---|---|---|---|
| T - 1 - 1.00 | 25.42 | 1.90 | 33.15 | | | 16.11 | 17.85 | 28 | 18 |
| T - 1 - 1.50 | | | | | | | | 114 | 38 |
| T - 1 - 2.00 | | | | | | | | 513 | 43 |
| T - 1 - 2.00 | | | | | | | | 550 | 45 |
| T - 1 - 2.00 | 31.16 | 1.92 | 31.90 | 1.53 | 23.00 | 49.57 | 57.07 | 519 | 41 |
| T - 1 - 2.50 | | | | | | | | 180 | 102 |
| T - 1 - 3.00 | 33.15 | 1.35 | 27.10 | | | 35.96 | 46.54 | 234 | 72 |
| T - 1 - 4.00 | | | | | | | | 304 | 49 |
| T - 1 - 4.00 | | | | | | | | | 51 |
| T - 1 - 4.00 | | | | | | | | | 55 |
| T - 1 - 4.25 | | | | | | | | 194 | 45 |
| T - 1 - 4.50 | | | | | | | | 54 | 50 |
| T - 1 - 4.60 | | | | | | | | 157 | 46 |
| T - 1 - 4.75 | | | | | | | | 482 | 86 |
| T - 1 - 5.00 | | | | | | | | 272 | 77 |
| T - 1 - 5.25 | | | | | | | | 522 | 89 |
| T - 1 - 5.50 | | | | | | | | 212 | 80 |
| T - 1 - 5.75 | | | | | | | | 220 | 70 |
| T - 1 - 6.00 | 30.69 | 1.13 | 27.45 | | | 25.02 | 72.37 | 286 | 62 |
| T - 1 - 6.00 | 22.13 | 1.04 | 26.55 | | | 24.61 | 61.85 | 316 | 70 |
| T - 1 - 6.00 | | | | | | | | | 46 |
| T - 1 - 6.00 | | | | | | | | 214 | 61 |
| T - 1 - 6.25 | | | | | | | | 126 | 58 |
| T - 1 - 6.50 | | | | | | | | 164 | 63 |
| T - 1 - 6.75 | | | | | | | | 100 | 67 |
| T - 1 - 7.00 | | | | | | | | 286 | 94 |
| T - 1 - 7.00 | 29.40 | 1.07 | 24.40 | | | 16.89 | 63.44 | 106 | 85 |
| T - 1 - 7.25 | | | | | | | | 196 | 58 |
| T - 1 - 7.40 | | | | | | | | 176 | 87 |
| T - 1 - 7.50 | | | | | | | | 106 | 75 |
| T - 1 - 7.60 | | | | | | | | 128 | 64 |
| T - 1 - 7.60 | | | | | | | | 129 | 62 |
| T - 1 - 7.60 | 23.38 | 0.86 | 21.60 | | | 23.48 | 81.61 | 131 | 64 |
| T - 1 - 7.75 | | | | | | | | 172 | 76 |
| T - 1 - 8.00 | 19.36 | 0.57 | 9.10 | | | 10.20 | 87.35 | 40 | 25 |
| T - 1 - 8.00 | | | | | | | | 348 | 86 |
| T - 1 - 8.25 | | | | | | | | 618 | 61 |
| T - 1 - 8.50 | | | | | | | | | 93 |
| T - 1 - 8.50 | | | | | | | | 532 | 104 |
| T - 1 - 8.50 | | | | | | | | 582 | 85 |
| T - 1 - 9.00 | | | | | | | | 323 | 118 |
| T - 1 - 9.00 | | | | | | | | 354 | 127 |
| T - 1 - 9.00 | 25.99 | 1.92 | 26.75 | | | 58.64 | 81.50 | 309 | 119 |
| T - 1 - 9.60 | | 1.58 | 28.00 | 1.03 | 53.50 | 49.57 | 67.50 | | |
| T - 1 - 9.60 | 27.98 | 1.52 | 30.85 | | | 51.84 | 81.50 | | |
| T - 1 -10.20 | | 1.86 | 34.15 | 2.53 | 22.00 | 65.45 | 43.68 | | |
| T - 1 -10.60 | 2.64 | 2.56 | 2.20 | | | 0.87 | 6.20 | | |
| T - 1 -10.70 | 2.88 | 1.90 | 28.00 | | | 0.76 | 6.64 | | |

Table 7.6 - Nordic main tailings data. Solid phase sample results of chemical and radioisotope analyses from locations T-1, T-2, T-3, T-7 and T-8 at various depths in concentration/gram.

| SAMPLE DESCRIPTION DEPTH (m) | K (mg/g) | Mg (mg/g) | Pb (mg/100g) | Silica Acid extract (mg/g) | Silica Fused w/ NaHCO3 (mg/g) | Soluble Sulphate (mg/g) | Total Sulphate (mg/g) | Th (ppm) | U (ppm) |
|---|---|---|---|---|---|---|---|---|---|
| T - 1 -10.77 | 17.25 | 2.80 | 14.00 | | | 5.86 | 51.35 | | |
| T - 1 -10.80 | 3.12 | 3.39 | 1.10 | | | 2.27 | 7.72 | | |
| T - 1 -11.18 | 14.98 | 2.99 | 1.30 | | | 0.52 | 0.56 | | |
| T - 1 -12.57 | | | | | | | | 425 | 77 |
| T - 2 - 1.00 | 27.64 | 0.90 | 37.60 | 0.51 | 31.50 | 40.50 | 42.73 | 21 | 16 |
| T - 2 - 1.40 | | | | | | | | 26 | 27 |
| T - 2 - 2.00 | 24.88 | 0.94 | 27.30 | | | 31.42 | 66.42 | 470 | 58 |
| T - 2 - 3.00 | | | | | | | | 110 | 50 |
| T - 2 - 4.00 | | | | | | | | 211 | 42 |
| T - 2 - 4.00 | | | | | | | | 196 | 40 |
| T - 2 - 4.00 | | | | | | | | 216 | 41 |
| T - 2 - 4.60 | 24.20 | 0.47 | 27.25 | | | 22.35 | 62.12 | 89 | 71 |
| T - 2 - 5.00 | | | | | | | | 269 | 55 |
| T - 2 - 5.79 | | | | | | | | 193 | 74 |
| T - 2 - 6.02 | | | | | | | | 287 | 63 |
| T - 2 - 6.93 | | | | | | | | 261 | 69 |
| T - 2 - 7.24 | | | | | | | | 347 | 74 |
| T - 2 - 8.00 | 24.23 | 1.65 | 37.25 | | | 54.11 | 73.96 | 480 | 78 |
| T - 2 - 8.31 | | | | | | | | 213 | 22 |
| T - 2 - 8.76 | | | | | | | | 407 | 149 |
| T - 2 - 8.76 | 32.63 | 2.13 | 40.20 | | | 45.03 | 42.73 | 421 | 153 |
| T - 2 - 8.76 | | | | | | | | 408 | 150 |
| T - 2 - 9.07 | | | | | | | | 629 | 100 |
| T - 2 - 9.07 | | | | | | | | 598 | 95 |
| T - 2 - 9.07 | | 2.84 | 53.40 | 3.55 | 29.00 | 85.87 | 105.19 | 623 | 118 |
| T - 2 - 9.61 | 36.53 | 1.23 | 47.15 | | | 76.79 | 107.35 | 587 | 141 |
| T - 2 - 9.77 | 37.40 | 2.14 | 45.00 | | | 10.29 | 78.11 | 756 | 73 |
| T - 2 - 9.79 | 25.90 | 1.89 | 44.40 | | | 10.06 | 94.42 | | |
| T - 2 - 9.87 | 40.72 | 4.55 | 47.60 | | | 76.79 | 93.09 | | |
| T - 2 - 9.94 | 26.99 | 1.20 | 42.85 | | | 7.23 | 70.73 | | |
| T - 2 -10.15 | 1.34 | 3.28 | 15.40 | | | 2.27 | 6.64 | | |
| T - 2 -10.25 | 15.79 | 2.56 | 0.75 | 0.51 | 14.00 | 1.93 | 0.44 | | |
| T - 2 -10.33 | 23.10 | 6.47 | 1.20 | | | 1.76 | 0.00 | | |
| T - 3 - 1.00 | | | | | | | | 34 | 15 |
| T - 3 - 1.30 | | | | | | | | 118 | 36 |
| T - 3 - 2.00 | | | | | | | | 80 | 72 |
| T - 3 - 2.60 | | | | | | | | 248 | 77 |
| T - 3 - 3.00 | | | | | | | | 150 | 66 |
| T - 3 - 3.00 | | | | | | | | 146 | 57 |
| T - 3 - 3.00 | | | | | | | | 139 | 44 |
| T - 3 - 4.00 | 27.50 | 1.49 | 45.00 | | | 55.24 | 59.96 | 394 | 70 |
| T - 3 - 4.30 | | | | | | | | 342 | 55 |
| T - 3 - 4.30 | | | | | | | | 356 | 51 |
| T - 3 - 4.30 | | | | | | | | 354 | 52 |
| T - 3 - 5.00 | 22.78 | 0.59 | 27.40 | | | 19.51 | 62.12 | 163 | 64 |
| T - 3 - 6.93 | | | | | | | | 814 | 325 |
| T - 3 - 6.93 | 38.75 | 2.84 | 8.00 | | | 8.81 | 71.41 | 870 | 296 |
| T - 3 - 6.93 | | | | | | | | 818 | 305 |

Table 7.7 - Nordic main tailings data. Solid phase sample results of chemical and radioisotope analyses from locations T-1, T-2, T-3, T-7 and T-8 at various depths in concentration/gram.

| SAMPLE DESCRIPTION DEPTH (m) | K (mg/g) | Mg (mg/g) | Pb (mg/100g) | Silica Acid extract (mg/g) | Silica Fused w/ NaHCO3 (mg/g) | Soluble Sulphate (mg/g) | Total Sulphate (mg/g) | Th (ppm) | U (ppm) |
|---|---|---|---|---|---|---|---|---|---|
| T - 3 - 7.25 | | | | | | | | 185 | 97 |
| T - 3 - 7.25 | | | | | | | | | 93 |
| T - 3 - 7.25 | | | | | | | | 426 | 85 |
| T - 3 - 7.50 | | | | | | | | 400 | 61 |
| T - 3 - 7.54 | | 3.27 | 35.95 | 3.55 | 26.50 | 60.91 | 94.42 | 394 | 59 |
| T - 3 - 7.75 | | | | | | | | 218 | 37 |
| T - 3 - 7.85 | | | | | | | | 728 | 51 |
| T - 3 - 7.85 | | | | | | | | 707 | 62 |
| T - 3 - 7.85 | 30.78 | 3.62 | 43.50 | | | 91.54 | 107.35 | 695 | 58 |
| T - 3 - 7.96 | | | | | | | | 20 | 37 |
| T - 3 - 7.97 | | | | | | | | 716 | 53 |
| T - 3 - 8.01 | | | | | | | | 12 | 9 |
| T - 3 - 8.06 | | 6.90 | 1.55 | 7.60 | 31.00 | 0.28 | 1.65 | 23 | 6 |
| T - 3 - 8.29 | | | | | | | | | |
| T - 3 - 8.53 | 36.79 | 0.71 | 30.15 | | | 2.38 | 57.07 | | |
| T - 7 - 1.00 | | | | | | | | 20 | 12 |
| T - 7 - 1.30 | | | | | | | | 28 | 11 |
| T - 7 - 2.00 | | | | | | | | 27 | 42 |
| T - 7 - 3.00 | | | | | | | | 370 | 49 |
| T - 7 - 3.00 | | | | | | | | 270 | 62 |
| T - 7 - 4.00 | | | | | | | | 183 | 48 |
| T - 7 - 5.00 | | | | | | | | 181 | 71 |
| T - 7 - 5.00 | | | | | | | | 186 | 72 |
| T - 7 - 5.00 | | | | | | | | 173 | 76 |
| T - 7 - 6.00 | | | | | | | | 183 | 68 |
| T - 7 - 6.40 | 29.60 | 0.90 | 32.20 | 1.53 | 18.50 | 31.42 | 61.85 | | |
| T - 7 - 6.90 | 24.44 | 1.18 | 53.00 | | | 46.17 | 49.19 | | |
| T - 7 - 6.90 | 27.18 | 1.34 | 56.25 | | | 47.30 | 56.73 | | |
| T - 7 - 7.00 | | | | | | | | 340 | 261 |
| T - 7 - 7.20 | 33.66 | 2.15 | 49.10 | | | 58.64 | 76.20 | | |
| T - 7 - 7.70 | 25.07 | 1.05 | 25.50 | 2.03 | 24.00 | 3.82 | 77.19 | | |
| T - 7 - 7.81 | 29.44 | 1.01 | 15.40 | | | 9.07 | 54.83 | | |
| T - 7 - 7.86 | 34.89 | 1.67 | 25.50 | 2.03 | 18.50 | 40.50 | 87.68 | | |
| T - 7 - 7.91 | 26.69 | 1.85 | 37.15 | | | 65.45 | 93.35 | | |
| T - 7 - 7.96 | | | | | | | | 201 | 30 |
| T - 7 - 8.38 | 15.49 | 2.84 | 4.00 | | | 3.40 | 14.73 | | |
| T - 7 - 8.99 | 14.09 | 8.33 | 1.88 | | | 2.09 | 2.02 | | |
| T - 8 - 1.00 | | | | | | | | 16 | 13 |
| T - 8 - 2.00 | | | | | | | | 15 | 13 |
| T - 8 - 3.00 | | | | | | | | 27 | 35 |
| T - 8 - 3.00 | | | | | | | | 26 | 31 |
| T - 8 - 4.00 | | | | | | | | 24 | 37 |
| T - 8 - 5.00 | | | | | | | | 184 | 42 |
| T - 8 - 6.00 | | | | | | | | 138 | 46 |
| T - 8 - 6.00 | | | | | | | | 133 | 48 |
| T - 8 - 6.00 | | | | | | | | 135 | 48 |
| T - 8 - 7.00 | | | | | | | | 215 | 74 |
| T - 8 - 7.60 | | 0.66 | 36.65 | | | 37.09 | 68.54 | | |

Solid Sample Data

Table 7.8 - Nordic main tailings data. Solid phase sample results of chemical and radioisotope analyses from locations T-1, T-2, T-3, T-7 and T-8 at various depths in concentration/gram.

| SAMPLE DESCRIPTION DEPTH (m) | K (mg/g) | Mg (mg/g) | Pb (mg/100g) | Silica Acid extract (mg/g) | Silica Fused w/ NaHCO3 (mg/g) | Soluble Sulphate (mg/g) | Total Sulphate (mg/g) | Th (ppm) | U (ppm) |
|---|---|---|---|---|---|---|---|---|---|
| T - 8 - 8.40 | 21.34 | 0.20 | 21.40 | 0.51 | 23.00 | 12.14 | 64.27 | | |
| T - 8 - 8.40 | 19.30 | 0.50 | 21.00 | 0.51 | 14.00 | 14.97 | 76.12 | | |
| T - 8 - 8.76 | | 0.90 | 30.35 | 2.03 | 20.50 | 21.78 | 70.46 | | |
| T - 8 - 9.07 | | | | | | | | 516 | 75 |
| T - 8 - 9.37 | | 2.18 | 4.80 | 2.03 | 21.00 | 23.48 | 9.24 | | |
| T - 8 - 9.98 | | | | | | | | 532 | 272 |
| T - 8 -10.29 | | | | | | | | 398 | 79 |
| T - 8 -10.29 | | | | | | | | 519 | 83 |
| T - 8 -10.29 | | | | | | | | 505 | 86 |
| T - 8 -11.05 | | | | | | | | 492 | 71 |
| T - 8 -11.20 | | | | | | | | 367 | 74 |
| T - 8 -11.44 | | | | | | | | 524 | 78 |
| T - 8 -11.49 | | | | | | | | 232 | 51 |
| T - 8 -11.60 | | | | | | | | 65 | 35 |
| T - 8 -11.65 | | | | | | | | | |
| T - 8 -11.65 | 18.57 | 1.14 | 18.00 | | | 20.08 | 59.96 | 147 | 33 |
| T - 8 -12.24 | 21.02 | 1.47 | 14.90 | | | 12.14 | 42.19 | | |

Table 7.9 - Nordic main tailings data. Liquid phase sample results of chemical and radioisotope analyses from locations T-1, T-2, T-3, T-7 and T-8 at various depths in concentration/litre.

||Water Sample Study

| SAMPLE DESCRIPTION | NORTHING (M) (x10) | ELEV.TOP PIEZO. (M) | TOTAL DEPTH (M) | WATER LEVEL (M) | PRESSURE POINT (M) | HYDRLC HEAD (M) | TEMP 'C | Eh (mV) | Ec (uS) | pH | Al (mg/L) |
|---|---|---|---|---|---|---|---|---|---|---|---|
| T1-P1 10-09-84 | 544.80 | 351.86 | 12.99 | 6.10 | 339.02 | 345.76 | | 230 | 3400 | 6.11 | 0.30 |
| T1-P2 10-09-84 | 544.80 | 351.86 | 8.36 | 4.45 | 343.65 | 347.41 | | 200 | 5200 | 5.96 | 0.50 |
| T1-P3 10-09-84 | 544.80 | 351.86 | 8.42 | 4.45 | 343.59 | 347.41 | | 170 | 6800 | 5.90 | 0.00 |
| T1-P4 10-09-84 | 544.80 | 351.86 | 6.95 | 4.34 | 345.06 | 347.52 | | 200 | 3800 | 6.02 | 0.00 |
| T1-P5 10-09-84 | 544.80 | 351.86 | 5.43 | 4.23 | 346.58 | 347.63 | | 270 | 3500 | 5.74 | 0.00 |
| T1-P6 10-09-84 | 544.80 | 351.86 | 3.86 | DRY | 348.15 | DRY | DRY | DRY | DRY | DRY | DRY |
| T2-P1 06-09-84 | 518.74 | 351.71 | 12.65 | 7.63 | 339.21 | 344.08 | 12.5 | 270 | 4750 | 5.83 | 4.95 |
| T2-P2 06-09-84 | 518.74 | 351.65 | 10.94 | 7.09 | 340.86 | 344.56 | 12.3 | 100 | 6500 | 6.23 | 0.00 |
| T2-P3 06-09-84 | 518.74 | 352.01 | 9.82 | 6.38 | 342.34 | 345.63 | | | | | 0.20 |
| T2-P4 06-09-84 | 518.74 | 352.01 | 8.30 | 6.20 | 343.86 | 345.81 | 19.0 | 400 | 4000 | 4.90 | 0.00 |
| T2-P5 06-09-84 | 518.74 | 352.04 | 6.86 | 6.01 | 345.33 | 346.03 | 22.0 | 450 | 3700 | 4.65 | 2.60 |
| T2-P6 06-09-84 | 518.74 | 352.04 | 5.82 | DRY | 346.37 | DRY | DRY | DRY | DRY | DRY | DRY |
| T2-P7 06-09-84 | 518.74 | 352.04 | 5.46 | DRY | 346.73 | DRY | DRY | DRY | DRY | DRY | DRY |
| T2-P8 06-09-84 | 518.74 | 352.01 | 3.99 | DRY | 348.17 | DRY | DRY | DRY | DRY | DRY | DRY |
| T2-P9 06-09-84 | 518.74 | 352.04 | 2.50 | DRY | 349.69 | DRY | DRY | DRY | DRY | DRY | DRY |
| T2-P10 06-09-84 | 518.74 | 352.04 | 10.75 | 5.75 | 341.44 | 346.29 | | 365 | 6000 | 5.12 | 0.00 |
| T2-P11 06-09-84 | 518.74 | 352.04 | 8.70 | 7.70 | 343.49 | 344.34 | 20.0 | 440 | 6000 | 4.62 | 0.87 |
| T3-CENTER 07-09-84 | 509.62 | 351.37 | 17.30 | 7.70 | 334.22 | 343.67 | 16.0 | 265 | 5000 | 5.90 | 0.50 |
| T3-1 07-09-84 | 509.62 | 351.37 | 16.11 | 7.73 | 335.41 | 343.64 | 12.0 | 245 | 4000 | 5.97 | 0.30 |
| T3-2 07-09-84 | 509.62 | 351.37 | 15.10 | 7.75 | 336.42 | 343.62 | 10.5 | 270 | 5000 | 6.12 | 0.25 |
| T3-3 07-09-84 | 509.62 | 351.37 | 14.20 | 7.70 | 337.32 | 343.67 | 10.5 | 240 | 4700 | 6.22 | 0.60 |
| T3-4 07-09-84 | 509.62 | 351.37 | 13.07 | 7.70 | 338.45 | 343.67 | 10.5 | 260 | 4600 | 6.15 | 0.20 |
| T3-5 07-09-84 | 509.62 | 351.37 | 12.00 | 7.70 | 339.52 | 343.67 | 11.0 | 265 | 4800 | 6.14 | 0.40 |
| T3-6 07-09-84 | 509.62 | 351.37 | 11.20 | 7.70 | 340.32 | 343.67 | 11.0 | 290 | 4900 | 5.96 | 0.31 |
| T3-P3 07-09-84 | 509.62 | 351.37 | 8.57 | 7.73 | 342.95 | 343.64 | 18.0 | 410 | 4750 | 4.95 | 1.50 |
| T7-CENTER 07-09-84 | 496.41 | 351.95 | 23.20 | 8.60 | 328.90 | 343.35 | 11.0 | 240 | 5000 | 6.10 | 2.84 |
| T7-1 07-09-84 | 496.41 | 351.95 | 19.08 | 8.55 | 333.02 | 343.40 | 11.0 | 230 | 4400 | 6.30 | 0.00 |
| T7-3 07-09-84 | 496.41 | 351.95 | 17.25 | 8.58 | 334.85 | 343.37 | 11.5 | 190 | 4600 | 6.40 | 0.00 |
| T7-4 07-09-84 | 496.41 | 351.95 | 15.10 | 8.53 | 337.00 | 343.42 | 11.5 | 210 | 4900 | 6.20 | 0.00 |
| T7-5 07-09-84 | 496.41 | 351.95 | 13.10 | 8.55 | 339.00 | 343.40 | 11.5 | 30 | 4800 | 6.70 | 0.00 |
| T7-6 07-09-84 | 496.41 | 351.95 | 11.08 | 8.55 | 341.02 | 343.40 | 12.5 | 240 | 4850 | 6.10 | 0.00 |
| T7-7 07-09-84 | 496.41 | 351.95 | 9.25 | 8.55 | 342.85 | 343.40 | 13.0 | 440 | 3500 | 5.10 | 26.49 |
| T7-P1 07-09-84 | 496.41 | 351.95 | 10.16 | 8.79 | 341.94 | 343.16 | 14.0 | 310 | 5000 | 5.88 | 0.30 |
| T7-P2 07-09-84 | 496.41 | 351.95 | 9.16 | 8.77 | 342.94 | 343.18 | 15.0 | 550 | 3200 | 3.23 | 56.90 |
| T7-P5 07-09-84 | 496.41 | 351.95 | 11.06 | 9.89 | 341.04 | 342.06 | 16.0 | 440 | 10000 | 4.16 | 0.40 |
| T7-PVCV SMALL TUBE 07-09-84 | 496.41 | 351.95 | 10.50 | 9.25 | 341.60 | 342.70 | 19.0 | 520 | 9000 | 4.51 | 171.23 |
| T8-P1 10/09/84 | 490.78 | 353.47 | 14.54 | 11.45 | 339.08 | 342.02 | 16.0 | 240 | 8000 | 5.89 | 0.20 |
| T8-P2 10/09/84 | 490.78 | 353.47 | 13.02 | 11.45 | 340.60 | 342.02 | 16.5 | 230 | 12000 | 5.73 | 0.15 |
| T8-P3 10/09/84 | 490.78 | 353.47 | 11.44 | 11.10 | 342.18 | 342.37 | 16.5 | 280 | 4000 | 5.87 | 0.00 |
| T8-P4 10/09/84 | 490.78 | 353.47 | 11.27 | 10.05 | 342.35 | 343.42 | 20.0 | 290 | 6000 | 5.55 | 0.15 |
| T8-P5 10/09/84 | 490.78 | 353.47 | 17.03 | 10.10 | 336.59 | 343.37 | 16.5 | 250 | 6500 | 6.00 | 2.41 |
| T8-P6 10/09/84 | 490.78 | 353.47 | 17.50 | 9.55 | 336.12 | 343.92 | 15.5 | 260 | 7000 | 5.78 | 2.73 |

Table 7.10 - Nordic main tailings data. Liquid phase sample results of chemical and radioisotope analyses from locations T-1, T-2, T-3, T-7 and T-8 at various depths in concentration/litre.

| SAMPLE DESCRIPTION | Ca (mg/L) | Fe (mg/L) | K (mg/L) | Mg (mg/L) | Mn (mg/L) | D.C.P. Na (mg/L) | Pb (mg/L) | Ra-226 (pCi/L) | Ra-226 (mBq/L) | SiO2 (mg/L) |
|---|---|---|---|---|---|---|---|---|---|---|
| T1-P1 10-09-84 | 457.0 | 295.0 | 38.25 | 450.00 | 20.00 | 21.920 | 0.000 | 1.80 | 66.60 | 34.40 |
| T1-P2 10-09-84 | 437.5 | 4625.0 | 73.25 | 633.60 | 17.40 | 6.560 | 0.000 | 147.45 | 5455.65 | 47.70 |
| T1-P3 10-09-84 | 385.0 | 3975.0 | 92.50 | 895.00 | 28.90 | 6.700 | 0.000 | 153.00 | 5661.00 | 55.40 |
| T1-P4 10-09-84 | 415.0 | 3612.0 | 36.00 | 182.50 | 6.24 | 8.160 | 0.000 | 144.20 | 5335.40 | 43.90 |
| T1-P5 10-09-84 | 435.0 | 630.0 | 19.00 | 75.00 | 4.82 | 7.330 | 0.000 | 114.95 | 4253.15 | 36.30 |
| T1-P6 10-09-84 | DRY | DRY | DRY | DRY | DRY | DRY | DRY | DRY | DRY | DRY |
| T2-P1 06-09-84 | 417.5 | 175.0 | 50.25 | 260.00 | 38.50 | 19.300 | 0.000 | 4.91 | 181.67 | 24.80 |
| T2-P2 06-09-84 | 417.5 | 500.0 | 147.50 | 1160.00 | 127.00 | 25.910 | 0.000 | | | 26.70 |
| T2-P3 06-09-84 | 437.5 | 5550.0 | 118.50 | 168.96 | | | 0.000 | 168.54 | 6235.98 | 49.60 |
| T2-P4 06-09-84 | 430.5 | 2100.0 | 24.25 | 75.00 | 1.67 | 3.469 | 0.000 | 231.30 | 8558.10 | 38.20 |
| T2-P5 06-09-84 | 417.5 | 925.0 | 22.50 | 12.80 | 1.22 | 4.020 | 0.000 | 218.40 | 8080.80 | 43.90 |
| T2-P6 06-09-84 | DRY | DRY | DRY | DRY | DRY | DRY | DRY | DRY | DRY | DRY |
| T2-P7 06-09-84 | DRY | DRY | DRY | DRY | DRY | DRY | DRY | DRY | DRY | DRY |
| T2-P8 06-09-84 | DRY | DRY | DRY | DRY | DRY | DRY | DRY | DRY | DRY | DRY |
| T2-P9 06-09-84 | DRY | DRY | DRY | DRY | DRY | DRY | DRY | DRY | DRY | DRY |
| T2-P10 06-09-84 | 696.0 | 4750.0 | | 114.00 | 9.04 | 13.690 | 0.000 | | | 12.02 |
| T2-P11 06-09-84 | 666.0 | 3620.0 | | 193.00 | 10.20 | 22.400 | 0.000 | | | 10.51 |
| T3-CENTER 07-09-84 | 515.0 | 440.0 | 82.50 | 352.50 | 42.00 | 25.200 | 0.000 | | | 26.70 |
| T3-1 07-09-84 | 495.0 | 175.0 | 82.50 | 350.00 | 42.40 | 27.510 | 0.000 | | | 26.70 |
| T3-2 07-09-84 | 495.0 | 450.0 | 81.50 | 383.50 | 42.90 | 27.210 | 0.000 | 131.76 | 4875.12 | 24.80 |
| T3-3 07-09-84 | 465.0 | 385.0 | 68.75 | 300.00 | 41.40 | 25.850 | 0.000 | 167.31 | 6190.47 | 22.90 |
| T3-4 07-09-84 | 447.5 | 305.0 | 72.50 | 260.00 | 39.30 | 27.500 | 0.000 | 73.50 | 2719.50 | 22.90 |
| T3-5 07-09-84 | 495.0 | 1475.0 | 85.50 | 331.00 | 39.10 | 60.160 | 0.000 | 1.90 | 70.30 | 22.90 |
| T3-6 07-09-84 | 487.5 | 2430.0 | | 268.00 | 36.60 | 25.280 | 0.000 | | | |
| T3-P3 07-09-84 | 457.5 | 2260.0 | | 175.00 | 10.20 | 6.010 | 0.322 | | | 64.90 |
| T7-CENTER 07-09-84 | 712.0 | 2380.0 | | 293.00 | 25.90 | 40.100 | <0.100 | | | |
| T7-1 07-09-84 | 679.0 | 1650.0 | | 311.00 | 23.60 | 48.800 | 0.000 | 24.37 | 901.69 | |
| T7-3 07-09-84 | 664.0 | 1640.0 | | 315.00 | 23.50 | 47.800 | <0.100 | | | |
| T7-4 07-09-84 | 704.0 | 1970.0 | | 288.00 | 25.40 | 43.290 | <0.100 | | | |
| T7-5 07-09-84 | 662.0 | 2020.0 | | 279.00 | 25.60 | 39.500 | <0.100 | | | |
| T7-6 07-09-84 | 682.0 | 1960.0 | | 273.00 | 26.70 | 41.030 | <0.100 | | | |
| T7-7 07-09-84 | 567.0 | 1560.0 | | 55.50 | 8.82 | 4.700 | <0.100 | | | |
| T7-P1 07-09-84 | 462.5 | 2838.0 | 78.00 | 495.00 | 24.50 | | 0.000 | | | 34.50 |
| T7-P2 07-09-84 | 382.5 | 1975.0 | 42.00 | 72.50 | 6.47 | 38.200 | 0.000 | 61.22 | 2265.14 | 99.30 |
| T7-P5 07-09-84 | 402.5 | 8040.0 | 83.00 | 265.00 | 9.47 | 12.780 | 0.000 | | | 95.50 |
| T7-PVCV SMALL TUBE 07-09-84 | 653.0 | 9140.0 | | 287.00 | 30.30 | 20.550 | 0.392 | | | 31.96 |
| T8-P1 10/09/84 | 380.0 | 5200.0 | 100.25 | 440.00 | 52.20 | | 0.000 | | | 45.80 |
| T8-P2 10/09/84 | 437.5 | 4990.0 | 117.25 | 790.00 | 95.70 | | 0.000 | 98.09 | 3629.33 | 34.40 |
| T8-P3 10/09/84 | 488.0 | 2840.0 | 59.00 | 200.00 | 9.29 | | 0.000 | | | 57.30 |
| T8-P4 10/09/84 | 425.0 | 4300.0 | 80.25 | 140.45 | 5.81 | | 0.000 | | | 47.70 |
| T8-P5 10/09/84 | 666.0 | 3660.0 | | 231.00 | 31.40 | | 0.124 | | | 11.20 |
| T8-P6 10/09/84 | 741.0 | 4660.0 | | 305.00 | 46.90 | | 0.000 | | | 8.17 |

Table 7.11 - Nordic main tailings data. Liquid phase sample results of chemical and radioisotope analyses from locations T-1, T-2, T-3, T-7 and T-8 at various depths in concentration/litre.

| | | | | Charge Balance | | | | | | |
|---|---|---|---|---|---|---|---|---|---|---|
| SAMPLE DESCRIPTION | Sulphate | Th | U | Al | Ca | Fe | K | Mg | Mn | Na |
| | (mg/L) | (mg/L) | (mg/L) | (mmol/L) | (mmol/L) | (mmol/L) | (mmol/L) | (mmol/L) | (mmol/L) | (mmol/L) |
| T1-P1 10-09-84 | 3760.13 | <0.100 | 0.604 | 0.03 | 22.8 | 10.6 | 0.98 | 37.02 | 1.09 | 0.954 |
| T1-P2 10-09-84 | 12260.13 | <0.100 | 0.765 | 0.06 | 21.8 | 165.6 | 1.87 | 52.12 | 0.95 | 0.285 |
| T1-P3 10-09-84 | 10023.29 | 0.142 | 0.849 | 0.00 | 19.2 | 142.4 | 2.37 | 73.63 | 1.58 | 0.292 |
| T1-P4 10-09-84 | 8173.42 | <0.100 | 0.678 | 0.00 | 20.7 | 129.4 | 0.92 | 15.01 | 0.34 | 0.355 |
| T1-P5 10-09-84 | 3760.13 | <0.100 | 0.624 | 0.00 | 21.7 | 22.6 | 0.49 | 6.17 | 0.26 | 0.319 |
| T1-P6 10-09-84 | DRY | DRY | DRY | DRY | DRY | DRY | DRY | DRY | DRY | DRY |
| T2-P1 06-09-84 | 30897.00 | <0.100 | 0.710 | 0.55 | 20.8 | 6.3 | 1.29 | 21.39 | 2.10 | 0.840 |
| T2-P2 06-09-84 | 6220.65 | <0.100 | 1.140 | 0.00 | 20.8 | 17.9 | 3.77 | 95.43 | 6.94 | 1.128 |
| T2-P3 06-09-84 | 10023.29 | 0.100 | 0.100 | 0.02 | 21.8 | 198.8 | 3.03 | 13.90 | 0.00 | 0.000 |
| T2-P4 06-09-84 | 5325.92 | <0.100 | 0.642 | 0.00 | 21.5 | 75.2 ) | 0.62 | 6.17 | 0.09 | 0.151 |
| T2-P5 06-09-84 | 3312.75 | 2.211 | 6.540 | 0.29 | 20.8 | 33.1 | 0.58 | 1.05 | 0.07 | 0.175 |
| T2-P6 06-09-84 | DRY | DRY | DRY | DRY | DRY | DRY | DRY | DRY | DRY | DRY |
| T2-P7 06-09-84 | DRY | DRY | DRY | DRY | DRY | DRY | DRY | DRY | DRY | DRY |
| T2-P8 06-09-84 | DRY | DRY | DRY | DRY | DRY | DRY | DRY | DRY | DRY | DRY |
| T2-P9 06-09-84 | DRY | DRY | DRY | DRY | DRY | DRY | DRY | DRY | DRY | DRY |
| T2-P10 06-09-84 | 7272.00 | 0.000 | 0.839 | 0.00 | 34.7 | 170.1 | 0.00 | 9.38 | 0.49 | 0.596 |
| T2-P11 06-09-84 | 6392.00 | <0.100 | 0.000 | 0.10 | 33.2 | 129.6 | 0.00 | 15.88 | 0.56 | 0.975 |
| T3-CENTER 07-09-84 | 3760.13 | <0.100 | 0.155 | 0.06 | 25.7 | 15.8 | 2.11 | 29.00 | 2.29 | 1.097 |
| T3-1 07-09-84 | 3983.80 | 0.000 | <0.100 | 0.03 | 24.7 | 6.3 | 2.11 | 28.79 | 2.32 | 1.197 |
| T3-2 07-09-84 | 3401.48 | 0.000 | 0.230 | 0.03 | 24.7 | 16.1 | 2.08 | 31.55 | 2.34 | 1.184 |
| T3-3 07-09-84 | 3536.45 | 0.000 | 0.000 | 0.07 | 23.2 | 13.8 | 1.76 | 24.68 | 2.26 | 1.125 |
| T3-4 07-09-84 | 3312.76 | <0.100 | 0.279 | 0.02 | 22.3 | 10.9 | 1.85 | 21.39 | 2.15 | 1.197 |
| T3-5 07-09-84 | 6668.02 | 0.000 | 0.244 | 0.04 | 24.7 | 52.8 | 2.19 | 27.23 | 2.14 | 2.618 |
| T3-6 07-09-84 | 5306.00 | <0.100 | 0.221 | 0.03 | 24.3 | 87.0 | 0.00 | 22.05 | 2.00 | 1.100 |
| T3-P3 07-09-84 | 7786.44 | 0.000 | 0.164 | 0.17 | 22.8 | 80.9 | 0.00 | 14.40 | 0.56 | 0.262 |
| T7-CENTER 07-09-84 | 5655.00 | 0.131 | 0.410 | 0.32 | 35.5 | 85.2 | 0.00 | 24.10 | 1.41 | 1.745 |
| T7-1 07-09-84 | 4832.00 | 0.000 | 0.406 | 0.00 | 33.9 | 59.1 | 0.00 | 25.58 | 1.29 | 2.124 |
| T7-3 07-09-84 | 4320.00 | <0.100 | 0.446 | 0.00 | 33.1 | 58.7 | 0.00 | 25.91 | 1.28 | 2.080 |
| T7-4 07-09-84 | 5270.00 | 0.000 | 0.471 | 0.00 | 35.1 | 70.5 | 0.00 | 23.69 | 1.39 | 1.884 |
| T7-5 07-09-84 | 5396.00 | 0.111 | 0.118 | 0.00 | 33.0 | 72.3 | 0.00 | 22.95 | 1.40 | 1.719 |
| T7-6 07-09-84 | 5458.00 | <0,100 | 0.128 | 0.00 | 34.0 | 70.2 | 0.00 | 22.46 | 1.46 | 1.785 |
| T7-7 07-09-84 | 3846.00 | 0.521 | 2.440 | 2.95 | 28.3 | 55.9 | 0.00 | 4.57 | 0.48 | 0.205 |
| T7-P1 07-09-84 | 6444.35 | <0.100 | 0.100 | 0.03 | 23.1 | 101.6 | 2.00 | 40.72 | 1.34 | 0.000 |
| T7-P2 07-09-84 | 5996.97 | 3.800 | 4.080 | 6.33 | 19.1 | 70.7 | 1.07 | 5.96 | 0.35 | 1.662 |
| T7-P5 07-09-84 | 17852.23 | 7.340 | 4.750 | 0.04 | 20.1 | 287.9 | 2.12 | 21.80 | 0.52 | 0.556 |
| T7-PVCV SMALL TUBE 07-09-84 | | 2.710 | 1.480 | 19.04 | 32.6 | 327.3 | 0.00 | 23.61 | 1.65 | 0.894 |
| T8-P1 10/09/84 | 14496.97 | 0.262 | 0.000 | 0.02 | 19.0 | 186.2 | 2.56 | 36.20 | 2.85 | 0.000 |
| T8-P2 10/09/84 | 12260.12 | 0.468 | 0.000 | 0.02 | 21.8 | 178.7 | 3.00 | 64.99 | 5.23 | 0.000 |
| T8-P3 10/09/84 | 7786.44 | 0.144 | 0.100 | 0.00 | 24.4 | 101.7 | 1.51 | 16.45 | 0.51 | 0.000 |
| T8-P4 10/09/84 | 11141.71 | 0.184 | 0.696 | 0.02 | 21.2 | 154.0 | 2.05 | 11.55 | 0.32 | 0.000 |
| T8-P5 10/09/84 | 7765.00 | 0.322 | 0.434 | 0.27 | 33.2 | 131.1 | 0.00 | 19.00 | 1.71 | 0.000 |
| T8-P6 10/09/84 | 9370.00 | 0.299 | 0.259 | 0.30 | 37.0 | 166.9 | 0.00 | 25.09 | 2.56 | 0.000 |

Table 7.12 - Nordic main tailings data. Liquid phase sample results of chemical and radioisotope analyses from locations T-1, T-2, T-3, T-7 and T-8 at various depths in concentration/litre.

| SAMPLE DESCRIPTION | Pb (mmol/L) | Ra-226 (mmol/L) | SiO2 (mmol/L) | Sulphate (Anions) (mmol/L) | Th (mmol/L) | U (mmol/L) | Total Cations (mmol/L) | Ion Balance (mmol/L) | Ion Balance Error |
|---|---|---|---|---|---|---|---|---|---|
| T1-P1 10-09-84 | 0.000000 | 1.61E-11 | 2.290 | 78.285 | 0.00086 | 0.0101 | 75.75 | -2.54 | -3.30% |
| T1-P2 10-09-84 | 0.000000 | 1.32E-09 | 3.176 | 255.255 | 0.00086 | 0.0129 | 245.94 | -9.32 | -3.72% |
| T1-P3 10-09-84 | 0.000000 | 1.37E-09 | 3.688 | 208.684 | 0.00245 | 0.0143 | 243.13 | 34.45 | 15.25% |
| T1-P4 10-09-84 | 0.000000 | 1.29E-09 | 2.923 | 170.170 | 0.00086 | 0.0114 | 169.63 | -0.54 | -0.32% |
| T1-P5 10-09-84 | 0.000000 | 1.03E-09 | 2.417 | 78.285 | 0.00086 | 0.0105 | 53.93 | -24.35 | -36.83% |
| T1-P6 10-09-84 | DRY | DRY | DRY | DRY | DRY | DRY | DRY | DRY | DRY |
| T2-P1 06-09-84 | 0.000000 | 4.39E-11 | 1.651 | 643.272 | 0.00086 | 0.0119 | 54.93 | -588.34 | -168.53% |
| T2-P2 06-09-84 | 0.000000 | 0.00E+00 | 1.777 | 129.513 | 0.00086 | 0.0192 | 147.80 | 18.29 | 13.19% |
| T2-P3 06-09-84 | 0.000000 | 1.51E-09 | 3.302 | 208.684 | 0.00172 | 0.0017 | 240.85 | 32.16 | 14.31% |
| T2-P4 06-09-84 | 0.000000 | 2.07E-09 | 2.543 | 110.885 | 0.00086 | 0.0108 | 106.27 | -4.61 | -4.25% |
| T2-P5 06-09-84 | 0.000000 | 1.95E-09 | 2.923 | 68.971 | 0.03811 | 0.1099 | 59.19 | -9.78 | -15.26% |
| T2-P6 06-09-84 | DRY | DRY | DRY | DRY | DRY | DRY | DRY | DRY | DRY |
| T2-P7 06-09-84 | DRY | DRY | DRY | DRY | DRY | DRY | DRY | DRY | DRY |
| T2-P8 06-09-84 | DRY | DRY | DRY | DRY | DRY | DRY | DRY | DRY | DRY |
| T2-P9 06-09-84 | DRY | DRY | DRY | DRY | DRY | DRY | DRY | DRY | DRY |
| T2-P10 06-09-84 | 0.000000 | 0.00E+00 | 0.800 | 151.402 | 0.00000 | 0.0141 | 216.12 | 64.72 | 35.22% |
| T2-P11 06-09-84 | 0.000000 | 0.00E+00 | 0.700 | 133.081 | 0.00086 | 0.0000 | 181.08 | 48.00 | 30.56% |
| T3-CENTER 07-09-84 | 0.000000 | 0.00E+00 | 1.777 | 78.285 | 0.00086 | 0.0026 | 77.79 | -0.49 | -0.63% |
| T3-1 07-09-84 | 0.000000 | 0.00E+00 | 1.777 | 82.942 | 0.00000 | 0.0084 | 67.20 | -15.74 | -20.97% |
| T3-2 07-09-84 | 0.000000 | 1.18E-09 | 1.651 | 70.818 | 0.00000 | 0.0039 | 79.66 | 8.84 | 11.75% |
| T3-3 07-09-84 | 0.000000 | 1.50E-09 | 1.525 | 73.628 | 0.00000 | 0.0000 | 68.41 | -5.22 | -7.35% |
| T3-4 07-09-84 | 0.000000 | 6.58E-10 | 1.525 | 68.971 | 0.00086 | 0.0047 | 61.39 | -7.58 | -11.63% |
| T3-5 07-09-84 | 0.000000 | 1.70E-11 | 1.525 | 138.827 | 0.00000 | 0.0041 | 113.27 | -25.56 | -20.28% |
| T3-6 07-09-84 | 0.000000 | 0.00E+00 | 0.000 | 110.470 | 0.00086 | 0.0037 | 136.53 | 26.06 | 21.10% |
| T3-P3 07-09-84 | 0.003108 | 0.00E+00 | 4.321 | 162.113 | 0.00000 | 0.0028 | 123.47 | -38.64 | -27.06% |
| T7-CENTER 07-09-84 | 0.000483 | 0.00E+00 | 0.000 | 117.736 | 0.00226 | 0.0069 | 148.35 | 30.61 | 23.01% |
| T7-1 07-09-84 | 0.000000 | 2.18E-10 | 0.000 | 100.602 | 0.00000 | 0.0068 | 121.98 | 21.37 | 19.21% |
| T7-3 07-09-84 | 0.000483 | 0.00E+00 | 0.000 | 89.942 | 0.00086 | 0.0075 | 121.15 | 31.21 | 29.57% |
| T7-4 07-09-84 | 0.000483 | 0.00E+00 | 0.000 | 109.721 | 0.00000 | 0.0079 | 132.65 | 22.93 | 18.92% |
| T7-5 07-09-84 | 0.000483 | 0.00E+00 | 0.000 | 112.344 | 0.00191 | 0.0020 | 131.45 | 19.10 | 15.67% |
| T7-6 07-09-84 | 0.000483 | 0.00E+00 | 0.000 | 113.635 | 0.00086 | 0.0022 | 129.93 | 16.29 | 13.38% |
| T7-7 07-09-84 | 0.000483 | 0.00E+00 | 0.000 | 80.073 | 0.00898 | 0.0410 | 92.41 | 12.33 | 14.30% |
| T7-P1 07-09-84 | 0.000000 | 0.00E+00 | 2.297 | 134.171 | 0.00086 | 0.0017 | 171.10 | 36.93 | 24.19% |
| T7-P2 07-09-84 | 0.000000 | 5.48E-10 | 6.611 | 124.856 | 0.06551 | 0.0686 | 111.94 | -12.91 | -10.91% |
| T7-P5 07-09-84 | 0.000000 | 0.00E+00 | 6.358 | 371.681 | 0.12653 | 0.0798 | 339.62 | -32.06 | -9.02% |
| T7-PVCV SMALL TUBE 07-09-84 | 0.003784 | 0.00E+00 | 2.128 | | 0.04672 | 0.0249 | 407.31 | | |
| T8-P1 10/09/84 | 0.000000 | 0.00E+00 | 3.049 | 301.825 | 0.00452 | 0.0000 | 249.87 | -51.95 | -18.83% |
| T8-P2 10/09/84 | 0.000000 | 8.78E-10 | 2.290 | 255.254 | 0.00807 | 0.0000 | 276.06 | 20.81 | 7.83% |
| T8-P3 10/09/84 | 0.000000 | 0.00E+00 | 3.815 | 162.113 | 0.00248 | 0.0017 | 148.35 | -13.77 | -8.87% |
| T8-P4 10/09/84 | 0.000000 | 0.00E+00 | 3.176 | 231.969 | 0.00317 | 0.0117 | 192.33 | -39.64 | -18.68% |
| T8-P5 10/09/84 | 0.001197 | 0.00E+00 | 0.746 | 161.666 | 0.00555 | 0.0073 | 186.05 | 24.38 | 14.03% |
| T8-P6 10/09/84 | 0.000000 | 0.00E+00 | 0.544 | 195.082 | 0.00515 | 0.0044 | 232.37 | 37.29 | 17.45% |

Table 7.13 - Nordic main tailings data. Solid phase samples. Summary of results from radioisotope analyses and activity ratios from locations T-1, T-2, T-3, T-7 and T-8 at various depths.

| | Solid Sample Study | | | | | | | | ACTIVITY RATIOS | | | |
|---|---|---|---|---|---|---|---|---|---|---|---|---|
| SAMPLE DESCRIPTION DEPTH (m) | Northing (m) (x10) | Elevation (m) | Pb-210 (mBq/g) +/-10% | Ra-224 (mBq/g) | Ra-226 (mBq/g) +/-10% | Th-228 (mBq/g) +/-20% | Th-230 (mBq/g) +/-20% | Th-232 (mBq/g) +/-20% | RATIO Pb-210/ Ra-226 | RATIO Ra-226/ Th-230 | RATIO Th-228/ Th-232 | RATIO Ra-224/ Th-228 |
| T - 1 - 1.00 | 544.80 | 350.79 | 13764.0 | | 17760.0 | 3219.0 | 1258.0 | 185.0 | 0.78 | 14.12 | 17.40 | |
| T - 1 - 1.50 | 544.80 | 350.79 | 7955.0 | | 9768.0 | 703.0 | 5106.0 | 851.0 | 0.81 | 1.91 | 0.83 | |
| T - 1 - 2.00 | 544.80 | 350.79 | 15873.0 | | 21201.0 | 1813.0 | 22126.0 | 2738.0 | 0.75 | 0.96 | 0.66 | |
| T - 1 - 2.00 | 544.80 | 350.79 | 15947.0 | | 17131.0 | 2220.0 | 23199.0 | 3034.0 | 0.93 | 0.74 | 0.73 | |
| T - 1 - 2.00 | 544.80 | 350.79 | 17760.0 | | 21423.0 | 2775.0 | 23680.0 | 3034.0 | 0.83 | 0.90 | 0.91 | |
| T - 1 - 2.50 | 544.80 | 350.79 | 13653.0 | | 14171.0 | 1073.0 | 8991.0 | 1332.0 | 0,96 | 1.58 | 0.81 | |
| T - 1 - 3.00 | 544.80 | 350.79 | 11803.0 | | 14726.0 | 888.0 | 13209.0 | 1332.0 | 0.80 | 1.11 | 0.67 | |
| T - 1 - 4.00 | 544.80 | 350.79 | 15799.0 | | 14245.0 | 407.0 | 2035.0 | 999.0 | 1.11 | 7.00 | 0.41 | |
| T - 1 - 4.00 | 544.80 | 350.79 | 18537.0 | | 18056.0 | 2368.0 | 9805.0 | 2627.0 | 1.03 | 1.84 | 0.90 | |
| T - 1 - 4.00 | 544.80 | 350.79 | 15799.0 | | 18167.0 | 1443.0 | 6327.0 | 1147.0 | 0.87 | 2.87 | 1.26 | |
| T - 1 - 4.25 | 544.80 | 350.79 | 12950.0 | | 12506.0 | 888.0 | 2775.0 | 962.0 | 1.04 | 4.51 | 0.92 | |
| T - 1 - 4.50 | 544.80 | 350.79 | 5846.0 | | 6105.0 | 333.0 | 851.0 | 148.0 | 0.96 | 7.17 | 2.25 | |
| T - 1 - 4.60 | 544.80 | 350.79 | 10471.0 | | 11840.0 | 814.0 | 8325.0 | 962.0 | 0.88 | 1.42 | 0.85 | |
| T - 1 - 4.75 | 544.80 | 350.79 | 32264.0 | | 21830.0 | 3330.0 | 6660.0 | 2035.0 | 1.48 | 3.28 | 1.64 | |
| T - 1 - 5.00 | 544.80 | 350.79 | 14615.0 | | 15540.0 | 2183.0 | 6919.0 | 1517.0 | 0.94 | 2.25 | 1.44 | |
| T - 1 - 5.25 | 544.80 | 350.79 | 31968.0 | | 25752.0 | 1036.0 | 3182.0 | 999.0 | 1.24 | 8.09 | 1.04 | |
| T - 1 - 5.50 | 544.80 | 350.79 | 12950.0 | | 13653.0 | 1036.0 | 1924.0 | 888.0 | 0.95 | 7.10 | 1.17 | |
| T - 1 - 5.75 | 544.80 | 350.79 | 13135.0 | | 16132.0 | 666.0 | 2701.0 | 851.0 | 0.81 | 5.97 | 0.78 | |
| T - 1 - 6.00 | 544.80 | 350.79 | 15651.0 | | 15836.0 | 407.0 | 3885.0 | 1221.0 | 0.99 | 4.08 | 0.33 | |
| T - 1 - 6.00 | 544.80 | 350.79 | 16502.0 | | 18500.0 | 1480.0 | 5106.0 | 1332.0 | 0.89 | 3.62 | 1.11 | |
| T - 1 - 6.00 | 544.80 | 350.79 | 18796.0 | | 18537.0 | 1517.0 | 6031.0 | 1295.0 | 1.01 | 3.07 | 1.17 | |
| T - 1 - 6.00 | 544.80 | 350.79 | 12950.0 | | 14208.0 | 1147.0 | 11729.0 | 1332.0 | 0.91 | 1.21 | 0.86 | |
| T - 1 - 6.25 | 544.80 | 350.79 | 10175.0 | | 9398.0 | 1036.0 | 3145.0 | 925.0 | 1.08 | 2.99 | 1.12 | |
| T - 1 - 6.50 | 544.80 | 350.79 | 13542.0 | | 14134.0 | 592.0 | 2664.0 | 592.0 | 0.96 | 5.31 | 1.00 | |
| T - 1 - 6.75 | 544.80 | 350.79 | 8806.0 | | 8954.0 | 370.0 | 2146.0 | 888.0 | 0.98 | 4.17 | 0.42 | |
| T - 1 - 7.00 | 544.80 | 350.79 | 19277.0 | | 14430.0 | 481.0 | 3885.0 | 814.0 | 1.34 | 3.71 | 0.59 | |
| T - 1 - 7.00 | 544.80 | 350.79 | 12247.0 | | 13468.0 | 740.0 | 4847.0 | 592.0 | 0.91 | 2.78 | 1.25 | |
| T - 1 - 7.25 | 544.80 | 350.79 | 5883.0 | | 4810.0 | 74.0 | 259.0 | 74.0 | 1.22 | 18.57 | 1.00 | |
| T - 1 - 7.40 | 544.80 | 350.79 | 17057.0 | | 20609.0 | 2331.0 | 9398.0 | 1036.0 | 0.83 | 2.19 | 2.25 | |
| T - 1 - 7.50 | 544.80 | 350.79 | 8954.0 | | 10989.0 | 296.0 | 2516.0 | 481.0 | 0.81 | 4.37 | 0.62 | |
| T - 1 - 7.60 | 544.80 | 350.79 | 10619.0 | | 12728.0 | 962.0 | 6031.0 | 703.0 | 0.83 | 2.11 | 1.37 | |
| T - 1 - 7.60 | 544.80 | 350.79 | 10619.0 | | 12469.0 | 2627.0 | 6697.0 | 777.0 | 0.85 | 1.86 | 3.38 | |
| T - 1 - 7.60 | 544.80 | 350.79 | 10360.0 | | 11507.0 | 666.0 | 8695.0 | 1332.0 | 0.90 | 1.32 | 0.50 | |
| T - 1 - 7.75 | 544.80 | 350.79 | 16539.0 | | 15096.0 | 555.0 | 2590.0 | 703.0 | 1.10 | 5.83 | 0.79 | |
| T - 1 - 8.00 | 544.80 | 350.79 | 3885.0 | | 6068.0 | 2109.0 | 14393.0 | 1036.0 | 0.64 | 0.42 | 2.04 | |
| T - 1 - 8.00 | 544.80 | 350.79 | 23754.0 | | 19610.0 | 1813.0 | 6105.0 | 2035.0 | 1.21 | 3.21 | 0.89 | |
| T - 1 - 8.25 | 544.80 | 350.79 | 35853.0 | | 24494.0 | 2627.0 | 6364.0 | 1554.0 | 1.46 | 3.85 | 1.69 | |
| T - 1 - 8.50 | 544.80 | 350.79 | 19388.0 | | 22459.0 | 925.0 | 7770.0 | 1036.0 | 0.86 | 2.89 | 0.89 | |
| T - 1 - 8.50 | 544.80 | 350.79 | 24901.0 | | 19092.0 | 666.0 | 2960.0 | 1036.0 | 1.30 | 6.45 | 0.64 | |
| T - 1 - 8.50 | 544.80 | 350.79 | 26307.0 | | 20239.0 | 3145.0 | 10360.0 | 2775.0 | 1.30 | 1.95 | 1.13 | |
| T - 1 - 9.00 | 544.80 | 350.79 | 18759.0 | | 20239.0 | 1924.0 | 14948.0 | 1554.0 | 0.93 | 1.35 | 1.24 | |
| T - 1 - 9.00 | 544.80 | 350.79 | 18685.0 | | 21497.0 | 1665.0 | 14652.0 | 1480.0 | 0.87 | 1.47 | 1.13 | |
| T - 1 - 9.00 | 544.80 | 350.79 | 15725.0 | | 18241.0 | 2738.0 | 16428.0 | 1887.0 | 0.86 | 1.11 | 1.45 | |
| T - 1 - 9.60 | 544.80 | 350.79 | 16761.0 | 1295.0 | 13579.0 | 1476.3 | 18107.8 | 1587.3 | 1.23 | 0.75 | 0.93 | 0.88 |
| T - 1 - 9.60 | 544.80 | 350.79 | 17908.0 | 1480.0 | 17782.2 | 1968.4 | 22618.1 | 2234.8 | 1.01 | 0.79 | 0.88 | 0.75 |
| T - 1 -10.20 | 544.80 | 350.79 | 20646.0 | 2849.0 | 20398.1 | 2886.0 | 26551.2 | 2667.7 | 1.01 | 0.77 | 1.08 | 0.99 |
| T - 1 -10.60 | 544.80 | 350.79 | 621.6 | 74.0 | 3307.8 | 59.2 | 292.3 | 25.9 | 0.19 | 11.32 | 2.29 | 1.25 |
| T - 1 -10.70 | 544.80 | 350.79 | 218.3 | 74.0 | 266.4 | 55.5 | 310.8 | 77.7 | 0.82 | 0.86 | 0.71 | 1.33 |

Radioisotopes Ratio Solid Sample Data

Table 7.14 - Nordic main tailings data. Solid phase samples. Summary of results from radioisotope analyses and activity ratios from locations T-1, T-2, T-3, T-7 and T-8 at various depths.

| | Solid Sample Study | | | | | | | | ACTIVITY RATIOS | | | |
|---|---|---|---|---|---|---|---|---|---|---|---|---|
| SAMPLE DESCRIPTION DEPTH (m) | Northing (m) (x10) | Elevation (m) | Pb-210 (mBq/g) +/-10% | Ra-224 (mBq/g) | Ra-226 (mBq/g) +/-10% | Th-228 (mBq/g) +/-20% | Th-230 (mBq/g) +/-20% | Th-232 (mBq/g) +/-20% | RATIO Pb-210/ Ra-226 | RATIO Ra-226/ Th-230 | RATIO Th-228/ Th-232 | RATIO Ra-224/ Th-228 |
| T - 1 -10.77 | 544.80 | 350.79 | 12062.0 | 2072.0 | 13908.3 | 1857.4 | 18396.4 | 1713.1 | 0.87 | 0.76 | 1.08 | 1.12 |
| T - 1 -10.80 | 544.80 | 350.79 | 225.7 | 70.3 | 336.7 | 85.1 | 188.7 | 51.8 | 0.67 | 1.78 | 1.64 | 0.83 |
| T - 1 -11.18 | 544.80 | 350.79 | 484.7 | 122.1 | 588.3 | 129.5 | 762.2 | 136.9 | 0.82 | 0.77 | 0.95 | 0.94 |
| T - 1 -12.57 | 544.80 | 350.79 | 18796.0 | | 17168.0 | 2146.0 | 25345.0 | 2442.0 | 1.09 | 0.68 | 0.88 | |
| T - 2 - 1.00 | 518.74 | 351.58 | 14689.0 | | 16391.0 | 370.0 | 444.0 | 22.2 | 0.90 | 36.92 | 16.67 | |
| T - 2 - 1.40 | 518.74 | 351.58 | 10138.0 | | 13764.0 | 666.0 | 1480.0 | 185.0 | 0.74 | 9.30 | 3.60 | |
| T - 2 - 2.00 | 518.74 | 351.58 | 12987.0 | | 17575.0 | 2886.0 | 18907.0 | 3293.0 | 0.74 | 0.93 | 0.88 | |
| T - 2 - 3.00 | 518.74 | 351.58 | 8140.0 | | 9805.0 | 1480.0 | 11211.0 | 1961.0 | 0.83 | 0.87 | 0.75 | |
| T - 2 - 4.00 | 518.74 | 351.58 | 14504.0 | | 12506.0 | 925.0 | 11211.0 | 1369.0 | 1.16 | 1.12 | 0.68 | |
| T - 2 - 4.00 | 518.74 | 351.58 | 18130.0 | | 16909.0 | 2220.0 | 10582.0 | 1221.0 | 1.07 | 1.60 | 1.82 | |
| T - 2 - 4.00 | 518.74 | 351.58 | 17834.0 | | 15762.0 | 1184.0 | 10841.0 | 1258.0 | 1.13 | 1.45 | 0.94 | |
| T - 2 - 4.60 | 518.74 | 351.58 | 15096.0 | | 15836.0 | 666.0 | 4921.0 | 629.0 | 0.95 | 3.22 | 1.06 | |
| T - 2 - 5.00 | 518.74 | 351.58 | 10693.0 | | 13061.0 | 2294.0 | 21090.0 | 2146.0 | 0.82 | 0.62 | 1.07 | |
| T - 2 - 5.79 | 518.74 | 351.58 | 22163.0 | | 18796.0 | 1332.0 | 11914.0 | 925.0 | 1.18 | 1.58 | 1.44 | |
| T - 2 - 6.02 | 518.74 | 351.58 | 25197.0 | | 23495.0 | 1628.0 | 17834.0 | 1776.0 | 1.07 | 1.32 | 0.92 | |
| T - 2 - 6.93 | 518.74 | 351.58 | 21571.0 | | 22829.0 | 1147.0 | 16465.0 | 1739.0 | 0.94 | 1.39 | 0.66 | |
| T - 2 - 7.24 | 518.74 | 351.58 | 32745.0 | | 27824.0 | 2479.0 | 22977.0 | 2442.0 | 1.18 | 1.21 | 1.02 | |
| T - 2 - 8.00 | 518.74 | 351.58 | 23495.0 | | 21978.0 | 2812.0 | 22718.0 | 2812.0 | 1.07 | 0.97 | 1.00 | |
| T - 2 - 8.31 | 518.74 | 351.58 | 14319.0 | | 14726.0 | 1184.0 | 10804.0 | 1591.0 | 0.97 | 1.36 | 0.74 | |
| T - 2 - 8.76 | 518.74 | 351.58 | 22089.0 | | 22459.0 | 2146.0 | 23569.0 | 2590.0 | 0.98 | 0.95 | 0.83 | |
| T - 2 - 8.76 | 518.74 | 351.58 | 21867.0 | | 25937.0 | 1887.0 | 21608.0 | 2849.0 | 0.84 | 1.20 | 0.66 | |
| T - 2 - 8.76 | 518.74 | 351.58 | 23902.0 | | 22866.0 | 1961.0 | 22903.0 | 2516.0 | 1.05 | 1.00 | 0.78 | |
| T - 2 - 9.07 | 518.74 | 351.58 | 33522.0 | | 26566.0 | 3626.0 | 29267.0 | 3256.0 | 1.26 | 0.91 | 1.11 | |
| T - 2 - 9.07 | 518.74 | 351.58 | 31968.0 | | 28897.0 | 3108.0 | 29822.0 | 3996.0 | 1.11 | 0.97 | 0.78 | |
| T - 2 - 9.07 | 518.74 | 351.58 | 30414.0 | | 26862.0 | 2997.0 | 28934.0 | 3737.0 | 1.13 | 0.93 | 0.80 | |
| T - 2 - 9.61 | 518.74 | 351.58 | 27491.0 | | 31931.0 | 3552.0 | 27306.0 | 3034.0 | 0.86 | 1.17 | 1.17 | |
| T - 2 - 9.77 | 518.74 | 351.58 | 37259.0 | | 42180.0 | 3996.0 | 42624.0 | 4810.0 | 0.88 | 0.99 | 0.83 | |
| T - 2 - 9.79 | 518.74 | 351.58 | 27972.0 | 2664.0 | 35786.4 | 2934.1 | 48421.9 | 2941.5 | 0.78 | 0.74 | 1.00 | 0.91 |
| T - 2 - 9.87 | 518.74 | 351.58 | 33633.0 | 5254.0 | 35989.9 | 4632.4 | 51788.9 | 5820.1 | 0.93 | 0.69 | 0.80 | 1.13 |
| T - 2 - 9.94 | 518.74 | 351.58 | 27750.0 | 3034.0 | 29326.2 | 2856.4 | 35353.5 | 5220.7 | 0.95 | 0.83 | 0.55 | 1.06 |
| T - 2 -10.15 | 518.74 | 351.58 | 321.9 | 7.4 | 492.1 | 14.8 | 236.8 | 37.0 | 0.65 | 2.08 | 0.40 | 0.50 |
| T - 2 -10.25 | 518.74 | 351.58 | 181.3 | 92.5 | 858.4 | 85.1 | 159.1 | 40.7 | 0.21 | 5.40 | 2.09 | 1.09 |
| T - 2 -10.33 | 518.74 | 351.58 | 233.1 | 44.4 | 318.2 | 96.2 | 103.6 | 18.5 | 0.73 | 3.07 | 5.20 | 0.46 |
| T - 3 - 1.00 | 509.62 | 350.83 | 15540.0 | | 17538.0 | 888.0 | 925.0 | 114.7 | 0.89 | 18.96 | 7.74 | |
| T - 3 - 1.30 | 509.62 | 350.83 | 12876.0 | | 13061.0 | 1221.0 | 6512.0 | 777.0 | 0.99 | 2.01 | 1.57 | |
| T - 3 - 2.00 | 509.62 | 350.83 | 9583.0 | | 9842.0 | 666.0 | 2516.0 | 222.0 | 0.97 | 3.91 | 3.00 | |
| T - 3 - 2.60 | 509.62 | 350.83 | 24383.0 | | 19055.0 | 1332.0 | 14800.0 | 1332.0 | 1.28 | 1.29 | 1.00 | |
| T - 3 - 3.00 | 509.62 | 350.83 | 11803.0 | | 10582.0 | 703.0 | 6549.0 | 703.0 | 1.12 | 1.62 | 1.00 | |
| T - 3 - 3.00 | 509.62 | 350.83 | 11655.0 | | 11618.0 | 555.0 | 7400.0 | 814.0 | 1.00 | 1.57 | 0.68 | |
| T - 3 - 3.00 | 509.62 | 350.83 | 11433.0 | | 11211.0 | 592.0 | 5846.0 | 666.0 | 1.02 | 1.92 | 0.89 | |
| T - 3 - 4.00 | 509.62 | 350.83 | 5476.0 | | 7511.0 | 407.0 | 1628.0 | 444.0 | 0.73 | 4.61 | 0.92 | |
| T - 3 - 4.30 | 509.62 | 350.83 | 26011.0 | | 27084.0 | 2183.0 | 23051.0 | 2553.0 | 0.96 | 1.17 | 0.86 | |
| T - 3 - 4.30 | 509.62 | 350.83 | 27232.0 | | 24457.0 | 1998.0 | 21904.0 | 2368.0 | 1.11 | 1.12 | 0.84 | |
| T - 3 - 4.30 | 509.62 | 350.83 | 27528.0 | | 23828.0 | 2072.0 | 21460.0 | 2257.0 | 1.16 | 1.11 | 0.92 | |
| T - 3 - 5.00 | 509.62 | 350.83 | 11359.0 | | 14874.0 | 1443.0 | 9250.0 | 1295.0 | 0.76 | 1.61 | 1.11 | |
| T - 3 - 6.93 | 509.62 | 350.83 | 48285.0 | | 49136.0 | 6549.0 | 41773.0 | 6808.0 | 0.98 | 1.18 | 0.96 | |
| T - 3 - 6.93 | 509.62 | 350.83 | 44474.0 | | 53465.0 | 4884.0 | 40959.0 | 6660.0 | 0.83 | 1.31 | 0.73 | |
| T - 3 - 6.93 | 509.62 | 350.83 | 48248.0 | | 44067.0 | 4514.0 | 39849.0 | 5661.0 | 1.09 | 1.11 | 0.80 | |

Radioisotopes Ratio Solid Sample Data

Table 7.15 - Nordic main tailings data. Solid phase samples. Summary of results from radioisotope analyses and activity ratios from locations T-1, T-2, T-3, T-7 and T-8 at various depths.

| SAMPLE DESCRIPTION DEPTH (m) | Solid Sample Study: Northing (m) (x10) | Elevation (m) | Pb-210 (mBq/g) +/-10% | Ra-224 (mBq/g) | Ra-226 (mBq/g) +/-10% | Th-228 (mBq/g) +/-20% | Th-230 (mBq/g) +/-20% | Th-232 (mBq/g) +/-20% | ACTIVITY RATIOS: RATIO Pb-210/ Ra-226 | RATIO Ra-226/ Th-230 | RATIO Th-228/ Th-232 | RATIO Ra-224/ Th-228 |
|---|---|---|---|---|---|---|---|---|---|---|---|---|
| T - 3 - 7.25 | 509.62 | 350.83 | 20868.0 | | 19166.0 | 777.0 | 4551.0 | 1036.0 | 1.09 | 4.21 | 0.75 | |
| T - 3 - 7.25 | 509.62 | 350.83 | 22089.0 | | 17131.0 | 1924.0 | 4662.0 | 851.0 | 1.29 | 3.67 | 2.26 | |
| T - 3 - 7.25 | 509.62 | 350.83 | 19869.0 | | 22792.0 | 1887.0 | 5550.0 | 1295.0 | 0.87 | 4.11 | 1.46 | |
| T - 3 - 7.50 | 509.62 | 350.83 | 22089.0 | | 17427.0 | 1850.0 | 4810.0 | 1332.0 | 1.27 | 3.62 | 1.39 | |
| T - 3 - 7.54 | 509.62 | 350.83 | 22422.0 | | 24679.0 | 2294.0 | 24198.0 | 2664.0 | 0.91 | 1.02 | 0.86 | |
| T - 3 - 7.75 | 509.62 | 350.83 | 12839.0 | | 12617.0 | 851.0 | 2257.0 | 592.0 | 1.02 | 5.59 | 1.44 | |
| T - 3 - 7.85 | 509.62 | 350.83 | 28194.0 | | 32116.0 | 2849.0 | 41329.0 | 3848.0 | 0.88 | 0.78 | 0.74 | |
| T - 3 - 7.85 | 509.62 | 350.83 | 29489.0 | | 34891.0 | 4810.0 | 42328.0 | 4995.0 | 0.85 | 0.82 | 0.96 | |
| T - 3 - 7.85 | 509.62 | 350.83 | 28194.0 | | 37481.0 | 3071.0 | 39257.0 | 3515.0 | 0.75 | 0.95 | 0.87 | |
| T - 3 - 7.96 | 509.62 | 350.83 | 2479.0 | | 3071.0 | 296.0 | 1110.0 | 185.0 | 0.81 | 2.77 | 1.60 | |
| T - 3 - 7.97 | 509.62 | 350.83 | 29970.0 | | 27972.0 | 1184.0 | 3330.0 | 666.0 | 1.07 | 8.40 | 1.78 | |
| T - 3 - 8.01 | 509.62 | 350.83 | 1406.0 | | 1813.0 | 148.0 | 74.0 | 18.5 | 0.78 | 24.50 | 8.00 | |
| T - 3 - 8.06 | 509.62 | 350.83 | 518.0 | | 518.0 | 74.0 | 222.0 | 74.0 | 1.00 | 2.33 | 1.00 | |
| T - 3 - 8.29 | 509.62 | 350.83 | 418.1 | 74.0 | 710.4 | 88.8 | 1098.9 | 107.3 | 0.59 | 0.65 | 0.83 | 0.83 |
| T - 3 - 8.53 | 509.62 | 350.83 | 1554.0 | 218.3 | 1872.2 | 203.5 | 1491.1 | 244.2 | 0.83 | 1.26 | 0.83 | 1.07 |
| T - 7 - 1.00 | 496.41 | 351.95 | 10027.0 | | 12506.0 | 481.0 | 1184.0 | 148.0 | 0.80 | 10.56 | 3.25 | |
| T - 7 - 1.30 | 496.41 | 351.95 | 13949.0 | | 17094.0 | 888.0 | 2183.0 | 296.0 | 0.82 | 7.83 | 3.00 | |
| T - 7 - 2.00 | 496.41 | 351.95 | 8103.0 | | 12136.0 | 629.0 | 740.0 | 66.6 | 0.67 | 16.40 | 9.44 | |
| T - 7 - 3.00 | 496.41 | 351.95 | 16095.0 | | 19610.0 | 888.0 | 18870.0 | 1628.0 | 0.82 | 1.04 | 0.55 | |
| T - 7 - 3.00 | 496.41 | 351.95 | 10841.0 | | 11803.0 | 1147.0 | 17020.0 | 2516.0 | 0.92 | 0.69 | 0.46 | |
| T - 7 - 4.00 | 496.41 | 351.95 | 14615.0 | | 14615.0 | 1850.0 | 8436.0 | 1110.0 | 1.00 | 1.73 | 1.67 | |
| T - 7 - 5.00 | 496.41 | 351.95 | 12432.0 | | 17242.0 | 1480.0 | 9879.0 | 1332.0 | 0.72 | 1.75 | 1.11 | |
| T - 7 - 5.00 | 496.41 | 351.95 | 12506.0 | | 15096.0 | 1406.0 | 8658.0 | 999.0 | 0.83 | 1.74 | 1.41 | |
| T - 7 - 5.00 | 496.41 | 351.95 | 12247.0 | | 19425.0 | 2183.0 | 9805.0 | 1517.0 | 0.63 | 1.98 | 1.44 | |
| T - 7 - 6.00 | 496.41 | 351.95 | 11914.0 | | 15244.0 | 1406.0 | 8547.0 | 1184.0 | 0.78 | 1.78 | 1.19 | |
| T - 7 - 6.40 | 496.41 | 351.95 | 14245.0 | 1480.0 | 18437.1 | 1420.8 | 14448.5 | 1139.6 | 0.77 | 1.28 | 1.25 | 1.04 |
| T - 7 - 6.90 | 496.41 | 351.95 | 30081.0 | 2960.0 | 29511.2 | 3204.2 | 28915.5 | 3193.1 | 1.02 | 1.02 | 1.00 | 0.92 |
| T - 7 - 6.90 | 496.41 | 351.95 | 27972.0 | 2775.0 | 28342.0 | 2516.0 | 26880.5 | 3178.3 | 0.99 | 1.05 | 0.79 | 1.10 |
| T - 7 - 7.00 | 496.41 | 351.95 | 26344.0 | | 31043.0 | 2072.0 | 17760.0 | 2886.0 | 0.85 | 1.75 | 0.72 | 0.00 |
| T - 7 - 7.20 | 496.41 | 351.95 | 28194.0 | 2960.0 | 27539.1 | 3204.2 | 32844.9 | 3470.6 | 1.02 | 0.84 | 0.92 | 0.92 |
| T - 7 - 7.70 | 496.41 | 351.95 | 14578.0 | 1517.0 | 14037.8 | 1716.8 | 15273.6 | 2604.8 | 1.04 | 0.92 | 0.66 | 0.88 |
| T - 7 - 7.81 | 496.41 | 351.95 | 7770.0 | 444.0 | 5846.0 | 532.8 | 4181.0 | 377.4 | 1.33 | 1.40 | 1.41 | 0.83 |
| T - 7 - 7.86 | 496.41 | 351.95 | 15355.0 | 2183.0 | 15318.0 | 1920.3 | 16265.2 | 2379.1 | 1.00 | 0.94 | 0.81 | 1.14 |
| T - 7 - 7.91 | 496.41 | 351.95 | 24198.0 | 2886.0 | 25382.0 | 2941.5 | 28893.3 | 4699.0 | 0.95 | 0.88 | 0.63 | 0.98 |
| T - 7 - 7.96 | 496.41 | 351.95 | 16021.0 | | 16354.0 | 1332.0 | 10952.0 | 1369.0 | 0.98 | 1.49 | 0.97 | |
| T - 7 - 8.38 | 496.41 | 351.95 | 2812.0 | 333.0 | 2797.2 | 355.2 | 1938.8 | 270.1 | 1.01 | 1.44 | 1.32 | 0.94 |
| T - 7 - 8.99 | 496.41 | 351.95 | 814.0 | 111.0 | 888.0 | 122.1 | 362.6 | 96.2 | 0.92 | 2.45 | 1.27 | 0.91 |
| T - 8 - 1.00 | 490.78 | 353.47 | 7474.0 | | 8954.0 | 703.0 | 407.0 | 44.4 | 0.83 | 22.00 | 15.83 | |
| T - 8 - 2.00 | 490.78 | 353.47 | 5920.0 | | 6438.0 | 259.0 | 296.0 | 48.1 | 0.92 | 21.75 | 5.38 | |
| T - 8 - 3.00 | 490.78 | 353.47 | 5402.0 | | 7178.0 | | 2220.0 | 2405.0 | 0.75 | 3.23 | 0.00 | |
| T - 8 - 3.00 | 490.78 | 353.47 | 6068.0 | | 7918.0 | 333.0 | 1739.0 | 148.0 | 0.77 | 4.55 | 2.25 | |
| T - 8 - 4.00 | 490.78 | 353.47 | 7178.0 | | 10989.0 | 296.0 | 481.0 | 77.7 | 0.65 | 22.85 | 3.81 | |
| T - 8 - 5.00 | 490.78 | 353.47 | 6697.0 | | 8991.0 | 666.0 | 10656.0 | 851.0 | 0.74 | 0.84 | 0.78 | |
| T - 8 - 6.00 | 490.78 | 353.47 | 7733.0 | | 8695.0 | 518.0 | 8325.0 | 703.0 | 0.89 | 1.04 | 0.74 | |
| T - 8 - 6.00 | 490.78 | 353.47 | 7622.0 | | 9324.0 | 629.0 | 8066.0 | 703.0 | 0.82 | 1.16 | 0.89 | |
| T - 8 - 6.00 | 490.78 | 353.47 | 8399.0 | | 8880.0 | 592.0 | 8140.0 | 888.0 | 0.95 | 1.09 | 0.67 | |
| T - 8 - 7.00 | 490.78 | 353.47 | 19499.0 | | 21497.0 | 1665.0 | 14837.0 | 1739.0 | 0.91 | 1.45 | 0.96 | |
| T - 8 - 7.60 | 490.78 | 353.47 | 18056.0 | 1591.0 | 14474.4 | 1539.2 | 17131.0 | 1502.2 | 1.25 | 0.84 | 1.02 | 1.03 |

Radioisotopes Ratio Solid Sample Data

Table 7.16 - Nordic main tailings data. Solid phase samples. Summary of results from radioisotope analyses and activity ratios from locations T-1, T-2, T-3, T-7 and T-8 at various depths.

| | Solid Sample Study | | | | | | | | ACTIVITY RATIOS | | | |
|---|---|---|---|---|---|---|---|---|---|---|---|---|
| SAMPLE DESCRIPTION DEPTH (m) | Northing (m) (x10) | Elevation (m) | Pb-210 (mBq/g) +/-10% | Ra-224 (mBq/g) | Ra-226 (mBq/g) +/-10% | Th-228 (mBq/g) +/-20% | Th-230 (mBq/g) +/-20% | Th-232 (mBq/g) +/-20% | RATIO Pb-210/ Ra-226 | RATIO Ra-226/ Th-230 | RATIO Th-228/ Th-232 | RATIO Ra-224/ Th-228 |
| T - 8 - 8.40 | 490.78 | 353.47 | 8991.0 | 1961.0 | 7437.0 | 1879.6 | 8376.8 | 703.0 | 1.21 | 0.89 | 2.67 | 1.04 |
| T - 8 - 8.40 | 490.78 | 353.47 | 7511.0 | 851.0 | 8658.0 | 1172.9 | 7440.7 | 1354.2 | 0.87 | 1.16 | 0.87 | 0.73 |
| T - 8 - 8.76 | 490.78 | 353.47 | 14652.0 | 1628.0 | 14999.8 | 1572.5 | 13149.8 | 1609.5 | 0.98 | 1.14 | 0.98 | 1.04 |
| T - 8 - 9.07 | 490.78 | 353.47 | 26640.0 | | 28823.0 | 5254.0 | 19055.0 | 2664.0 | 0.92 | 1.51 | 1.97 | |
| T - 8 - 9.37 | 490.78 | 353.47 | 16687.0 | 1406.0 | 15351.3 | 973.1 | 10855.8 | 862.1 | 1.09 | 1.41 | 1.13 | 1.44 |
| T - 8 - 9.98 | 490.78 | 353.47 | 41736.0 | | 42809.0 | 5624.0 | 40145.0 | 3811.0 | 0.97 | 1.07 | 1.48 | |
| T - 8 -10.29 | 490.78 | 353.47 | 24790.0 | | 26973.0 | | | | 0.92 | | | |
| T - 8 -10.29 | 490.78 | 353.47 | 30081.0 | | 26196.0 | 3293.0 | 31302.0 | 3700.0 | 1.15 | 0.84 | 0.89 | |
| T - 8 -10.29 | 490.78 | 353.47 | 29045.0 | | 31524.0 | 1924.0 | 21201.0 | 2109.0 | 0.92 | 1.49 | 0.91 | |
| T - 8 -11.05 | 490.78 | 353.47 | 23347.0 | | 24013.0 | 1665.0 | 25530.0 | 2664.0 | 0.97 | 0.94 | 0.63 | |
| T - 8 -11.20 | 490.78 | 353.47 | 22385.0 | | 22200.0 | 1776.0 | 21127.0 | 2257.0 | 1.01 | 1.05 | 0.79 | |
| T - 8 -11.44 | 490.78 | 353.47 | 33781.0 | | 32893.0 | 2553.0 | 28379.0 | 2627.0 | 1.03 | 1.16 | 0.97 | |
| T - 8 -11.49 | 490.78 | 353.47 | 12543.0 | | 12432.0 | 518.0 | 15170.0 | 962.0 | 1.01 | 0.82 | 0.54 | |
| T - 8 -11.60 | 490.78 | 353.47 | 5328.0 | | 6956.0 | 1184.0 | 2183.0 | 222.0 | 0.77 | 3.19 | 5.33 | |
| T - 8 -11.65 | 490.78 | 353.47 | 9324.0 | 1110.0 | 9224.1 | 865.8 | 10145.4 | 965.7 | 1.01 | 0.91 | 0.90 | 1.28 |
| T - 8 -11.65 | 490.78 | 353.47 | 9805.0 | | 10434.0 | 925.0 | 9287.0 | 888.0 | 0.94 | 1.12 | 1.04 | |
| T - 8 -12.24 | 490.78 | 353.47 | 6845.0 | | 7422.2 | 740.0 | 7248.3 | 825.1 | 0.92 | 1.02 | 0.90 | |

Table 7.17 - Nordic main tailings data. Additional data from location T-5. Solid and liquid phase samples for comparison of radioisotope activities at various depths.

| | | Solid Sample | | | | | Liquid Sample | | | | | | |
|---|---|---|---|---|---|---|---|---|---|---|---|---|---|
| Depth m | Piezometer No. | $^{228}Th$ pCi/g | $^{232}Th$ pCi/g | $^{230}Th$ pCi/g | $^{226}Ra$ pCi/g | $^{210}Pb$ pCi/g | $^{228}Th$ pCi/L | $^{232}Th$ pCi/L | $^{230}Th$ pCi/l | $^{226}Ra$ pCi/L | $^{210}Pb$ pCi/L | $^{223}Ra$ pCi/L | Remarks |
| 4.70 | | 11 | 11 | 32 | 105 | 125 | | | | | | | |
| 4.80 | | 10 | 7 | 42 | 110 | 107 | | | | | | | |
| 5.00 | | 33 | 11 | 64 | 164 | 206 | | | | | | | |
| 5.40 | | 8 | 7 | 28 | 162 | 115 | | | | | | | |
| 5.58 | P5 | 24 | 21 | 66 | 303 | 287 | 160±33 | 0.9±0.6 | 40±1.4 | 86±6 | 1951±87 | 439±18 | |
| 5.75 | | 26 | 40 | 152 | 296 | 353 | | | | | | | |
| 6.00 | | 9 | 8 | 52 | 125 | 159 | | | | | | | |
| 6.25 | | 24 | 13 | 52 | 111 | 163 | | | | | | | |
| 6.50 | | 14 | 15 | 44 | 182 | 176 | | | | | | | |
| 6.60 | P7 | 20.8±1.9 | 19.7±1.8 | 242.8±13.4 | 250±11.2 | 304±14 | 104±11 | 5.8±1.2 | 8.9±1.5 | 29±3 | 2114±94 | 460±18 | |
| 6.75 | P3 | 21 | 15 | 58 | 331 | 314 | 128±14 | 3.9±0.9 | 14.1±1.7 | 81±4 | 2421±103 | 694±24 | |
| 7.00 | | 8 | 17 | 55 | 281 | 332 | | | | | | | |
| 7.25 | P1 | 25 | 6 | 43 | 176 | 223 | 4±2 | $\leq$0.5 | $\leq$0.5 | 137±5 | 31±10 | 444±14 | Water table |
| 7.50 | | 63 | 65 | 238 | 556 | 653 | | | | | | | |
| 7.75 | | 11 | 13 | 36 | 130 | 164 | | | | | | | |
| 8.00 | P2 | 14 | 10 | 31 | 292 | 312 | $\leq$0.5 | $\leq$0.5 | 1.1±0.6 | 239±10 | 288±10 | 2360±71 | |
| 8.10 | P8 | 17.5±2 | 10.8±2 | 110.1±7 | 182.2±8.6 | 154±7 | 41±7 | 0.5 | 0.5 | 17±2 | 2785±121 | 492±17 | |
| 8.50 | | 15 | 17 | 60 | 180 | 183 | | | | | | | |
| 8.75 | P9 | 8 | 5 | 24 | 141 | 167 | 5±2 | 0.5 | 0.5 | 186±8 | 382±25 | 317±14 | |
| 9.00 | P4 | 40 | 16 | 65 | 349 | 323 | 123±18 | 0.8±0.4 | 0.9±0.7 | 52±4 | 3473±142 | 1007±38 | |
| 9.25 | | 11 | 6 | 23 | 156 | 129 | | | | | | | |
| 9.75 | | 6 | 3 | 36 | 144 | 158 | | | | | | | |
| 10.00 | P11 | 37 | 31 | 104 | 338 | 280 | 3±2 | 0.6±0.5 | 0.7±0.4 | 126±6 | 62±9 | 160±8 | |
| 11.70 | P12 | 6.1±1.2 | 7.6±1.2 | 67.4±4.8 | 171.8±8.2 | 164±8 | 10±4 | 1.2±0.2 | 3.7±1.2 | 97±6 | 639±32 | 761±26 | |
| 13.40 | P13 | 26.2±2.6 | 25.2±2.5 | 299.5±17 | 343.9±15.2 | 336±15 | 112±18 | 15±2 | 16±2 | 112±18 | 3430±18 | 670±15 | |
| 15.10 | | 16.3±1.5 | 12.2±1.2 | 112.5±6.6 | 141.3±7.3 | 126±6 | 0.5 | 0.5 | 0.5 | 139±7 | 55±12 | 52±5 | |
| 16.00 | | 9.1±1.5 | 8.9±1.5 | 131.4±8.5 | 206±10.4 | 136±7 | | | | | | | |
| 16.20 | | 10.2±1.3 | 11.8±1.4 | 123.7±7.5 | 200.3±9.5 | 163±7 | | | | | | | |
| 16.30 | Bundle 5 | 11.9±1.4 | 17.7±1.8 | 139.8±8.2 | 195.5±9.2 | 170±8 | 20±11 | $\leq$0.5 | $\leq$0.5 | 104±8 | 16±8 | 62±8 | Peat zone |
| 24 | | | | | | | 7±5 | 10±2 | 67±6 | 30±3 | 109±12 | 72±8 | |

Table 7.18 - Nordic main tailings data. Additional data from location T-5. Solid and liquid phase comparison of radioisotope activity ratios. Activity ratio = daughter activity/parent activity at various depths.

| | SOLID PHASE | | | LIQUID PHASE | | |
|---|---|---|---|---|---|---|
| SAMPLE DESCRIPTION DEPTH (m) | RATIO Pb-210/ Ra-226 | RATIO Ra-226/ Th-230 | RATIO Th-228/ Th-232 | RATIO Pb-210/ Ra-226 | RATIO Ra-226/ Th-230 | RATIO Th-228/ Th-232 |
| P - 5 - 5.58 | 0.95 | 4.59 | 1.14 | 22.69 | 2.15 | 177.78 |
| P - 7 - 6.60 | 1.22 | 1.03 | 1.02 | 72.90 | 3.26 | 17.93 |
| P - 3 - 6.75 | 0.95 | 5.71 | 1.40 | 29.89 | 5.74 | 32.82 |
| P - 1 - 7.25 | 1.27 | 4.09 | 4.17 | 0.23 | 274.00 | 8.00 |
| P - 2 - 8.00 | 1.07 | 9.42 | 1.40 | 1.21 | 217.27 | 1.00 |
| P - 8 - 8.10 | 0.85 | 1.65 | 1.62 | 163.82 | 34.00 | 82.00 |
| P - 9 - 8.75 | 1.18 | 5.88 | 1.60 | 2.05 | 372.00 | 10.00 |
| P - 4 - 9.00 | 0.93 | 5.37 | 2.50 | 66.79 | 57.78 | 153.75 |
| P - 11 - 10.00 | 0.83 | 3.25 | 1.19 | 0.49 | 180.00 | 5.00 |
| P - 12 - 11.70 | 0.95 | 2.55 | 0.80 | 6.59 | 26.22 | 8.33 |
| P - 13 - 13.40 | 0.98 | 1.15 | 1.04 | 30.63 | 7.00 | 7.47 |
| 15.10 | 0.89 | 1.26 | 1.34 | 0.40 | 278.00 | 1.00 |
| B - 5 - 16.30 | 0.87 | 1.40 | 0.67 | 0.15 | 208.00 | 40.00 |

Table 7.19 - Solubility of major radioisotopes and related sulphate salts in uranium tailings

| Salts | Solubility (g/100 mL) | Temperature °C |
|---|---|---|
| $RaSo_4$ | 0.000002 | 25 |
| $PbSO_4$ | 0.00425 | 25 |
| $Th(SO_4).4\ H_2O$ | 9.41 | 17 |
| $Th(SO_4).6\ H_2O$ | 1.63 | 16 |
| $Th(SO_4).8\ H_2O$ | 1.88 | 25 |
| $Th(SO_4).9\ H_2O$ | 1.57 | 20 |
| $U(SO_4)\ .4\ H_2O$ | 23.0 | 11 |
| $U(SO_4)\ .8\ H_2O$ | 11.3 | 18 |
| Pb-sulphide | 0.000008 | 24 |
| Po-sulphide | Insoluble | - |
| Bi-sulphide | 0.000018 | 18 |

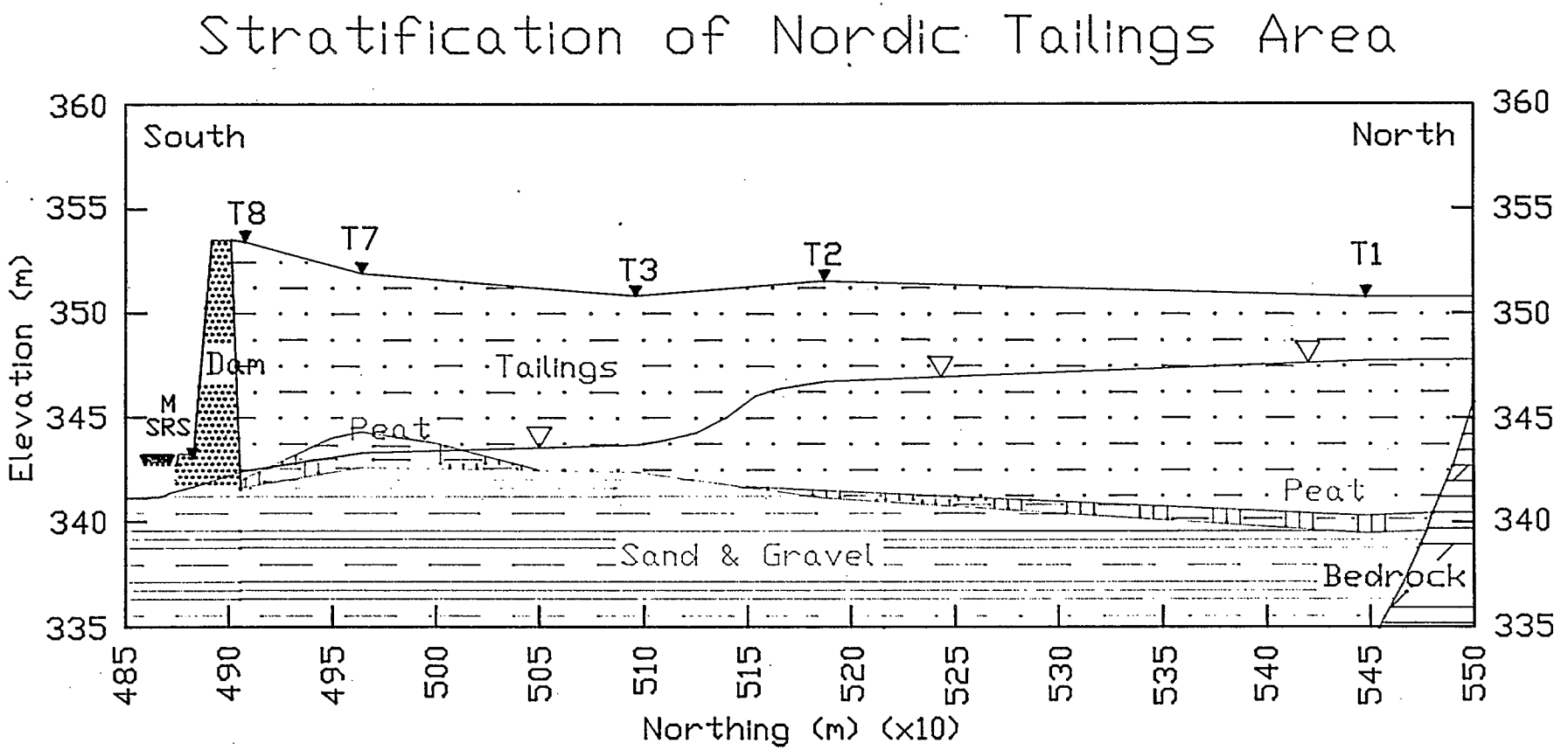


Fig. 7.1 - General stratification of Nordic main tailings area. Vertical north-south profile. Elevation (m) ASL versus Northing (m) (x10).

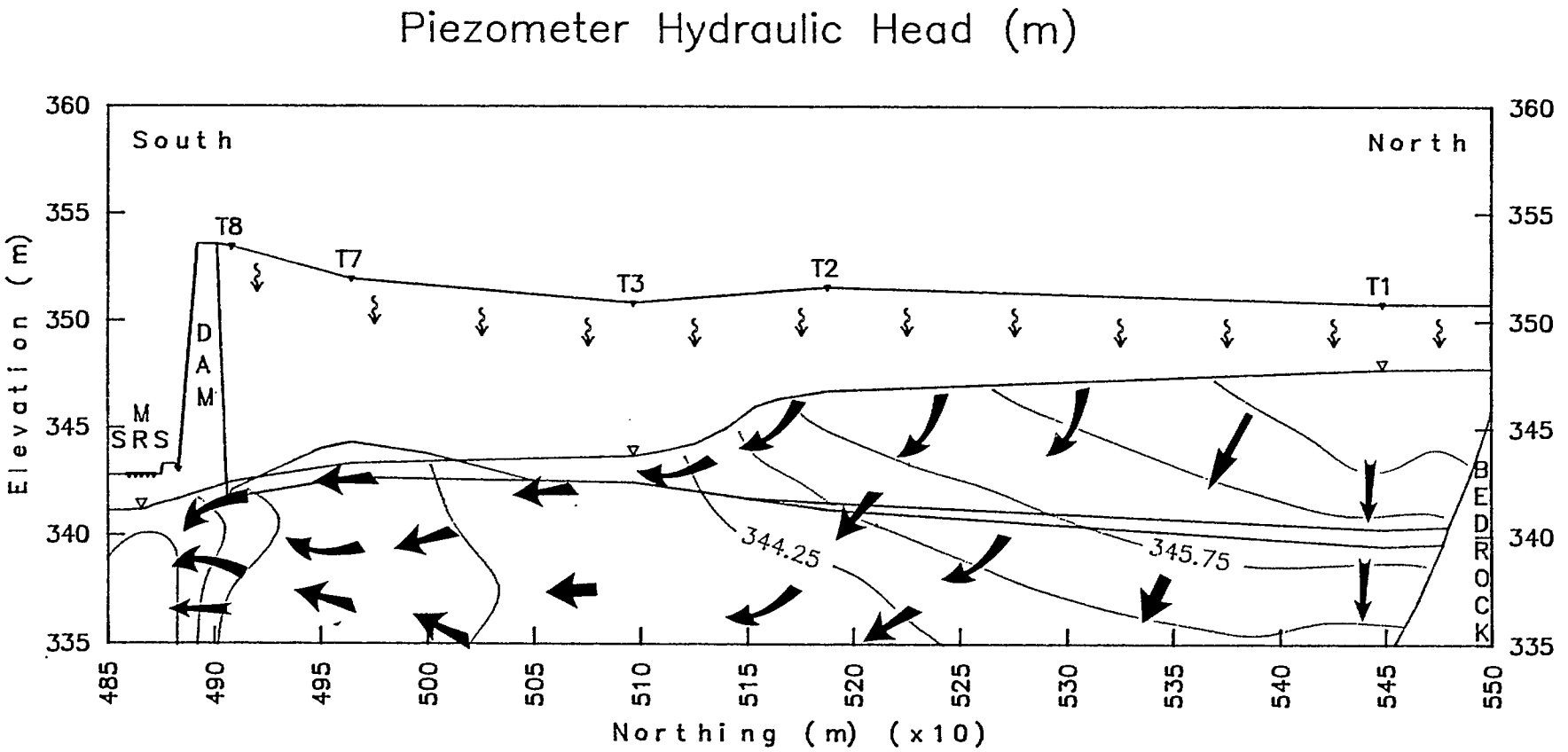


Fig. 7.2 - General groundwater flow pattern of Nordic main tailings. Vertical north-south profile. Based on data interpretation of hydraulic head into equipotential line contour mapping.

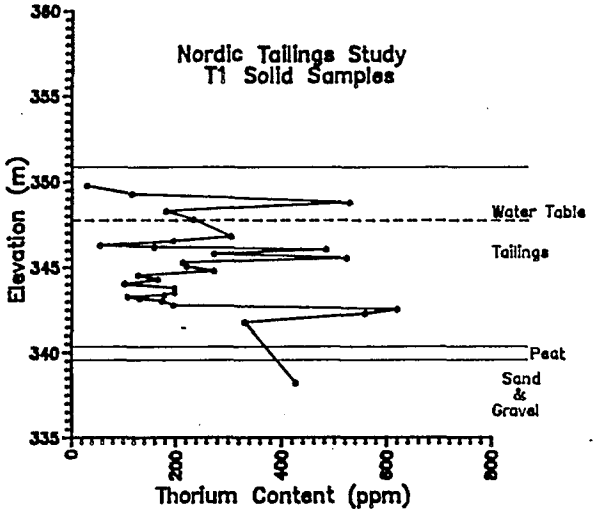


Fig. 7.3 - Nordic main tailings data. Location T-1, solid phase concentration of thorium at various depths.

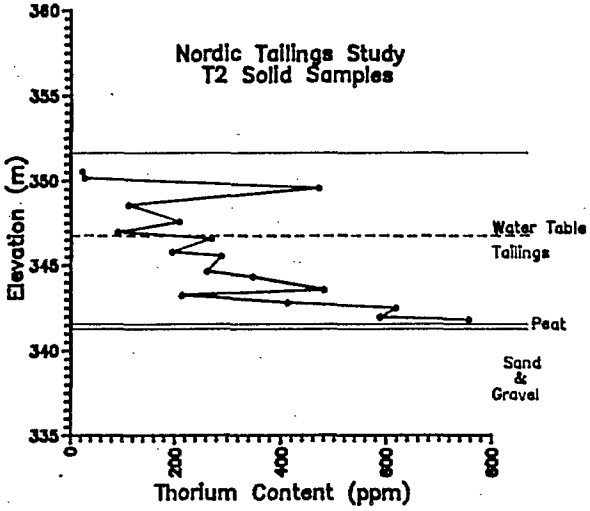


Fig. 7.4 - Nordic main tailings data. Location T-2, solid phase concentration of thorium at various depths.

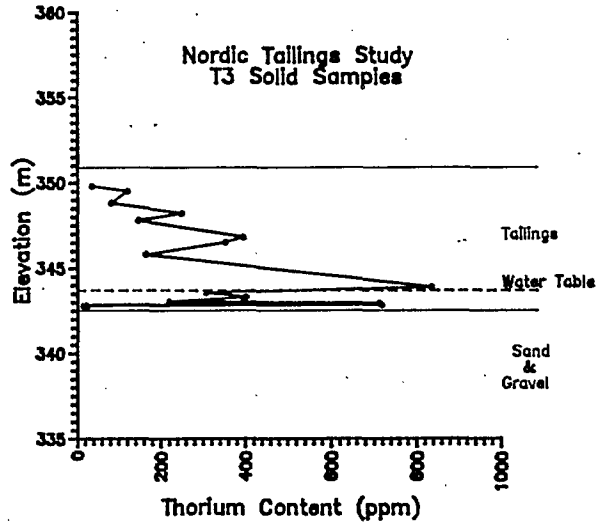


Fig. 7.5 - Nordic main tailings data. Location T-3, solid phase concentration of thorium at various depths.

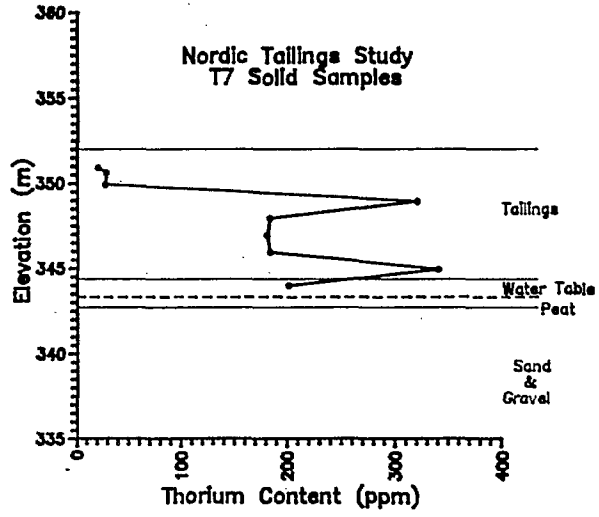


Fig. 7.6 - Nordic main tailings data. Location T-7, solid phase concentration of thorium at various depths.

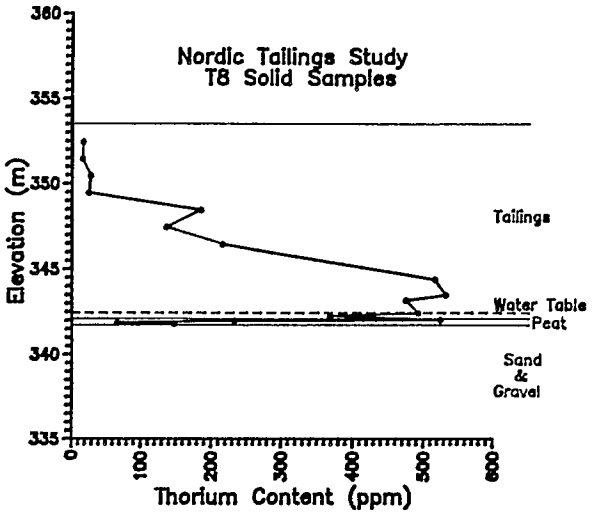


Fig. 7.7 - Nordic main tailings data. Location T-8, solid phase concentration of thorium at various depths.

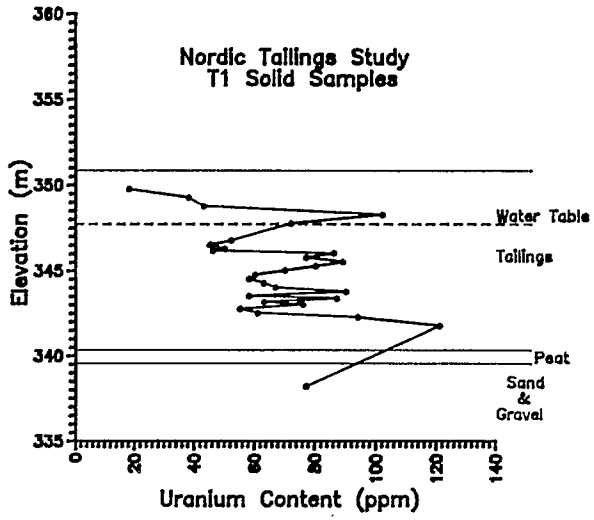


Fig. 7.8 - Nordic main tailings. Location T-1, solid phase concentration of uranium at various depths.

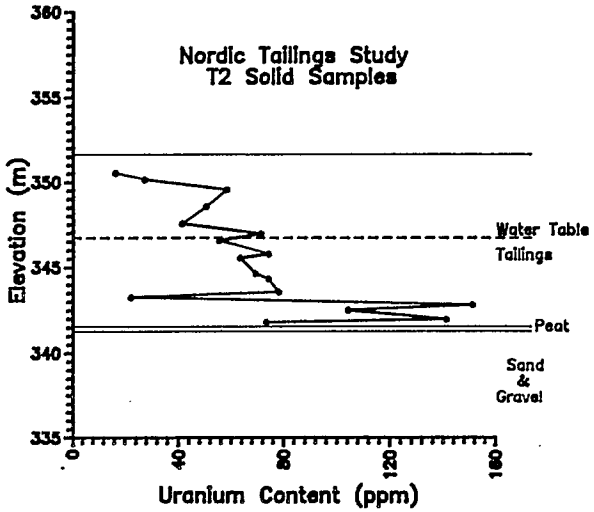


Fig. 7.9 - Nordic main tailings. Location T-2, solid phase concentration of uranium at various depths.

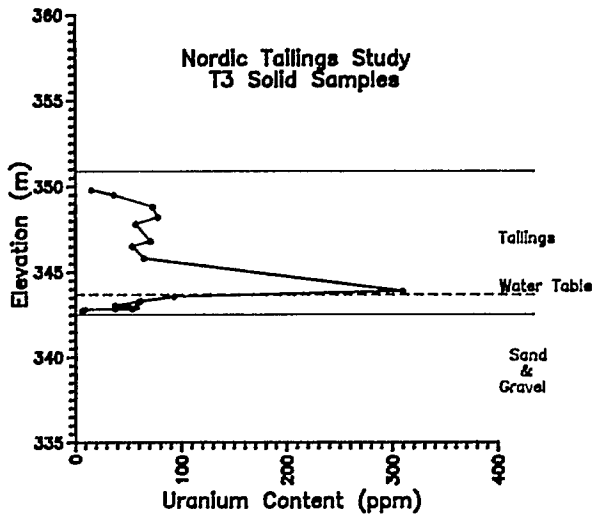


Fig. 7-10 - Nordic main tailings data. Location T-3, solid phase concentration of uranium at various depths.

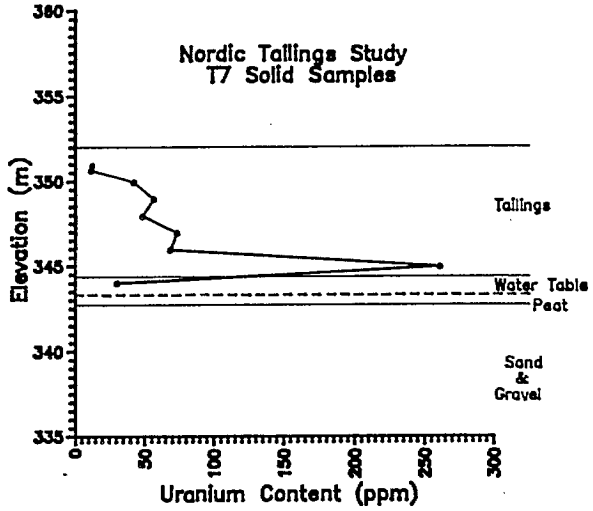


Fig. 7.11 - Nordic main tailings data. Location T-7, solid phase concentration of uranium at various depths.

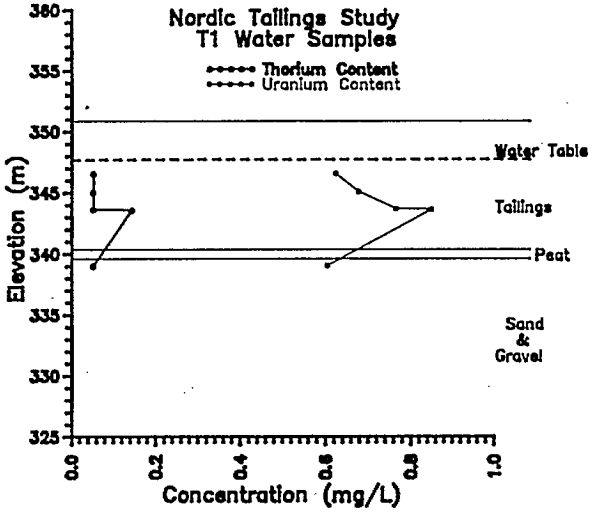


Fig. 7.13 - Nordic main tailings data. Location T-1, liquid phase concentration of thorium and uranium at various depths.

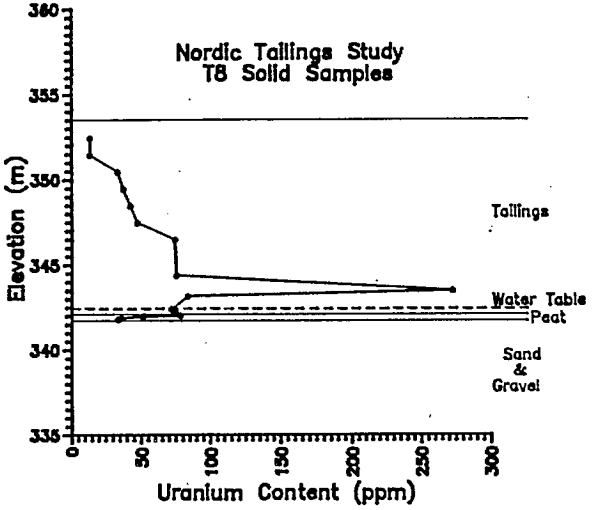


Fig. 7.12 - Nordic main tailings data. Location T-8, solid phase concentration of uranium at various depths.

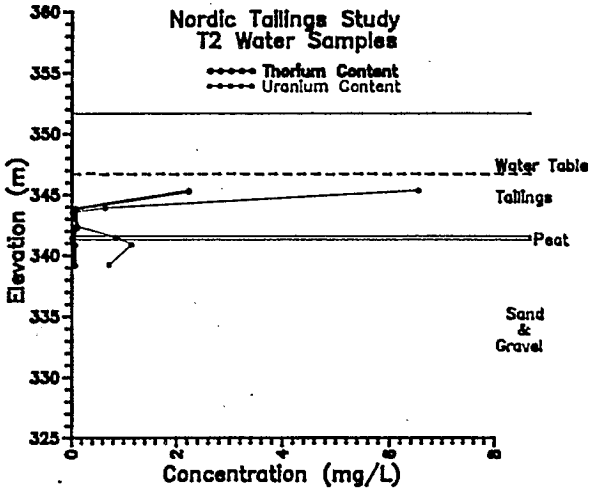


Fig. 7.14 - Nordic main tailings data. Location T-2, liquid phase concentration of thorium and uranium at various depths.

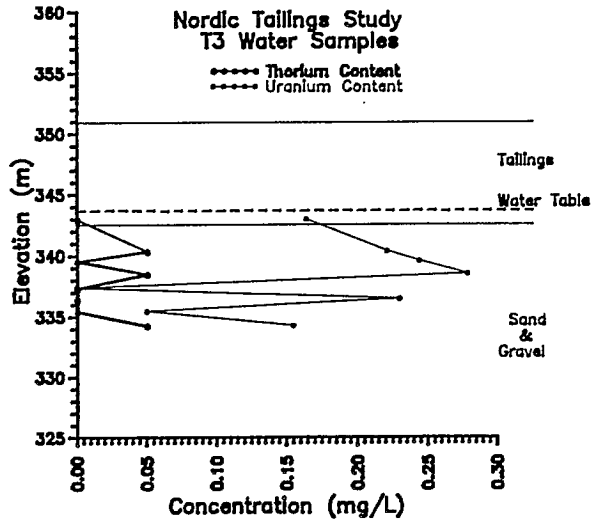


Fig. 7.15 - Nordic main tailings data. Location T-3, liquid phase concentration of thorium and uranium at various depths.

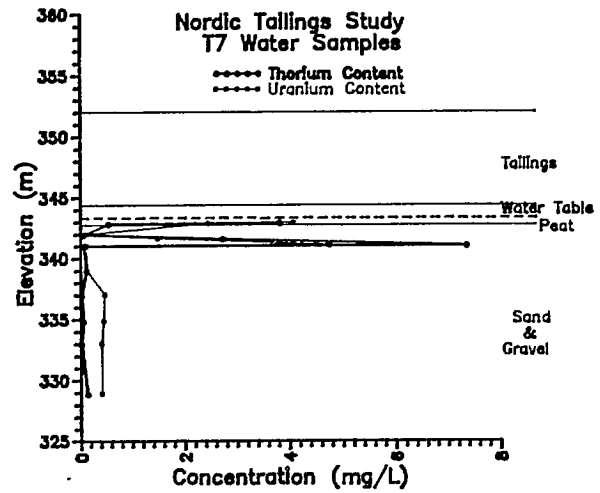


Fig. 7.16 - Nordic main tailings data. Location T-7, liquid phase concentration of thorium and uranium at various depths.

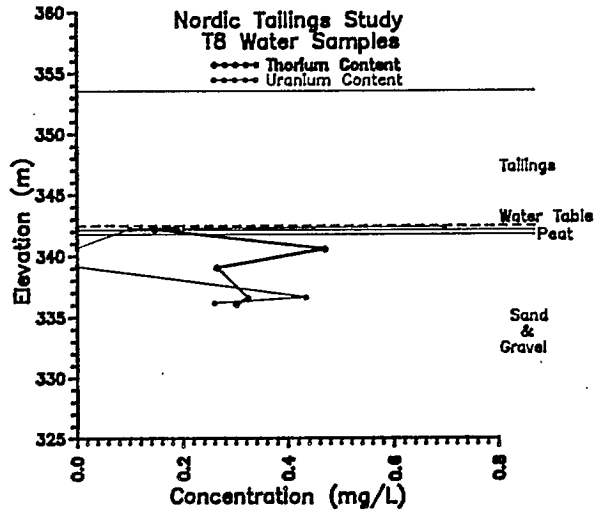


Fig. 7.17 - Nordic main tailings data. Location T-8, liquid phase concentration of thorium and uranium at various depths.

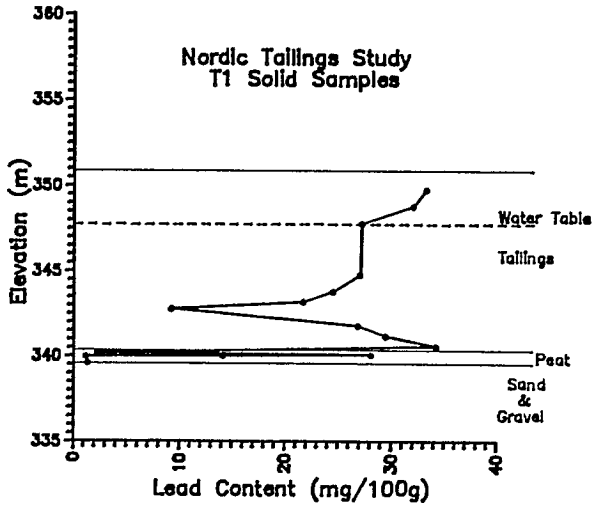


Fig. 7.18 - Nordic main tailings data. Location T-1, solid phase concentration of lead at various depths.

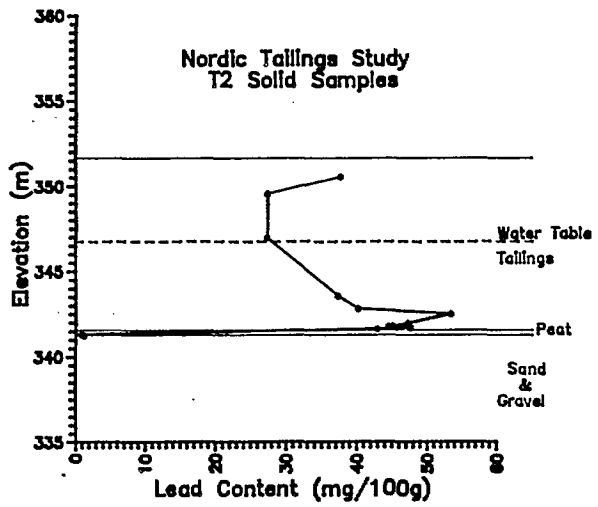


Fig. 7.19 - Nordic main tailings data. Location T-2, solid phase concentration of lead at various depths.

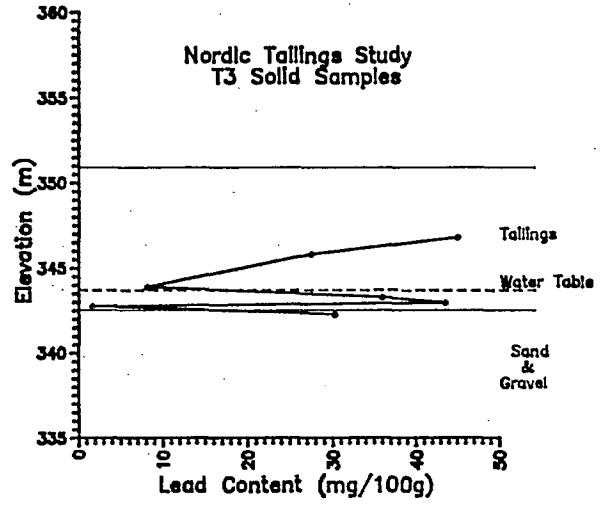


Fig. 7.20 - Nordic main tailings data. Location T-3, solid phase concentration of lead at various depths.

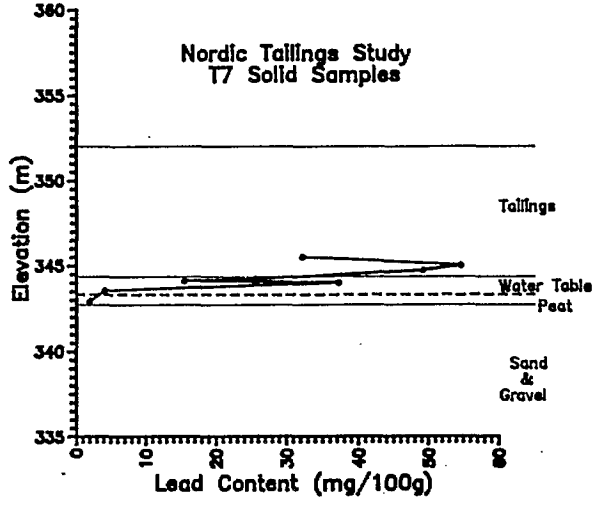


Fig. 7.21 - Nordic main tailings data. Location T-7, solid phase concentration of lead at various depths.

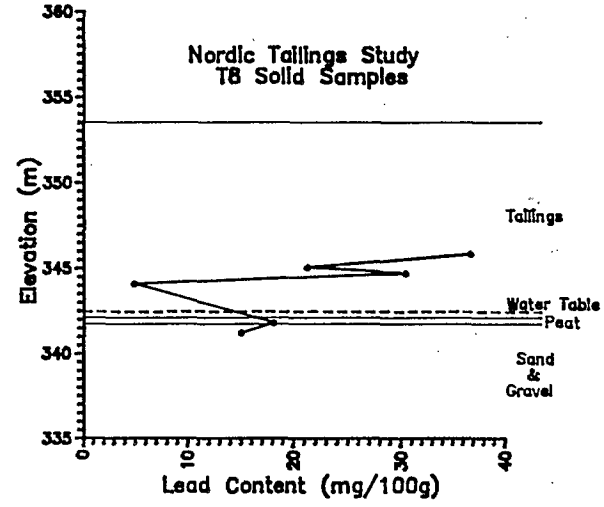


Fig. 7.22 - Nordic main tailings data. Location T-8, solid phase concentration of lead at various depths.

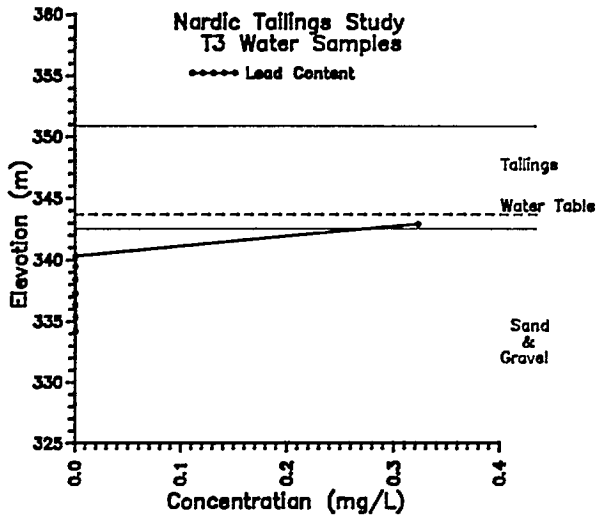


Fig. 7.23 - Nordic main tailings data. Location T-3, liquid phase concentration of lead at various depths.

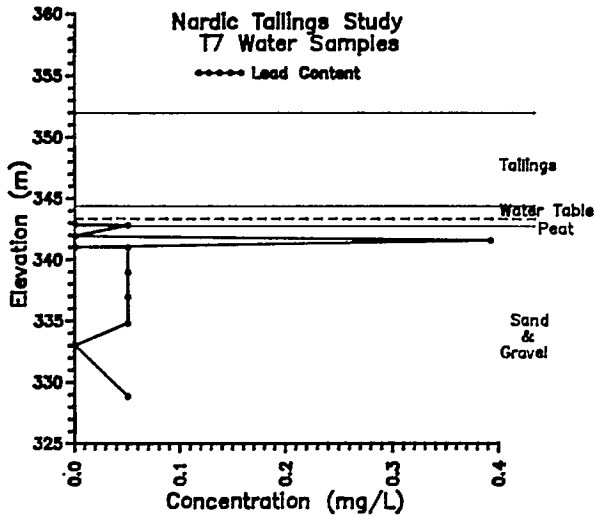


Fig. 7.24 - Nordic main tailings data. Location T-7, liquid phase concentration of lead at various depths.

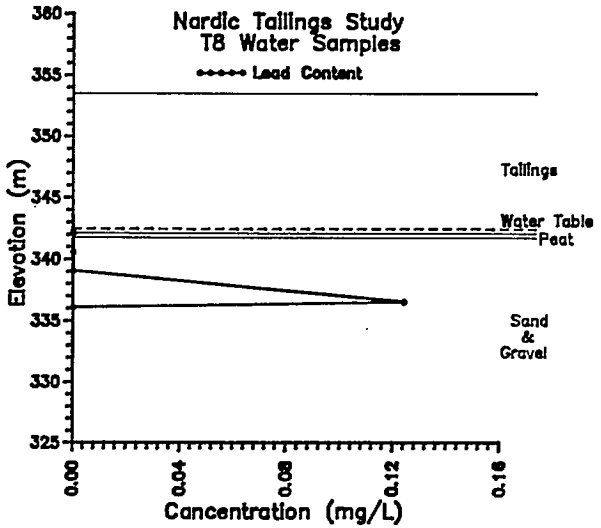


Fig. 7.25 - Nordic main tailings data. Location T-8, liquid phase concentration of lead at various depths.

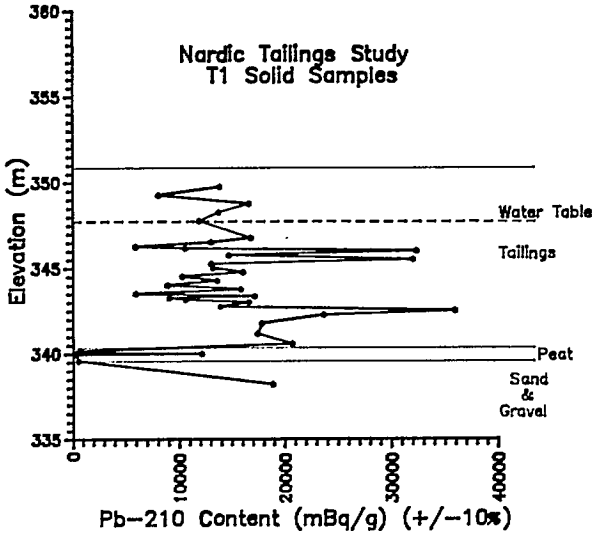


Fig. 7.26 - Nordic main tailings data. Location T-1, solid phase concentration of $^{210}Pb$ at various depths.

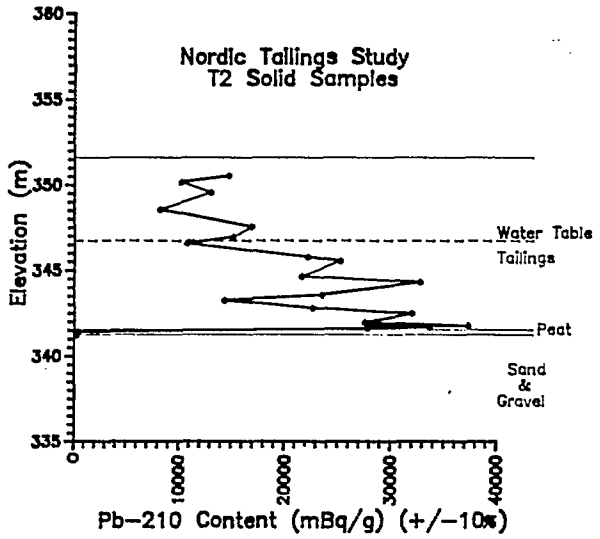


Fig. 7.27 - Nordic main tailings data. Location T-2, solid phase concentration of $^{210}Pb$ at various depths.

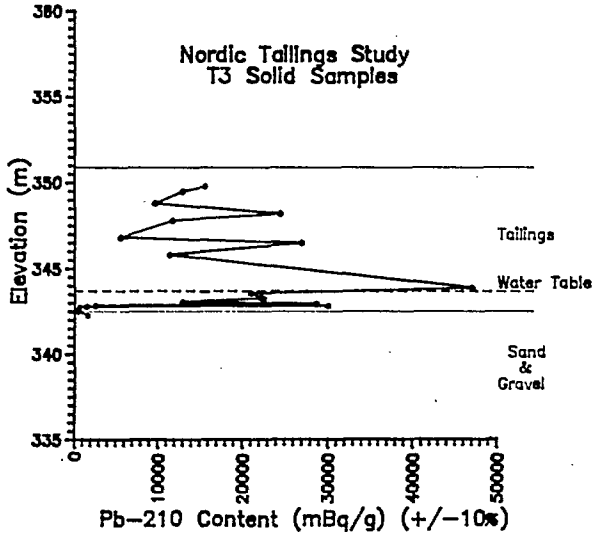


Fig. 7.28 - Nordic main tailings data. Location T-3, solid phase concentration of $^{210}Pb$ at various depths.

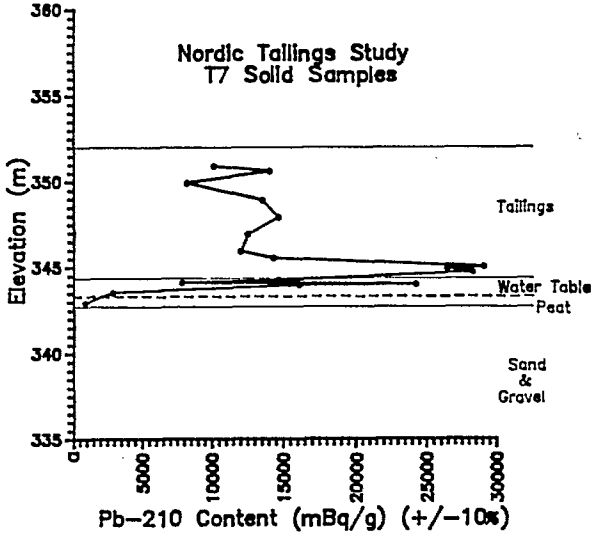


Fig. 7.29 - Nordic main tailings data. Location T-7, solid phase concentration of $^{210}Pb$ at various depths.

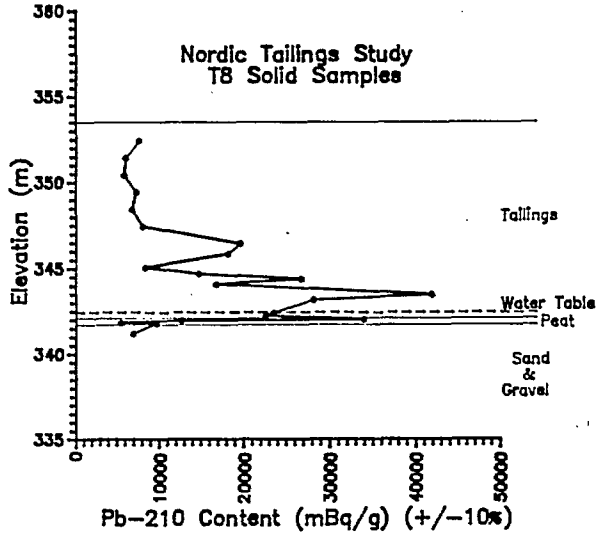


Fig. 7.30 - Nordic main tailings data. Location T-8, solid phase concentration of $^{210}Pb$ at various depths.

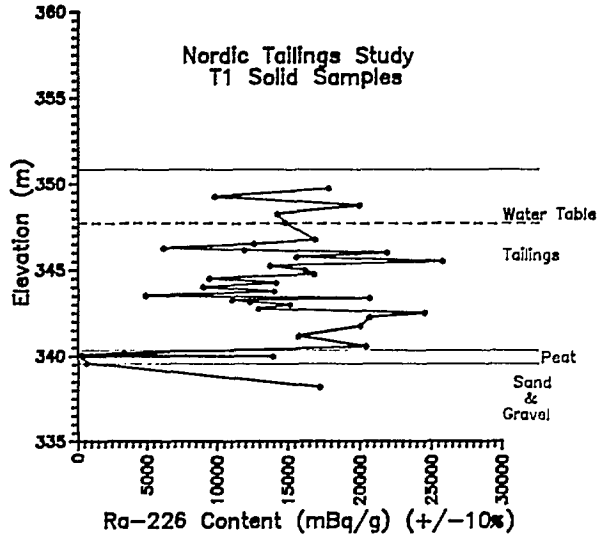


Fig. 7.31 - Nordic main tailings data. Location T-1, solid phase concentration of $^{226}Ra$ at various depths.

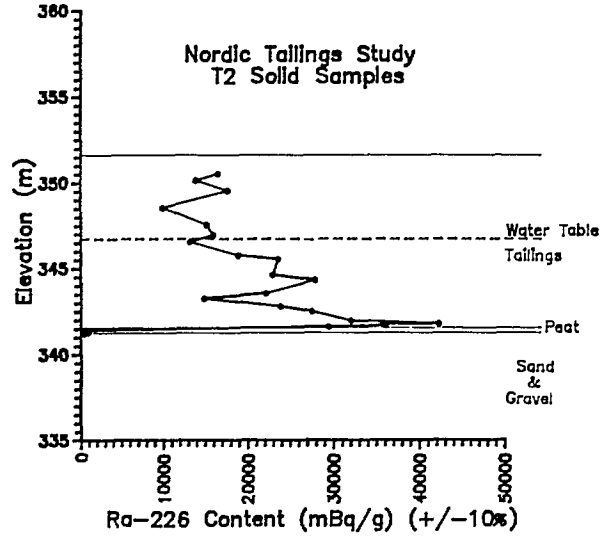


Fig. 7.32 - Nordic main tailings data. Location T-2, solid phase concentration of $^{226}Ra$ at various depths.

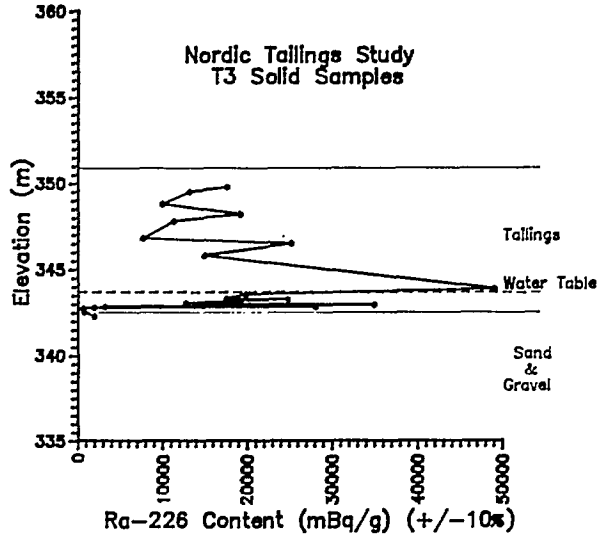


Fig. 7.33 - Nordic main tailings data. Location T-3, solid phase concentration of $^{226}Ra$ at various depths.

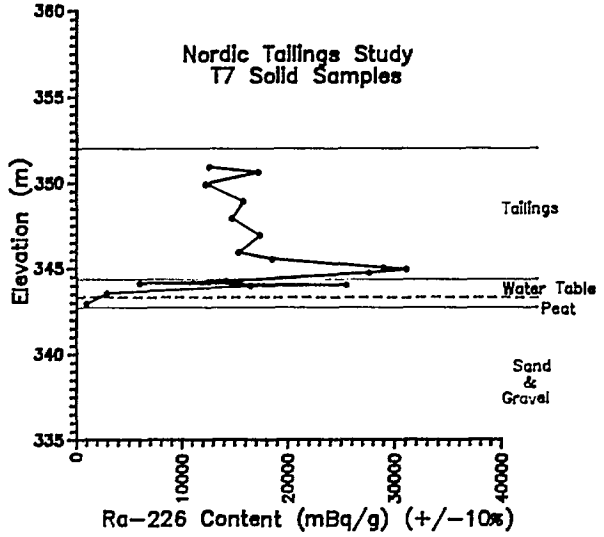


Fig. 7.34 - Nordic main tailings data. Location T-7, solid phase concentration of $^{226}Ra$ at various depths.

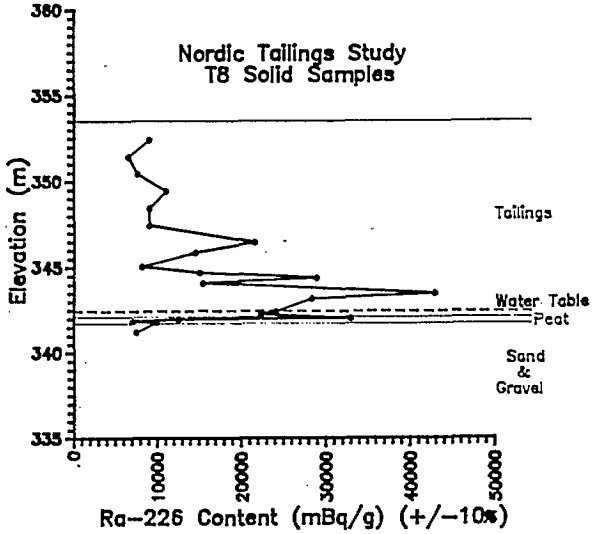


Fig. 7.35 - Nordic main tailings data. Location T-8, solid phase concentration of $^{226}Ra$ at various depths.

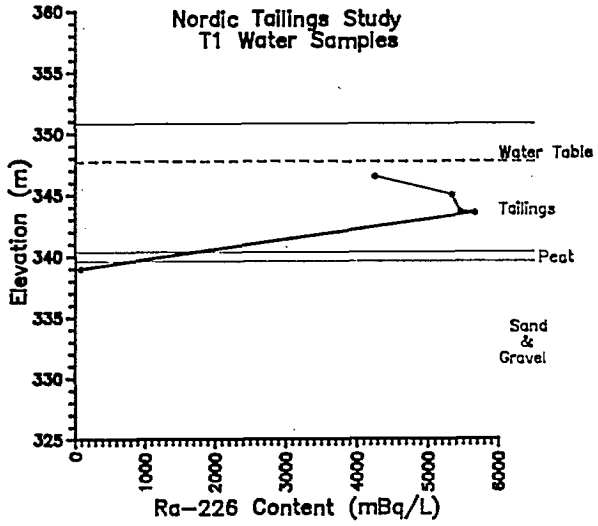


Fig. 7.36 - Nordic main tailings data. Location T-1, liquid phase concentration of $^{226}Ra$ at various depths.

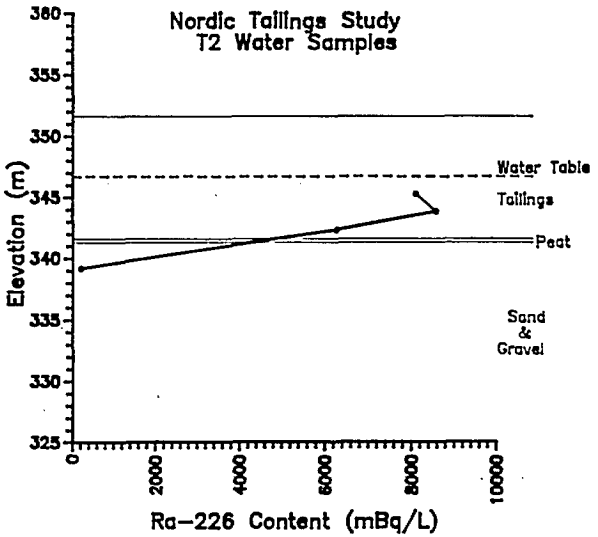


Fig. 7.37 - Nordic main tailings data. Location T-2, liquid phase concentration of $^{226}Ra$ at various depths.

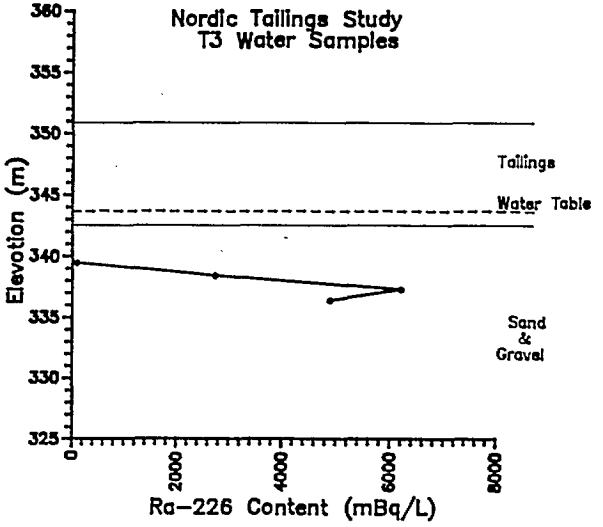


Fig. 7.38 - Nordic main tailings data. Location T-3, liquid phase concentration of $^{226}Ra$ at various depths.

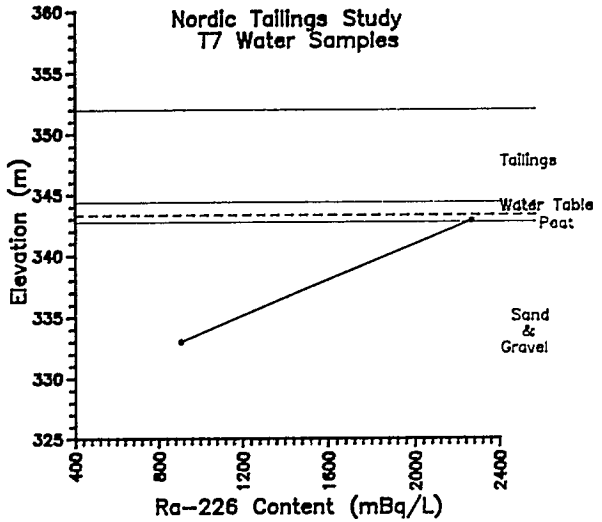


Fig. 7.39 - Nordic main tailings data. Location T-7, liquid phase concentration of $^{226}Ra$ at various depths.

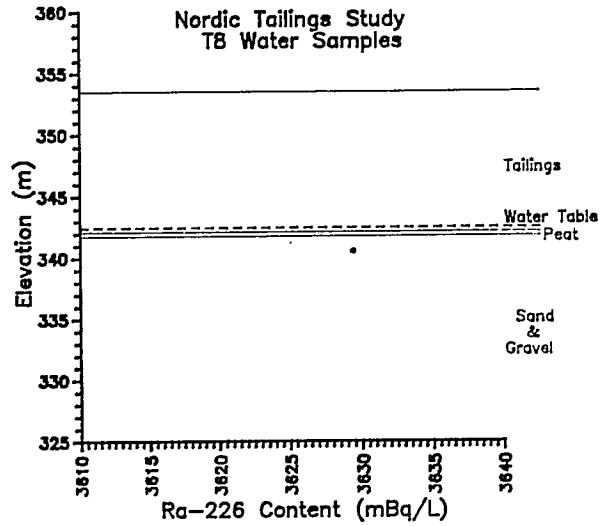


Fig. 7.40 - Nordic main tailings data. Location T-8, liquid phase concentration of $^{226}Ra$ at various depths.

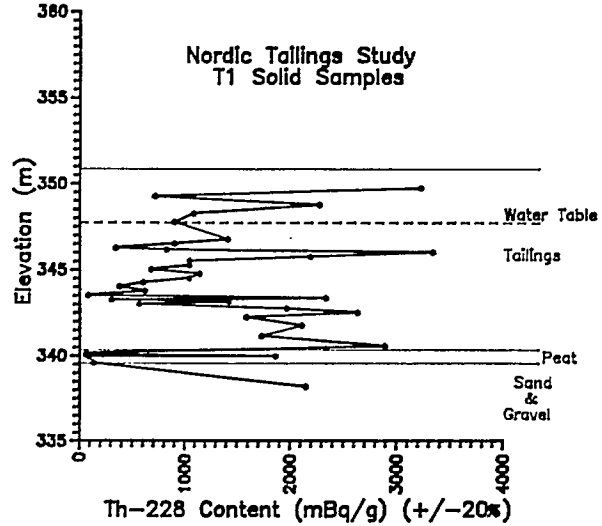


Fig. 7.41 - Nordic main tailings data. Location T-1, solid phase concentration of $^{228}Th$ at various depths.

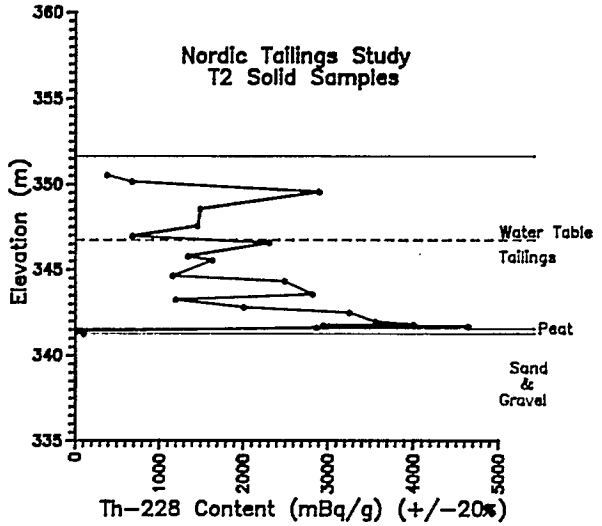


Fig. 7.42 - Nordic main tailings data. Location T-2, solid phase concentration of $^{228}Th$ at various depths.

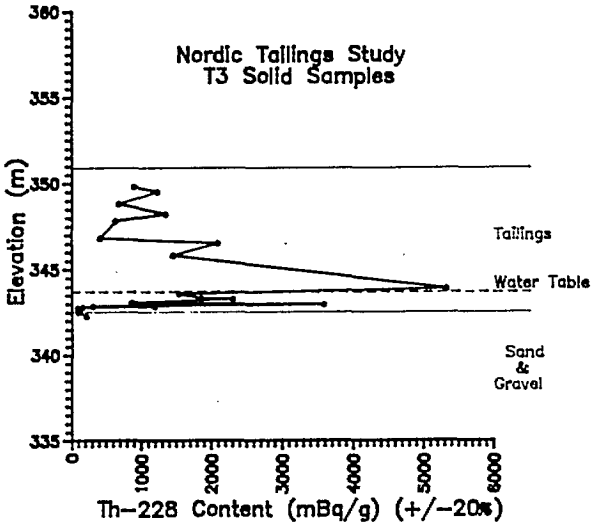


Fig. 7.43 - Nordic main tailings data. Location T-3, solid phase concentration of $^{228}Th$ at various depths.

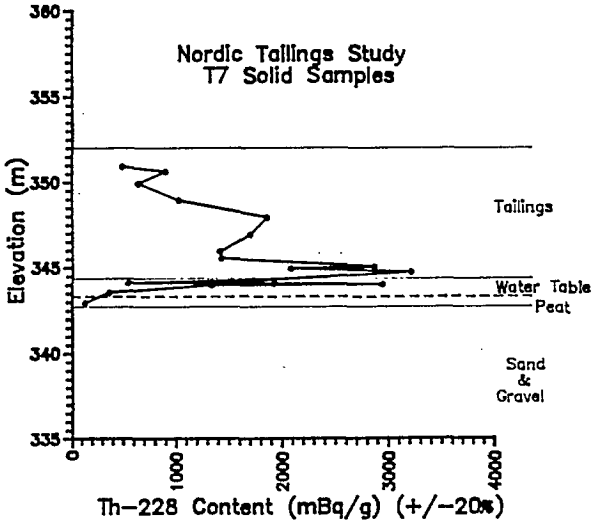


Fig. 7.44 - Nordic main tailings data. Location T-7, solid phase concentration of $^{228}Th$ at various depths.

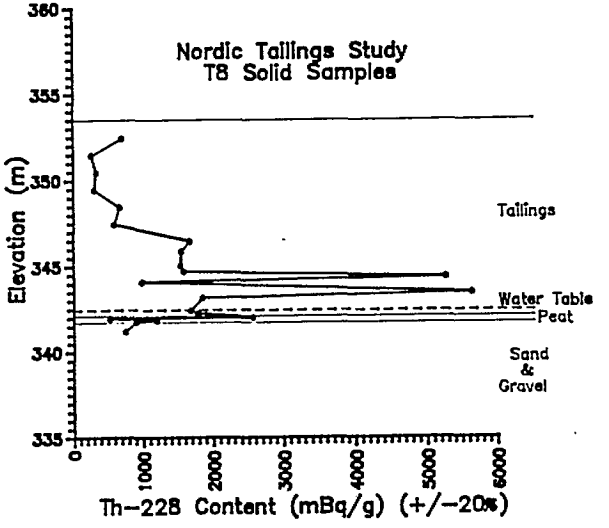


Fig. 7.45 - Nordic main tailings data. Location T-8, solid phase concentration of $^{228}Th$ at various depths.

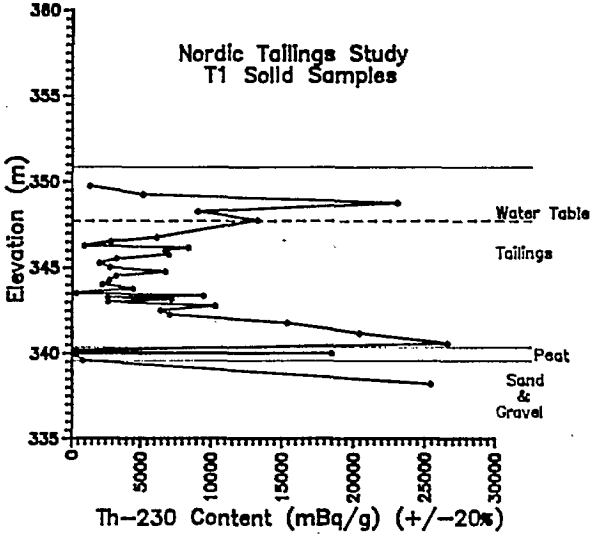


Fig. 7.46 - Nordic main tailings data. Location T-1, solid phase concentration of $^{230}Th$ at various depths.

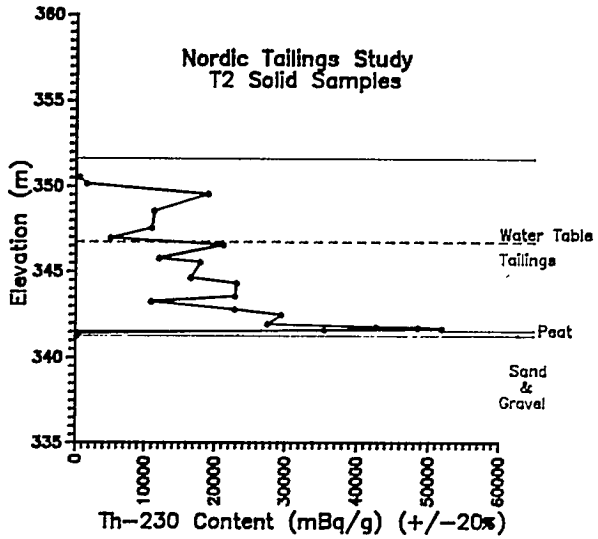


Fig. 7.47 - Nordic main tailings data. Location T-2, solid phase concentration of $^{230}Th$ at various depths.

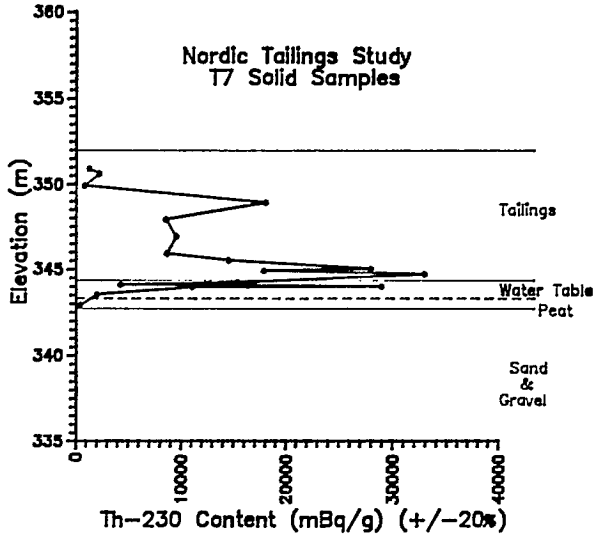


Fig. 7.49 - Nordic main tailings data. Location T-7, solid phase concentration of $^{230}Th$ at various depths.

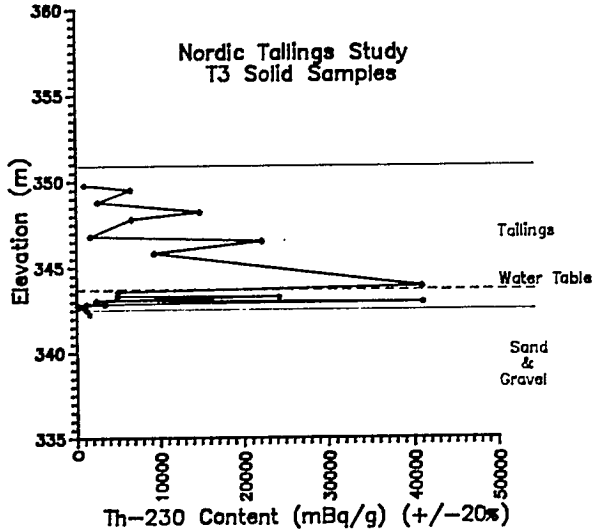


Fig. 7.48 - Nordic main tailings data. Location T-3, solid phase concentration of $^{230}Th$ at various depths.

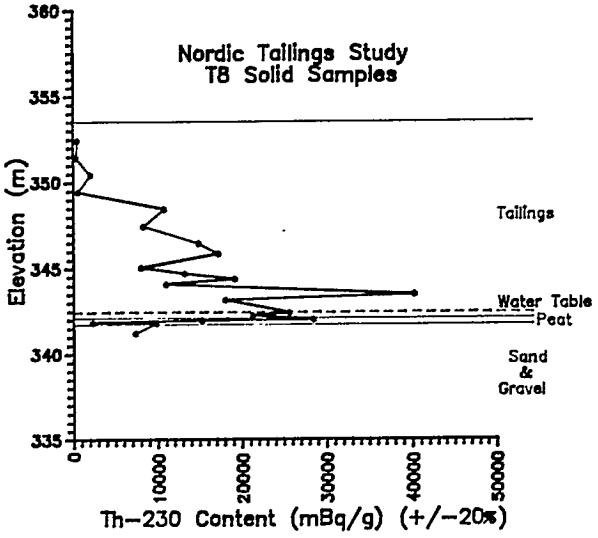


Fig. 7.50 - Nordic main tailings data. Location T-8, solid phase concentration of $^{230}Th$ at various depths.

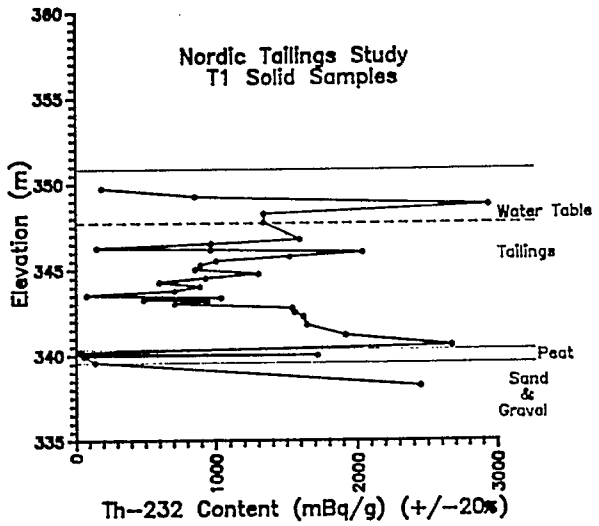


Fig. 7.51 - Nordic main tailings data. Location T-1, solid phase concentration of $^{232}Th$ at various depths.

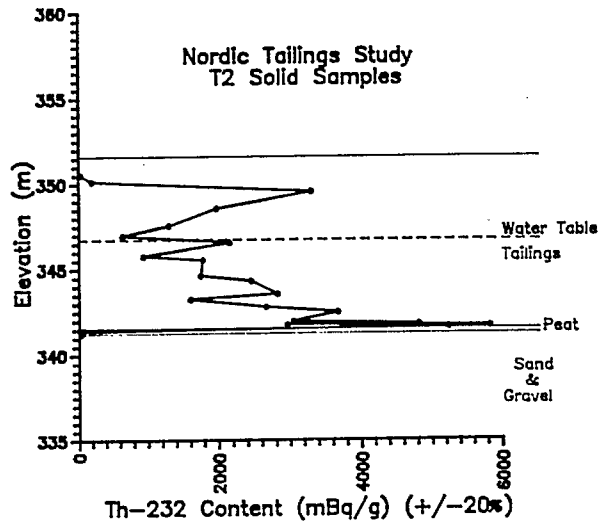


Fig. 7.52 - Nordic main tailings data. Location T-2, solid phase concentration of $^{232}Th$ at various depths.

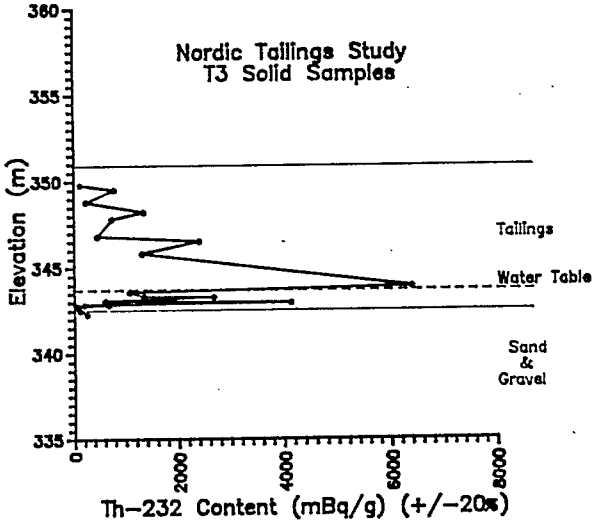


Fig. 7.53 - Nordic main tailings data. Location T-3, solid phase concentration of $^{232}Th$ at various depths.

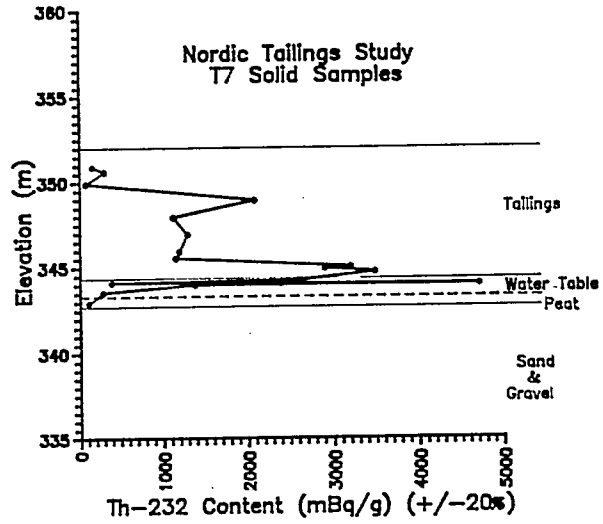


Fig. 7.54 - Nordic main tailings data. Location T-7, solid phase concentration of $^{232}Th$ at various depths.

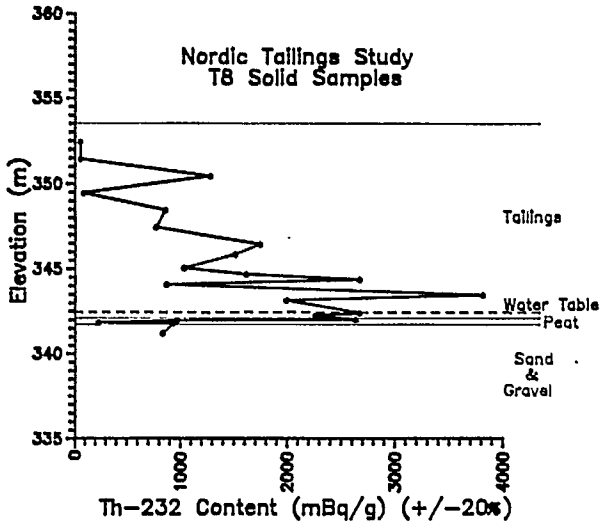


Fig. 7.55 - Nordic main tailings data. Location T-8, solid phase concentration of $^{232}Th$ at various depths.

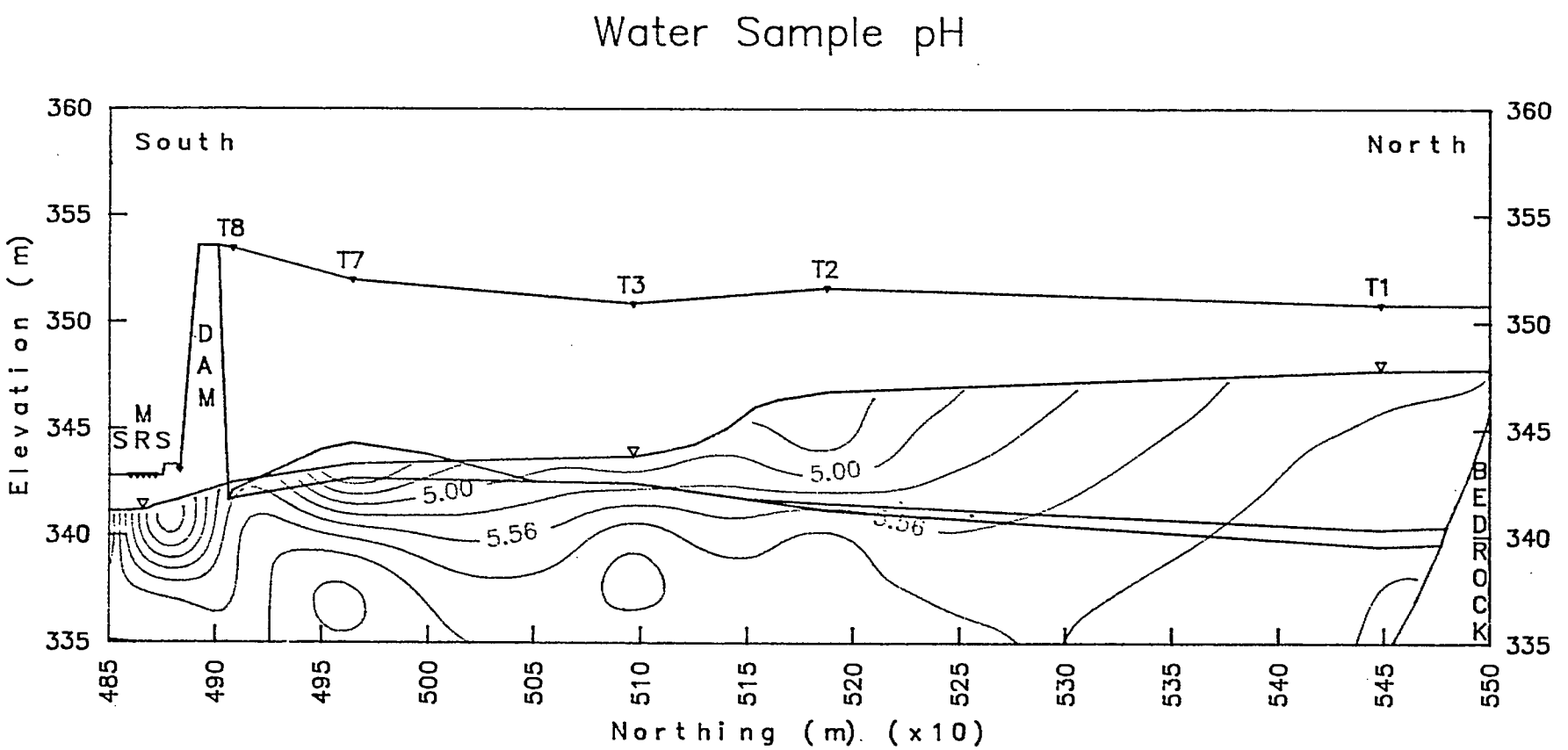


Fig. 7.56 - Nordic main tailings. Vertical north-south profile liquid phase, pH, contour map at various depths.

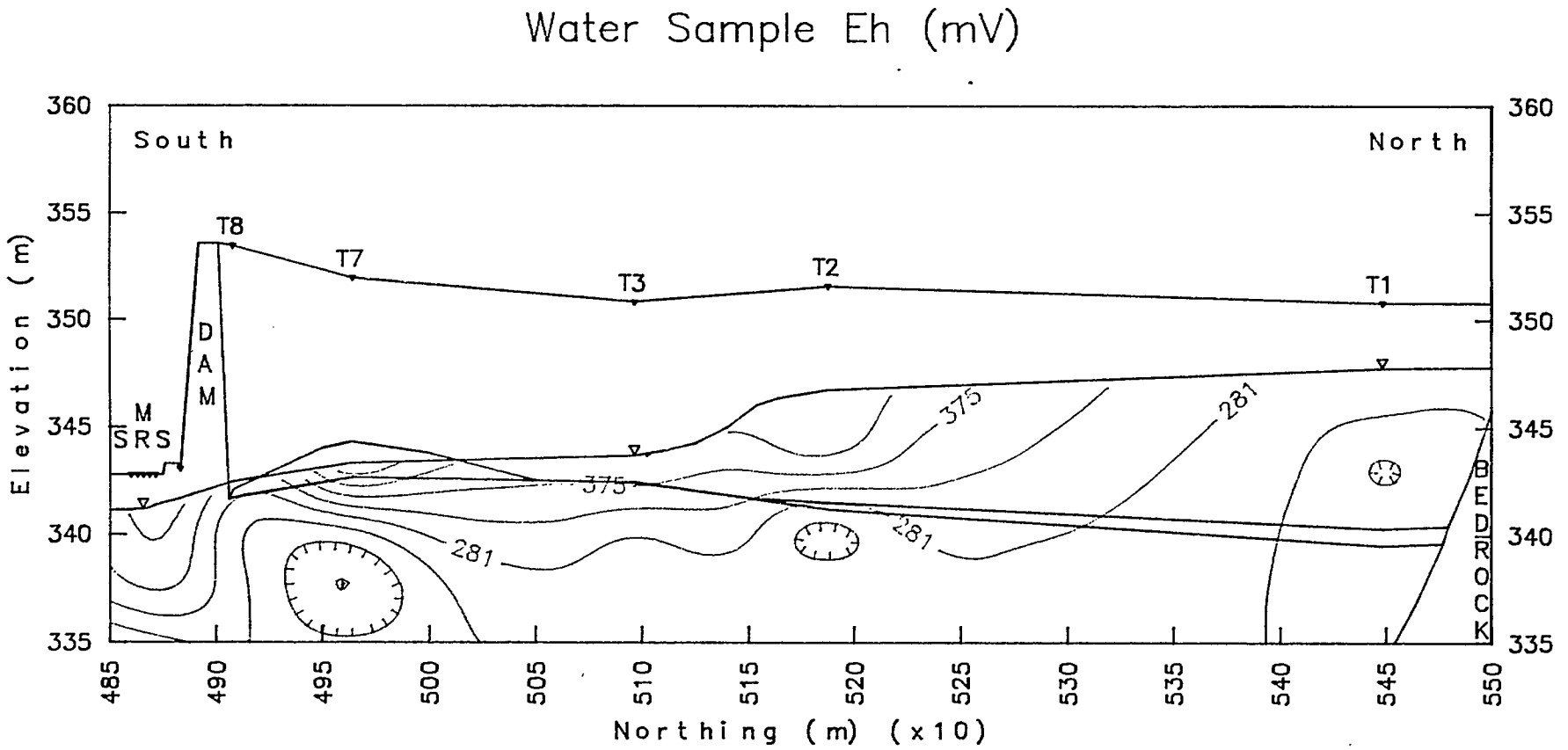


Fig. 7.57 - Nordic main tailings. Vertical north-south profile liquid phase, Eh (mV), contour map at various depths.

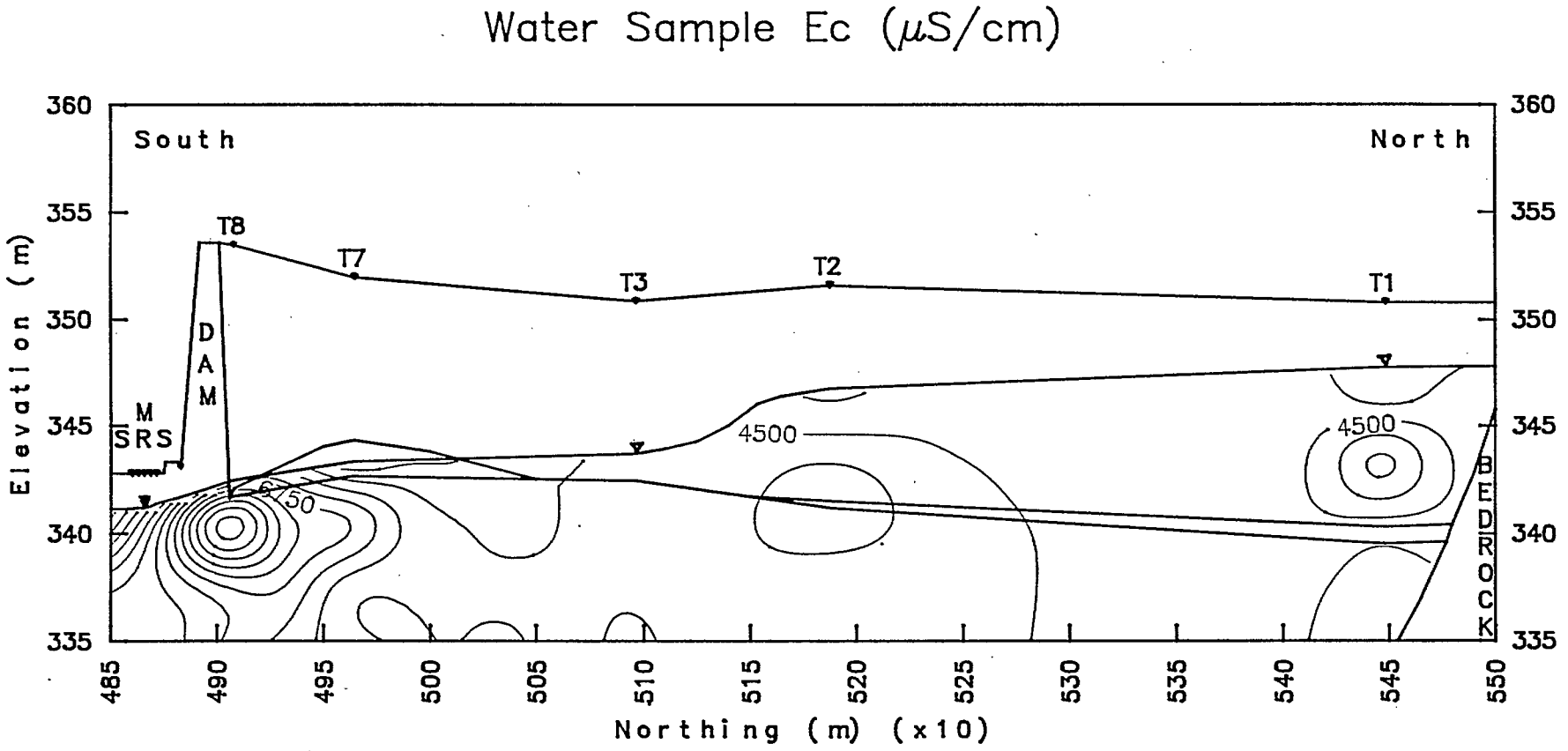


Fig. 7.58 - Nordic main tailings. Vertical north-south profile of liquid sample Ec (μS/cm), contour map at various depths.

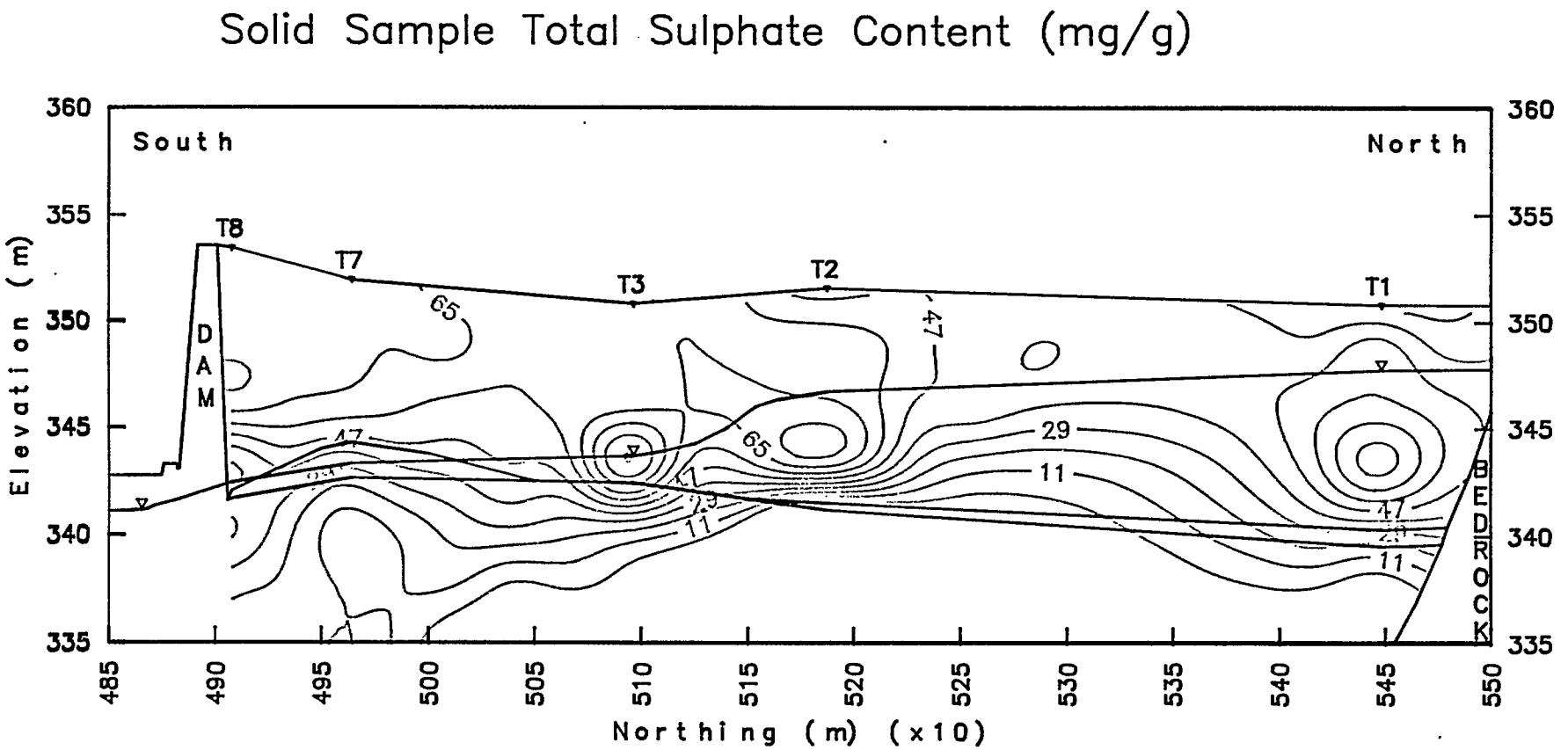


Fig. 7.59 - Nordic main tailings. Vertical north-south profile solid sample of total sulphate content (mg/g), contour map at various depths.

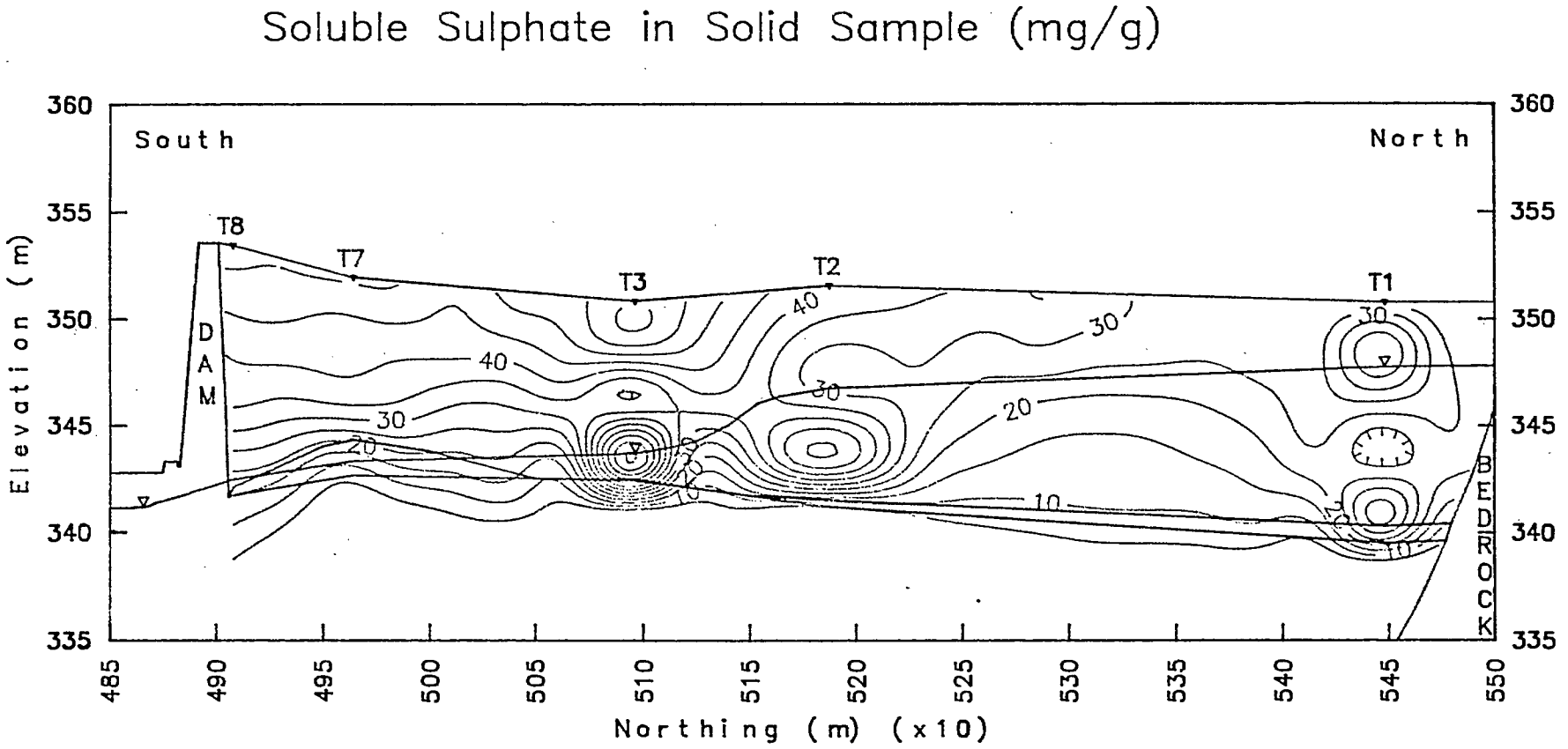


Fig. 7.60 - Nordic main tailings. Vertical north-south profile of soluble sulphate in solid sample (mg/g), contour map at various depths.

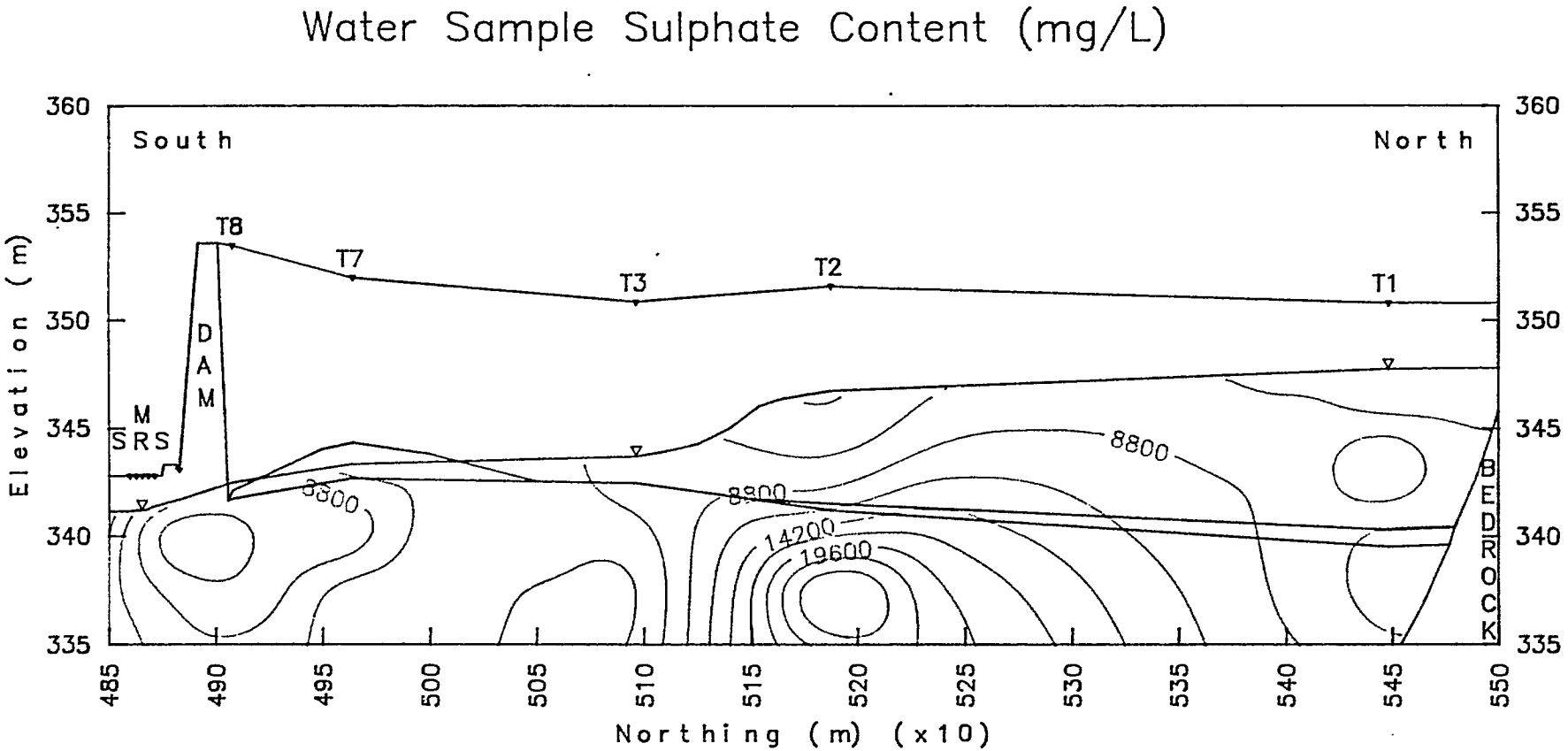


Fig. 7.61 - Nordic main tailings. Vertical north-south profile of liquid sample, sulphate content (mg/L), contour map at various depths.

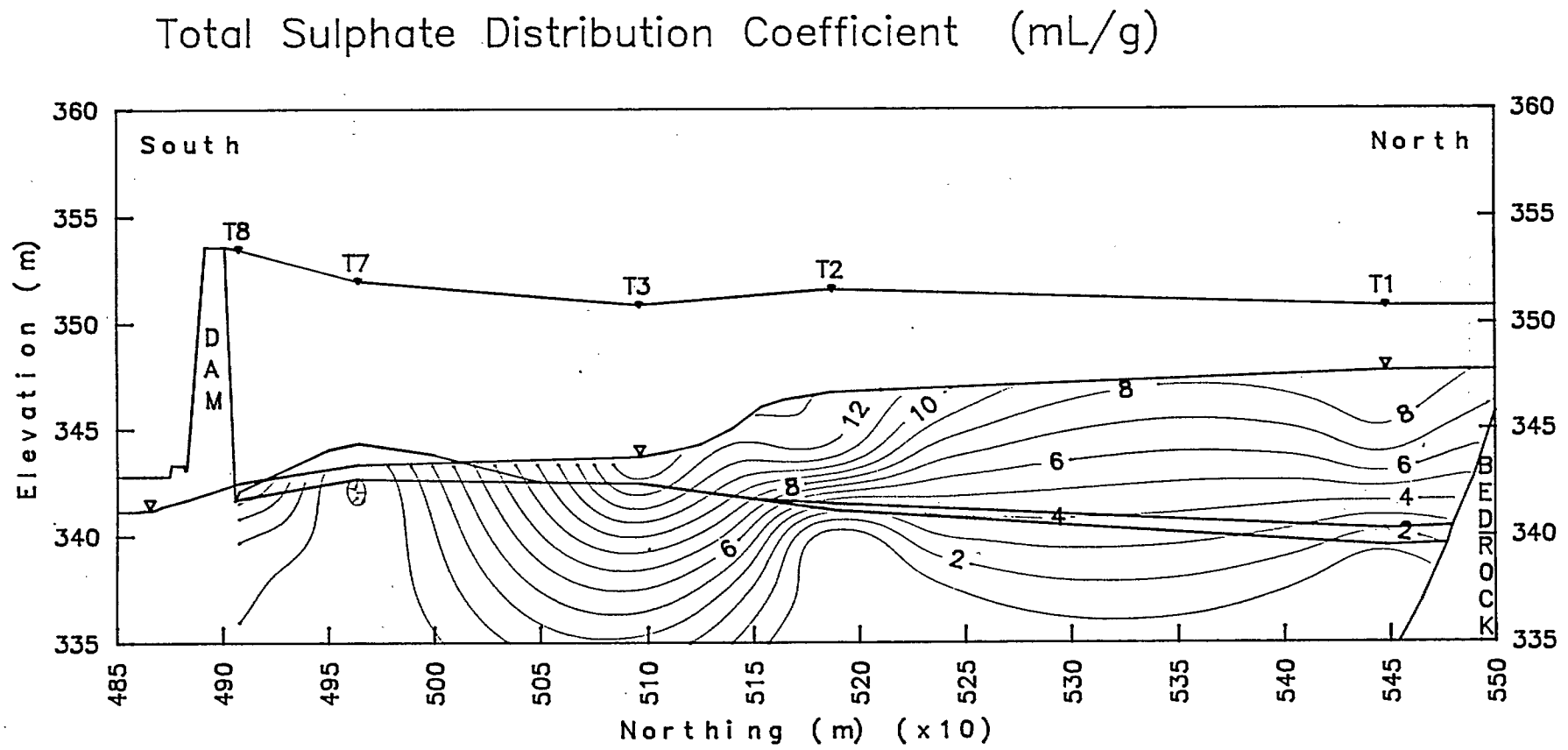


Fig. 7.62 - Nordic main tailings. Vertical north-south profile solid/liquid distribution coefficient (mL/g), contour map at various depths.
(Based on total sulphate in bulk mass.)

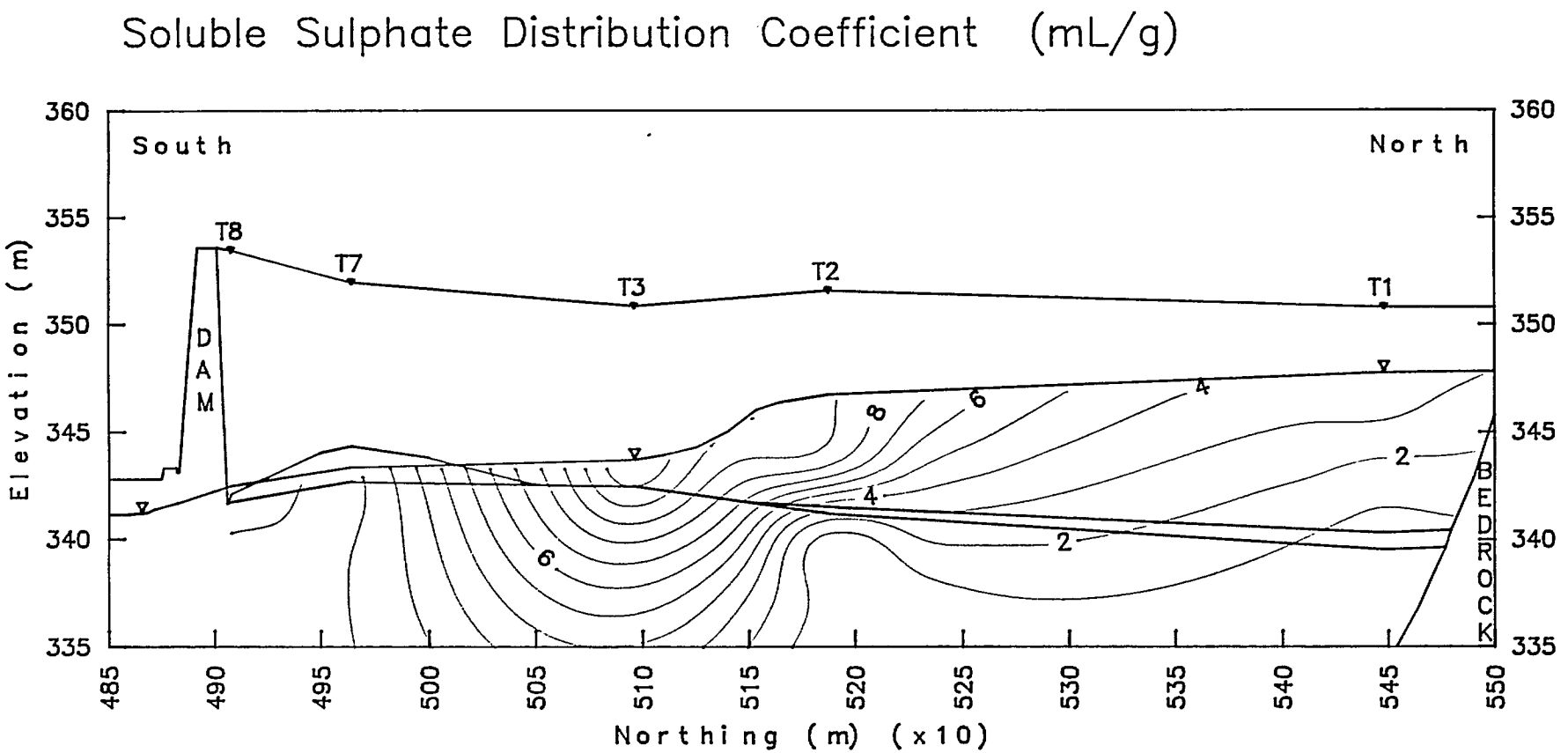


Fig. 7.63 - Nordic main tailings. Vertical north-south profile solid/liquid distribution coefficient of soluble sulphate (mL/g), contour map at various depths. (Based on total soluble sulphate on bulk mass.)

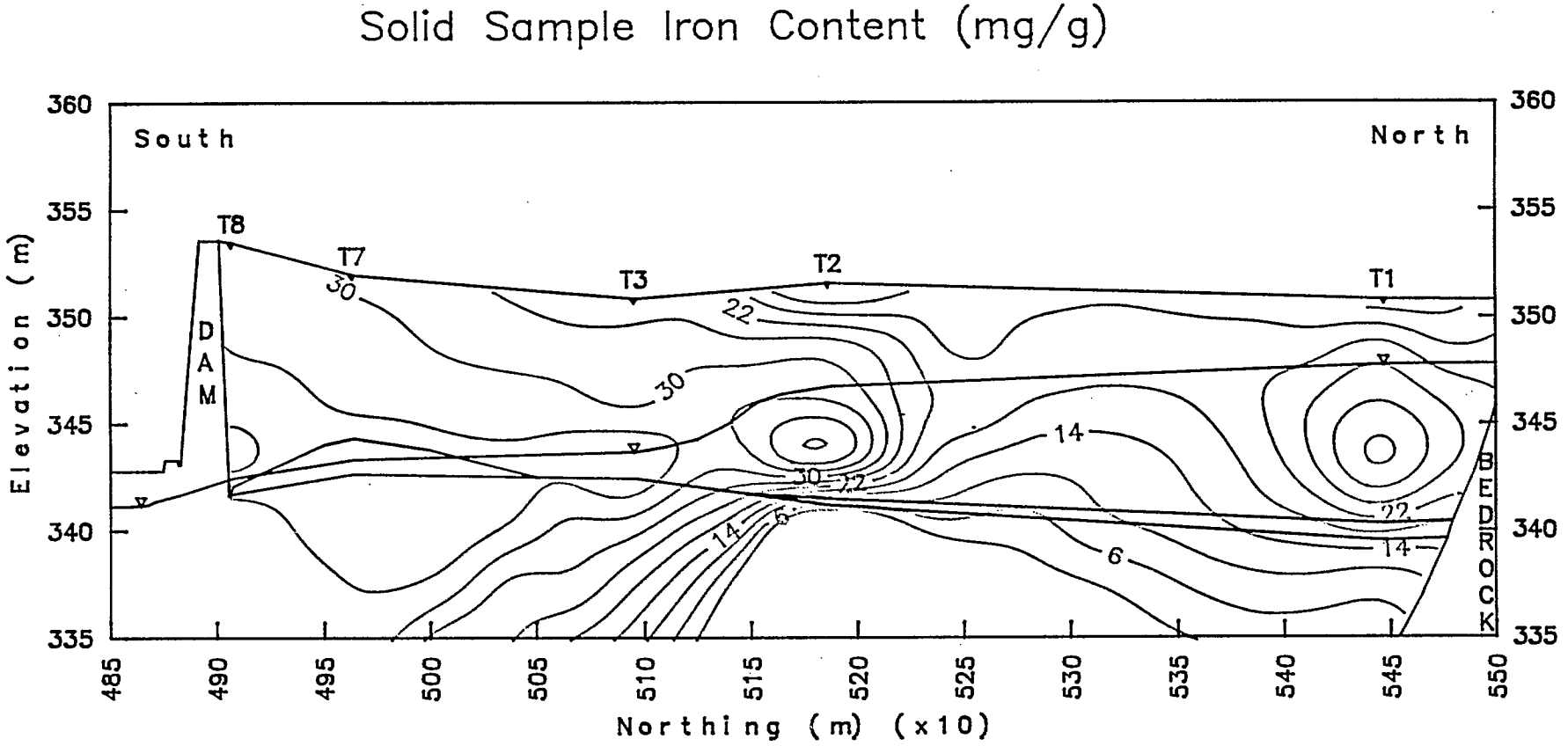


Fig. 7.64 - Nordic main tailings. Vertical north-south profile of solid sample, iron content (mg/g), contour map at various depths.

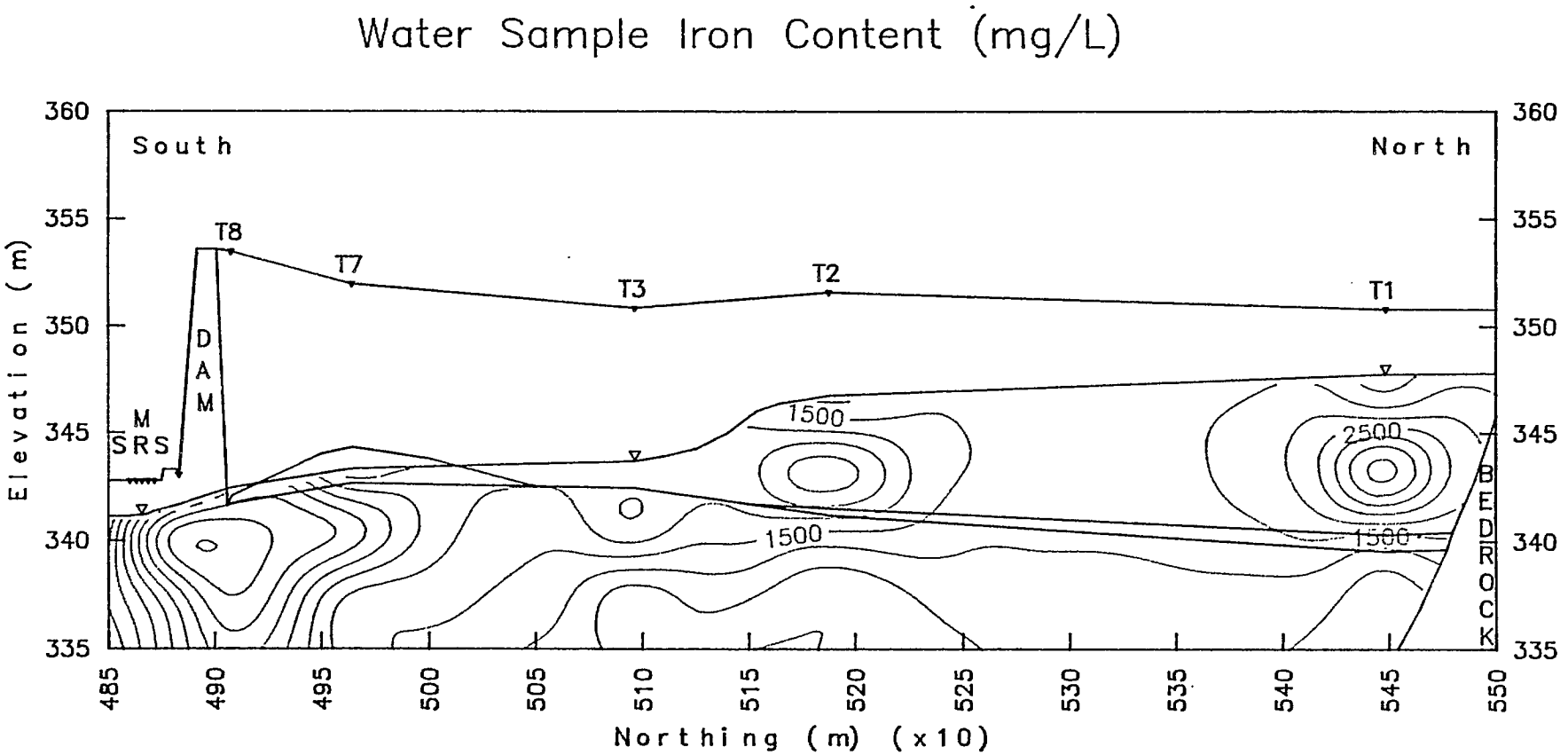


Fig. 7.65 - Nordic main tailings. Vertical north-south profile of liquid sample, iron content (mg/L), contour map at various depths.

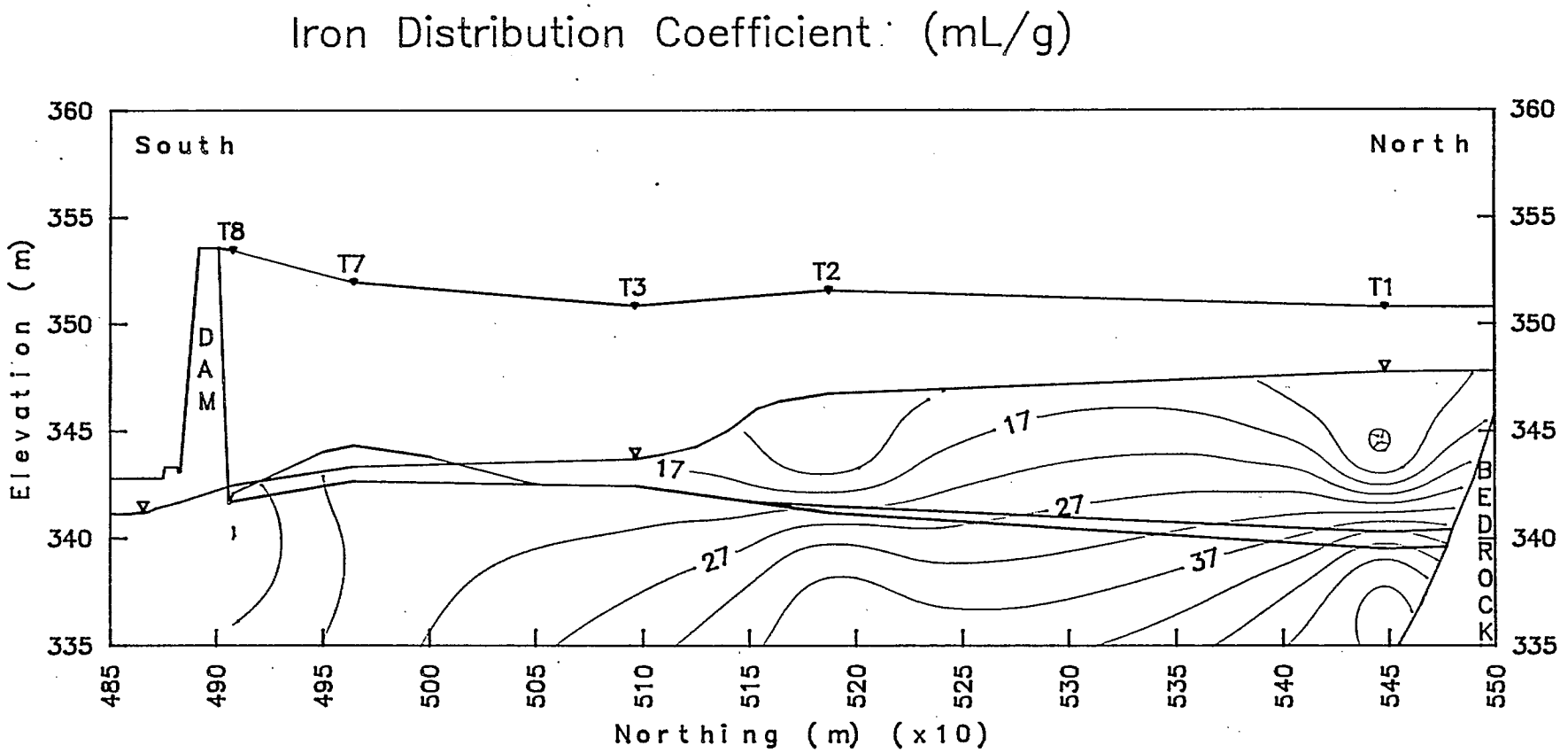


Fig. 7.66 - Nordic main tailings. Vertical north-south profile solid/liquid distribution coefficient of iron (mL/g), contour map at various depths. (Based on iron in bulk mass.)

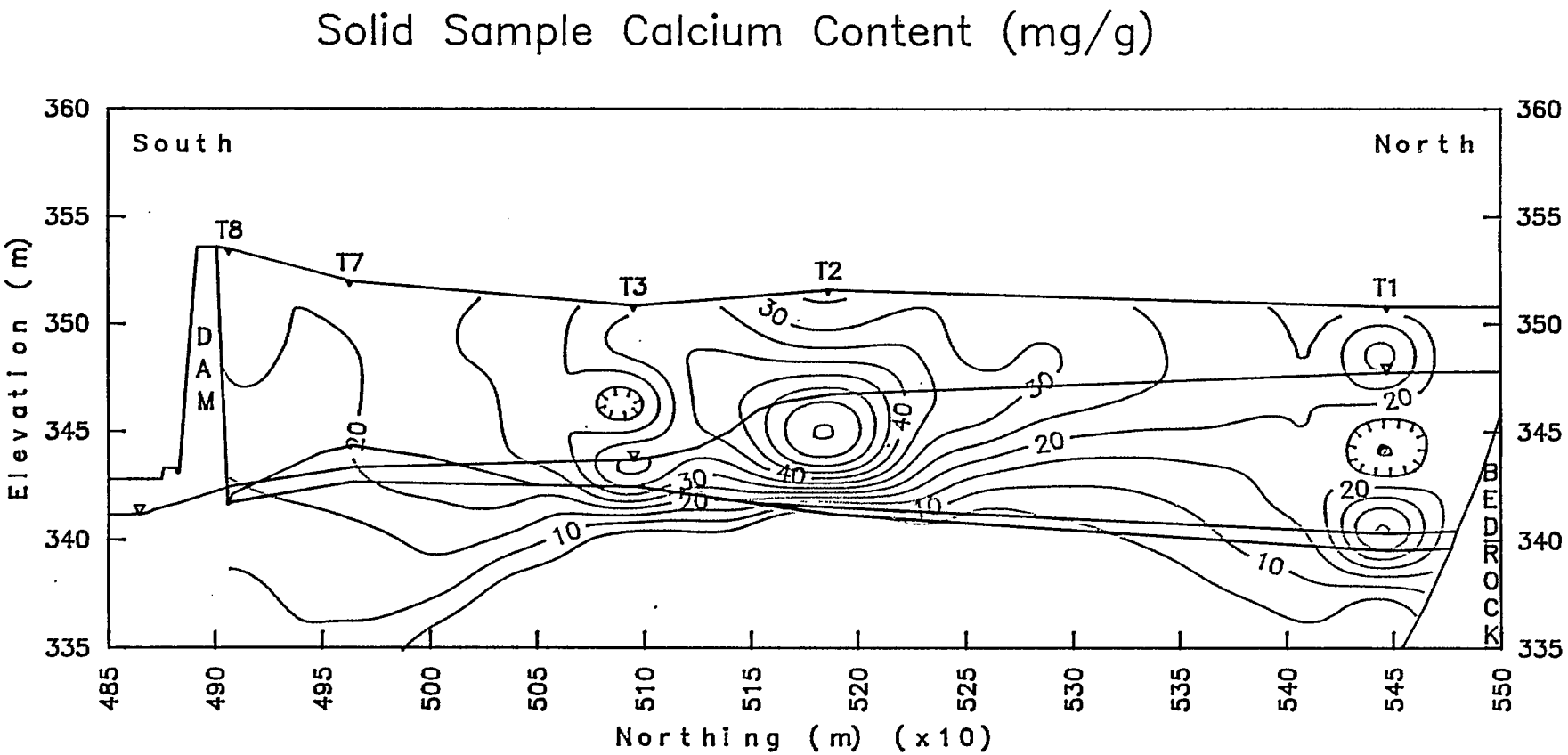


Fig. 7.67 - Nordic main tailings. Vertical north-south profile of solid sample, calcium content (mg/g), contour map at various depths.

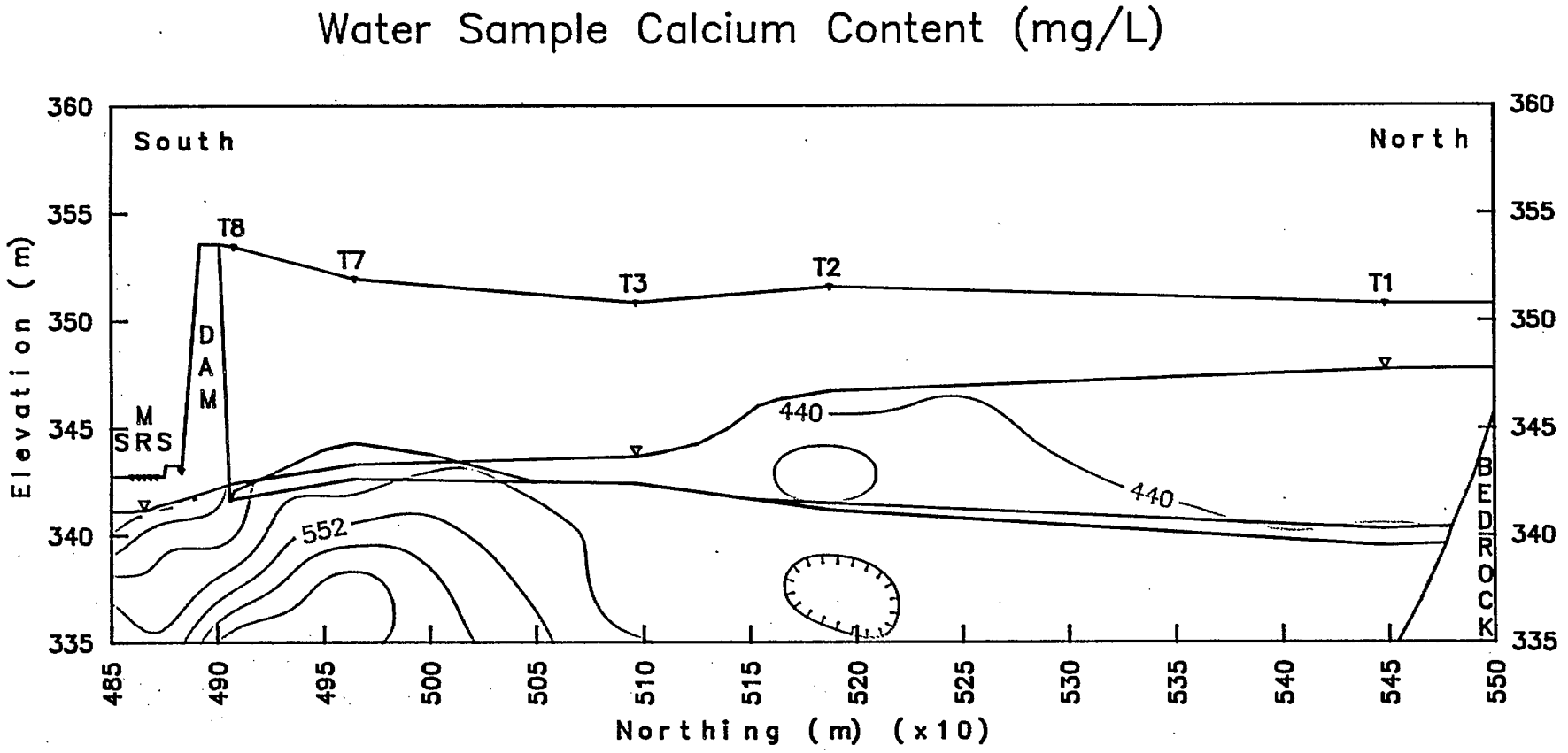


Fig. 7.68 - Nordic main tailings. Vertical north-south profile of liquid sample, calcium content (mg/L), contour map at various depths.

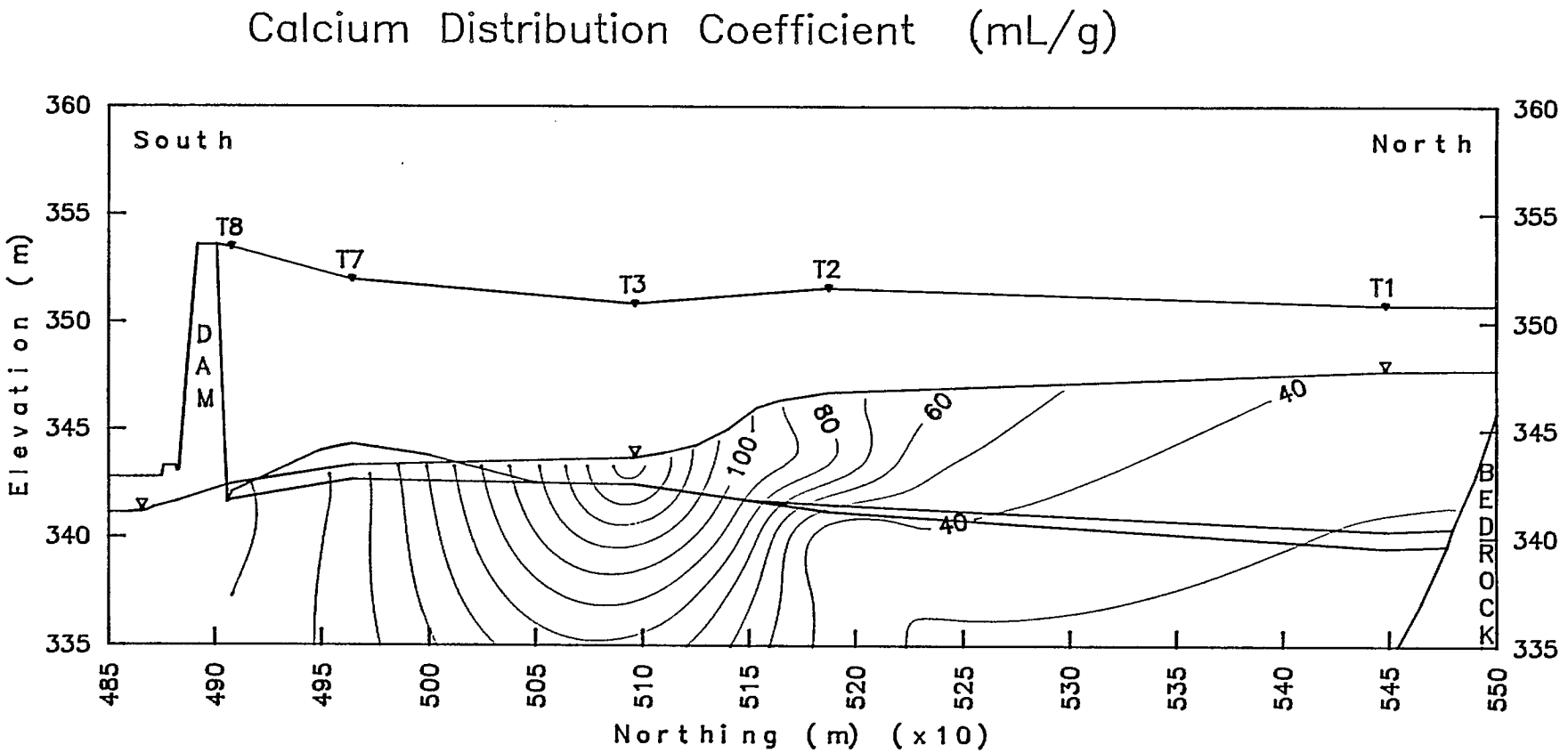


Fig. 7.69 - Nordic main tailings. Vertical north-south profile solid/liquid distribution coefficient of calcium (mL/g), contour map at various depths. (Based on total calcium in bulk mass.)

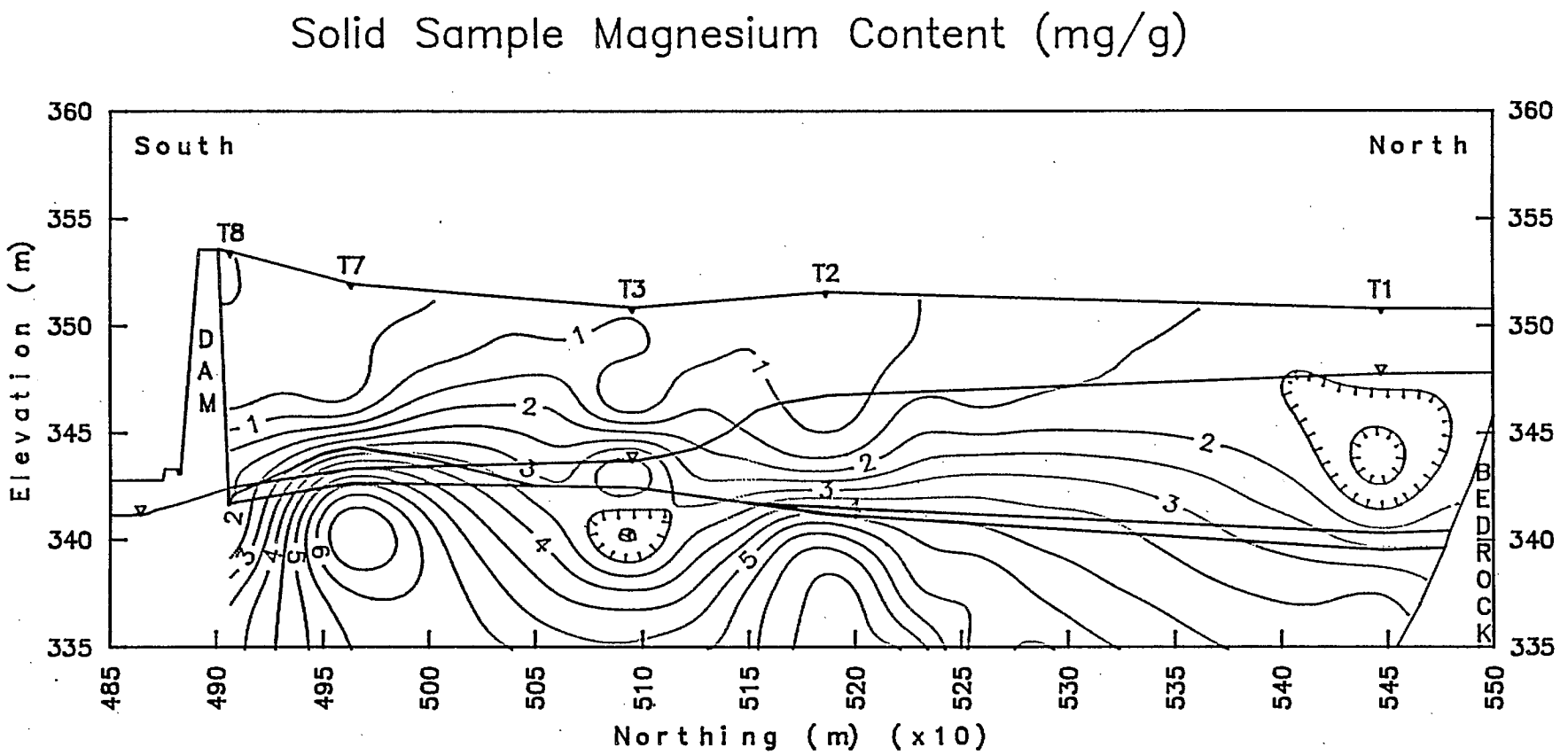


Fig. 7.70 - Nordic main tailings. Vertical north-south profile of solid sample magnesium content (mg/g), contour map at various depths.

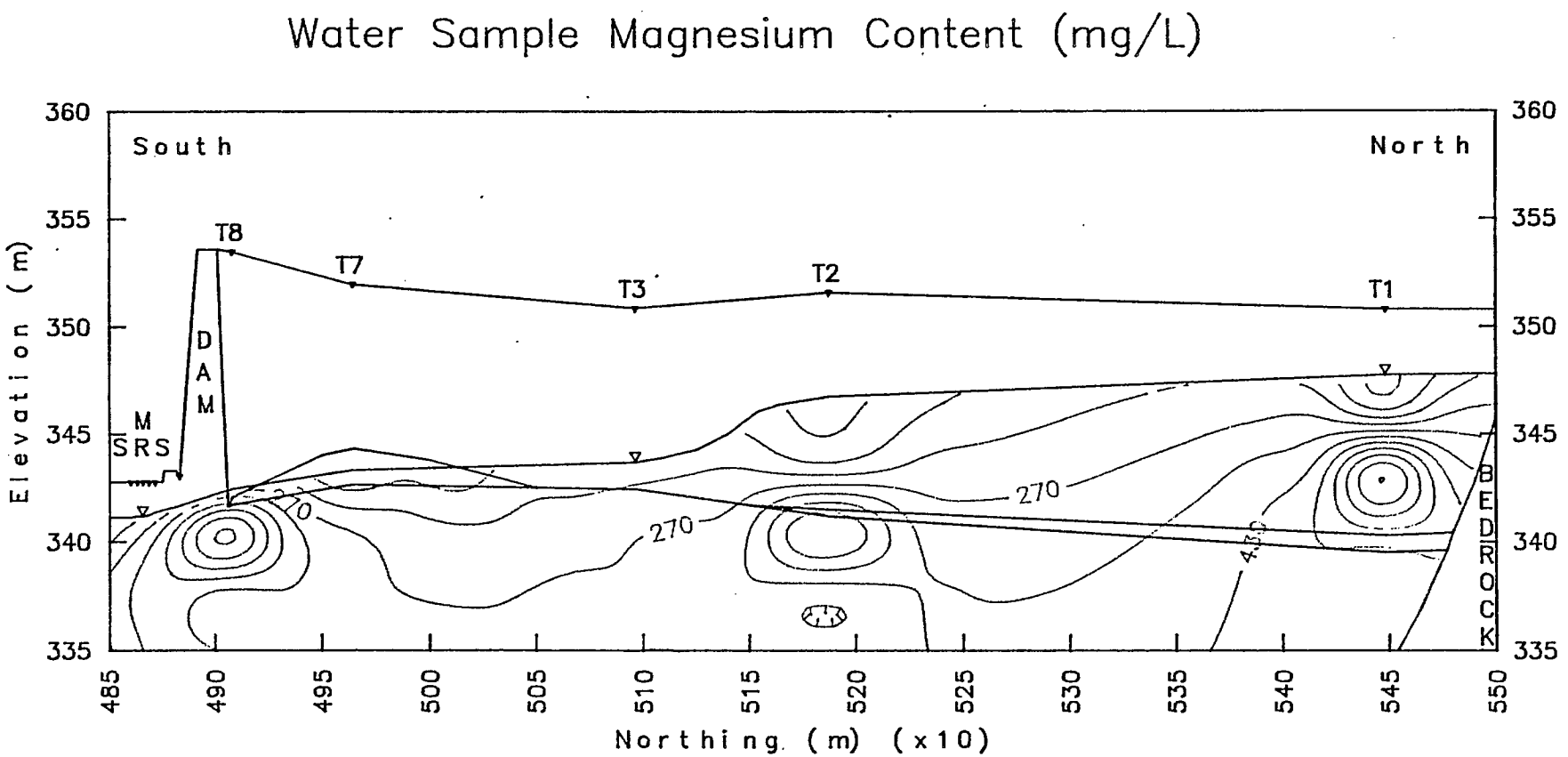


Fig. 7.71 - Nordic main tailings. Vertical north-south profile of liquid sample magnesium content (mg/L), contour map at various depths.

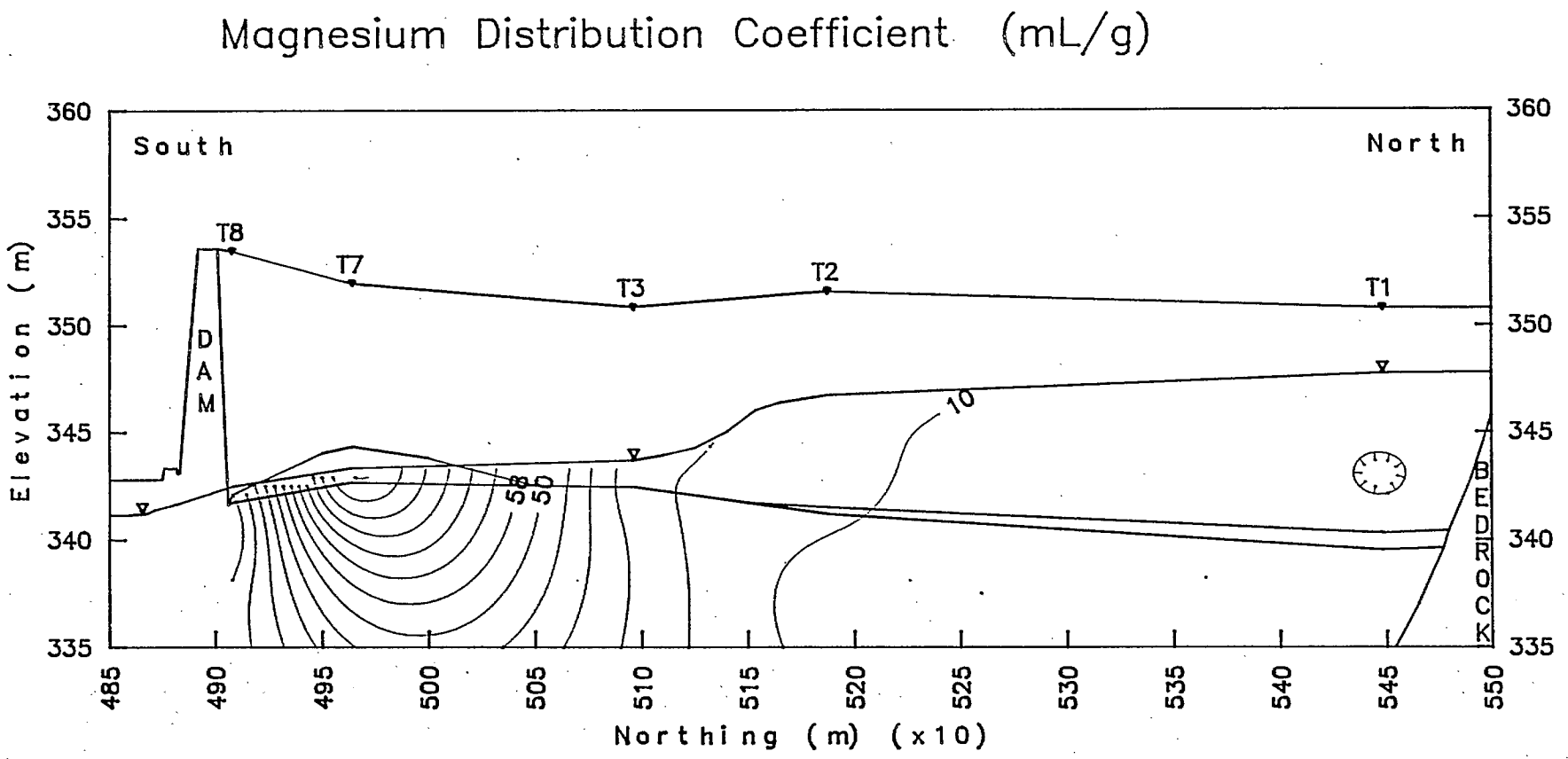


Fig. 7.72 - Nordic main tailings. Vertical north-south profile solid/liquid distribution coefficient of magnesium (mL/g), contour map at various depths. (Based on total magnesium in bulk mass.)

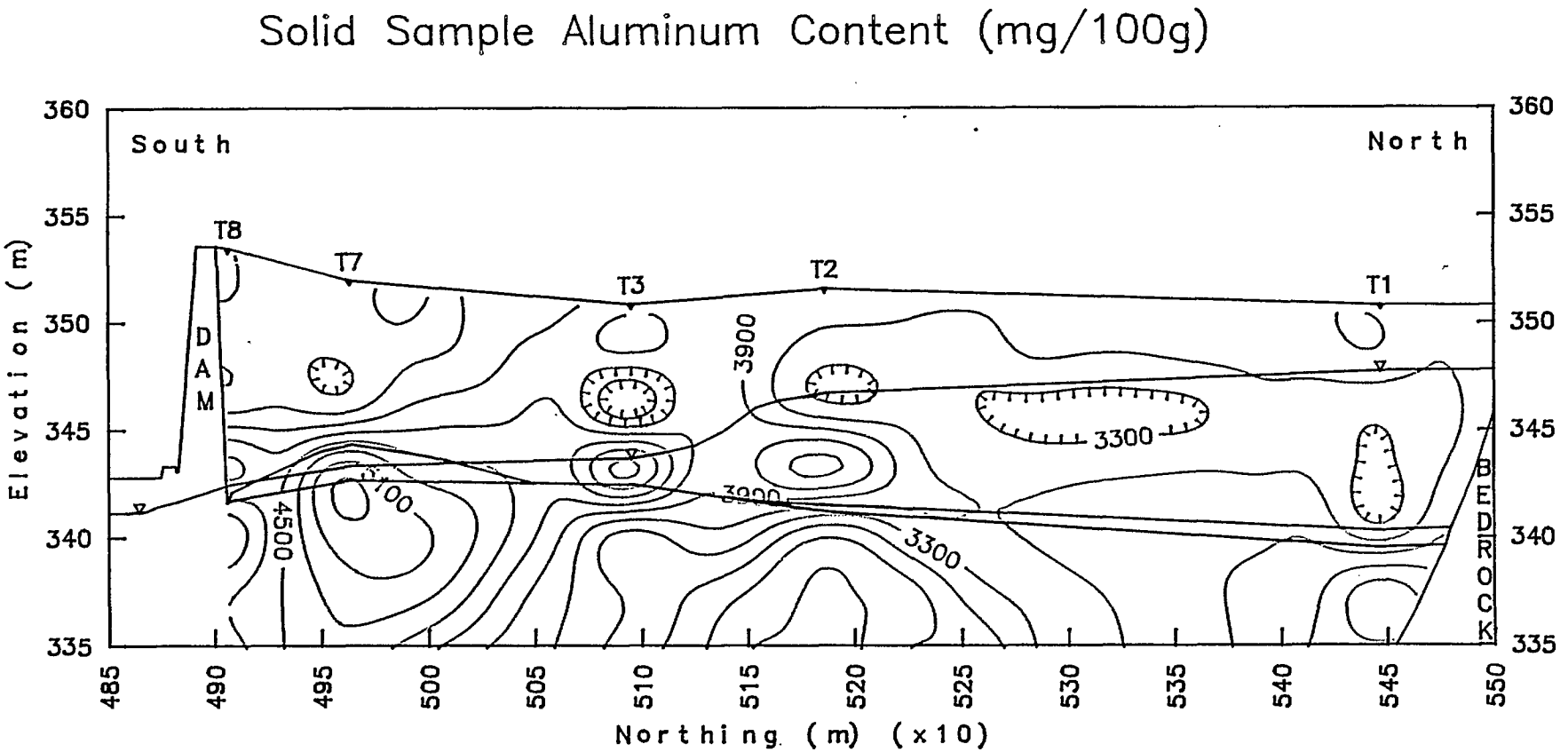


Fig. 7.73 - Nordic main tailings. Vertical north-south profile of solid sample aluminum content (mg/100 g), contour map at various depths.

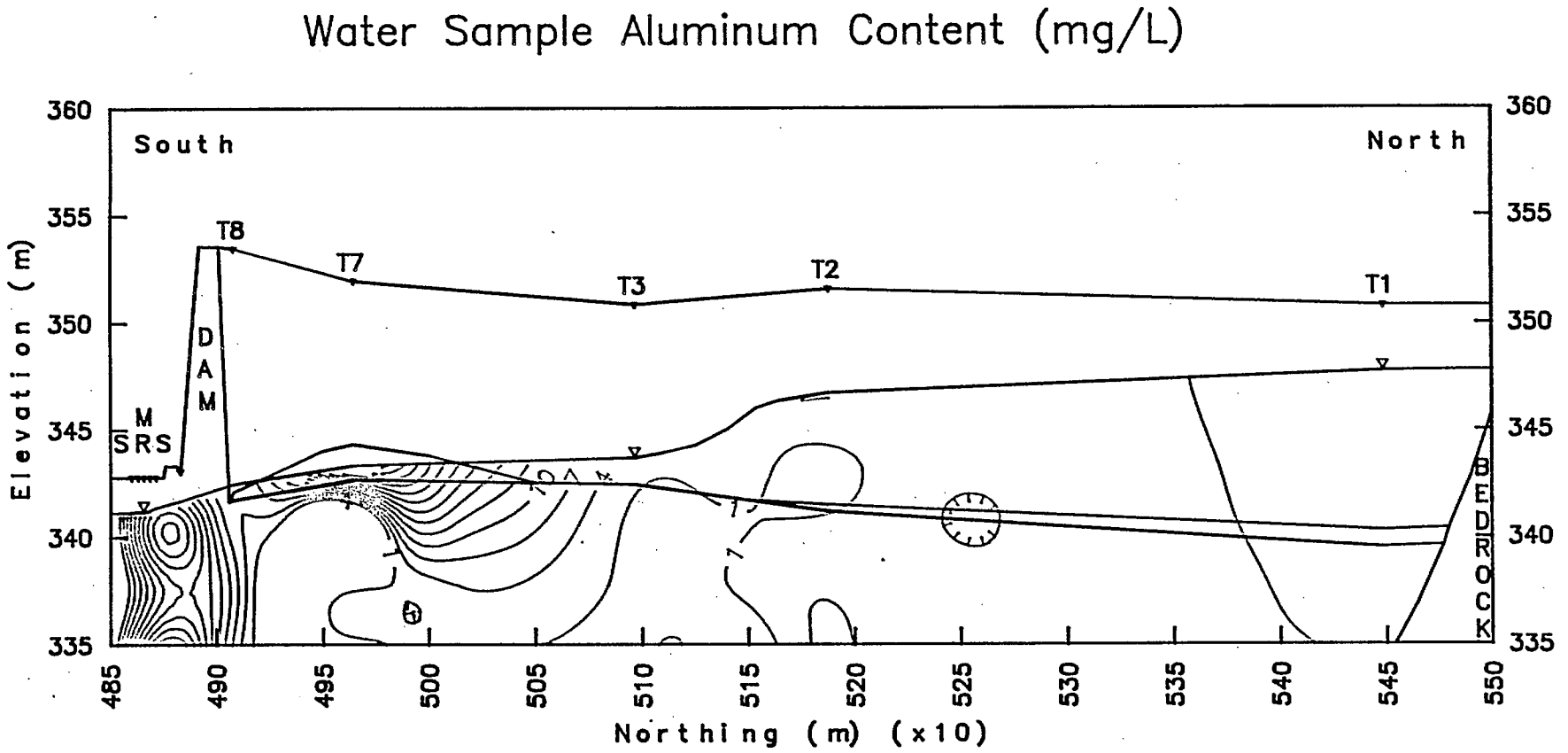


Fig. 7.74 - Nordic main tailings. Vertical north-south profile of liquid sample aluminum content (mg/L), contour map at various depths.

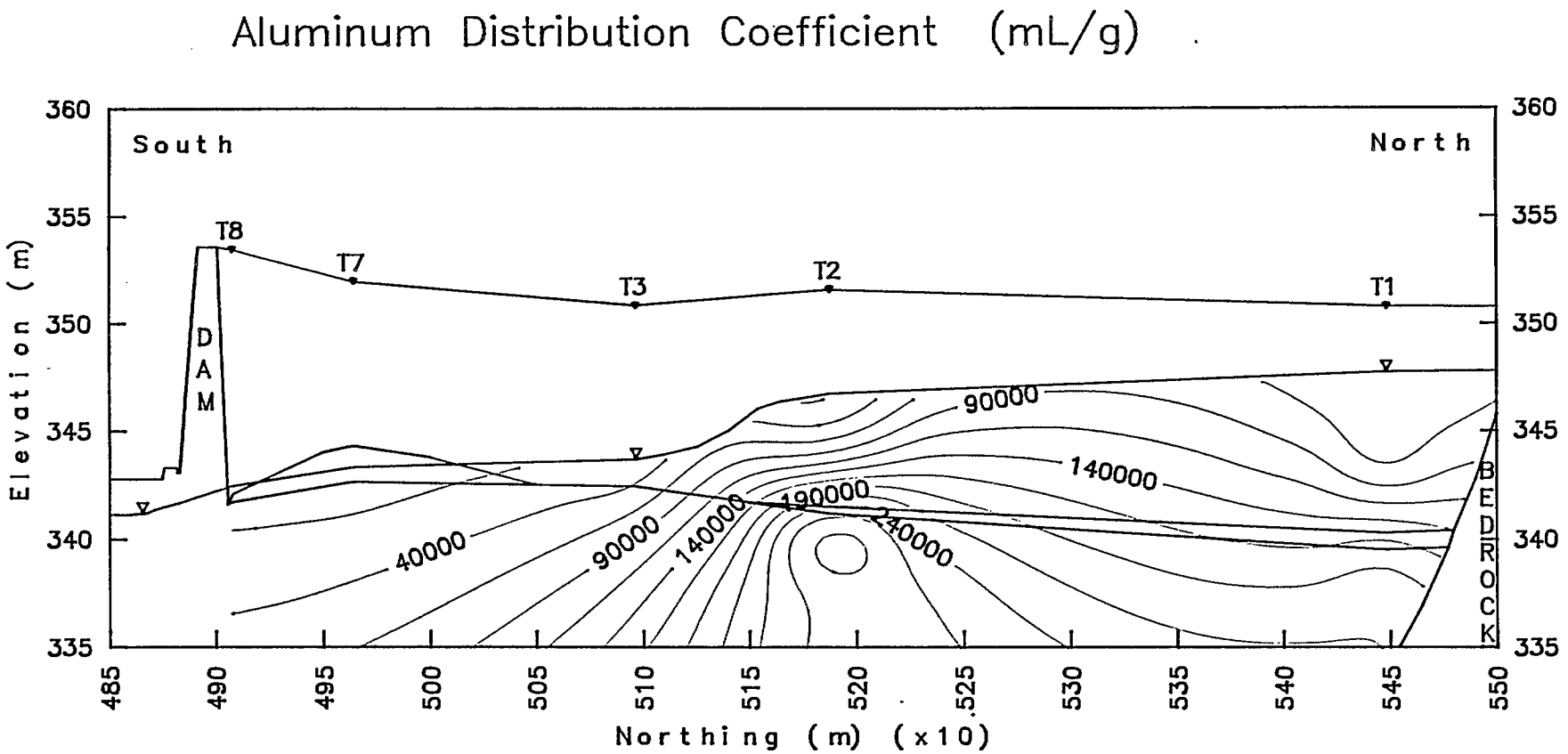


Fig. 7.75 - Nordic main tailings. Vertical north-south profile solid/liquid distribution coefficient of aluminum (mL/g), contour map at various depths. (Based on aluminum in bulk mass.)

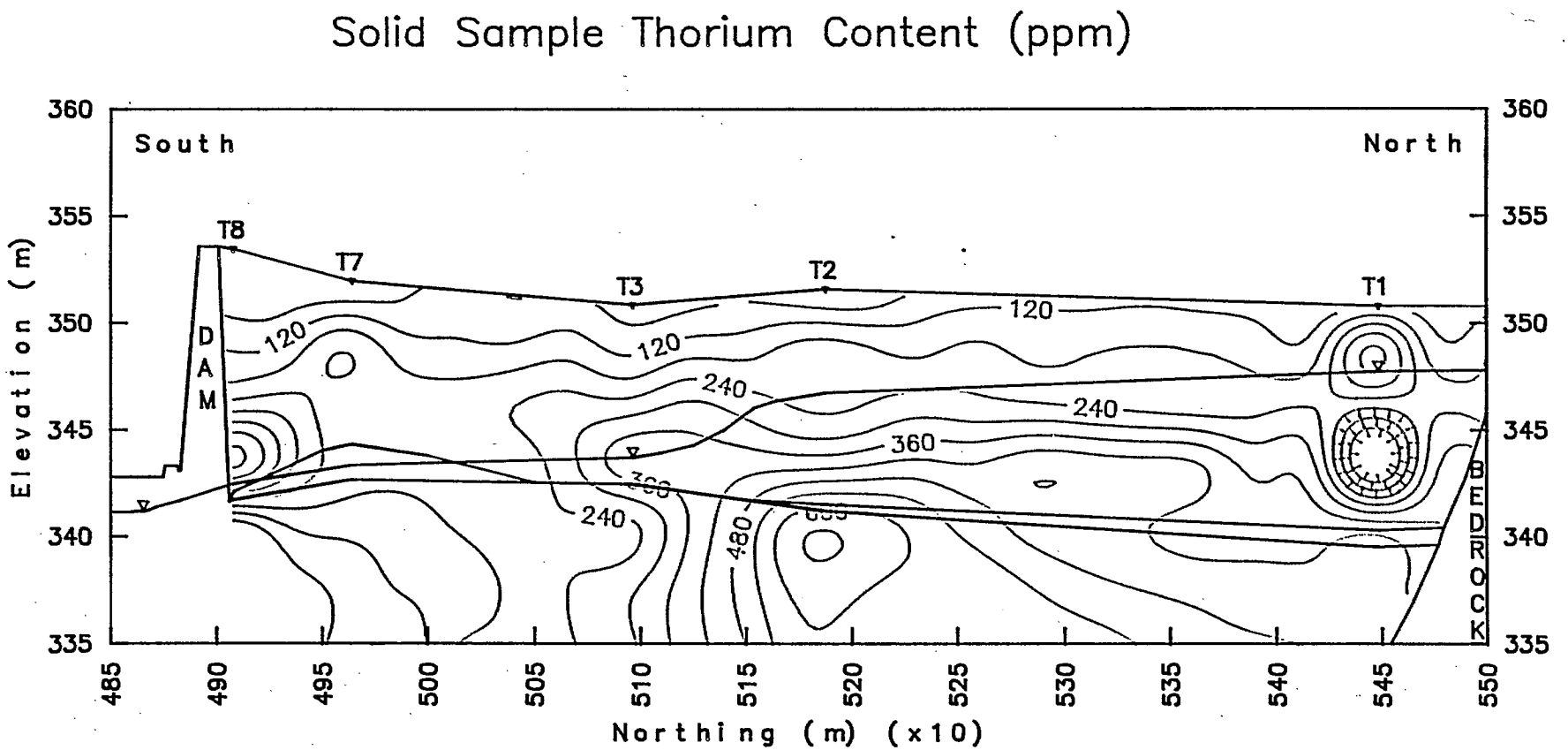


Fig. 7.76 - Nordic main tailings. Vertical north-south profile of solid sample thorium content (ppm), contour map at various depths.

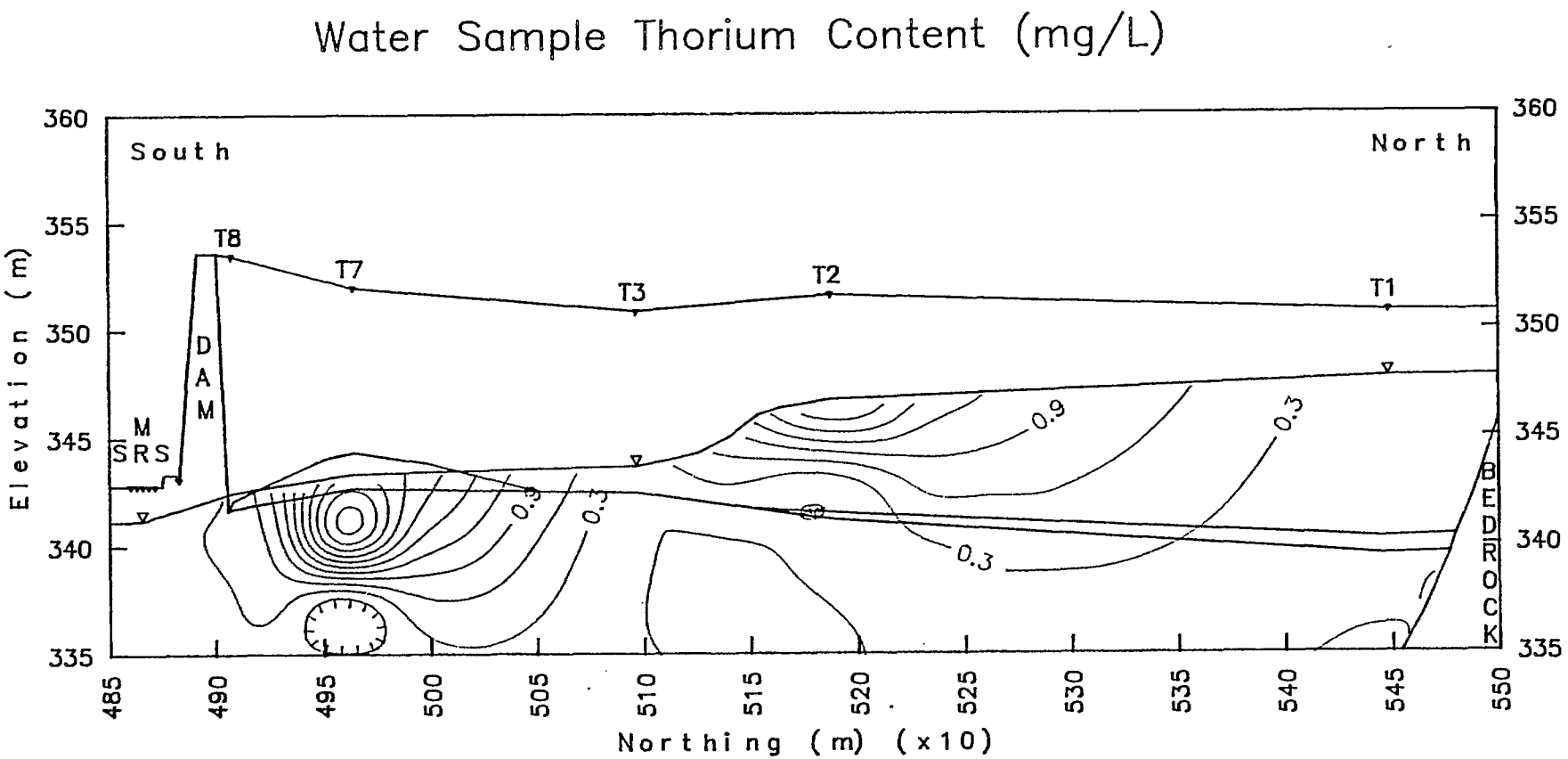


Fig. 7.77 - Nordic main tailings. Vertical north-south profile of liquid sample thorium content (mg/L), contour map at various depths.

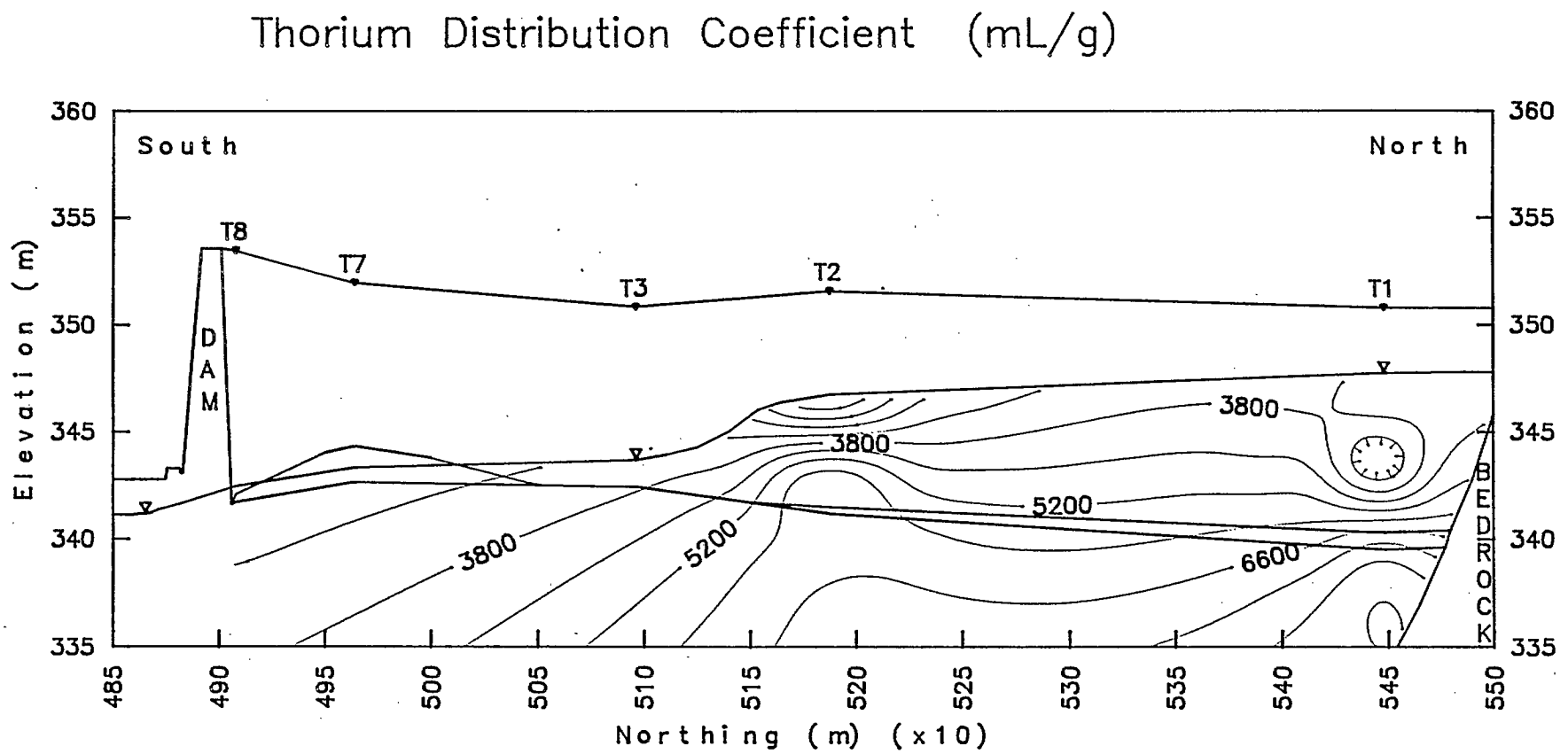


Fig. 7.78 - Nordic main tailings. Vertical north-south profile solid/liquid distribution coefficient of thorium (mL/g), contour map at various depths. (Based on thorium in bulk mass.)

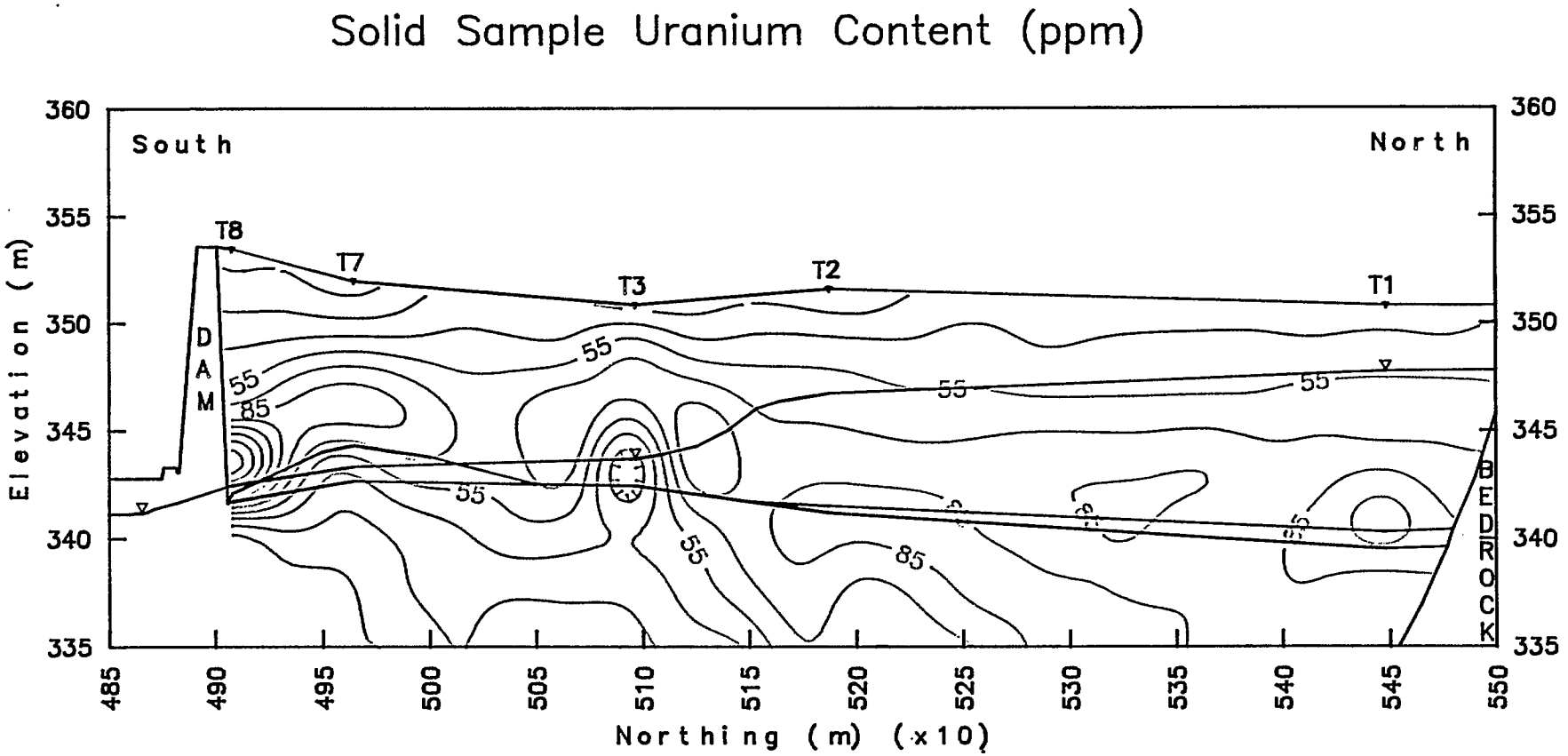


Fig. 7.79 - Nordic main tailings. Vertical north-south profile of solid sample uranium content (ppm), contour map at various depths.

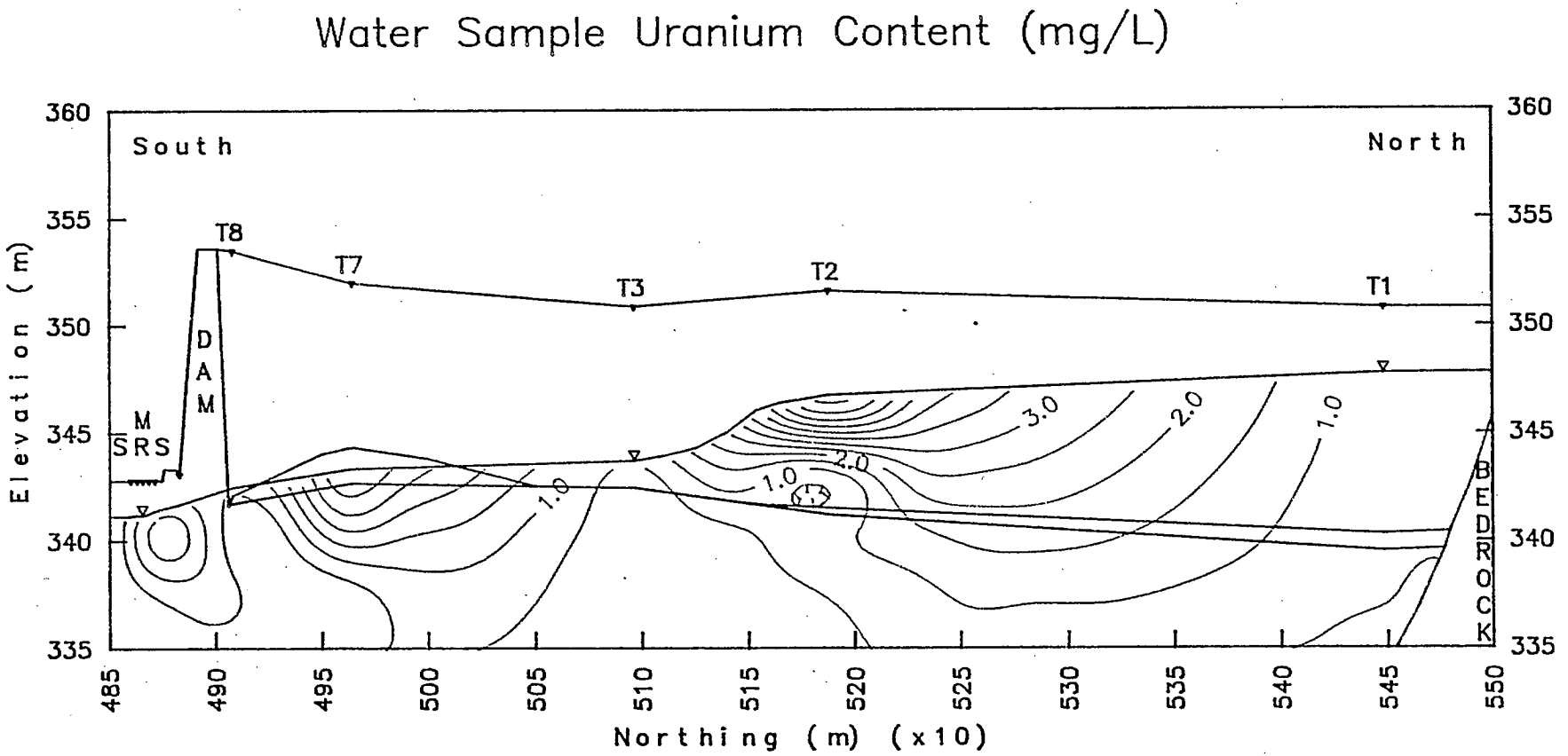


Fig. 7.80 - Nordic main tailings. Vertical north-south profile of liquid sample uranium content (mg/L), contour map at various depths.

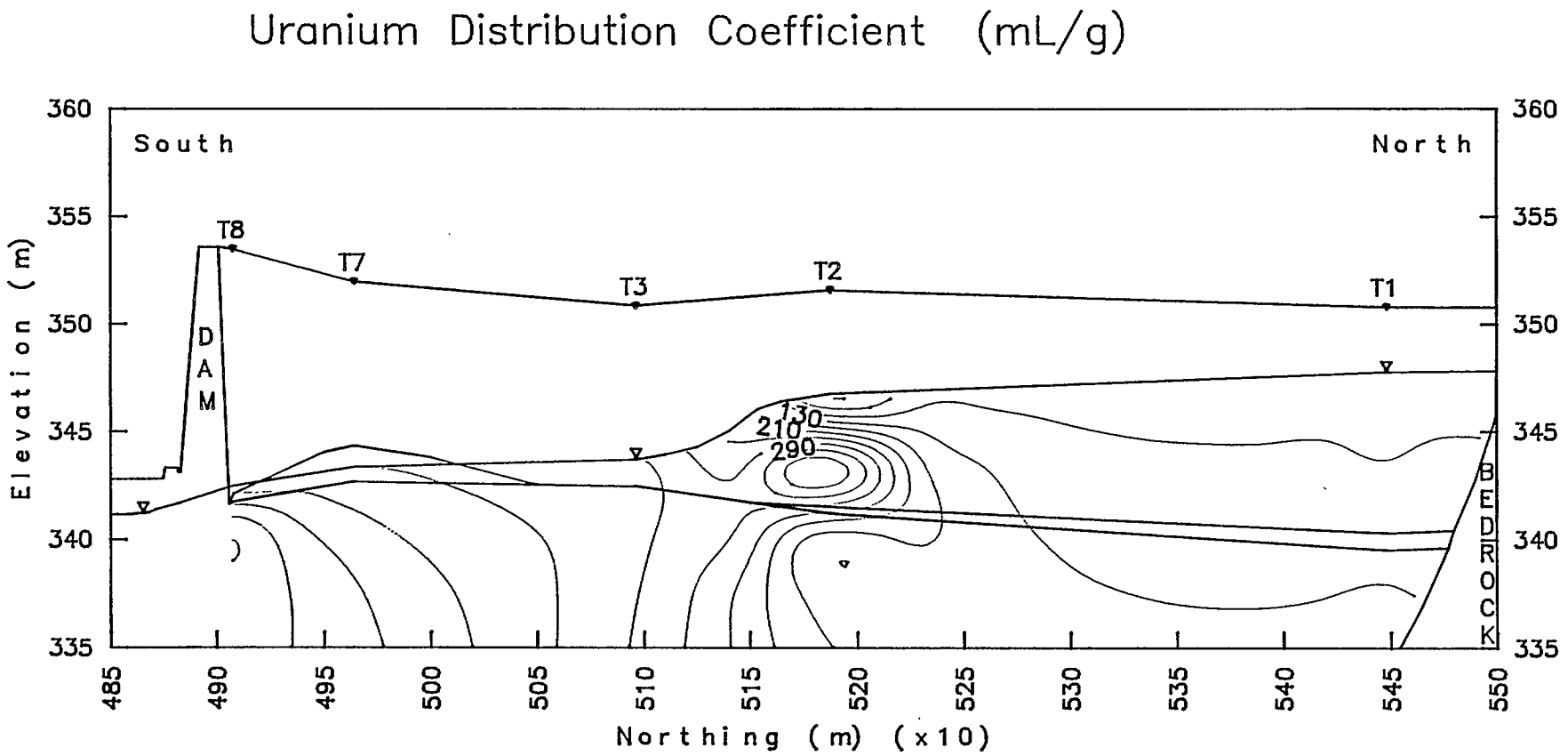


Fig. 7.81 - Nordic main tailings. Vertical north-south profile solid/liquid distribution coefficient of uranium (mL/g), contour map at various depths. (Based on uranium in bulk mass.)

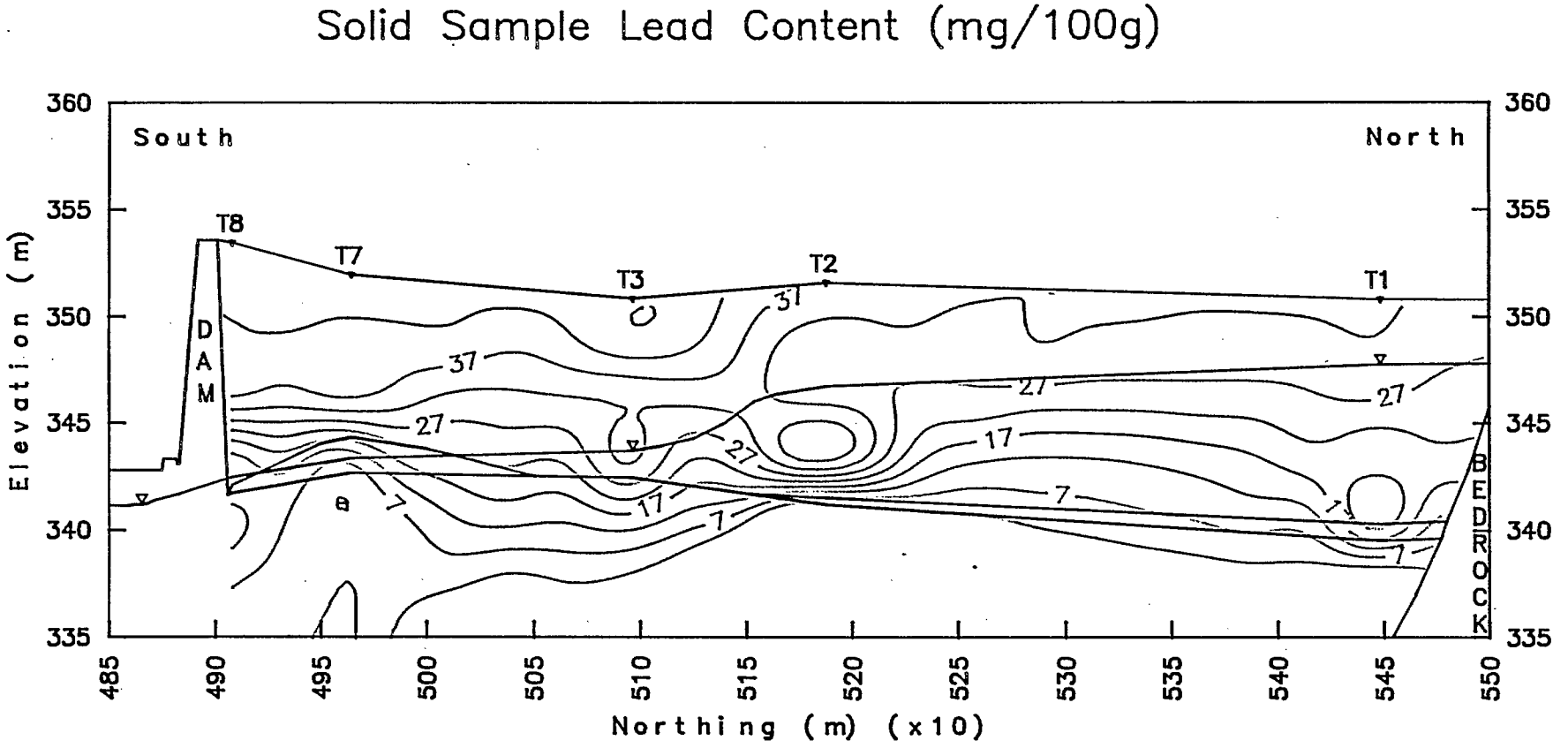


Fig. 7.82 - Nordic main tailings. Vertical north-south profile of solid sample lead content (mg/100 g), contour map at various depths.

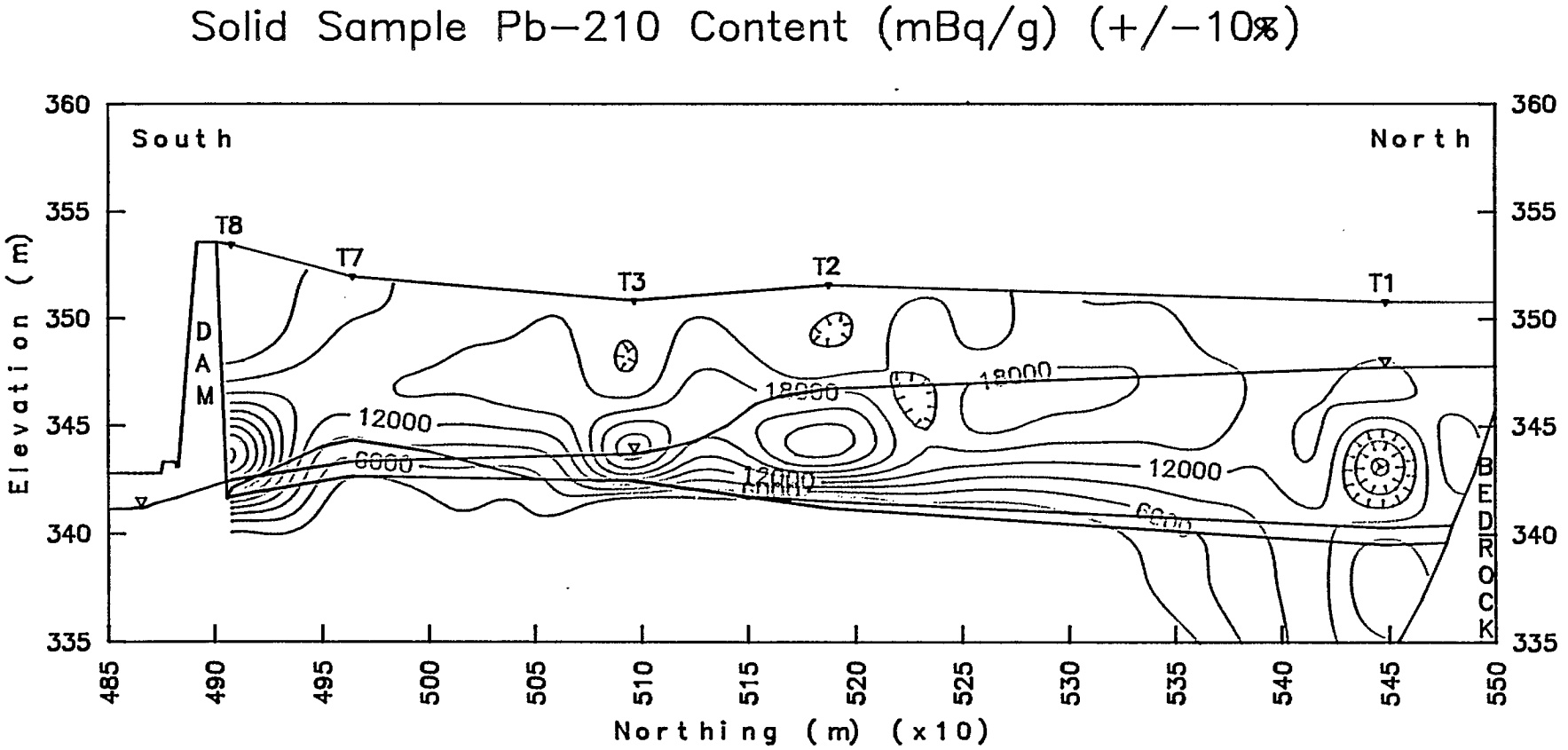


Fig. 7.83 - Nordic main tailings. Vertical north-south profile of solid sample $^{210}Pb$ content (mBq/g) (±10%), contour map at various depths.

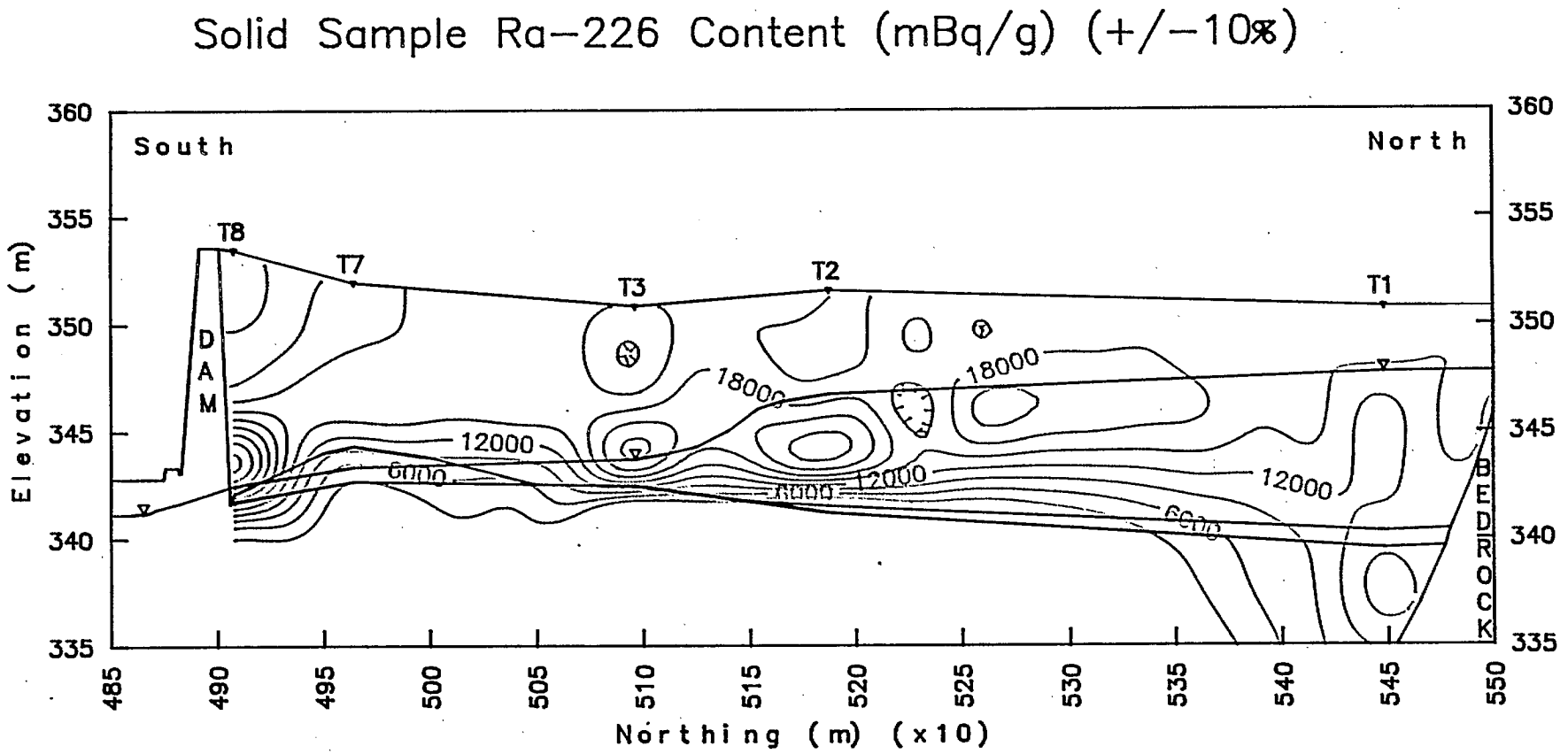


Fig. 7.84 - Nordic main tailings. Vertical north-south profile of solid sample $^{226}Ra$ content (mBq/g) (±10%), contour map at various depths.

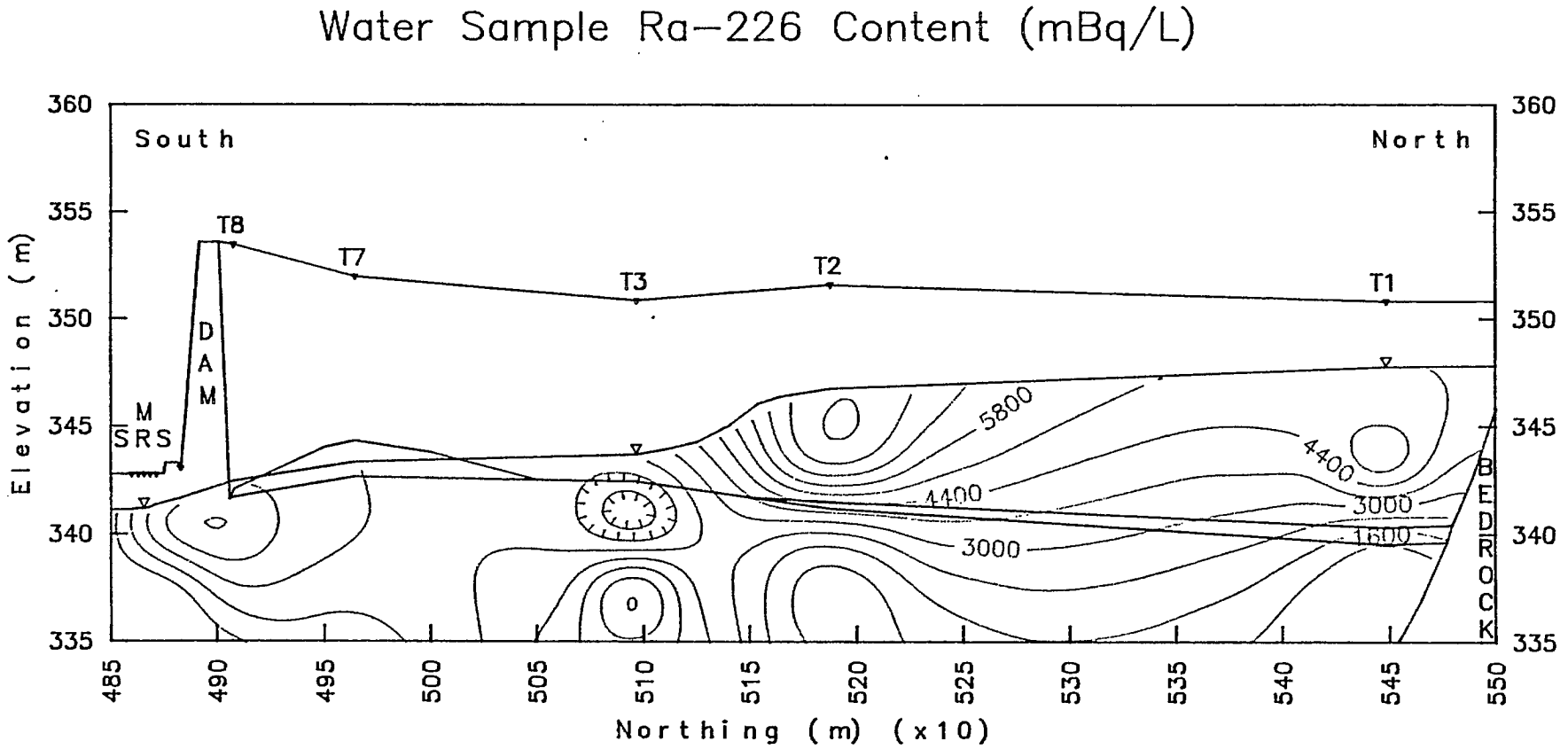


Fig. 7.85 - Nordic main tailings. Vertical north-south profile of liquid sample $^{226}Ra$ content (mBq/L), contour map at various depths.

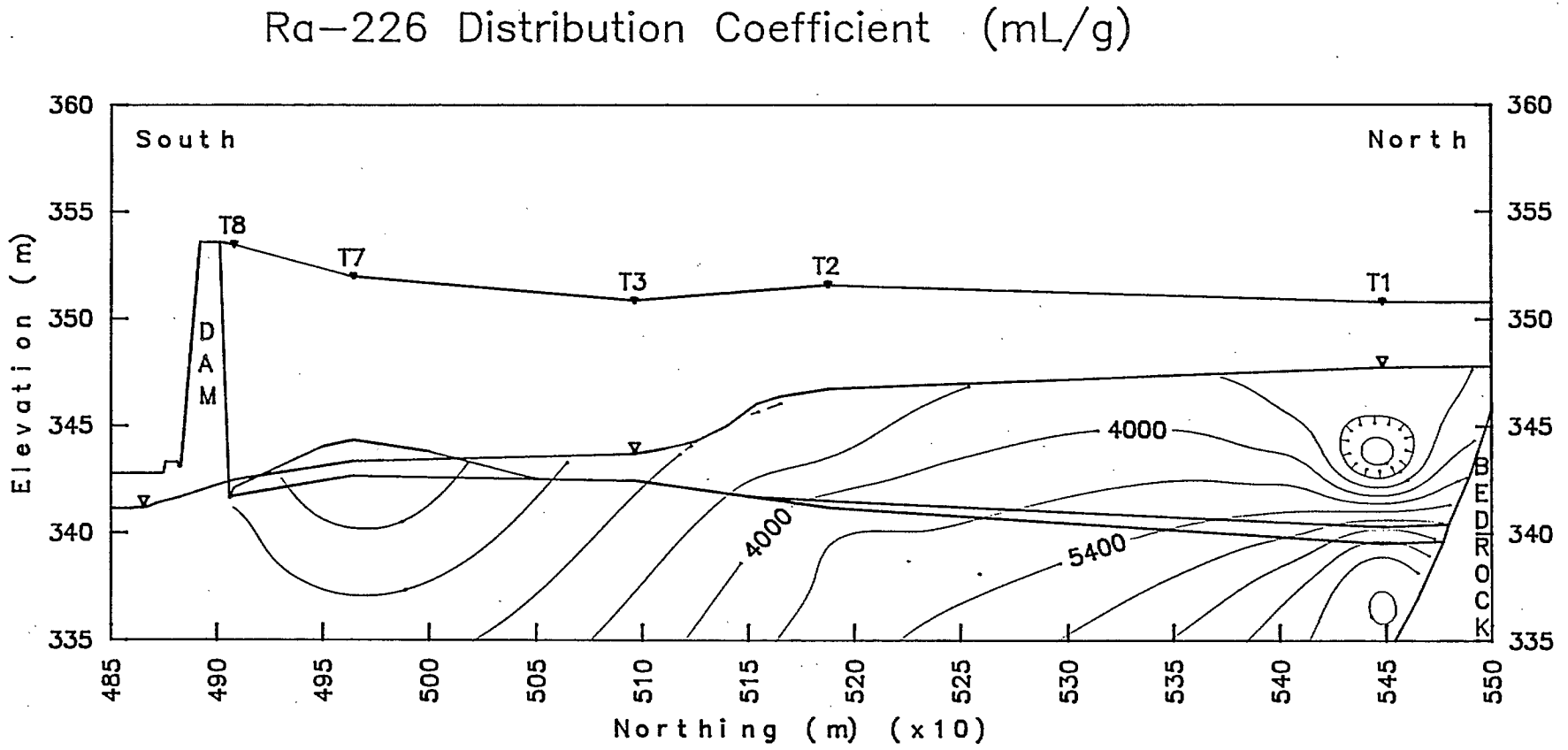


Fig. 7.86 - Nordic main tailings. Vertical north-south profile solid/liquid distribution coefficient of $^{226}Ra$ (mL/g), contour map at various depths. (Based on $^{226}Ra$ in bulk mass.)

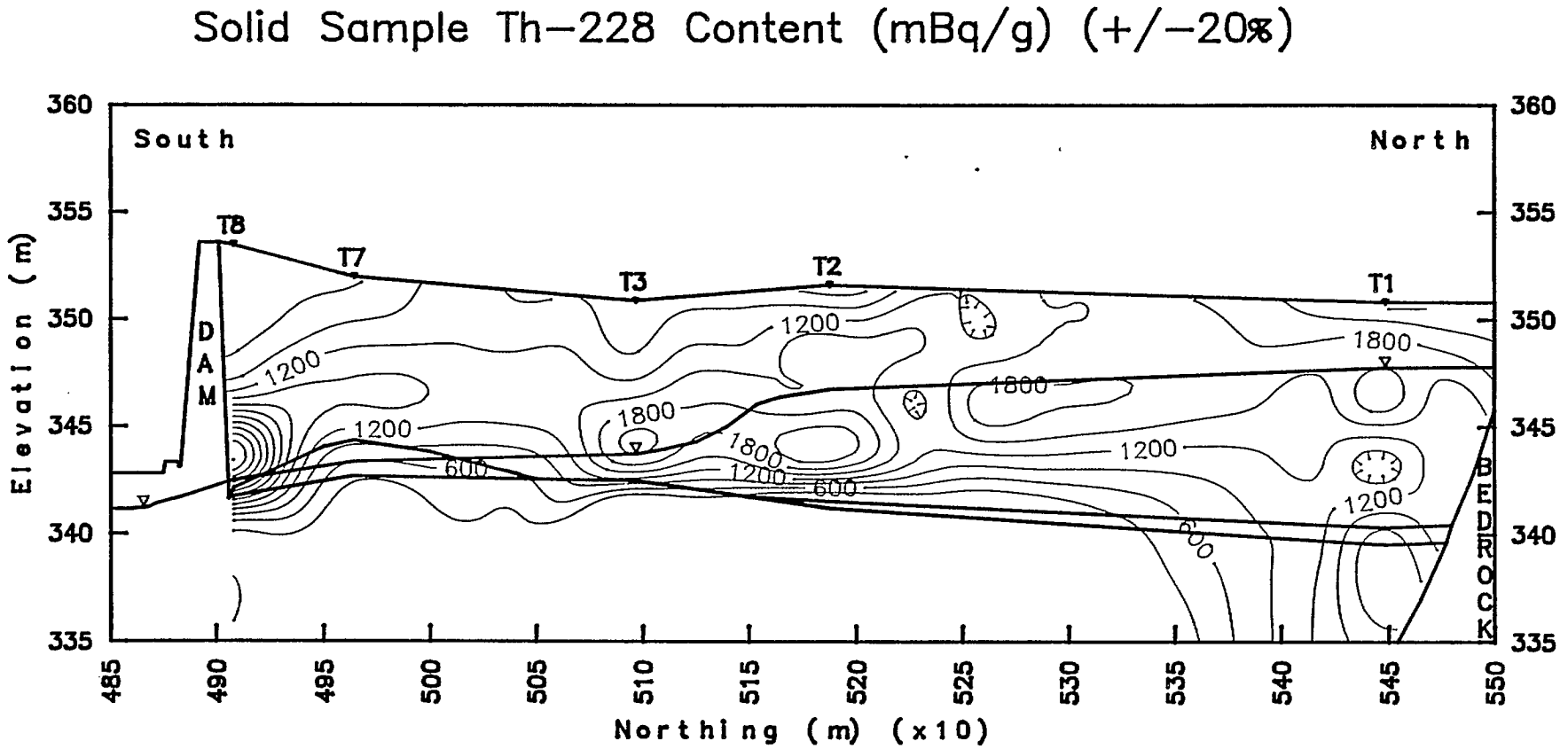


Fig. 7.87 - Nordic main tailings. Vertical north-south profile of solid sample $^{228}Th$ content (mBq/g) (±20%), contour map at various depths.

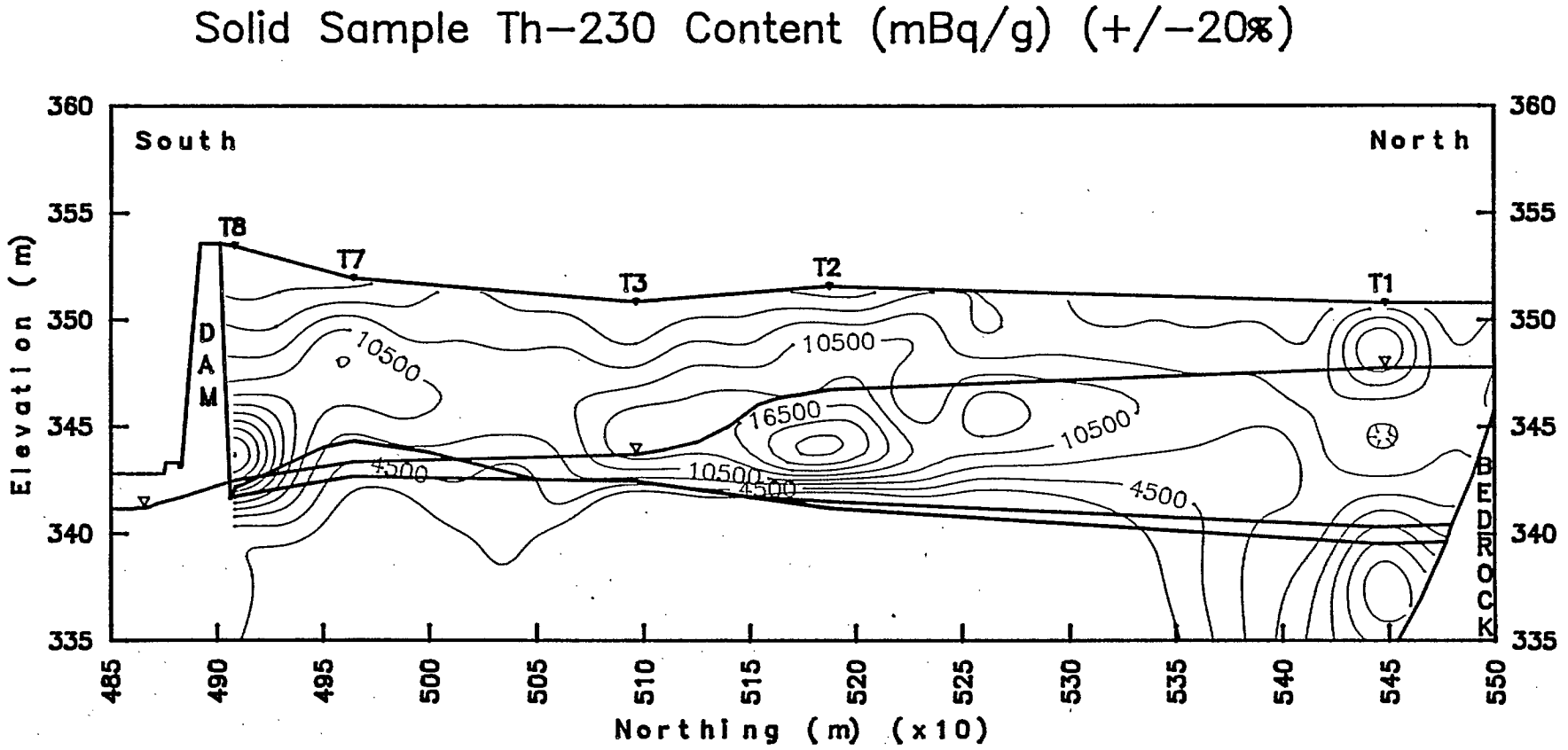


Fig. 7.88 - Nordic main tailings. Vertical north-south profile of solid sample $^{230}Th$ content (mBq/g) (±20%), contour map at various depths.

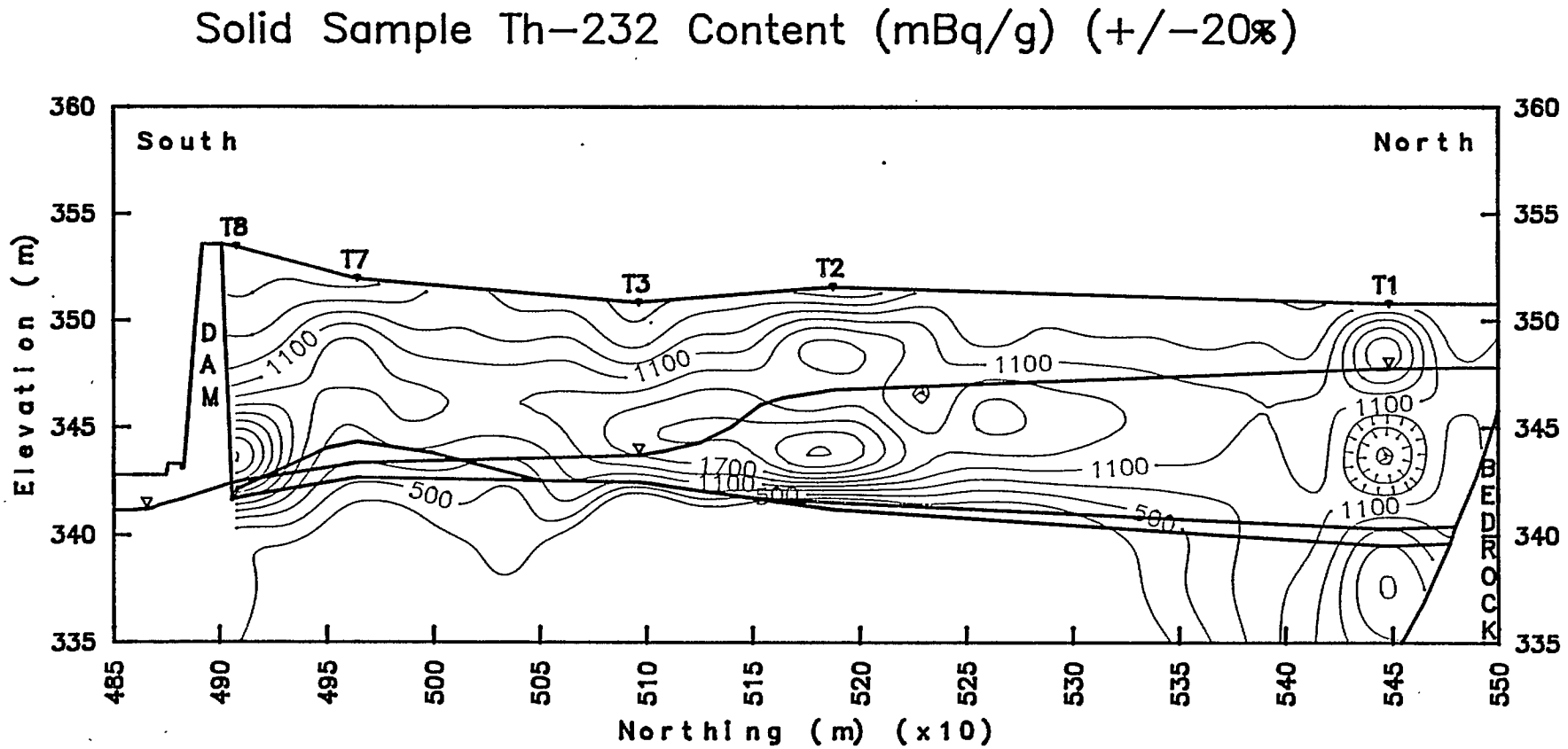


Fig. 7.89 - Nordic main tailings. Vertical north-south profile of solid sample $^{232}Th$ content (mBq/g) (±20%), contour map at various depths.

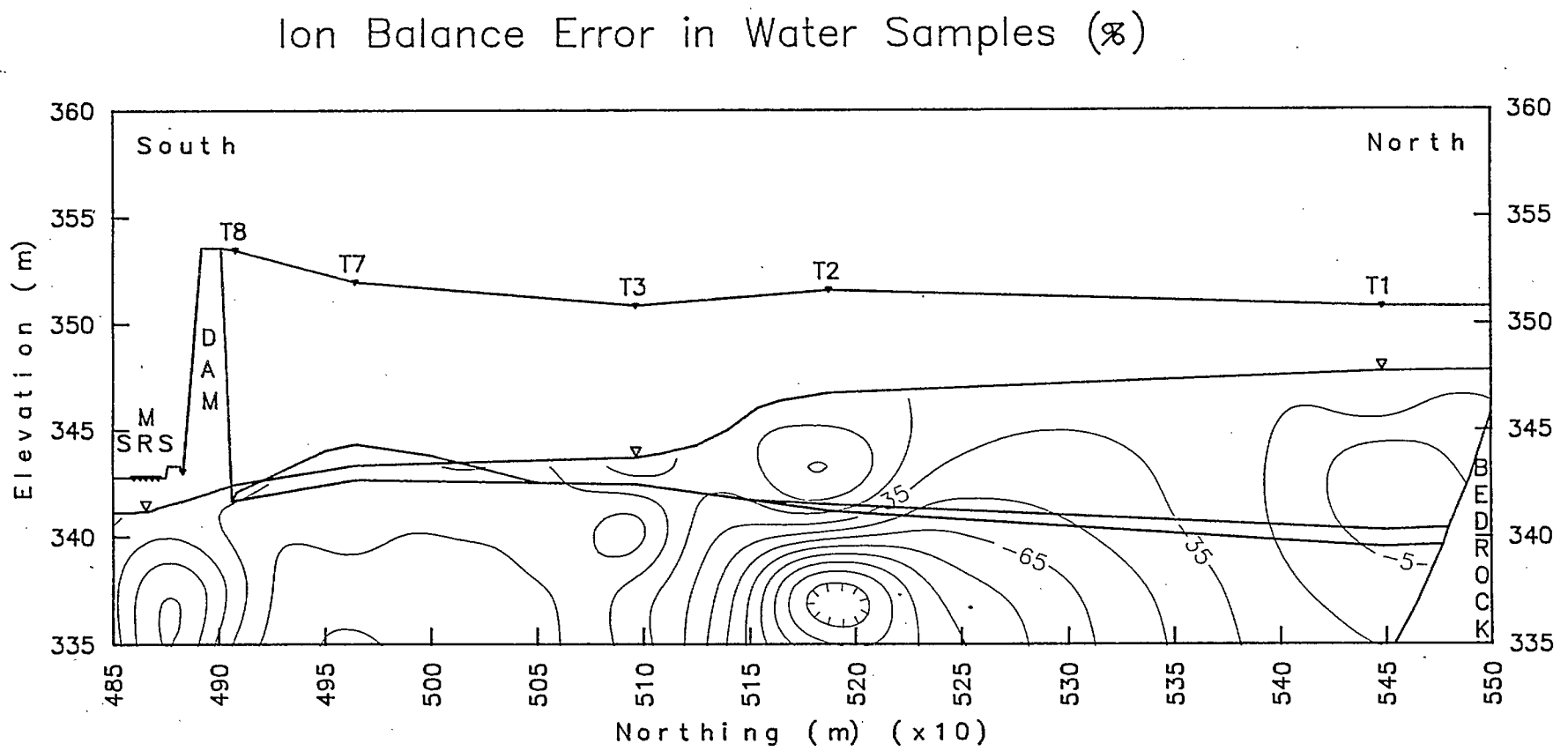


Fig. 7.90 - Nordic main tailings. Vertical north-south profile of ion balance error in water samples (%), contour map at various depths.

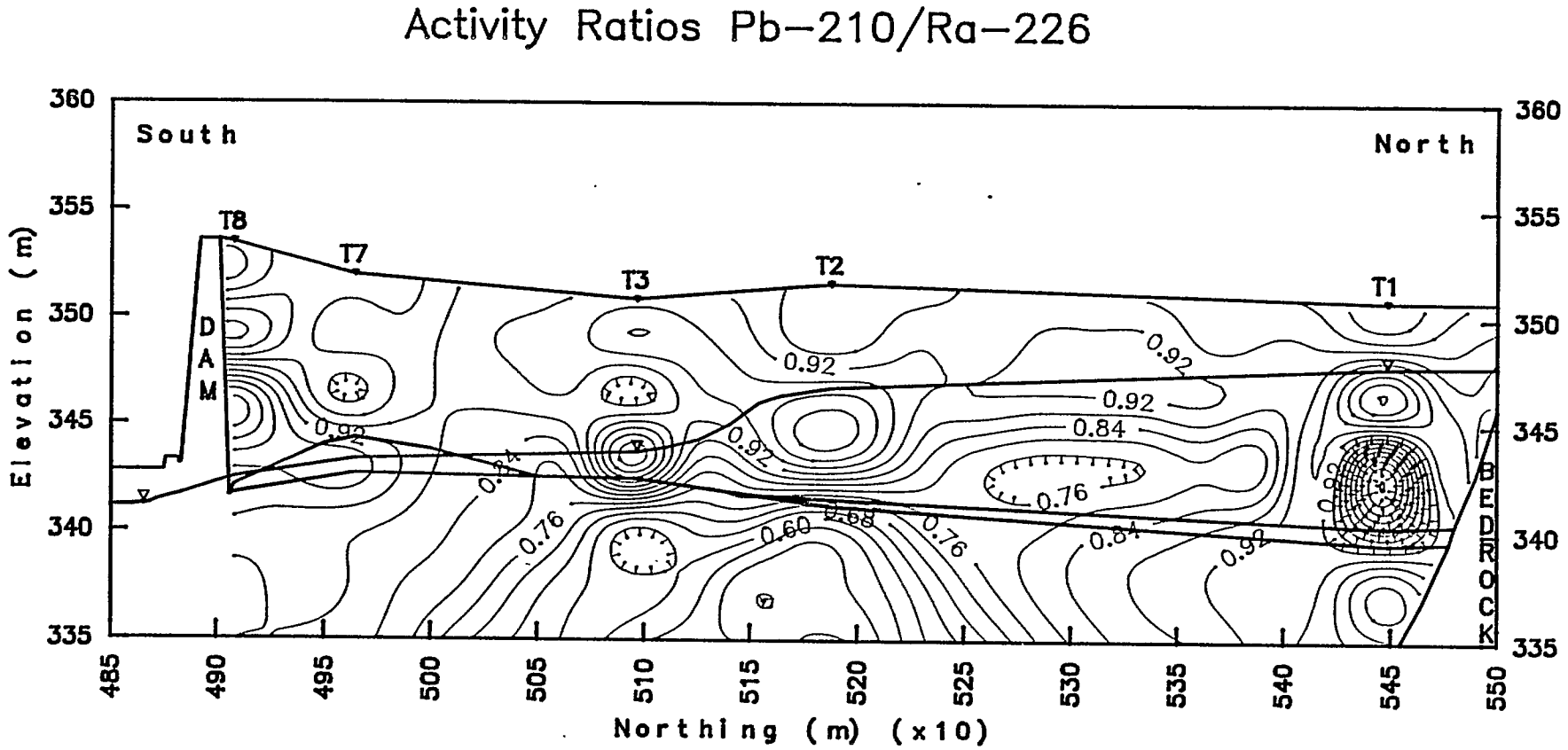


Fig. 7.91 - Nordic main tailings. Vertical north-south profile of solid phase activity ratios $^{210}Pb/^{226}Ra$, contour map with depth.

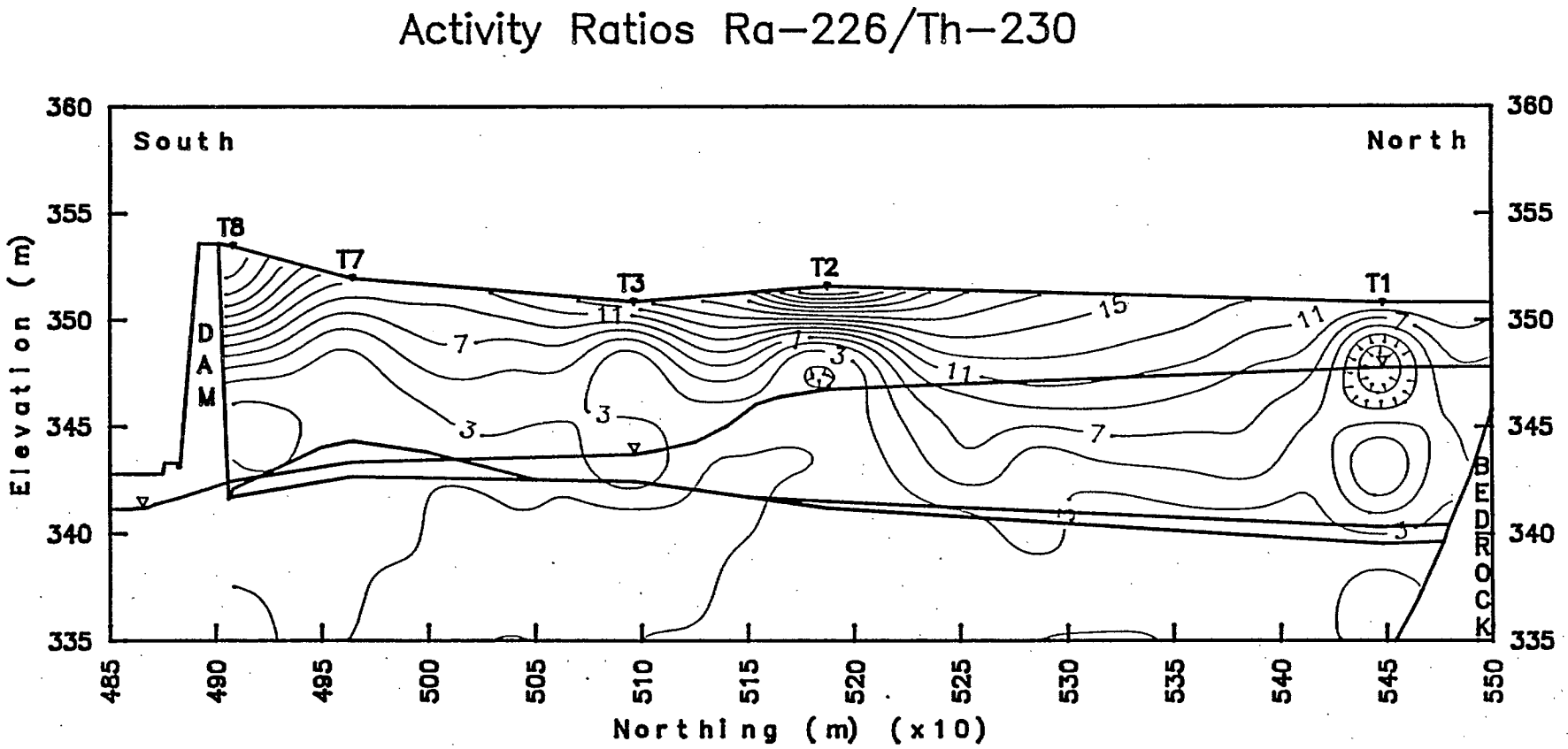


Fig. 7.92 - Nordic main tailings. Vertical north-south profile of solid phase activity ratios $^{226}Ra/^{230}Th$ , contour map with depth.

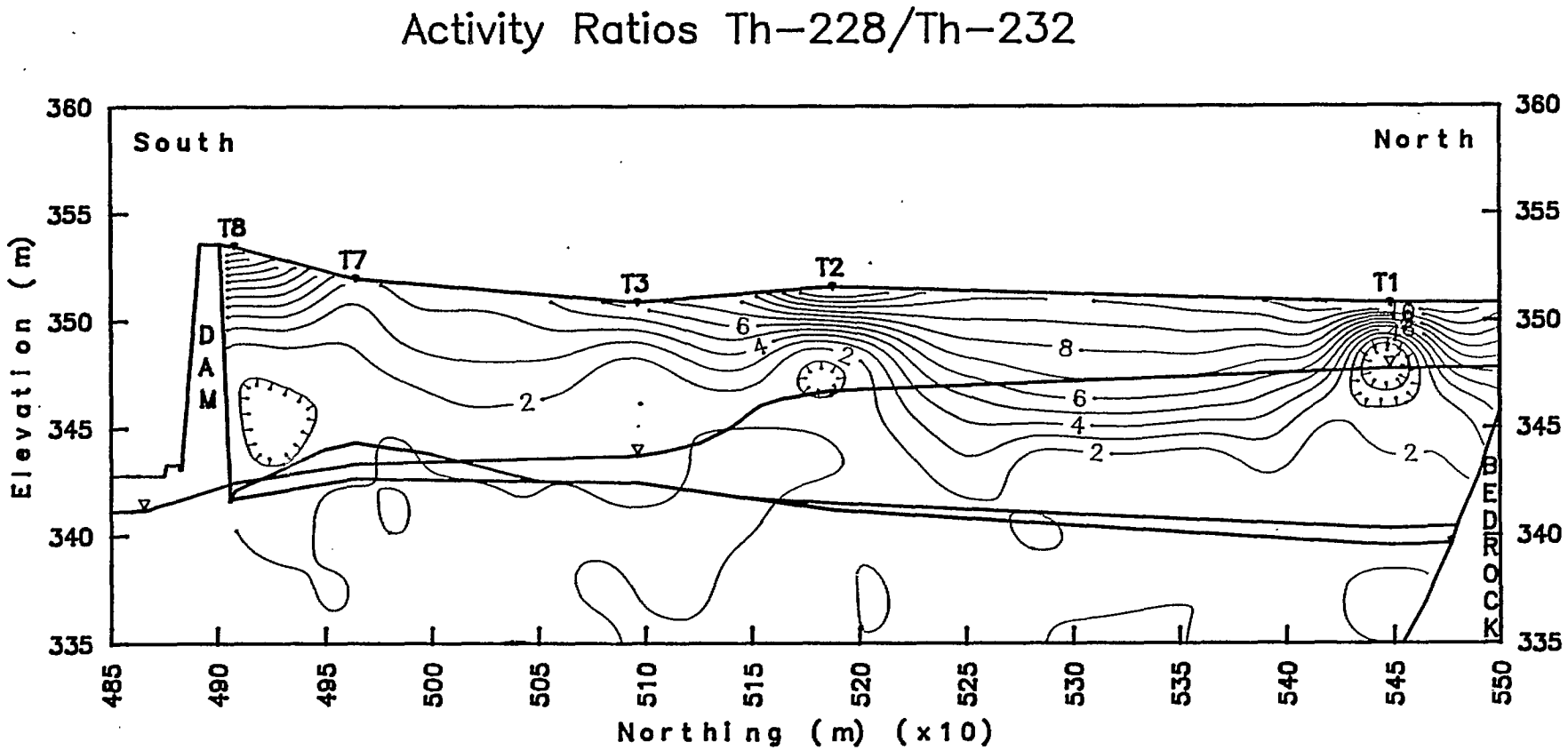


Fig. 7.93 - Nordic main tailings. Vertical north-south profile of solid phase activity ratios $^{228}Th/^{232}Th$, contour map with depth.

# CHAPTER 8

## SAMPLING METHOD AND TIMING SEQUENCE - LABORATORY EXPERIMENT

The existence of paradoxical secular disequilibrium has been shown in Chapter 7. The behaviour of this paradoxical secular disequilibrium is time-dependent as a result of the dynamics of nuclear decay chains and geochemistry processes. This Chapter will be devoted to the important role of sampling techniques and the timing sequence in identifying and characterizing this disequilibrium.

### 8.1 LABORATORY EXPERIMENT

A laboratory experiment was designed to exhibit the dynamic changes in the activity of the liquid phase. The design was based on related experiences in the field investigation, especially on radium analyses using alpha-spectroscopy (reference 47, Figures 16 to 18), in which some abnormality in the radium spectrum was observed. It was concluded that this abnormality was caused by the ingrowth of $^{233}Ra$ and $^{224}Ra$ isotopes within the sampling bottle a few weeks after sampling. Since the resolution of the technique for radium analyses at that time was very low, no further investigation was planned to test for the mechanism.

The laboratory facility at Elliot Lake Laboratory, at the present time is still very limited for doing analyses on the trans- uranium series, therefore, only alpha-particle emitting radium species were used in this experimental design. However, suitable radium alpha-emitters with short half-lives (11 d for $^{223}Ra$, and 3.6 d for $^{224}Ra$, respectively) could be used, and therefore rapid changes were expected. A new technique with high resolution alpha-spectroscopy for radium analysis, recently published, was used in this

experiment in order to identify the $^{223}Ra$ and $^{224}Ra$ (56).

## 8.2 EXPERIMENTAL DESIGN

In this experimental design, only natural radioisotopes from uranium tailings were used, and no spiked standard (such as that designed by Veska (26)) was added to enhance the limit of detection so only true paradoxical secular disequilibrium events that occurred naturally were observed.

A 100 L acid washed plastic container was used, and approximately 100 kg of the top layer of the tailings sample from Nordic main tailings was put into it and flooded with water.

A half inch pipe, 50 cm high, with side holes surrounded by a glass wool filter, and a rubber plug on the bottom, was installed in the centre of the tailings as a sampling port, Figure 8.1.

The sample was put aside for two years, because of other priorities. From time to time air was blown into the tube to keep the oxidation and low pH condition in effect. Since the sample had no porewater removed, it was expected that the solid and liquid phase would come to chemical equilibrium, as well as radioisotope equilibrium on some short-lived radioisotope species such as $^{227}Th$ (18 d), $^{228}Th$ (1.9 y), $^{223}Ra$ (11 d) and $^{224}Ra$ (3.6 d).

A 4 L liquid phase sample was extracted from the mixture using a peristaltic pump and passed through a 0.45 μm filter. The sample bottle was labelled 'RDE', for Radioisotope Disequilibrium Experiment, and some of the standard chemical parameters were measured, such as pH, Eh, Ec and temperature. Then 10 mL concentrated hydrochloric acid was added to the liquid phase sample to preserve and stabilize it. The time of liquid and solid phase separation was noted, and a 250 mL sample cut was taken for radium analysis. On three separate occasions liquid samples were extracted and analyzed for radium content. The radium planchets (56) were labelled

RDE-1, RDE-2 and RDE-3, respectively.

The separation times for $Ba(Ra)SO_4$ from the EDTA solution were noted for RDE-1, RDE-2 and RDE-3. These data were used later to determine the amount of $^{227}Th$ and $^{228}Th$ in the liquid phase at time of separation from the solid phase.

The radium samples on each planchet were periodically counted at 6000 sec intervals up to 600 hours from the liquid separation time. Several radium spectra were obtained from each planchet, and the integration of $^{226}Ra$, ($^{223}Ra$+$^{224}Ra$), $^{215}Po$, $^{214}Po$ and $^{212}Po$ peaks were recorded every 6000 sec. The data were used later on $^{226}Ra$, $^{223}Ra$ and $^{224}Ra$ determinations.

It should be noted here that this is the first time 'High Resolution Alpha-Spectroscopy for Radium Analysis' (56) has been employed and tested for field use.

## 8.3 RESULTS AND DISCUSSION

The radioisotope disequilibrium experimental data are shown in Tables 8.1 to 8.11. Some typical spectra of mixed radium species are shown in Figures 8.2 to 8.4. These three Figures were obtained from the same planchet and show a gradual transformation of spectra with time as the radium decays into its daughters.

An example of the decay curve of mixed radium species is shown in Figures 8.5 and 8.6.

The raw data for RDE-1 are shown in Table 8.1, and the standard information, such as time of sample collection, time of radium species separation from the liquid phase sample, and the $^{133}Ba$ recovery factor to correct the radium activity are also shown.

Table 8.2 shows the processed data based on the ln (natural logarithm) function of corrected radium counts to 100% yield.

In Figure 8.6, an example using RDE-3 data shows the decay curve of mixed radium species of ln (count rate/6000 sec) versus time in hours. The $^{212}Po$ (8.78 MeV) daughter of $^{224}Ra$ (3.6 d) shows a rapid increase in activity caused by the short half-life of its parent. After reaching $T_{max}$ in approximately 40 hours, the $^{212}Po$ (daughter) came to secular equilibrium with $^{224}Ra$ (parent), and the decay curve was parallel with its parent.

Therefore, the antilog of the projection of the linear regression of $^{212}Po$ decay curve, between $T_{max}$ and 700 hours to t=0, in which radium was separated from the liquid phase sample, determined the activity of pure $^{224}Ra$ (Table 8.3).

From Tables 8.1 to 8.10, the activity of $^{223}Ra$ (5.71 MeV) and $^{224}Ra$ (5.68 MeV), as unresolveable twin peaks, was determined from the first data obtained before too much $^{222}Rn$ and other daughter isotopes interfered with the twin peaks.

By subtracting the activity of the determined $^{224}Ra$ from the corrected twin peaks of $^{223}Ra$ and $^{224}Ra$, the activity of $^{223}Ra$ was obtained. The same routine was carried out for RDE-2 and RDE-3 samples to obtain the activities of $^{223}Ra$ and $^{224}Ra$.

Compiled data for RDE-1, RDE-2 and RDE-3 are shown in Table 8.11. The activities of $^{223}Ra$ and $^{224}Ra$ are arranged as a function of time after liquid phase separation from the solid.

Using Equation 2, (Chapter 2.2.2), $^{227}Th$ and $^{228}Th$ can be calculated as follows:

$$N_2 = \frac{\lambda_1}{\lambda_2 - \lambda_1} N_1^0 \left(e^{-\lambda_1 t} - e^{-\lambda_2 t}\right) + N_2^0 e^{-\lambda_2 t} \qquad \text{Eq 2}$$

where, $N_1$ = number of parent atoms, $N_2$ = number of daughter atoms. Since, $N = \frac{A}{\lambda}$, where $A_1$ is the activity of the parent and $A_2$ is the activity of the daughter, we have:

$$\frac{A_2}{\lambda_2} = \frac{\lambda_1}{\lambda_2 - \lambda_1}\left(\frac{A_1{}^0}{\lambda_1}\right)\left(e^{-\lambda_1 t} - e^{-\lambda_2 t}\right) + \left(\frac{A_1{}^0}{\lambda_2}\right) e^{-\lambda_2 t}$$

By multiplying it with $\lambda_2 e^{\lambda_2 t}$, the above equation becomes:

$$A_2 e^{\lambda_2 t} = \frac{\lambda_2}{\lambda_2 - \lambda_1} A_1{}^0\left(e^{(\lambda_2 - \lambda_1)t} - 1\right) + A_2{}^0$$

A plot of:

$$A_2 e^{\lambda_2 t} \text{ vs. } \frac{\lambda_2}{\lambda_2 - \lambda_1}\left(e^{(\lambda_2 - \lambda_1)t} - 1\right)$$

will be linear with slope $A_1{}^0$ and intercept $A_2{}^0$, where $A_1{}^0$ and $A_2{}^0$ are the activities of parent and daughter isotopes at time t = 0, when the liquid phase was separated from the solid, respectively.

Table 8.11 displays the calculated results for $^{227}Th$, $^{223}Ra$, $^{228}Th$ and $^{224}Ra$. The ratio of daughter/parent activities was calculated as follows:

$$\frac{^{224}Ra}{^{228}Th} = \frac{50\ (Bq/L)}{338\ (Bq/L)} = 0.148, \text{ and}$$

$$\frac{^{223}Ra}{^{227}Th} = \frac{50\ (Bq/L)}{690\ (Bq/L)} = 0.073$$

It can be seen from these ratios that the daughter/parent isotopes, $^{223}Ra/^{227}Th$ and $^{224}Ra/^{228}Th$ are not in equilibrium, and yet it was expected that they should be, since the sample had been stored for two years without any of the liquid phase being removed. Thus the type of secular disequilibrium observed here can also be classified as paradoxical.

It is also important to mention here that, because of the dynamic growth of $^{223}Ra$ (11.7 d), and $^{224}Ra$ (3.6 d), and the dynamic decay of $^{227}Th$ (18.2 d), and $^{228}Th$ (1.98 y), secular equilibrium is reached in the sample container within days after the liquid phase separation. Consequently the timing sequence for sampling and geochemical mechanism is assuming an important role in the field study (see Table 8.11).

For the sampling technique of the future, the timing sequence should be included in the design to synchronize the the time required for field sampling with the time needed to analyze the short-lived radionuclides in either solid or liquid phase samples before secular equilibrium is reached in

the isolated sample container.

Liquid or solid samples that have been stored for too long (years) might lose their integrity as a tool for hydrogeochemical evolution study of radioisotope species as most short-lived radioisotopes would have reached their secular equilibrium. It would then be impossible to evaluate the condition of the sample or the formation of these radioisotopes in the tailings pile at the time of sampling.

## 8.4 APPLICATION TO RADIOISOTOPES IN A GROUNDWATER SPRING

Based on the above data and experiment, a similar mechanism can also be applied to the enrichment of some radioisotopes from the sample obtained from an active groundwater spring, as the spring water can be classified as liquid extraction from the main bulk mass of the geological formation. This can be explained by evaluating the previous experimental data.

For example, as shown in Table 8.11, $^{228}Th$ at the time of liquid separation had an activity of 338 $\pm$ 8 Bq/L, and $^{224}Ra$ activity was only 50 $\pm$ 80 Bq/L. After it had been stored in the bottle for T = 390 hours, the $^{224}Ra$ activity grew and reached 320.7 Bq/L. This could only be explained by the fact that, in isolation, the Ra-224 isotope which grew from its parent $^{228}Th$ did not have the solid phase to attach to, adsorb to, or coprecipitate with, and probably did not have the right condition to precipitate. (In this case hydrochloric acid was added to prevent it precipitating.)

Therefore, in the natural groundwater spring, a particular daughter isotope can grow from its parent with time and distance from the source, and reflect an enrichment, or increase in activity ratio, between daughter/parent in combination with geochemical effects (1,5-14,22-26).

The important role of the radon species in radioisotope disequilibrium should be noted in this thesis, especially as radon gas is classified as an

inert gas. Inert gases do not react with other chemical species and remain static in the liquid phase as dissolved gas.

Fleischer (Figure 1, (60)), discussed the mechanism of $^{222}Ra$ release from solids, which is an ejection of $^{222}Rn$ into the liquid phase, especially in the saturation zone, due to alpha-recoil as $^{226}Ra$ decays.

The dissolved $^{222}Rn$, which is highly mobile, moves with the liquid phase at the same velocity downward in the tailings pile, and is the main cause of enrichment of $^{210}Pb$ in the liquid phase at T-3 site, as observed by Dalton (40).

In the groundwater spring, the dissolved radon concentration is expected to be very high in comparison with its parent, the radium species. With time and distance, because of the agitation and turbulence as the spring water flows away from the source, the radon gas escapes into the air. Therefore, this again causes separation of gas from the liquid phase and may result in rapid decreases of $^{210}Pb$ with time and distance from the source.

Unpublished data from an artesian spring water sample from a nearby Elliot Lake area (April 1978), showed $^{222}Rn$ concentrations of 421 pCi/L (15.6 Bq/L), and $^{226}Ra$ concentrations as high as 65 pCi/L (2.4 Bq/L).

The $^{222}Rn$ measurement could be approximately 20 times lower than expected as the spring water was sampled directly from the mouth of the spring where there was a lot of turbulence and gas bubbles escaping into the air before the sample bottle could be closed. Other measurements carried out by the Ontario Ministry of the Environment, between 1978 and 1982, from the same well, showed values of 10,000 to 12,000 pCi/L.

Hess et al. (61) reported concentration values for Rn-222 of up to 30,000 pCi/L (1,110 Bq/L) in the United States.

The follow-up study on this particular artesian well near Elliot Lake, where it was believed to be located on the borderline of low grade

uranium ore, was never carried out.

However, based on the cell model by Morin (30), assuming a one cubic meter cell of tailings with 45% porosity and grain density of 2.7 g/mL, and an average $^{226}Ra$ concentration of 300 pCi/g (11.1 Bq/g), the partition of solid and void space are 450 litres void and 550 litres solid. Thus, the total solid mass is 1,485 kg, and the total $^{226}Ra$ available in the solid mass is 445.5 x $10^6$ pCi (16.5 x $10^6$ Bq).

If the void space is saturated with water, and if the $^{226}Ra$ and $^{222}Rn$ are in secular equilibrium and homogeneously mixed, then the concentration of $^{222}Rn$ in the steady state water phase can be expected to be as high as (total available $^{222}Rn$ in secular equilibrium with $^{226}Ra$/the volume of void space =) 0.99 x $10^6$ pCi/L, or 36,630 Bq/L.

Under dynamic conditions, where the liquid phase is always being replaced (depending on the flow rate), and taking into consideration that some of the $^{222}Rn$ will be absorbed by the solid, secular disequilibrium is anticipated, and therefore, lower concentration than 0.99 x $10^6$ pCi/L is expected.

In the rock formation, the porosity and permeability of the rock may be less than in the tailings material, however, the magnitude of the radon release will not differ much, varying only between 400 x $10^6$ pCi/L to 0.99 x $10^6$ pCi/L.

## 8.5 CONCLUSIONS AND RECOMMENDATIONS

It is clear from the laboratory experiment described above that the timing of sampling and analytical techniques for the investigation of disequilibrium phenomena is critically important. Broad assumptions concerning equilibrium states for radioisotopes in an apparently isolated system must be carefully examined. Factors which can affect the accuracy of

isotope measurements and models, as seen in the laboratory experiment, include:

1. Careful sampling, sample preservation and preparation.
2. Planning for timing sequences starting with
   - liquid phase separation;
   - radium-species separation; and
   - time interval in alpha-counting.
3. The use of a good high resolution alpha-spectroscopy system is essential to obtain a clear spectrum separation of the radium species and its daughters.
4. The limited time shelf-life of a stored sample.

In Table 8.11, when the initial $^{223}Ra$ and $^{224}Ra$ peaks were counted, a large statistical error was observed caused by technical difficulties during alpha-counting, when a timing error occurred from vacuum breakdown at a critical moment resulting in twin peaks.

For the future analyses of radium species and their daughters it is recommended that the high resolution alpha-spectroscopy should be combined with a convoluted software program to evaluate complex alpha-spectra with greater accuracy, and to eliminate doubt in separating twin peaks. The thorium species could be analyzed directly as mentioned in Chapter 6.4 and compared with the method described in Chapter 8.2 for greater precision and accuracy.

Table 8.1 - Radioisotope disequilibrium experimental data, RDE-1.

RAW DATA

| # | REMARK CHN.FROM-TO | TIME (Hrs.) FROM T=0 | Ra-226 790-970 | Ra-(223+224) 981-1161 | Po-215 1394-1494 | Po-214 1496-1578 | Po-212 1660-1840 |
|---|---|---|---|---|---|---|---|
| | # MeV.FROM-TO | | 4.03-4.91 | 4.97-5.85 | 6.98-7.47 | 7.48-7.88 | 8.28-9.16 |
| 1 | PROBE 1 | 1.83 | 4381 | 34147 | 2073 | 45 | 1403 |
| 2 | | 100.08 | 3525 | 18147 | 1796 | 1131 | 8178 |
| 3 | t(collect sample): | 148.00 | 3450 | 13537 | 1627 | 1522 | 6279 |
| 4 | 10:00, Oct. 7,1987 | 174.33 | 3286 | 11945 | 1548 | 1494 | 4747 |
| 5 | t(separation): | 241.83 | 3158 | 8587 | 1379 | 1841 | 2778 |
| 6 | 10:50, Oct. 9,1987 | 291.83 | 3103 | 7435 | 1373 | 2058 | 1959 |
| 7 | | 311.58 | 2996 | 5909 | 1075 | 1924 | 1442 |
| 8 | pH: 2.0 | 484.33 | 3050 | 4449 | 930 | 2184 | 1085 |
| 9 | Eh: +434.2 mV | 676.03 | 2761 | 3448 | 637 | 2059 | 140 |
| 10 | Ec: 15650 | 1180.03 | 2670 | 3001 | 396 | 2113 | 25 |
| 11 | temp: 68.9 F | 1185.13 | 2660 | 3045 | 393 | 2082 | 28 |
| 12 | BA-133 RECOVERY: | 1186.98 | 2611 | 3009 | 344 | 2096 | 19 |
| 13 | 67.21% | 1212.85 | 2779 | 3071 | 404 | 2133 | 22 |
| 14 | | 1190.72 | 2690 | 2991 | 372 | 2036 | 19 |
| 15 | | 1192.58 | 2651 | 3064 | 386 | 2122 | 18 |
| 16 | | 1194.45 | 2584 | 3032 | 382 | 2087 | 21 |
| 17 | | 1196.30 | 2627 | 2986 | 414 | 2062 | 19 |
| 18 | | 1198.17 | 2666 | 3020 | 384 | 2082 | 13 |
| 19 | | 1200.02 | 2664 | 2988 | 376 | 2169 | 18 |
| 20 | | 1201.88 | 2655 | 2997 | 395 | 2135 | 21 |
| 21 | | 1203.75 | 2664 | 2929 | 350 | 2080 | 20 |
| 22 | | 1205.60 | 2798 | 2918 | 339 | 2065 | 20 |
| 23 | | 1207.47 | 2749 | 2964 | 386 | 2103 | 17 |
| 24 | | 1209.33 | 2521 | 2955 | 360 | 2111 | 22 |
| 25 | | 1211.20 | 2742 | 3060 | 366 | 2126 | 13 |
| 26 | | 1213.07 | 2747 | 3037 | 370 | 2079 | 21 |
| 27 | | 1214.93 | 2634 | 2921 | 375 | 2088 | 15 |
| 28 | | 1216.82 | 2610 | 3056 | 358 | 2068 | 25 |
| 29 | | 1218.68 | 2715 | 2991 | 367 | 2052 | 16 |
| 30 | | 1220.55 | 2591 | 3036 | 410 | 2106 | 12 |
| 31 | | 1222.40 | 2758 | 3027 | 388 | 2081 | 21 |
| 32 | | 1224.27 | 2636 | 2998 | 399 | 2121 | 22 |
| 33 | | 1226.12 | 2759 | 3007 | 405 | 2105 | 26 |
| 34 | | 1227.98 | 2707 | 3061 | 390 | 2115 | 24 |
| 35 | | 1229.83 | 2671 | 3085 | 433 | 2055 | 15 |

Table 8.2 - Radioisotope disequilibrium experimental data, RDE-1. Processed data $\ln(A_{ic})$, derived from Table 8.1, where $A_{ic} = A_i \times (100\%/\%\ ^{133}Ba\ \text{recovery})$.

PROCESSED DATA

| # | REMARK CHN.FROM-TO | TIME (Hrs.) FROM T=0 | Ra-226 2848-3028 | Ra-(223+224) 3039-3219 | Po-215 3452-3552 | Po-214 3554-3638 | Po-212 3718-3898 |
|---|---|---|---|---|---|---|---|
| # | MeV.FROM-TO | | 4.03-4.91 | 4.97-5.85 | 6.98-7.47 | 7.48-7.88 | 8.28-9.16 |
| 1 | PROBE 1 | 1.83 | 8.78 | 10.84 | 8.03 | 4.20 | 8.09 |
| 2 | | 100.08 | 8.57 | 10.20 | 7.89 | 7.43 | 9.85 |
| 3 | t(collect sample): | 148.00 | 8.54 | 9.91 | 7.79 | 7.73 | 9.59 |
| 4 | 10:00, Oct. 7,1987 | 174.33 | 8.49 | 9.79 | 7.74 | 7.71 | 9.31 |
| 5 | t(separation): | 241.83 | 8.46 | 9.46 | 7.63 | 7.92 | 8.77 |
| 6 | 10:50, Oct. 9,1987 | 291.83 | 8.44 | 9.31 | 7.62 | 8.03 | 8.42 |
| 7 | | 311.58 | 8.40 | 9.08 | 7.38 | 7.96 | 8.12 |
| 8 | pH: 2.0 | 484.33 | 8.42 | 8.80 | 7.23 | 8.09 | 7.83 |
| 9 | Eh: +434.2 mV | 676.03 | 8.32 | 8.54 | 6.85 | 8.03 | 5.79 |
| 10 | Ec: 15650 | 1180.03 | 8.29 | 8.40 | 6.38 | 8.05 | 4.06 |
| 11 | temp: 68.9 F | 1185.13 | 8.28 | 8.42 | 6.37 | 8.04 | 4.18 |
| 12 | BA-133 RECOVERY: | 1186.98 | 8.26 | 8.41 | 6.24 | 8.05 | 3.79 |
| 13 | 67.21% | 1212.85 | 8.33 | 8.43 | 6.40 | 8.06 | 3.93 |
| 14 | | 1190.72 | 8.29 | 8.40 | 6.32 | 8.02 | 3.79 |
| 15 | | 1192.58 | 8.28 | 8.42 | 6.35 | 8.06 | 3.73 |
| 16 | | 1194.45 | 8.25 | 8.41 | 6.34 | 8.04 | 3.89 |
| 17 | | 1196.30 | 8.27 | 8.40 | 6.42 | 8.03 | 3.79 |
| 18 | | 1198.17 | 8.29 | 8.41 | 6.35 | 8.04 | 3.41 |
| 19 | | 1200.02 | 8.28 | 8.40 | 6.33 | 8.08 | 3.73 |
| 20 | | 1201.88 | 8.28 | 8.40 | 6.38 | 8.06 | 3.89 |
| 21 | | 1203.75 | 8.28 | 8.38 | 6.26 | 8.04 | 3.84 |
| 22 | | 1205.60 | 8.33 | 8.38 | 6.22 | 8.03 | 3.84 |
| 23 | | 1207.47 | 8.32 | 8.39 | 6.35 | 8.05 | 3.68 |
| 24 | | 1209.33 | 8.23 | 8.39 | 6.28 | 8.05 | 3.93 |
| 25 | | 1211.20 | 8.31 | 8.42 | 6.30 | 8.06 | 3.41 |
| 26 | | 1213.07 | 8.32 | 8.42 | 6.31 | 8.04 | 3.89 |
| 27 | | 1214.93 | 8.27 | 8.38 | 6.32 | 8.04 | 3.55 |
| 28 | | 1216.82 | 8.26 | 8.42 | 6.28 | 8.03 | 4.06 |
| 29 | | 1218.68 | 8.30 | 8.40 | 6.30 | 8.02 | 3.62 |
| 30 | | 1220.55 | 8.26 | 8.42 | 6.41 | 8.05 | 3.33 |
| 31 | | 1222.40 | 8.32 | 8.41 | 6.36 | 8.04 | 3.89 |
| 32 | | 1224.27 | 8.27 | 8.40 | 6.39 | 8.06 | 3.93 |
| 33 | | 1226.12 | 8.32 | 8.41 | 6.40 | 8.05 | 4.10 |
| 34 | | 1227.98 | 8.30 | 8.42 | 6.36 | 8.05 | 4.02 |
| 35 | | 1229.83 | 8.29 | 8.43 | 6.47 | 8.03 | 3.55 |

Table 8.3 - Linear regression data, RDE-1.
Evaluation for $^{226}Ra$, $^{223}Ra$ and $^{224}Ra$.

| REGRESSION DATA AND FINAL COUNTS FOR T=0 | Linear regression of ln ($^{212}Po$) at 100% yield |
|---|---|
| **Regression Output:** | |
| Constant | 10.09 |
| Std Err of Y Est | 0.26 |
| R Squared | 0.98 |
| No. of Observations | 34 |
| Degrees of Freedom | 32 |
| X Coefficient(s) | -0.00522 |
| Std Err of Coef. | 0.000115 |
| Ra-226 (100% Recovery): | 3974 |
| Ra-224 (100% Recovery): | 24159 |
| Ra-223 (100% Recovery): | 26650 |

$^{226}Ra$ (100% recovery) was obtained from the last $^{226}Ra$ raw data after t = 1000 hours, and corrected using $^{133}Ba$ recovery to a 100% yield.

$^{224}Ra$ (100% recovery) was obtained by means of linear regression interpolation of antilog ln A($^{212}Po$) at t=0.

$^{223}Ra$ (100% recovery) was obtained by means of subtracting the activity A($^{224}Ra$) at 100% yield from the first data of A($^{233}Ra$ + $^{224}Ra$) at 100% yield at t=0.

Table 8.4 - Radioisotope disequilibrium experimental data, RDE-2

RAW DATA

| RDE | REMARK CHN.FROM-TO | TIME (Hrs.) FROM T=0 | Ra-226 790-970 | Ra-(223+224) 981-1161 | Po-215 1394-1494 | Po-214 1496-1578 | Po-212 1660-1840 |
|---|---|---|---|---|---|---|---|
| | MeV.FROM-TO | | 4.03-4.91 | 4.97-5.85 | 6.98-7.47 | 7.48-7.88 | 8.28-9.16 |
| 1 | PROBE 1 | 1.83 | 5007 | 65295 | 4422 | 61 | 1943 |
| 2 | 1987 10 14 - 16:20 | 18.08 | 5182 | 63524 | 4687 | 535 | 21799 |
| 3 | | 41.92 | 4971 | 52933 | 4354 | 768 | 25060 |
| 4 | pH: 2.0 | 113.92 | 3976 | 31425 | 3545 | 1247 | 15082 |
| 5 | | 163.33 | 3765 | 22959 | 3373 | 1767 | 10306 |
| 6 | Eh: +434.2 mV | 377.83 | 3002 | 7828 | 2000 | 1919 | 2242 |
| 7 | | 721.00 | 2655 | 3471 | 952 | 1931 | 156 |
| 8 | | 786.45 | 2704 | 3585 | 861 | 2019 | 88 |
| 9 | Ec: 15650 | 1050.02 | 2717 | 3044 | 557 | 2006 | 46 |

ln $A_{ic}$ versus time

PROCESSED DATA

| RDE | REMARK CHN.FROM-TO | TIME (Hrs.) FROM T=0 | Ra-226 2848-3028 | Ra-(223+224) 3039-3219 | Po-215 3452-3552 | Po-214 3554-3638 | Po-212 3718-3898 |
|---|---|---|---|---|---|---|---|
| | MeV.FROM-TO | | 4.03-4.91 | 4.97-5.85 | 6.98-7.47 | 7.48-7.88 | 8.28-9.16 |
| 1 | PROBE 1 | 1.83 | 8.91 | 11.48 | 8.78 | 4.50 | 8.41 |
| 2 | 1987 10 14 - 16:20 | 18.08 | 8.94 | 11.45 | 8.84 | 6.67 | 10.82 |
| 3 | | 41.92 | 8.90 | 11.27 | 8.77 | 7.03 | 10.96 |
| 4 | pH: 2.0 | 113.92 | 8.68 | 10.74 | 8.56 | 7.52 | 10.46 |
| 5 | | 163.33 | 8.62 | 10.43 | 8.51 | 7.87 | 10.08 |
| 6 | Eh: +434.2 mV | 377.83 | 8.40 | 9.35 | 7.99 | 7.95 | 8.55 |
| 7 | | 721.00 | 8.27 | 8.54 | 7.25 | 7.95 | 5.88 |
| 8 | | 786.45 | 8.29 | 8.57 | 7.15 | 8.00 | 5.31 |
| 9 | Ec: 15650 | 1050.02 | 8.30 | 8.41 | 6.71 | 7.99 | 4.66 |

where $A_{ic} = A_i \times (100\%/\%\ ^{133}Ba \text{ recovery})$

Table 8.5 - Linear regression data, RDE-2.
Evaluation for $^{226}Ra$, $^{223}Ra$ and $^{224}Ra$

| REGRESSION DATA AND FINAL COUNTS FOR T=0 | Linear regression of ln ($^{212}Po$) at 100% yield |
|---|---|
| **Regression Output:** | |
| Constant | 11.32 |
| Std Err of Y Est | 0.06 |
| R Squared | 1.00 |
| No. of Observations | 6 |
| Degrees of Freedom | 4 |
| X Coefficient(s) | -0.00756 |
| Std Err of Coef. | 0.000080 |
| Ra-226 (100% Recovery): | 4008 |
| Ra-224 (100% Recovery): | 82562 |
| Ra-223 (100% Recovery): | 13767 |

$^{226}Ra$ (100% recovery) was obtained from the last $^{226}Ra$ raw data after t = 1000 hours, and corrected using $^{133}Ba$ recovery to a 100% yield.

$^{224}Ra$ (100% recovery) was obtained by means of linear regression interpolation of antilog ln A($^{212}Po$) at t=0.

$^{223}Ra$ (100% recovery) was obtained by means of subtracting the activity A($^{224}Ra$) at 100% yield from the first data of A($^{223}Ra$ + $^{224}Ra$) at 100% yield at t=0.

Table 8.6 - Radioisotope disequilibrium experimental data, RDE-3.

| | | | RAW DATA | | | | |
|---|---|---|---|---|---|---|---|
| # | REMARK<br>CHN.FROM-TO | TIME (Hrs.)<br>FROM T=0 | Ra-226<br>2848-3028 | Ra-(223+224)<br>3039-3219 | Po-215<br>3452-3552 | Po-214<br>3554-3638 | Po-212<br>3718-3898 |
| | MeV.FROM-TO | | 4.03-4.91 | 4.97-5.85 | 6.98-7.47 | 7.48-7.88 | 8.28-9.16 |
| 1 | PROBE #1 | 1.67 | 8505 | 87994 | 6616 | 234 | 2704 |
| 2 | | 3.53 | 8567 | 88322 | 6691 | 331 | 6458 |
| 3 | | 5.38 | 8646 | 86239 | 6718 | 387 | 10194 |
| 4 | | 7.23 | 8685 | 86230 | 6795 | 490 | 13453 |
| 5 | 16:00 87,10,23 | 9.08 | 8746 | 85454 | 6732 | 589 | 16420 |
| 6 | 23 Oct 87 | 10.95 | 8707 | 84868 | 6815 | 650 | 19111 |
| 7 | | 12.80 | 8622 | 82911 | 6700 | 737 | 21455 |
| 8 | | 14.65 | 8561 | 82610 | 6777 | 828 | 23412 |
| 9 | | 16.50 | 8353 | 81956 | 6874 | 917 | 25075 |
| 10 | | 18.35 | 8538 | 81028 | 6661 | 970 | 26704 |
| 11 | Sample: | 20.22 | 8413 | 80036 | 6648 | 978 | 27684 |
| 12 | RAMIXPR1 | 22.07 | 8297 | 79708 | 6778 | 992 | 28517 |
| 13 | TRIAL 1 | 23.92 | 8225 | 78616 | 6700 | 1070 | 29672 |
| 14 | | 25.77 | 8410 | 76974 | 6608 | 1096 | 29748 |
| 15 | time of separation: | 27.63 | 8062 | 75720 | 6637 | 1143 | 30212 |
| 16 | 15:50 | 29.48 | 7994 | 74965 | 6643 | 1179 | 31014 |
| 17 | | 31.33 | 8087 | 73773 | 6531 | 1150 | 30973 |
| 18 | pH: 2.0 | 33.18 | 7935 | 73350 | 6376 | 1291 | 31462 |
| 19 | Eh: +434.2 mV | 35.05 | 7892 | 71836 | 6431 | 1263 | 31256 |
| 20 | Ec: 15650 | 36.90 | 7897 | 71094 | 6545 | 1298 | 31264 |
| 21 | temp: 68.9 F | 38.75 | 7643 | 69908 | 6363 | 1303 | 31791 |
| 22 | Ba-133 RECOVERY | 40.60 | 7727 | 69605 | 6353 | 1360 | 31749 |
| 23 | 68.78% | 42.45 | 7608 | 68845 | 6297 | 1330 | 31486 |
| 24 | | 44.32 | 7766 | 68479 | 6479 | 1316 | 31023 |
| 25 | | 46.17 | 7557 | 67400 | 6320 | 1366 | 31138 |
| 26 | | 48.02 | 7407 | 66525 | 6265 | 1373 | 30525 |
| 27 | | 49.87 | 7486 | 65869 | 6356 | 1378 | 30791 |
| 28 | | 51.73 | 7562 | 65089 | 6176 | 1390 | 31004 |
| 29 | | 53.58 | 7414 | 64513 | 6224 | 1476 | 30638 |
| 30 | | 55.43 | 7226 | 63612 | 6345 | 1456 | 30028 |
| 31 | | 73.75 | 6803 | 55670 | 5891 | 1525 | 26603 |
| 32 | | 75.62 | 6743 | 55185 | 5869 | 1522 | 26779 |
| 33 | | 77.47 | 6853 | 54752 | 5905 | 1567 | 26261 |
| 34 | | 79.32 | 6614 | 53488 | 6040 | 1477 | 25897 |
| 35 | | 81.17 | 6560 | 52253 | 5694 | 1524 | 24827 |
| 36 | | 83.03 | 6369 | 51960 | 5786 | 1616 | 24576 |
| 37 | | 84.88 | 6442 | 51137 | 5702 | 1567 | 24520 |
| 38 | | 86.75 | 6333 | 50671 | 5657 | 1601 | 24278 |
| 39 | | 88.60 | 6404 | 50963 | 5733 | 1617 | 24082 |
| 40 | | 90.45 | 6442 | 50008 | 5724 | 1609 | 23676 |
| 41 | | 96.58 | 6269 | 48151 | 5566 | 1606 | 22666 |
| 42 | | 98.43 | 6202 | 47823 | 5690 | 1656 | 22250 |
| 43 | | 100.30 | 6165 | 46715 | 5534 | 1700 | 21953 |
| 44 | | 102.15 | 6091 | 46193 | 5653 | 1824 | 21838 |
| 45 | | 104.00 | 5980 | 45437 | 5494 | 1643 | 21088 |

Table 8.7 - Radioisotope disequilibrium experimental data, RDE-3.

| # | REMARK CHN.FROM-TO | TIME (Hrs.) FROM T=0 | RAW DATA Ra-226 2848-3028 | Ra-(223+224) 3039-3219 | Po-215 3452-3552 | Po-214 3554-3638 | Po-212 3718-3898 |
|---|---|---|---|---|---|---|---|
| | MeV.FROM-TO | | 4.03-4.91 | 4.97-5.85 | 6.98-7.47 | 7.48-7.88 | 8.28-9.16 |
| 46 | | 105.87 | 5919 | 44426 | 5666 | 1729 | 20892 |
| 47 | | 107.72 | 5906 | 44087 | 5455 | 1702 | 20767 |
| 48 | | 109.57 | 5916 | 44340 | 5487 | 1737 | 20428 |
| 49 | | 111.42 | 6071 | 43520 | 5514 | 1674 | 20173 |
| 50 | | 113.28 | 5894 | 43261 | 5603 | 1732 | 19979 |
| 51 | | 673.98 | 2834 | 3763 | 1394 | 1503 | 294 |
| 52 | | 675.83 | 2899 | 3769 | 1441 | 1486 | 252 |
| 53 | | 677.68 | 2947 | 3798 | 1328 | 1526 | 279 |
| 54 | | 679.70 | 2962 | 3806 | 1351 | 1565 | 254 |
| 55 | | 681.38 | 2814 | 3667 | 1283 | 1638 | 270 |
| 56 | | 683.25 | 2823 | 3869 | 1364 | 1571 | 250 |
| 57 | | 685.10 | 2985 | 3634 | 1283 | 1617 | 220 |
| 58 | | 686.95 | 2934 | 3755 | 1289 | 1587 | 243 |
| 59 | | 688.80 | 2937 | 3727 | 1328 | 1611 | 285 |
| 60 | | 690.65 | 2955 | 3622 | 1302 | 1618 | 210 |
| 61 | | 692.50 | 2944 | 3843 | 1269 | 1651 | 223 |
| 62 | | 694.37 | 2999 | 3881 | 1271 | 1607 | 207 |
| 63 | | 696.22 | 2916 | 3769 | 1299 | 1654 | 176 |
| 64 | | 698.07 | 2878 | 3712 | 1229 | 1609 | 201 |
| 65 | | 699.92 | 2911 | 3798 | 1279 | 1572 | 199 |
| 66 | | 701.77 | 2986 | 3845 | 1249 | 1750 | 205 |
| 67 | | 703.63 | 3016 | 3813 | 1258 | 1717 | 223 |
| 68 | | 705.48 | 2863 | 3726 | 1243 | 1698 | 206 |
| 69 | | 707.33 | 2835 | 3707 | 1230 | 1683 | 209 |
| 70 | | 709.18 | 3964 | 3737 | 1285 | 1736 | 193 |
| 71 | | 711.03 | 2980 | 3668 | 1208 | 1721 | 211 |
| 72 | | 712.88 | 2882 | 3809 | 1231 | 1753 | 164 |
| 73 | | 714.75 | 2897 | 3730 | 1242 | 1670 | 174 |
| 74 | | 716.60 | 2938 | 3863 | 1274 | 1732 | 165 |
| 75 | | 718.45 | 2896 | 3788 | 1255 | 1731 | 185 |
| 76 | | 720.57 | 2945 | 3730 | 1193 | 1725 | 179 |
| 77 | | 722.15 | 2874 | 3919 | 1246 | 1719 | 175 |
| 78 | | 724.02 | 2892 | 3882 | 1246 | 1725 | 170 |
| 79 | | 725.87 | 3013 | 3909 | 1243 | 1793 | 171 |
| 80 | | 727.72 | 2867 | 3859 | 1282 | 1742 | 179 |
| 81 | | 761.20 | 3142 | 3744 | 1272 | 1667 | 152 |
| 82 | | 1085.48 | 2996 | 2964 | 687 | 1780 | 48 |
| 83 | | 1087.35 | 3023 | 2943 | 675 | 1701 | 46 |
| 84 | | 1089.20 | 2991 | 3025 | 703 | 1659 | 54 |
| 85 | | 1091.07 | 2924 | 3054 | 697 | 1720 | 38 |
| 86 | | 1092.92 | 3017 | 3167 | 702 | 1738 | 42 |
| 87 | | 1483.92 | 2890 | 2634 | 411 | 1628 | 81 |
| 88 | | 1485.65 | 2832 | 2648 | 411 | 1565 | 95 |
| 89 | | 1487.58 | 2954 | 2663 | 431 | 1601 | 81 |
| 90 | | 1489.50 | 2933 | 2626 | 398 | 1607 | 69 |

Table 8.8 - Radioisotope disequilibrium experimental data, RDE-3.

PROCESSED DATA

| # | REMARK | TIME (Hrs.) | Ra-226 | Ra-(223+224) | Po-215 | Po-214 | Po-212 |
|---|---|---|---|---|---|---|---|
| | CHN.FROM-TO | FROM T=0 | 2848-3028 | 3039-3219 | 3452-3552 | 3554-3638 | 3718-3898 |
| | MeV.FROM-TO | | 4.03-4.91 | 4.97-5.85 | 6.98-7.47 | 7.48-7.88 | 8.28-9.16 |
| 1 | PROBE #1 | 1.67 | 9.42 | 11.76 | 9.17 | 5.83 | 8.72 |
| 2 | | 3.53 | 9.43 | 11.76 | 9.18 | 6.18 | 9.59 |
| 3 | | 5.38 | 9.44 | 11.74 | 9.19 | 6.33 | 10.05 |
| 4 | | 7.23 | 9.44 | 11.74 | 9.20 | 6.57 | 10.33 |
| 5 | 16:00 87,10,23 | 9.08 | 9.45 | 11.73 | 9.19 | 6.75 | 10.53 |
| 6 | 23 Oct 87 | 10.95 | 9.45 | 11.72 | 9.20 | 6.85 | 10.68 |
| 7 | | 12.80 | 9.44 | 11.70 | 9.18 | 6.98 | 10.79 |
| 8 | | 14.65 | 9.43 | 11.70 | 9.20 | 7.09 | 10.88 |
| 9 | | 16.50 | 9.40 | 11.69 | 9.21 | 7.20 | 10.95 |
| 10 | | 18.35 | 9.43 | 11.68 | 9.18 | 7.25 | 11.01 |
| 11 | Sample: | 20.22 | 9.41 | 11.66 | 9.18 | 7.26 | 11.05 |
| 12 | RAMIXPR1 | 22.07 | 9.40 | 11.66 | 9.20 | 7.27 | 11.08 |
| 13 | TRIAL 1 | 23.92 | 9.39 | 11.65 | 9.18 | 7.35 | 11.12 |
| 14 | | 25.77 | 9.41 | 11.63 | 9.17 | 7.37 | 11.12 |
| 15 | time of separation: | 27.63 | 9.37 | 11.61 | 9.17 | 7.42 | 11.14 |
| 16 | 15:50 | 29.48 | 9.36 | 11.60 | 9.18 | 7.45 | 11.16 |
| 17 | | 31.33 | 9.37 | 11.58 | 9.16 | 7.42 | 11.16 |
| 18 | pH: 2.0 | 33.18 | 9.35 | 11.58 | 9.13 | 7.54 | 11.18 |
| 19 | Eh: +434.2 mV | 35.05 | 9.35 | 11.56 | 9.14 | 7.52 | 11.17 |
| 20 | Ec: 15650 | 36.90 | 9.35 | 11.55 | 9.16 | 7.54 | 11.17 |
| 21 | temp: 68.9 F | 38.75 | 9.32 | 11.53 | 9.13 | 7.55 | 11.19 |
| 22 | Ba-133 RECOVERY | 40.60 | 9.33 | 11.52 | 9.13 | 7.59 | 11.19 |
| 23 | 68.78% | 42.45 | 9.31 | 11.51 | 9.12 | 7.57 | 11.18 |
| 24 | | 44.32 | 9.33 | 11.51 | 9.15 | 7.56 | 11.16 |
| 25 | | 46.17 | 9.30 | 11.49 | 9.13 | 7.59 | 11.17 |
| 26 | | 48.02 | 9.28 | 11.48 | 9.12 | 7.60 | 11.15 |
| 27 | | 49.87 | 9.30 | 11.47 | 9.13 | 7.60 | 11.16 |
| 28 | | 51.73 | 9.31 | 11.46 | 9.10 | 7.61 | 11.16 |
| 29 | | 53.58 | 9.29 | 11.45 | 9.11 | 7.67 | 11.15 |
| 30 | | 55.43 | 9.26 | 11.43 | 9.13 | 7.66 | 11.13 |
| 31 | | 73.75 | 9.20 | 11.30 | 9.06 | 7.70 | 11.01 |
| 32 | | 75.62 | 9.19 | 11.29 | 9.05 | 7.70 | 11.02 |
| 33 | | 77.47 | 9.21 | 11.28 | 9.06 | 7.73 | 11.00 |
| 34 | | 79.32 | 9.17 | 11.26 | 9.08 | 7.67 | 10.98 |
| 35 | | 81.17 | 9.16 | 11.24 | 9.02 | 7.70 | 10.94 |
| 36 | | 83.03 | 9.13 | 11.23 | 9.04 | 7.76 | 10.93 |
| 37 | | 84.88 | 9.14 | 11.22 | 9.02 | 7.73 | 10.93 |
| 38 | | 86.75 | 9.13 | 11.21 | 9.01 | 7.75 | 10.92 |
| 39 | | 88.60 | 9.14 | 11.21 | 9.03 | 7.76 | 10.91 |
| 40 | | 90.45 | 9.14 | 11.19 | 9.03 | 7.76 | 10.89 |
| 41 | | 96.58 | 9.12 | 11.16 | 9.00 | 7.76 | 10.85 |
| 42 | | 98.43 | 9.11 | 11.15 | 9.02 | 7.79 | 10.83 |
| 43 | | 100.30 | 9.10 | 11.13 | 8.99 | 7.81 | 10.82 |
| 44 | | 102.15 | 9.09 | 11.11 | 9.01 | 7.88 | 10.81 |
| 45 | | 104.00 | 9.07 | 11.10 | 8.99 | 7.78 | 10.78 |

Processed data $\ln(A_{ic})$, derived from Table 8.6, where $A_{ic} = A_i \times (100\%/\%\ ^{133}Ba \text{ recovery})$.

Table 8.9 - Radioisotope disequilibrium experimental data, RDE-3.

| | | PROCESSED DATA | | | | |
|---|---|---|---|---|---|---|
| # | REMARK<br>CHN.FROM-TO | TIME (Hrs.)<br>FROM T=0 | Ra-226<br>2848-3028 | Ra-(223+224)<br>3039-3219 | Po-215<br>3452-3552 | Po-214<br>3554-3638 | Po-212<br>3718-3898 |
| | MeV.FROM-TO | | 4.03-4.91 | 4.97-5.85 | 6.98-7.47 | 7.48-7.88 | 8.28-9.16 |
| 46 | | 105.87 | 9.06 | 11.08 | 9.02 | 7.83 | 10.77 |
| 47 | | 107.72 | 9.06 | 11.07 | 8.98 | 7.81 | 10.76 |
| 48 | | 109.57 | 9.06 | 11.07 | 8.98 | 7.83 | 10.75 |
| 49 | | 111.42 | 9.09 | 11.06 | 8.99 | 7.80 | 10.73 |
| 50 | | 113.28 | 9.06 | 11.05 | 9.01 | 7.83 | 10.72 |
| 51 | | 673.98 | 8.32 | 8.61 | 7.61 | 7.69 | 6.50 |
| 52 | | 675.83 | 8.35 | 8.61 | 7.65 | 7.68 | 6.35 |
| 53 | | 677.68 | 8.36 | 8.62 | 7.57 | 7.70 | 6.45 |
| 54 | | 679.70 | 8.37 | 8.62 | 7.58 | 7.73 | 6.36 |
| 55 | | 681.38 | 8.32 | 8.58 | 7.53 | 7.78 | 6.42 |
| 56 | | 683.25 | 8.32 | 8.64 | 7.59 | 7.73 | 6.34 |
| 57 | | 685.10 | 8.38 | 8.57 | 7.53 | 7.76 | 6.21 |
| 58 | | 686.95 | 8.36 | 8.61 | 7.54 | 7.74 | 6.31 |
| 59 | | 688.80 | 8.36 | 8.60 | 7.57 | 7.76 | 6.47 |
| 60 | | 690.65 | 8.37 | 8.57 | 7.55 | 7.76 | 6.17 |
| 61 | | 692.50 | 8.36 | 8.63 | 7.52 | 7.78 | 6.23 |
| 62 | | 694.37 | 8.38 | 8.64 | 7.52 | 7.76 | 6.15 |
| 63 | | 696.22 | 8.35 | 8.61 | 7.54 | 7.79 | 5.99 |
| 64 | | 698.07 | 8.34 | 8.59 | 7.49 | 7.76 | 6.12 |
| 65 | | 699.92 | 8.35 | 8.62 | 7.53 | 7.73 | 6.11 |
| 66 | | 701.77 | 8.38 | 8.63 | 7.50 | 7.84 | 6.14 |
| 67 | | 703.63 | 8.39 | 8.62 | 7.51 | 7.82 | 6.23 |
| 68 | | 705.48 | 8.33 | 8.60 | 7.50 | 7.81 | 6.15 |
| 69 | | 707.33 | 8.32 | 8.59 | 7.49 | 7.80 | 6.16 |
| 70 | | 709.18 | 8.46 | 8.60 | 7.53 | 7.83 | 6.08 |
| 71 | | 711.03 | 8.37 | 8.58 | 7.47 | 7.82 | 6.17 |
| 72 | | 712.88 | 8.34 | 8.62 | 7.49 | 7.84 | 5.92 |
| 73 | | 714.75 | 8.35 | 8.60 | 7.50 | 7.79 | 5.98 |
| 74 | | 716.60 | 8.36 | 8.63 | 7.52 | 7.83 | 5.93 |
| 75 | | 718.45 | 8.35 | 8.61 | 7.51 | 7.83 | 6.04 |
| 76 | | 720.57 | 8.36 | 8.60 | 7.46 | 7.83 | 6.01 |
| 77 | | 722.15 | 8.34 | 8.65 | 7.50 | 7.82 | 5.99 |
| 78 | | 724.02 | 8.34 | 8.64 | 7.50 | 7.83 | 5.96 |
| 79 | | 725.87 | 8.39 | 8.65 | 7.50 | 7.87 | 5.96 |
| 80 | | 727.72 | 8.34 | 8.63 | 7.53 | 7.84 | 6.01 |
| 81 | | 761.20 | 8.43 | 8.60 | 7.52 | 7.79 | 5.84 |
| 82 | | 1085.48 | 8.38 | 8.37 | 6.91 | 7.86 | 4.69 |
| 83 | | 1087.35 | 8.39 | 8.36 | 6.89 | 7.81 | 4.65 |
| 84 | | 1089.20 | 8.38 | 8.39 | 6.93 | 7.79 | 4.81 |
| 85 | | 1091.07 | 8.36 | 8.40 | 6.92 | 7.82 | 4.46 |
| 86 | | 1092.92 | 8.39 | 8.43 | 6.93 | 7.83 | 4.56 |
| 87 | | 1483.92 | 8.34 | 8.25 | 6.39 | 7.77 | 5.22 |
| 88 | | 1485.65 | 8.32 | 8.26 | 6.39 | 7.73 | 5.37 |
| 89 | | 1487.58 | 8.37 | 8.26 | 6.44 | 7.75 | 5.22 |
| 90 | | 1489.50 | 8.36 | 8.25 | 6.36 | 7.76 | 5.05 |

Processed data $\ln(A_{ic})$, derived from Table 8.7, where $A_{ic} = A_i$ x (100%/% $^{133}Ba$ recovery).

Table 8.10 - Linear regression data RDE-3.
Evaluation for $^{226}Ra$, $^{223}Ra$ and $^{224}Ra$

| REGRESSION DATA AND FINAL COUNTS FOR T=0 | Linear regression of ln ($^{212}Po$) at 100% yield | |
|---|---|---|
| **Regression Output:** | | |
| Constant | | 11.42 |
| Std Err of Y Est | | 0.34 |
| R Squared | | 0.98 |
| No. of Observations | | 66 |
| Degrees of Freedom | | 64 |
| X Coefficient(s) | -0.00713 | |
| Std Err of Coef. | 0.00012 | |
| Ra-226 (100% Recovery): | | 4375 |
| Ra-224 (100% Recovery): | | 91230 |
| Ra-223 (100% Recovery): | | 36712 |

$^{226}Ra$ (100% recovery) was obtained from the last $^{226}Ra$ raw data after t = 1000 hours, and corrected using $^{133}Ba$ recovery to a 100% yield.

$^{224}Ra$ (100% recovery) was obtained by means of linear regression interpolation of antilog ln A($^{212}Po$) at t=0.

$^{223}Ra$ (100% recovery) was obtained by means of subtracting the activity A($^{224}Ra$) at 100% yield from the first data of A($^{223}Ra$ + $^{224}Ra$) at 100% yield at t=0.

Table 8.11 - Compiled data for RDE-1, RDE-2 and RDE-3. $^{228}Th$, $^{223}Ra$ and $^{224}Ra$ at time 0 were evaluated based on the concentration of $^{223}Ra$ and $^{224}Ra$ observed as a function of time after liquid phase extraction from the solid phase.

| SAMPLE DESCRIPTION | TIME OF LIQUID EXTRACTION FROM SOLID PHASE | TIME OF SEPERATION FOR RADIUM SPECIES | TIME FROM EXTRACTION = (hrs) |
|---|---|---|---|
| RDE-1 | 07-Oct-87 -10 : 0 | 09-Oct-87 -10 :50 | 48.83 |
| RDE-2 | 07-Oct-87 -10 : 0 | 14-Oct-87 -16 :20 | 174.33 |
| RDE-3 | 07-Oct-87 -10 : 0 | 23-Oct-87 -16 : 0 | 390.00 |

| SAMPLE DESCRIPTION | COUNTS AT 100% RECOVERY | | | CONTENT (pCi/L) | | | CONTENT (mBq/L) | | |
|---|---|---|---|---|---|---|---|---|---|
| | RA-226 | Ra-224 | Ra-223 | Ra-226 | Ra-224 | Ra-223 | Ra-226 | Ra-224 | Ra-223 |
| RDE-1 | 3974 | 24159 | 26650 | 378 | 2295 | 2532 | 13970 | 84930 | 93684 |
| RDE-2 | 4008 | 82562 | 13766 | 381 | 7844 | 1308 | 14090 | 290242 | 48394 |
| RDE-3 | 4375 | 91230 | 36712 | 416 | 8668 | 3488 | 15380 | 320714 | 129059 |

| | |
|---|---|
| Ra-223 CONTENT AT LIQUID SEPARATION FROM SOLID PHASE (Bq/L) : | 50 +/- 80 |
| Th-227 CONTENT AT LIQUID SEPARATION FROM SOLID PHASE (Bq/L) : | 690 +/- 100 |
| Ra-224 CONTENT AT LIQUID SEPARATION FROM SOLID PHASE (Bq/L) : | 50 +/- 130 |
| Th-228 CONTENT AT LIQUID SEPARATION FROM SOLID PHASE (Bq/L) : | 338 +/- 8 |

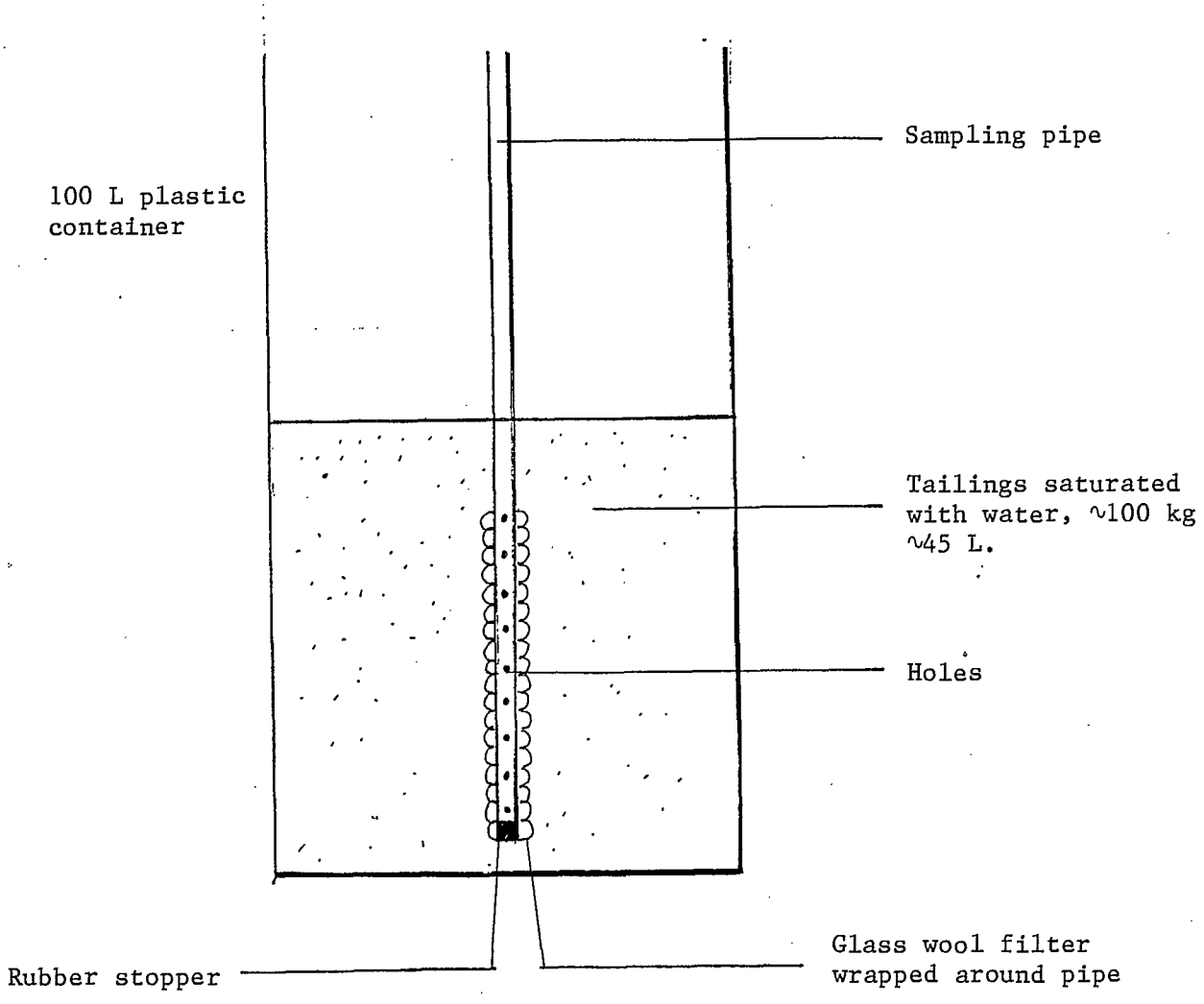


Fig. 8.1 - Laboratory experimental design for testing paradoxical secular disequilibrium in uranium tailings.

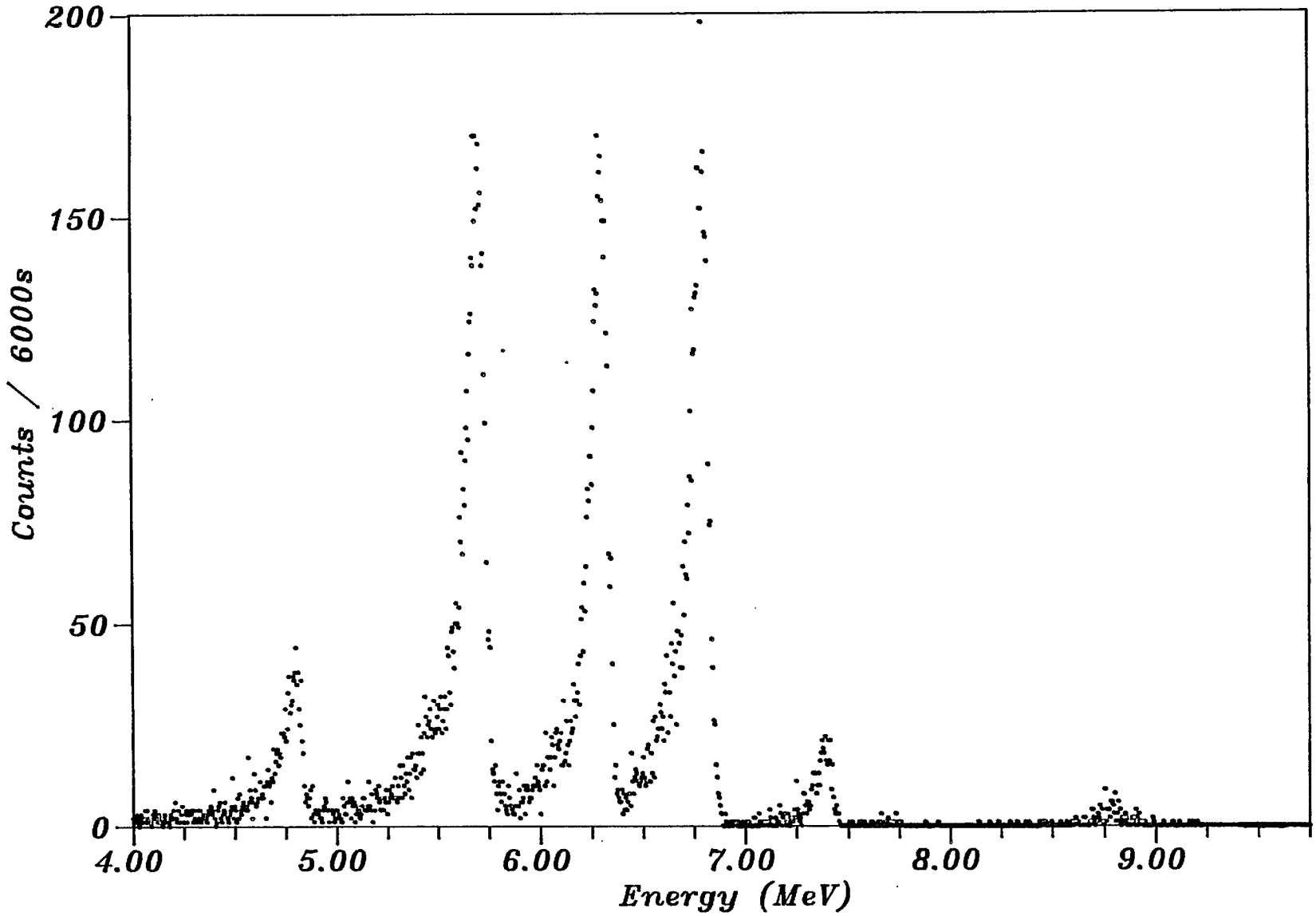


Fig. 8.2 - Mixed radium alpha spectrum. T=0 : 2.10 hours.

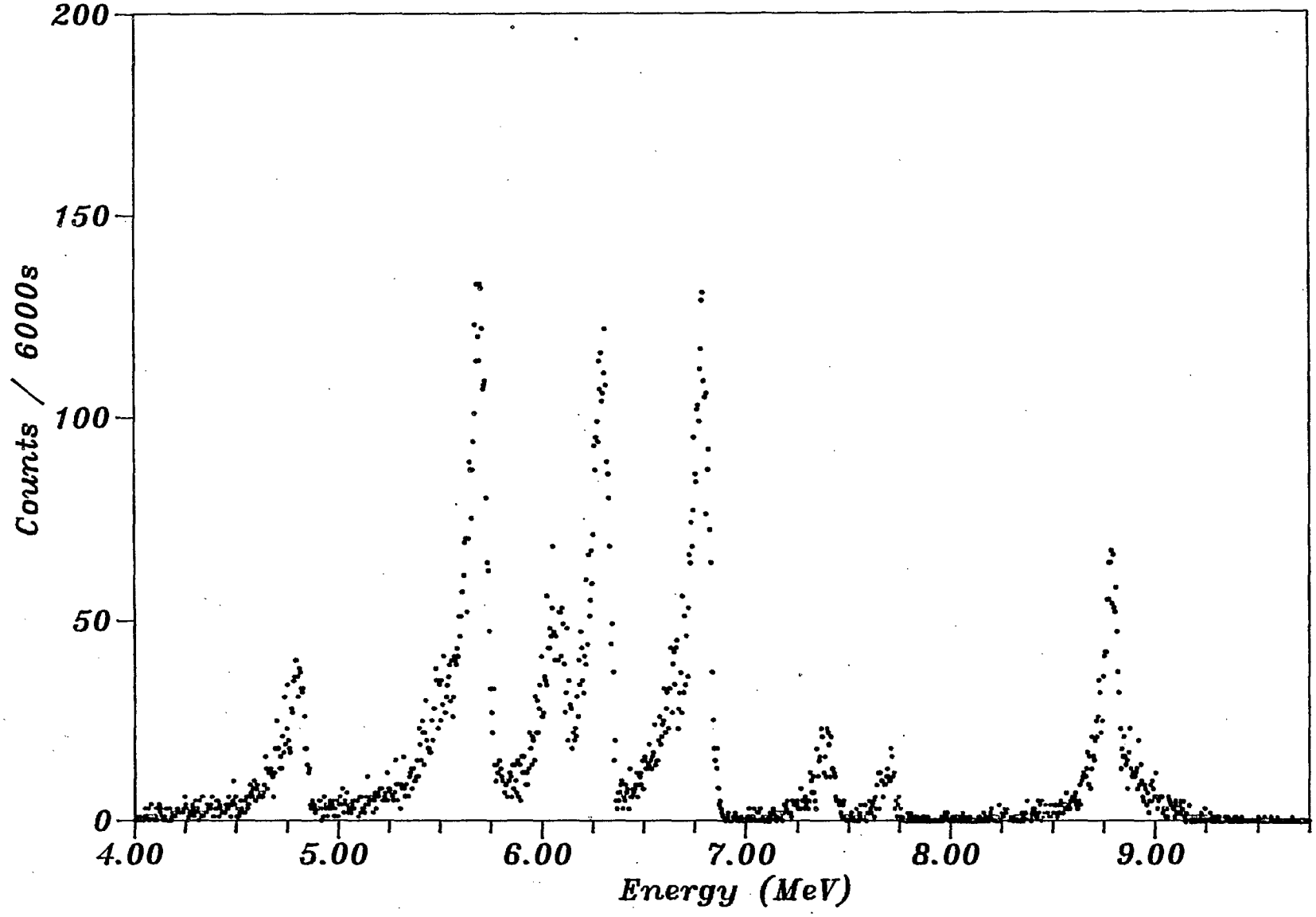


Fig. 8.3 - Mixed radium alpha spectrum. Time from T=0 : 30.80 hours.

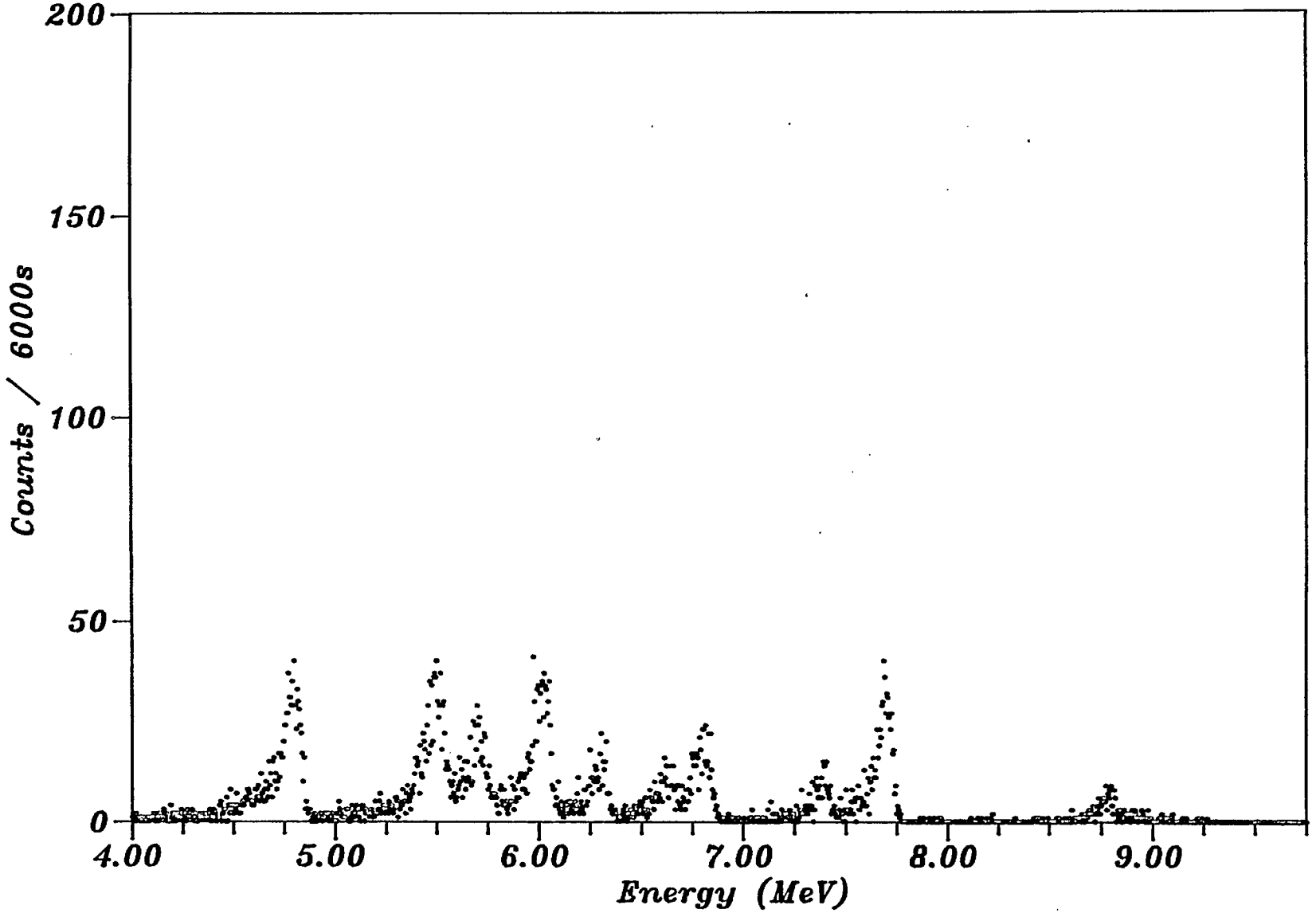


Fig. 8.4 - Mixed radium alpha spectrum. Time from T=0 : 303.72 hours.

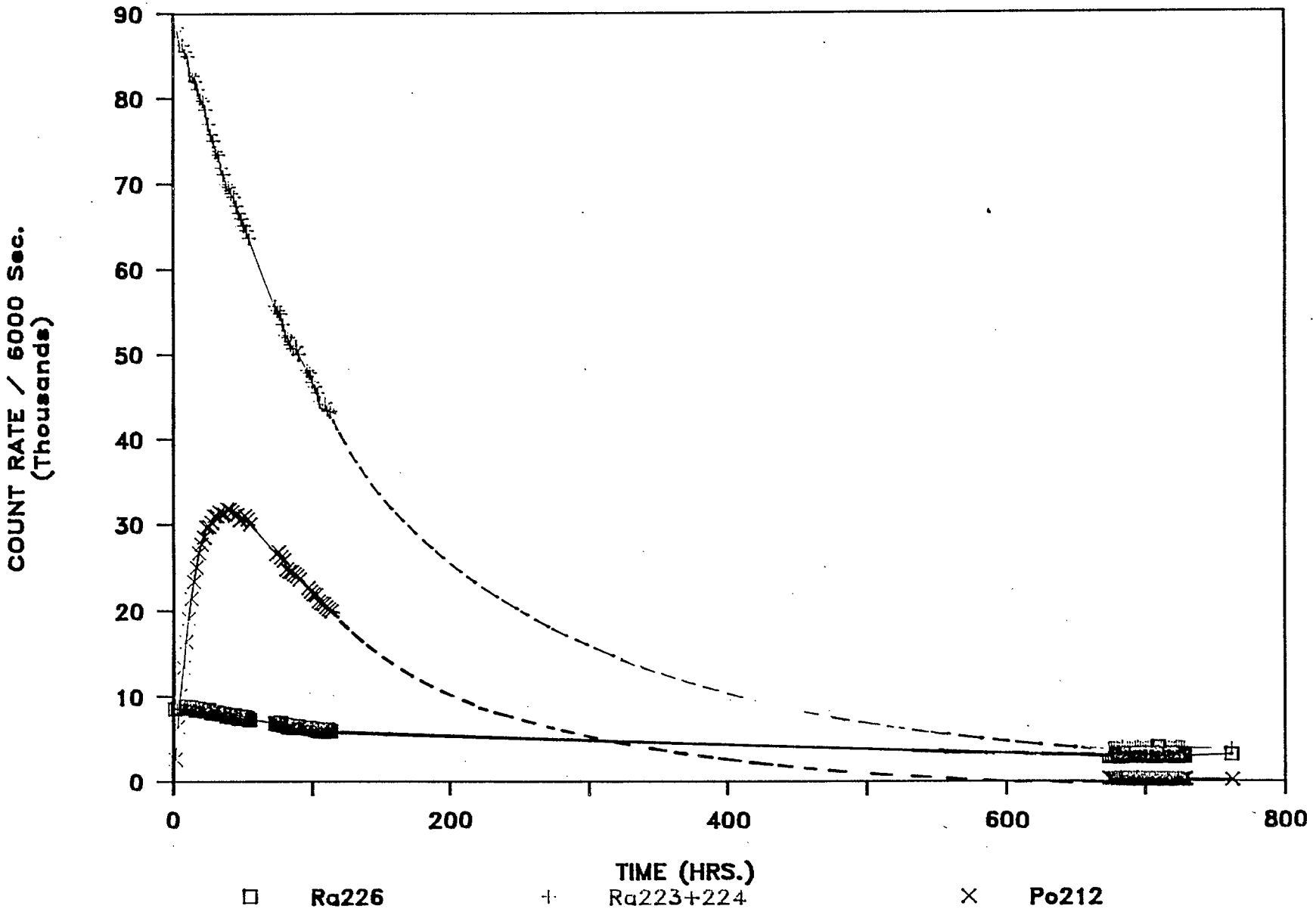


Fig. 8.5 - Decay curve of mixed radium species. (RDE-3) count rate versus time.

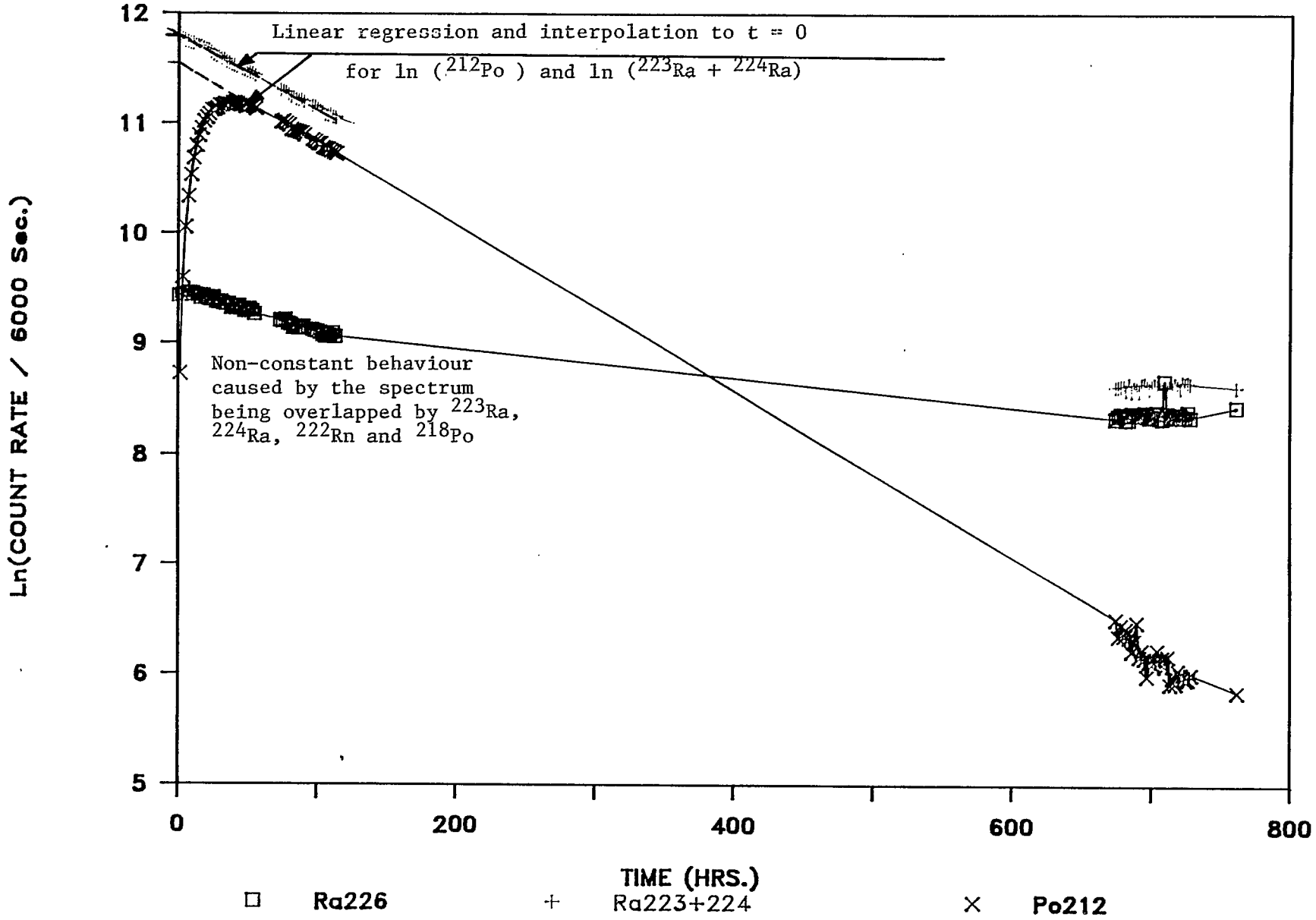


Fig. 8.6 - Decay curve of mixed radium species. (RDE-3) Ln(count rate) versus time.

# CHAPTER 9

## CONCLUSIONS

At the time when the tailings are placed in its containment, the ratios between daughter/parent isotopes should have been near 1.0 (equilibrium), with the exception of those for the uranium-species which were already extracted in the mill.

The data obtained from the T-5 area in this study showed that the activity ratio between daughter/parent, especially for $^{210}Pb/^{226}Ra$ in the liquid phase is as high as 164. This was approximately 200 times larger than the ratio in the solid phase. This anomalous secular disequilibrium should be called "Paradoxical secular disequilibrium" since its behaviour is very irregular and beyond the boundary of the expected ratio for secular equilibrium, which is less than 1.0.

In this study, data from the solid phase were also obtained to demonstrate the hydrogeochemical interaction between liquid and solid phase in the uranium tailings bulk mass. In some cases, these data show the existence of paradoxical secular disequilibrium in the solid phase.

The activity ratios of daughter/parent isotopes for $^{210}Pb/^{226}Ra$ isotopes in the solid tailings had values of less than 1.0. However the activity ratios for $^{226}Ra/^{230}Th$ and $^{228}Th/^{232}Th$ showed an unusual pattern with a high ratio of approximately 20:1 close to the surface of the tailings which then decreased with depth and approached 1.0 at the peat layer.

The mechanism of paradoxical secular disequilibrium in liquid and solid phases can be explained with reference to the basic rule of secular equilibrium, which has often been ignored, that the sample should be undisturbed, and no parent or daughter substances removed or allowed to

escape for a period of time long enough for secular equilibrium to be established. Therefore, in a disturbed and non-isolated system, paradoxical secular disequilibrium can exist:

1. In the solid phase, if the parent is removed by a leaching process, or a daughter is gained by reprecipitation and adsorption at a faster rate than the time required to reach equilibrium, and vice versa.
2. In the liquid phase, if the daughter activity is gained by preferential leaching, or if the parent isotopes reprecipitate at a faster rate than the time needed to reach equilibrium.

The solubilities of the sulphates which increase in value progressively from radium through lead, thorium and uranium (VI) species, is the major controlling factor in radioisotope disequilibrium.

It may be concluded that the behaviour of $^{210}Pb/^{226}Ra$ ratio (less than 1.0) in the solid phase is caused by preferential leaching of $^{210}Pb$ over $^{226}Ra$ and at a faster rate than the $^{226}Ra$ production of its daughter $^{210}Pb$ to reach secular equilibrium. The activity in the liquid phase is controlled by the pH, solubility or chemical equilibrium constant of $^{210}Pb$ $(SO_4)$, and the residence time of porewater. This ratio in the liquid phase is sometimes very high, caused by the higher availability of $^{210}Pb$ with the increased $^{226}Ra$ activity present in the bulk mass, and higher solubility of lead sulphate with decreases in pH (acidic condition).

A similar process occurs for the $^{226}Ra/^{230}Th$ activity ratio in the solid phase, where the thorium sulphate is more soluble than the radium sulphate.

Important differences between the activity ratios of $^{226}Ra/^{230}Th$ and $^{210}Pb/^{226}Ra$ were observed. The $^{226}Ra/^{230}Th$ values are mostly between 1 and 10. These values were a result of the higher solubility of thorium sulphate compared to the radium sulphate, and the slow rate of $^{226}Ra$ production from

its parent $^{230}Th$.

$^{210}Pb$ ($SO_4$), a product of a much faster rate of decay from $^{226}Ra$ (1.6 x $10^3$ y), has a solubility higher than radium sulphate, but less than thorium sulphate. Thus the $^{210}Pb/^{226}Ra$ ratio was close to or less than 1.0 in the solid phase.

In the case of $^{228}Th/^{232}Th$ activity ratio, although $^{228}Th$ and $^{230}Th$ supposedly behave the same as chemical thorium (same solubility), the result showed a ratio between 20:1 which indicates a chemical segregation to two different elements. A review of the $^{232}Th$ decay series shows that the $^{228}Th$ is not a direct daughter of $^{232}Th$, but results from several decay chain steps, i,e., $^{232}Th$ (1.4 x $10^{10}$ y) → $^{228}Ra$ (6.7 y) → $^{228}Ac$ (6.1 h) → $^{228}Th$.

For thorium which undergoes dynamic hydrogeochemical processes, the $^{232}Th$ (which is more soluble) is leached at a faster rate than $^{228}Ra$, while the $^{228}Th$ is produced indirectly, at a faster rate from $^{228}Ra$. It can then be concluded that the decay events, and the solubility of thorium and radium are the major controlling factors in the hydrogeochemical processes that caused the paradoxical disequilibrium between $^{228}Th$ and $^{232}Th$.

This study gives more complete evidence of disequilibrium than studies by other investigators in this field (1,4 to 26,57,58), as it outlines more fully the comprehensive interaction between the solid and liquid phases.

For example, Veska (26) who extensively studied the $^{234}U/^{238}U$ ratio in the liquid phase, recognized a continuous trend of relative $^{234}U$ enrichment in the isolated system, and believed this was caused by preferential leaching of $^{234}U$ in the 6+ oxidation state, and a stronger absorption of $^{238}U$ in the 4+ state. This explanation, however, was contradicted by Morin (27) who mentioned that $^{238}U$ or $^{234}U$ can exist in a 4+, 5+ or 6+ state.

Based on this study, a scenario can be deduced to explain how the $^{234}U/^{238}U$ ratio can result from the $^{238}U$ chain of decay in the solid phase

where $^{238}U$, $^{234}Th$, $^{234}Pa$ and $^{234}U$ are assumed to be at or near secular equilibrium. As the solid phase is leached by low pH water, the $^{238}U$ and $^{234}U$ are leached out at an equal rate as they both behave as chemical uranium. However, $^{234}Th$ and $^{234}Pa$ were leached out at a slower rate than the uranium, resulting in retardation of these species as the $^{234}U$ was being continuously produced. This causes an increase in the activity ratio of $^{234}U/^{238}U$ in the solid. The increased activity ratio in the solid phase is, of course, reversed in the liquid phase.

Through a simple laboratory experiment (Chapter 8) the impact on sampling, timing and analyses has indicated the parameters required for planning of future work and for evaluating work done in the past.

For example, the explanation given by CBCL Ltd. (58) in regard to $^{234}U/^{238}U$ activity ratio of 1.13 average, believed to be caused by mass recoil and ejection of $^{234}U$ was inaccurate.

As discussed previously in this thesis, $^{234}U$ is not a direct daughter of $^{238}U$ because $^{234}Th$ and $^{234}Pa$ are produced in between (63). Both $^{234}Th$ and $^{234}Pa$ could also be ejected and recoiled by their parents into solution and later adsorbed, precipitated and coprecipitated as the dynamic processes of hydrogeochemistry progress. It was also mentioned by CBCL Ltd. that the uranium deposition is considered to be an on-going process, i.e., the hydrogeochemical process is still very active. Therefore, it can be concluded that the age measurement as reported by CBCL Ltd could be seriously in error as $^{238}U$ and $^{234}U$ could be continuously added to the peat layer as the hydrogeochemical processes continue. Thus, caution should be taken in radioactive dating of geological strata and serious consideration should be given to the hydrogeochemical processes.

This study can also be utilized to explain the enrichment of radon gas species in groundwater and to give some information on the pathway to the

surface.

From the results of this study,it is clear that interpretation of data in dynamic situations must be done very carefully, especially when dealing with radiochemistry and related subjects, such as radioisotope dating, pathway analysis of radioisotopes in the food chain of biological matter (biomonitoring).

It is also seen in this study that the solid phase system acts as an indicator of the long term effects of the slow processes of dynamic hydrogeochemical evolution. Solid phase results are extremely valuable, in particular, in the study of the evolution of radioisotope species from uranium tailings. By comparison, the liquid phase system is a much faster, short term indicator of the happenings on a day to day basis. Sometimes the changes are so rapid (such as those connected with the oxidation mechanism of iron species), that complex problems arise in the design of mathematical models for the long term tailings events. The long term modelling could probably be simplified and improved by using only an empirical model based on the solid phase system.

When dealing with hydrogeochemical processes and field data interpretation of radioisotope migration, one must have an in-depth understanding of the physics of radioisotope decay, the chemical behaviour of the isotopes, and the groundwater hydrology of the system. It is clear too, that the timing of sampling, analytical techniques and sample storage for the investigation of disequilibrium phenomena is extremely important.

In conclusion, because of the many ways in which separation or removal of daughter isotopes can occur (hydrogeochemical or gas separation), even in a very tight rock formation with a very low water permeability (e.g., $10^{-9}$ to $10^{-12}$ cm/s), true secular equilibrium probably never exists. Many determinations of such equilibrium are limited by the counting statistics of

the instrument.

Most of the paradoxical secular disequilibrium shown in this study and in the data obtained by many other researchers was found by isolating the liquid phase and solid phase (either by natural separation such as in groundwater springs or by manual liquid sample extraction using piezometers). The possibility of paradoxical disequilibrium is often ignored by field investigators in their data interpretation.

Although paradoxical secular disequilibrium actually has nothing to do with the existence of secular equilibrium for series members, it does tell much about the pathways and processes for these isotopes.

## RECOMMENDATIONS

Future disequilibrium studies would be aided by more improvements in high resolution alpha-spectroscopy including a convoluted software program to evaluate complex alpha spectra. Methods of direct analyses for $^{238}U$, $^{235}U$ and $^{232}Th$ series decay chains should also be upgraded for field use (for liquid and solid phases). In situ measurements of gamma spectra using borehole logging techniques as a non-destructive method for field measurement would also give valuable data.

Furthermore, in future research, it is imperative to repeat this study every five years, especially on the Nordic Main tailings area, and include the study of the activity ratio within the liquid phase and the solid phase at the same time. The information will be extremely useful as an aid in the development of mathematical models for the long-term prediction of tailings behaviour.

Variations of sites and types of tailings should also be considered such as Agnew Lake Mine's tailings, Ontario, and a few othere in Saskatchewan.

The results of this type of study will also help in decision making

for designing of:

1. future tailings - such as deep water disposal, wet barrier etc.
2. remedial action to correct problems from and past and present tailings deposition using different types of engineering or biological covers such as: consolidated tailings, wet barriers or wet land reducing bacteria, etc.

The objective of the design is to limit the release of contaminants to the environment without much human involvement in the future.

For instance, research involving a wet barrier on top of the tailings is planned for the near future. An impervious dam will be built to contain the porewater, and it is expected that sulphide reducing bacteria will slowly colonize the saturated zone. Under such conditions, it is expected that the contaminant migration will be drastically reduced and thus allow secular equilibrium to exist in the solid phase. Therefore, paradoxical secular disequilibrium can also be used as an indicator of contaminant migration within the uranium tailings deposition.

Another interesting area of study is the scavenging elements and their behaviour, such as the hydroxides of iron, aluminum and manganese as there are possibilities that these elements could be used in the future as scrubbers, and if later on were further processed by nature into insoluble solid minerals (oxidation into hardpan etc.).

Caution should be taken in radioisotope dating of geological strata (or archeological) as there are numerous possibilities where serious errors can vastly mislead the conclusion. One of them is hydrogeochemical interaction between liquid and solid phases. Even in a very tight formation with a permeability of $10^{-9}$ to $10^{-12}$ cm/sec, and taking into account the geological time of many thousands of years, significant porewater must have been transported from one place to another, i.e., parent and daughter

isotopes could have been removed or added during that time.

Furthermore, the type of rock could be very important since some types are more soluble than others. However, the chance of making errors is smaller when dealing with the solid phase sample in general, as the solid phase is a much larger sample in mass ratio in comparison to the liquid phase sample. Also, as previously mentioned, the solid phase reacts much more slowly to change of time in comparison to the liquid phase.

The radioisotope chosen should be chemically insoluble and have a half life suitable for the time scale range required. Several activity ratios of the radioisotope members should be done to test the logic.

## REFERENCES


1. Morin, K.A., Cherry, J.A., "Variations in natural-decay-series disequilibrium along groundwater flowpaths"; Report MR 09-04, Morwikj Enterprises; 1987.

2. Lederer, C.M., Hollander, J.M. and Perlman, I., "Table of isotopes"; Sixth edition, Lawrence Radiation Laboratory, University of California, Berkeley, CA; John Wiley & Sons Inc., New York; 1968.

3. Friedlander, G., Kennedy, J.W., Miller, J.M., "Nuclear and Radiochemistry"; Second edition, John Wiley & Sons Inc., New York; 1964.

4. Cherry, J.A., Shepherd, T.A. and Morin, K.A., "Chemical composition and geochemical behaviour of contaminated groundwater at uranium tailings impoundments"; SME-AIME Annual Meeting, Dallas, Texas, 14-18 February, 1982. Preprint No. 82-114.

5. Cowart, J.B., "Uranium isotopes and $^{226}Ra$ content in the deep groundwaters of the Tri-State region, U.S.A."; J. of Hydrology, vol. 54, pp. 185-193, 1981.

6. Cowart, J.B., "The relationship of uranium isotopes to oxidation/reduction in the Edwards Carbonate Aquifer of Texas"; Earth and Planetary Science Letters, vol. 48, pp. 277-283, 1980.

7. Davidson, M.R. and Dickson, B.L., "A porous model for steady state transport of radium in groundwater"; Water Resources Research, vol. 22, pp. 34-44, 1986.

8. Frohlich, K., Gellerman, R. and Runge, K., "On the migration of uranium isotopes in sandstone aquifers"; Proc. Int. Symp on Migration in the Terrestrial Environment of Long-Lived Radionuclides from the Fuel Cycle; Knoxville, TN, 27-31 July 1981; IAEA-SM 275/88p.

9. Haji-Djafari, S., Antommaria, P.E. and Crouse, H.L., "Attenuation of radionuclides and toxic elements by in situ soils at a uranium tailings pond in central Wyoming"; Proc. ASTM Symp. on Permeability and Groundwater Contaminant Transport; Zummer, T.F. and Riggs, C.O. (Eds.); pp. 221-242, Philadelphia, 1979.

10. Highland, W.R., Murdock, L.T. and Kemp, E., "Design and seepage modelling studies of below-grade disposal West Gas Hills, Wyoming"; Symp. on Uranium Mill Tailings Management; Colorado State University, Fort Collins, CO., pp. 537-556; 1981.

11. Hoffman, G.L. and Playton, S.J., "Evaluation of the ground water hydrology in the vicinity of petrotomics' tailings reservoir, Shirley Basin, Wyoming"; Preliminary Report, Hydro-Engineering, Casper, Wyoming, 1981.

12. Kaufman, N.I., Rydell, H.S. and Osmond, J.K., "$^{234}U/^{238}U$ disequilibrium as an aid to hydrologic study of the Floridan Aquifer"; J. Hydrology, vol. 9, pp. 374-386, 1969.

13. Kronfeld, J., "Uranium deposition and Th-234 alpha-recoil: an explanation for extreme U-234/U-238 fractionation within the Trinity Aquifer"; Earth and Planetary Science Letters, vol. 21, pp. 327-330; 1974.

14. Laul, J.C., Smith, M.R. and Hubbard, N., "Behaviour of natural uranium, thorium and radium isotopes in the Wolfcamp Brine aquifers, Palo Duro Basin, Texas"; Proc. Symp. Materials Research Society, vol. 44, pp. 475-482; 1985.

15. Moffett, D. and Tellier, M., "Radiological investigations of an abandoned uranium tailings area"; J. Environmental Quality, vol. 7, pp. 310-314, 1978.

16. Morin, K.A., "Prediction of subsurface contaminated transport of acidic seepage from uranium tailings impoundments"; Ph.D. Thesis, Department of Earth Sciences, University of Waterloo, Ontario; 1983.

17. Morin, M.A. and Cherry, J.A., "Field investigation of a small-diameter cylindrical, contaminated groundwater plume emanating from a pyritic uranium-tailings impoundment"; ASTM Special Publication ASTM-SP-963 (in press), 1987. Based on ASTM Symp. on Field Methods for Groundwater Contamination Studies and Their Standardization, Cocoa Beach, Florida, 2-6 February, 1986.

18. Morin, K.A. and Cherry, J.A., "Trace amounts of siderite near a uranium tailings impoundment, Elliot Lake, Ontario, and its implication in controlling contaminant migration in a sand aquifer"; Chemical Geology, vol. 56, pp. 117-134, 1986.

19. Morin, K.A. and Cherry, J.A., "Migration of acidic groundwater seepage from uranium-tailings impoundments. 3. Simulation of conceptual model with application to seepage area A and other case studies"; J. of Contaminant Hydrology, vol. 2, No. 4, pp. 288-340; 1987.

20. Morin, K.A., Cherry, J.A., Dave, N.K., Lim, T.P. and Vivyurka, A.J., "Migration of acidic groundwater seepage from uranium tailings impoundments. 1. Field study and conceptual hydrology model"; J. of Contaminant Hydrology, vol. 2, No. 4, pp. 288-340; 1987.

21. Morin, K.A., Cherry, J.A., Dave, N.K., Lim, T.P. and Vivyurka, A.J., "Migration of acidic groundwater seepage from uranium tailings impoundments. 2. Geochemical behaviour of radionuclides in groundwater"; J. of Contaminant Hydrology, vol. 2, No. 4, pp. 288-340; 1987.

22. Osmond, J.K. and Cowart, J.B., "U-234/U-238 variations in a sandstone aquifer"; EOS, vol. 55, p. 458, 1974.

23. Taylor, M.J., "Radionuclide movement in seepage and its control"; Proc. 1st Int. Conf. on Uranium Mine Waste Disposal SME-AIME, pp. 205-244, Vancouver, B.C., 19-21 May, 1980.

24. Taylor, M.J. and Antommaria, P.E., "Immobilization of radionuclides at uranium tailings disposal sites"; Proc. Symp. on Uranium Mill Tailings Management, Colorado State University, Fort Collins, CO., 20-21 November, 1978.

25. Titayeva, N.A., Filonov, V.A., Ovchenkov, V.Y., Veksler, T.I., Orlova, A.V. and Tyrina, A.S., "Behaviour of uranium and thorium isotopes in crystalline rocks and surface waters in a cold wet climate"; Geochemistry International, vol. 10, pp. 1146-1151, 1973.

26. Veska, E., "Origin and subsurface migrations of radionuclides from waste rock at an abandoned uranium mine near Bancroft, Ontario"; Ph.D. Thesis, University of Waterloo, Ontario, 1983.

27. Morin, K.A., "A critical examination of the condition of electro-neutrality in groundwater"; Proc. Int. Groundwater Symp., Int. Assoc. of Hydrogeologists, Halifax, Nova Scotia, May 1-5, 1988.

28. Blair, R., Cherry, J.A., Lim, T.P. and Vivyurka, A.J., Groundwater monitoring and contaminant occurrence at an abandoned tailings area, Elliot Lake, Ontario"; Proc. 1st Int. Conf. on Uranium Mine Waste Disposal, SME-AIME, May 19-21, 1980, Chapter 29, p. 411.

29. Cherry, J.A., Blackport, R.J., Dubrovsky, N., Gilham, R.W., Reardon, E.L., Smyth, D.J.A., Lim, T.P., and Murray, D., "Subsurface hydrology and geochemical evolution of inactive pyritic tailings in the Elliot Lake uranium district, Canada"; Proc. Symp. Uranium Mill Tailings Management, Fort Collins, CO., November 24-25, 1980.

30. Morin, K.A., Cherry, J.A., Lim, T.P. and Vivyurka, A.J., "Contaminant migration in a sand aquifer near an inactive uranium tailings impoundment Elliot Lake, Ontario"; Can. Geotech. J., vol. 19, No., 1, pp, 49-62, 1982. (Prize award winner Can. Geotech. Society, best paper 1983.)

31. Dave, N.K., Lim, T.P. and Vivyurka, A.J., "Chemical and radioisotope distribution profiles in an abandoned uranium tailings pile"; Proc. 4th Symp. on Uranium Mill Tailings Management, Fort Collins, CO., 26-28 October, 1981, Session 4, p. 343.

32. Dave, N.K., Lim, T.P. and Vivyurka, A.J., "Chemical and radioisotopes stratification in an abandoned uranium tailings pile"; Proc. Int. Conf. on Radiation Hazards in Mining: Control Measurement and Medical Aspects, Golden, CO., 4-9 October, 1981.

33. Robertson, J.A., "Geology of Township 149 and Township 150"; Geologic Report 57, Ontario Department of Mines.

34. Wardrop, W.L. and Associates Ltd., "Nordic West Arm tailings pond hydraulic investigation"; DSS Contract OSQ 78-00072; CANMET, Energy, Mines and Resources Canada, 1978.

35. Morrison Beatty Ltd., "Hydrogeologic investigation of the Nordic tailings ponds, Elliot Lake, Ontario"; DSS Contract OSQ 79-00105, CANMET, Energy, Mines and Resources Canada, 1979.

36. Furman, N.H. (Ed.) "Standard methods of chemical analysis"; Sixth edition, vol. 1; D. Van Nostrand Co. Inc., Princeton, New Jersey, 1962.

37. Nordstrom, D.K., "Aqueous pyrite oxidation and the formation of secondary iron sulphate and iron oxide/hydroxide minerals"; prepared for Acid Sulphate Soil Symp., Annual Meeting SSSA, Fort Collins, CO., August 6, 1979.

38. Dalton, L., "Analysis of drilling samples from the West Arm of the tailings basin, Nordic Mine"; Division Report MSL-INT 79-26, CANMET, Energy, Mines and Resources Canada, 1979.

39. Dalton, L., "Analysis of drilling samples from the West Arm of the tailings basin, Nordic Mine, Phase 2"; Division Report MSL-INT 79-103, CANMET, Energy, Mines and Resources Canada; 1979

40. Dalton, L., "Analysis of drilling samples from the Nordic Lake tailings basin"; Division Report MSL-INT 81-7; CANMET, Energy, Mines and Resources Canada, 1980.

41. Lim, T.P., Cloutier, N., Boucher, Y., Dave, N.K., "Performance test of the Spectraspan V sequential atomic emission spectrometer"; Division Report MRP/MRL 85-47(TR), CANMET, Energy, Mines and Resources Canada, March 1985.

42. Smithson, G.L., Dalton, J.L. and Masson, D.L., "Radiochemical procedures for the determination of selective members of the uranium and thorium series"; CANMET Report 78-22, CANMET, Energy, Mines and Resources Canada; 1979.

43. Chiu, N.W. and Dean, J.R., "Radioanalytical methods manual"; National Uranium Tailings Program, CANMET, Report NUTP-3E, Monenco Consultants Limited; 1986.

44. Michel, J, Moore, W.S. and King, P.T., "γ-ray spectrometry for determination of radium-228 and radium-226 in natural waters"; Anal. Chem., vol. 53, pp. 1885-1889; 1981.

45. Trahey, N.M., Voeks, A.M. and Soriano.M.D., Report NBL-303, USDOE, Argonne, IL., pp. 116-117; 1982.

46. Schery, S.D., "Determination of lead-210 in environmental samples by γ-spectrometry with high-parity germanium detectors"; Anal. Chem., vol. 52, pp. 1957-1958; 1980.

47. Lim, T.P. and Dave, N.K., "A rapid method of radium-226 analysis in water samples using an alpha spectroscopic technique"; CIM Bull., vol. 74, No. 833, pp 97-105; 1981.

48. Dean, J.R. and Chiu, N., "Indirect measurement of thorium-228 and radium-224 by high resolution α-spectrometry"; Nucl. Instrum. Methods Phys. Res. Sect. A. vol. 223, No. 2-3, pp. 253-258; 1984.

49. Sill, C.W., "Determination of radium-226 by high resolution alpha-spectroscopy"; NTIS Report DE83-014 959, EG&G Inc., Idaho Falls, Idaho. U.S.A., 1983.

50. Chiu, N. and Dean, J.R., "Internal procedure manual"; Monenco Analytical Laboratories, Calgary, Canada; 1983.

51. Sill, C.W. and Williams, R.L., "Preparation of actinides for α-spectroscopy without electrodeposition"; Anal. Chem., vol. 53, pp. 412-415; 1981.

52. Durham, R.W. and Joshi, H.R., "Determination of $^{228}Th$ in environmental samples from uranium mining and milling operations"; J. Radioanal. Chem., vol. 52, No. 1, pp. 181-188; 1979.

53. Freeze, R.A., Cherry, J.A., "Groundwater", Chapters 5 and 6, pp. 167-236, Prentice-Hall Inc., Englewood Cliffs, New Jersey; 1979.

54. Surfer Information Manual, for Surfer Version 3.0, Golden Software Inc., Golden, Colorado.

55. CRC Handbook of Chemistry and Physics; Weast, R.C. (Ed.), 60th Edition, CRC Press Inc., Boca Raton, Florida; 1979.

56. Lim, T.P., Dave, N.K. and Cloutier, N.K., "High resolution alpha-spectroscopy for radium analysis - the effects of sample thickness and filter pore size"; Division Report M&ET/MRL 87-12(J), 1987.

57. Music, S. and Ristic, M., "Adsorption of trace elements or radionuclides on hydrous iron oxides"; J. Radioanal. & Nucl. Chem. Articles, vol. 120, No. 2, pp. 797-799, 1987.

58. CBCL Limited, "A study of naturally occurring, radionuclide bearing deposits at Portland Creek, Newfoundland"; Final Report for National Uranium Tailings Program; DSS Contract OSQ84-00074; Energy, Mines and Resources Canada; 1985.

59. Hvorslev, M.J., "Time lag and soil permeability in groundwater observations"; Bull. 36; U.S. Army Corps. Engrs., Waterways Exp. Sta., Vickburg, Miss.

60. Fleischer, R.L., "Moisture and $^{222}Rn$ Emanation"; Health Phys. vol. 52, No. 6, pp. 797-799, June 1987.

61. Mess, C.T., Vietti, M.A. and Mage, D.T., "Radon from drinking water - evaluation of waterborne transfer into house air"; Envir. Geochem. & Health, vol. 9, No. 3-4, pp. 68-73, 1987.

62. Ivanovich, M. and Harmon, R.S., "Uranium series disequilibrium-applications to environmental problems"; Oxford University Press, 1982.

63. Kigoshi, K., "Alpha-recoil thorium-234: dissolution into water and the uranium-234/uranium-238 disequilibrium in nature"; Science, 173:47-48, 2 July, 1971.